

---

# Macromolecules Containing Metal and Metal-Like Elements

## Volume 6

---

### Transition Metal-Containing Polymers

**Edited by**

**Alaa S. Abd-El-Aziz**

*Department of Chemistry, The University of Winnipeg, Winnipeg, Manitoba,  
Canada*

**Charles E. Carraher Jr.**

*Department of Chemistry and Biochemistry, Florida Atlantic University,  
Boca Raton, Florida, and Florida Center for Environmental Studies, Palm  
Beach Gardens, Florida*

**Charles U. Pittman Jr.**

*Department of Chemistry, Mississippi State University, Mississippi State,  
Mississippi*

**Martel Zeldin**

*Department of Chemistry, University of Richmond, Richmond, Virginia*

 **WILEY-INTERSCIENCE**

A John Wiley & Sons, Inc., Publication



---

**Macromolecules  
Containing Metal and  
Metal-Like Elements**

**Volume 6**

---



---

# Macromolecules Containing Metal and Metal-Like Elements

## Volume 6

---

### Transition Metal-Containing Polymers

**Edited by**

**Alaa S. Abd-El-Aziz**

*Department of Chemistry, The University of Winnipeg, Winnipeg, Manitoba, Canada*

**Charles E. Carraher Jr.**

*Department of Chemistry and Biochemistry, Florida Atlantic University, Boca Raton, Florida, and Florida Center for Environmental Studies, Palm Beach Gardens, Florida*

**Charles U. Pittman Jr.**

*Department of Chemistry, Mississippi State University, Mississippi State, Mississippi*

**Martel Zeldin**

*Department of Chemistry, University of Richmond, Richmond, Virginia*

 **WILEY-INTERSCIENCE**

A John Wiley & Sons, Inc., Publication

Copyright © 2006 by John Wiley & Sons, Inc. All rights reserved.

Published by John Wiley & Sons, Inc., Hoboken, New Jersey.  
Published simultaneously in Canada.

No part of this publication may be reproduced, stored in a retrieval system, or transmitted in any form or by any means, electronic, mechanical, photocopying, recording, scanning, or otherwise, except as permitted under Section 107 or 108 of the 1976 United States Copyright Act, without either the prior written permission of the Publisher, or authorization through payment of the appropriate per-copy fee to the Copyright Clearance Center, Inc., 222 Rosewood Drive, Danvers, MA 01923, (978) 750-8400, fax (978) 750-4470, or on the web at [www.copyright.com](http://www.copyright.com). Requests to the Publisher for permission should be addressed to the Permissions Department, John Wiley & Sons, Inc., 111 River Street, Hoboken, NJ 07030, (201) 748-6011, fax (201) 748-6008, or online at <http://www.wiley.com/go/permission>.

**Limit of Liability/Disclaimer of Warranty:** While the publisher and author have used their best efforts in preparing this book, they make no representations or warranties with respect to the accuracy or completeness of the contents of this book and specifically disclaim any implied warranties of merchantability or fitness for a particular purpose. No warranty may be created or extended by sales representatives or written sales materials. The advice and strategies contained herein may not be suitable for your situation. You should consult with a professional where appropriate. Neither the publisher nor author shall be liable for any loss of profit or any other commercial damages, including but not limited to special, incidental, consequential, or other damages.

For general information on our other products and services or for technical support, please contact our Customer Care Department within the United States at (800) 762-2974, outside the United States at (317) 572-3993 or fax (317) 572-4002.

Wiley also publishes its books in a variety of electronic formats. Some content that appears in print may not be available in electronic formats. For more information about Wiley products, visit our web site at [www.wiley.com](http://www.wiley.com).

***Library of Congress Cataloging-in-Publication Data:***

ISBN-13 978-0-471-68445-9  
ISBN-10 0-471-68445-7  
ISSN 1545-438X

Printed in the United States of America

10 9 8 7 6 5 4 3 2 1

---

# Contributors

---

**Alaa S. Abd-El-Aziz**, Department of Chemistry, The University of Winnipeg, Winnipeg, Manitoba, R3B 2E9, CANADA

**Charles E. Carraher Jr.**, Department of Chemistry, Florida Atlantic University, Boca Raton, FL 33431 and Florida Center for Environmental Studies, Palm Beach Gardens, FL 33410

**Alison Y. Cheng**, Department of Chemistry, University of Toronto, 80 St. George Street, Toronto, Ontario, M5S 3H6, CANADA

**Scott B. Clendenning**, Department of Chemistry, University of Toronto, 80 St. George Street, Toronto, Ontario, M5S 3H6, CANADA

**Gulzhian I. Dzhardimalieva**, Institute of Problems of Chemical Physics, Russian Academy of Sciences, Chernogolovka, Moscow Region 142432, RUSSIA

**Ian Manners**, Department of Chemistry, University of Toronto, 80 St. George Street, Toronto, Ontario, M5S 3H6, CANADA

**A. D. Pomogailo**, Institute of Problems of Chemical Physics, Russian Academy of Sciences, Chernogolovka, Moscow Region 142432, RUSSIA

**Ikuyoshi Tomita**, Department of Electronic Chemistry, Interdisciplinary Graduate School of Science and Engineering, Tokyo Institute of Technology, Nagatsuta-cho 4529, Midoriku, Yokohama 226-8502, JAPAN

**David R. Tyler**, Department of Chemistry, University of Oregon, Eugene, OR 97403



---

# Contents

---

<b>Preface</b>	<b>xi</b>
<b>Series Preface</b>	<b>xiii</b>
<b>1. Introduction</b>	<b>1</b>
<i>Alaa S. Abd-El-Aziz and Charles E. Carraher Jr.</i>	
I. Coverage	2
II. General Concepts	3
III. Historical	5
IV. Polymers Containing Bis(Cyclopentadienyl) Metal Complexes	7
A. Polymerization of Olefin-Functionalized Metallocenes	8
B. Alkyne Metathesis Polymerization of Substituted Metallocenes	11
C. Polycondensation of Metallocenes	13
D. Ring-Opening Polymerization	15
E. Coordination of Metals to Cyclopentadienyl Rings	18
F. Introduction of Metallocenes into Preformed Polymers	20
V. Arene-Transition Metal Polymers	21
A. Polymerization of Olefin-Containing Arenes	21
B. Ring-Opening Metathesis Polymerization of Substituted Norbornenes	22
C. Nucleophilic Aromatic Substitution Polymerization of Chloroarene Complexes	23
D. Polycondensation of Arene Complexes	27
E. Coordination of Organometallic Moieties to Arenes	29
F. Supramolecular Assembly of Polymers	30
VI. Polymers with Metal-Coordinated Cyclobutadienes	31
VII. Polymers Containing Metal Carbonyl Complexes	32
VIII. Polymers with Metal-Carbon $\sigma$ -Bonds	34
A. Transition Metal Polyynes	34
B. Metal-Aryl and Metal-Alkyl Systems	37
IX. Metal-Metal Bonded Systems	38
X. Conclusion	41
XI. References	41

<b>2. Lithographic Applications of Highly Metallized Polyferrocenylsilanes</b>	<b>49</b>
<i>Alison Y. Cheng, Scott B. Clendenning, and Ian Manners</i>	
I. Introduction	50
II. Polyferrocenylsilanes as Electron Beam Lithography Resists	52
III. Polyferrocenylsilanes as Reactive Ion Etch Resists	53
IV. Polyferrocenylsilanes as UV Photoresists	55
V. Conclusions	56
VI. Acknowledgments	56
VII. References	57
<b>3. Polymers Possessing Reactive Metallacycles in the Mainchain</b>	<b>59</b>
<i>Ikuyoshi Tomita</i>	
I. Introduction	60
II. Synthesis and Reactions of Organometallic Polymers Possessing Metallacycles in the Mainchain	61
A. Cobaltcyclopentadiene-Containing Polymers	61
B. Conversion of Cobaltcyclopentadiene-Containing Polymers into Polymers Possessing Various Mainchain Structures	63
i. Conversion into Other Organometallic Polymers	63
ii. Conversion into Organic Polymers with Various Functional Groups in the Mainchain	66
C. Synthesis and Reactions of Titanacycle-Containing Polymers	69
i. Polymers Containing Titanacyclopentadiene Unit in the Mainchain	69
ii. Polymers Possessing Other Titanacycle Units	73
III. Summary	74
IV. References	75
<b>4. Mechanistic Aspects of the Photodegradation of Polymers Containing Metal–Metal Bonds Along Their Backbones</b>	<b>77</b>
<i>David R. Tyler</i>	
I. Introduction	78
II. General Overview of Polymer Photodegradation	79
A. The Auto-Oxidation Mechanism	79
B. Reactions of Hydroperoxide Species That Lead to Backbone Degradation	80
C. Other Photochemical Degradation Mechanisms	82
D. Methods for Intentionally Making Polymers Photodegradable	83
III. Metal–Metal Bond-Containing Polymers	85
A. Synthesis and Characterization	85
B. Synthesis of the Difunctional Dimers	86
C. Synthesis of the Polymers	88
D. Characterization of the Polymers	90

---

E. Photochemical Reactions in Solution	91
F. Photochemistry in the Solid State	94
IV. Factors Controlling the Rate of Photochemical Degradation	95
A. Cage Effects	95
B. The Effect of Tensile Stress on Photodegradation	98
i. Theories of Stress-Induced Photodegradation	98
ii. Stress-Induced Changes in $\phi_{\text{homolysis}}$ ; the Plotnikov Hypothesis	99
iii. Stress-Induced Changes in $k_{\text{recombination}}$ ; the Decreased Radical Recombination Efficiency Hypothesis	100
iv. Stress-Induced Changes in the Rates of Radical Reactions Subsequent to Radical Formation	100
v. The Zhurkov Equation	100
vi. Quantum Yields as a Function of Stress for Polymer 3	101
C. Other Factors Affecting Photochemical Degradation Rates of Polymers	102
i. Absorbed Light Intensity	103
ii. Polymer Morphology	104
iii. Oxygen Diffusion	105
iv. Chromophore Concentration	106
V. Acknowledgments	106
VI. References	106
<b>5. Zirconocene and Hafnocene-Containing Macromolecules</b>	<b>111</b>
<i>Charles E. Carraher Jr.</i>	
I. General	112
II. Introduction	113
III. Inorganic Supported Zirconocene and Hafnocene Catalysts	116
IV. Other Supports	119
V. Condensation Reactions with Monomeric Lewis Bases	121
VI. Zirconocene and Hafnocene Reactions with Already Existing Polymers	137
VII. Miscellaneous	139
VIII. Summary	143
IX. References	143
<b>6. Compositional and Structural Irregularities of Macromolecular Metal Complexes</b>	<b>147</b>
<i>Anatolii D. Pomogailo, Gulzhian I. Dzhardimalieva</i>	
I. Introduction	148
II. Basic Transformations of Macroligands in Binding $\text{MX}_n$	150
A. Conformational Changes in Polymer Chains	150
B. Macroligand Structuring Processes	152

C.	Macroligand Decomposition in $MX_n$ -Polymer Systems	155
D.	Changes in Origin of Functional Groups of Polymers in Their Reactions with $MX_n$	159
III.	Transformation of Transition Metal Compounds in Reactions with Polymers	161
A.	Oxidation-Reduction Conversion of Transition Metals	161
B.	Monomerization of Transition Metal Dimer Complexes in Reactions with Polymers	162
C.	Composite Inhomogeneity of Macromolecular Complexes	164
IV.	Problem of Topochemistry of Macromolecular Complexes	166
A.	Topochemistry of Polymer Macroligand Functional Layers	166
B.	Topochemistry of Diamagnetic Complexes That Are Fixed to the Polymers	167
C.	Topochemistry of Polymer-Bonded Paramagnetic Complexes	168
D.	The Main Data on MMC Topochemistry	172
V.	Problems of Unit Variability in Metal-Containing Polymers Obtained by Copolymerization of Metal-Containing Monomers	172
A.	Unit Variability Due to Elimination of a Metal-Containing Group During Polymerization	175
B.	Unit Variability Due to Different Valence States of the Transition Metal Ions	177
C.	Unit Variability Due to the Presence of Stable Metal Isotopes	179
D.	Anomalies in Metallopolymeric Chains Caused by the Diversity of Chemical Binding of a Metal to Polymerizable Ligands	180
E.	Unit Variability Due to Qualitatively and Quantitatively Different Ligand Environments of the Metal	183
F.	Extra-Coordination as a Spatial and Electronic Anomaly of the Polyhedron	186
G.	Exchange Interactions Between Metal Ions Incorporated in the Chain	188
H.	Change in the Nuclearity of Metal Sites as a Type of Unit Variability	190
I.	Stereoregularity of Metallopolymeric Chains	192
J.	Unit Variability Due to Chirality in Pendant Groups	194
K.	Unsaturation and Structurization of Metallopolymers	196
L.	Cyclization During Polymerization	197
VI.	Some Practical Applications of Unit Variability of Metal-Containing Polymers	198
VII.	Acknowledgments	202
VIII.	References	202

---

# Preface

---

Almost 70 of the approximately 115 elements are transition metals. These are elements with electrons successively added to their “d” or “f” subshells and have both filled and unfilled orbitals suitable for bonding. They exhibit a variety of oxidation states and bond formations, such as sigma and pi bonds or coordination bonds as are found in typical chelate structures. These characteristics are the reason that transition metal-containing macromolecules exist in a wide variety of structures including linear, two-dimensional, three-dimensional, dendrite, and assemblies. Many of these polymers are often referred to as organometallic polymers. We have, somewhat arbitrarily, separated this class from coordination polymers, which have been covered in Volumes 1, 3, and 5.

The interest in transition metal-containing polymers stems from the optical, biological, thermal, catalytic, electrical, and magnetic properties of these materials. They are candidates as essential materials for a wide variety of applications for the 21st century because of these properties. They are used in the coatings, colorants, pharmaceutical, aerospace, and communications industries. They can serve as precursors for ceramics.

This volume begins with a general review that includes an overview of the general types of polymers already synthesized. Different approaches to their synthesis and background information are included to help the reader to understand transition metal-containing macromolecules. This information provides an introduction to both Volumes 6 and 7 of this series. Activity in this important area is increasing exponentially. New materials, properties, synthetic routes, and common applications constitute the root of this rapid development.

Most polymers are useful because of their inactivity; however, metal-containing polymers are finding uses because of their chemical reactivity in diverse areas such as catalysis, photodegradation, and lithography. This volume contains reviews of each of these important areas that illustrate the possible application of metal-containing macromolecules in this important emerging area of reactive materials.



---

# Series Preface

---

Most traditional macromolecules are composed of less than 10 elements (mainly C, H, N, O, S, P, Cl, F), whereas metal and semi-metal-containing polymers allow properties that can be gained through the inclusion of nearly 100 additional elements. Macromolecules containing metal and metal-like elements are widespread in nature with metalloenzymes supplying a number of essential physiological functions including respiration, photosynthesis, energy transfer, and metal ion storage.

Polysiloxanes (silicones) are one of the most studied classes of polymers. They exhibit a variety of useful properties not common to non-metal-containing macromolecules. They are characterized by combinations of chemical, mechanical, electrical, and other properties that, when taken together, are not found in any other commercially available class of materials. The initial footprints on the moon were made by polysiloxanes. Polysiloxanes are currently sold as high-performance caulks, lubricants, antifoaming agents, window gaskets, O-rings, contact lens, and numerous and variable human biological implants and prosthetics, to mention just a few of their applications.

The variety of macromolecules containing metal and metal-like elements is extremely large, not only because of the large number of metallic and metalloid elements, but also because of the diversity of available oxidation states, the use of combinations of different metals, the ability to include a plethora of organic moieties, and so on. The appearance of new macromolecules containing metal and metal-like elements has been enormous since the early 1950s, with the number increasing explosively since the early 1990s. These new macromolecules represent marriages among many disciplines, including chemistry, biochemistry, materials science, engineering, biomedical science, and physics. These materials also form bridges between ceramics, organic, inorganic, natural and synthetic, alloys, and metallic materials. As a result, new materials with specially designated properties have been made as composites, single- and multiple-site catalysts, biologically active/inert materials, smart materials, nanomaterials, and materials with superior conducting, nonlinear optical, tensile strength, flame retardant, chemical inertness, superior solvent resistance, thermal stability, solvent resistant, and other properties.

There also exist a variety of syntheses, stabilities, and characteristics, which are unique to each particular material. Further, macromolecules containing metal and metal-like elements can be produced in a variety of geometries, including linear, two-dimensional, three-dimensional, dendritic, and star arrays.

In this book series, macromolecules containing metal and metal-like elements will be defined as large structures where the metal and metalloid atoms are (largely) covalently bonded into the macromolecular network within or pendant to the polymer

backbone. This includes various coordination polymers where combinations of ionic, sigma-, and pi-bonding interactions are present. Organometallic macromolecules are materials that contain both organic and metal components. For the purposes of this series, we will define metal-like elements to include both the metalloids as well as materials that are metal-like in at least one important physical characteristic such as electrical conductance. Thus the term includes macromolecules containing boron, silicon, germanium, arsenic, and antimony as well as materials such as poly(sulfur nitride), conducting carbon nanotubes, polyphosphazenes, and polyacetylenes.

The metal and metalloid-containing macromolecules that are covered in this series will be essential materials for the twenty-first century. The first volume is an overview of the discovery and development of these substances. Succeeding volumes will focus on thematic reviews of areas included within the scope of metallic and metalloid-containing macromolecules.

Alaa S. Abd-El-Aziz  
Charles E. Carraher Jr.  
Charles U. Pittman Jr.  
Martel Zeldin

---

## CHAPTER 1

# Introduction

### **Alaa S. Abd-El-Aziz**

*Department of Chemistry, The University of Winnipeg, Winnipeg, Manitoba, Canada*

### **Charles Carraher Jr.**

*Department of Chemistry and Biochemistry, Florida Atlantic University, Florida, and Florida Center for Environmental Studies, Palm Beach Gardens, Florida*

#### CONTENTS

I. COVERAGE	2
II. GENERAL CONCEPTS	3
III. HISTORICAL	5
IV. POLYMERS CONTAINING BIS(CYCLOPENTADIENYL) METAL COMPLEXES	7
A. Polymerization of Olefin-Functionalized Metallocenes	8
B. Alkyne Metathesis Polymerization of Substituted Metallocenes	11
C. Polycondensation of Metallocenes	13
D. Ring-Opening Polymerization	15
E. Coordination of Metals to Cyclopentadienyl Rings	18
F. Introduction of Metallocenes into Preformed Polymers	20

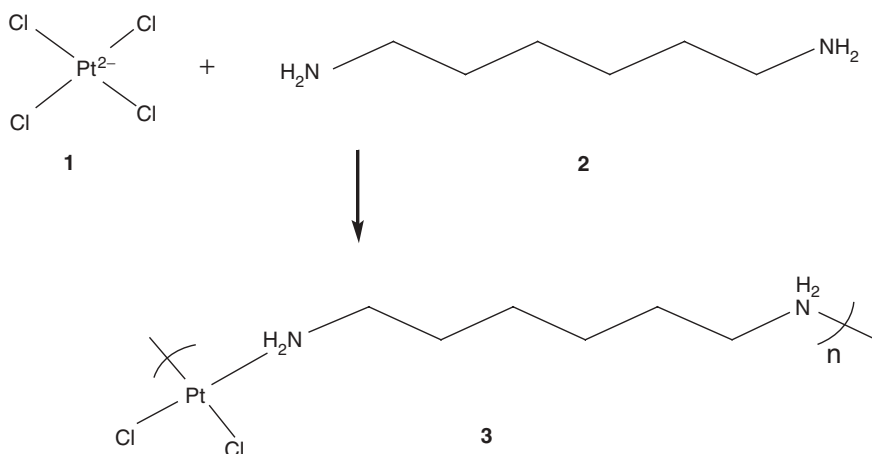
*Macromolecules Containing Metal and Metal-Like Elements,  
Volume 6: Transition Metal-Containing Polymers*, edited by Alaa S. Abd-El-Aziz,  
Charles E. Carraher Jr., Charles U. Pittman Jr., and Martel Zeldin.  
Copyright © 2006 John Wiley & Sons, Inc.

V. ARENE-TRANSITION METAL POLYMERS	21
A. Polymerization of Olefin-Containing Arenes	21
B. Ring-Opening Metathesis Polymerization of Substituted Norbornenes	22
C. Nucleophilic Aromatic Substitution Polymerization of Chloroarene Complexes	23
D. Polycondensation of Arene Complexes	27
E. Coordination of Organometallic Moieties to Arenes	29
F. Supramolecular Assembly of Polymers	30
VI. POLYMERS WITH METAL-COORDINATED CYCLOBUTADIENES	31
VII. POLYMERS CONTAINING METAL CARBONYL COMPLEXES	32
VIII. POLYMERS WITH METAL-CARBON $\sigma$ -BONDS	34
A. Transition Metal Polyynes	34
B. Metal-Aryl and Metal-Alkyl Systems	37
IX. METAL-METAL BONDED SYSTEMS	38
X. CONCLUSIONS	41
XI. REFERENCES	41

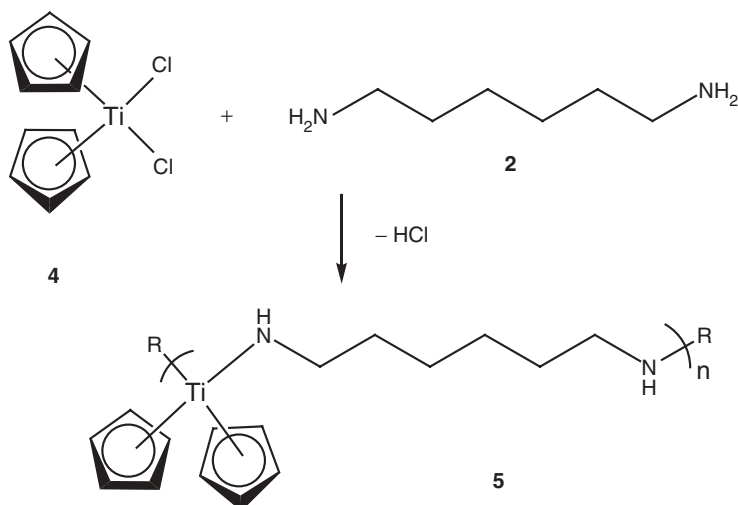
## I. COVERAGE

Transition metal-containing macromolecules come in a wide variety of structures. While volume 5 of this series dealt with metal coordination polymers, in this book we focus on transition metal-containing polymers where the metal is bonded to at least one organic group through  $\sigma$ - and/or  $\pi$ -bonds. Many of the macromolecules covered in this volume are often referred to as organometallic polymers. The term *organometallic compound* refers to compounds that contain at least one metal-carbon (M-C) bond, whether the bond is  $\sigma$  or  $\pi$  or some combination of both types of bonding.<sup>1-5</sup>

The line that divides classical and nonclassical metal complexes, organometallic complexes, and coordination compounds is imperfect. For instance, what constitutes a coordination reaction and a condensation reaction? Piperidine is an organic compound, that can react with metal-containing sites in two different ways. If the N-proton is retained, then the reaction is a coordination reaction and the resulting product a coordination compound. In this case, the nitrogen donates its lone pair of electrons to the metal site. However, if the proton is lost, then the reaction is described as a condensation reaction with the product called a condensation product. Polymers formed from such condensation reactions are covered in this volume. Schemes 1 and 2 depict reactions that illustrate the difference between coordination and condensation reactions using 1,6-hexanediamine.<sup>5-13</sup>



**Scheme 1** Coordination reaction between tetrachloroplatinate and 1,6-hexanediamine.



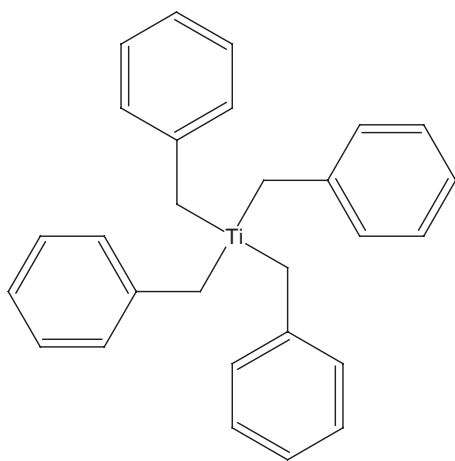
**Scheme 2** Condensation reaction between titanocene dichloride and 1,6-hexanediamine.

## II. GENERAL CONCEPTS

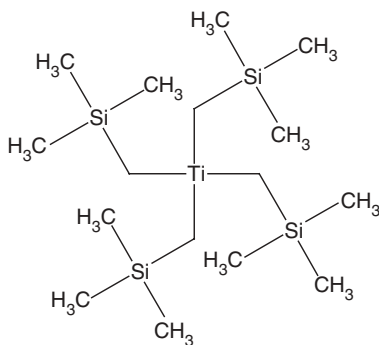
The elementary chemistry of transition metals can be understood using traditional chemistry terms. This is easily illustrated with the chemistry of titanium. Titanium, the second transition element, has an outer or valence electron configuration of  $4s^2, 3d^2$ . Its most common oxidation state is +4, with titanium losing or sharing four electrons. While compounds with titanium in the  $-1, 0, +2,$  and  $+3$  exist; they are easily oxidized to titanium +4. The energy for removal of four electrons is high,

so most titanium +4 compounds are covalent rather than ionic. Ferrocene, for example, when viewed according to the 18-electron rule, has 8 valence electrons, ( $4s^23d^6$ ), and each cyclopentadienyl (Cp) ion contributes 5 electrons giving a total of 10 electrons contributed by the two Cp units for a total of 18 electrons. Not all of the transition metals require the 18 electrons, some seek only 16 electrons. For titanocene dichloride, the titanium atom already has 4 electrons  $4s^23d^2$ , with each Cp contributing 5 electrons for a total of 10 electrons. Each chloride supplies 1 electron for a total of 2, giving a total of 16 electrons. Titanocene dichloride, however, has a vacant hybrid orbital; and to obtain 18 electrons, it can bind to double bonds. Deviations from the 16/18-electron rule are common in neutral bis(cyclopentadienyl) complexes. Thus  $Cp_2VCl_2$  has 5 valence electrons derived from the vanadium atom, 10 total electrons from the two Cp groups, and 2 total electrons from the two chlorides for a total of 17 valence electrons.

The compounds of titanium will be briefly described to illustrate the behavior and structural considerations in common organometallic compounds. Organotitanium compounds have been extensively studied because of their use in the production of stereoregular polymers. Here, we will briefly focus on some organotitanium(IV) compounds. Alkyl titanium complexes can be made using bulky groups, where titanium hydride elimination is impossible. Structures **6** and **7**, are examples of two of these compounds.



6



7

A number of Cp derivatives of Ti exist. Titanocene dichloride exists as a distorted tetrahedron, with the planes of the Cp rings facing the titanium metal. This is unlike ferrocene and cobalticinium salts for which the metal atoms are sandwiched between the parallel Cp rings. The structure of titanocene dichloride is similar to that of many of the other  $\pi$ -bonded Cp structures. Numerous derivatives of the titanocene moiety exist. These derivatives consist of various substituents, including alkyl, aryl,

halides, thiols, carbonyls, and ethers. There are also numerous compounds containing substituents on the ring. All of these derivatives have a distorted tetrahedral geometry about the titanium atom.

For many classical Lewis acid-base reactions, the Cp rings appear inert and condensation reactions occur with other substituents on the metal. In Figure 1, typical reactions with titanocene dichlorides that result in the formation of polymers are described.

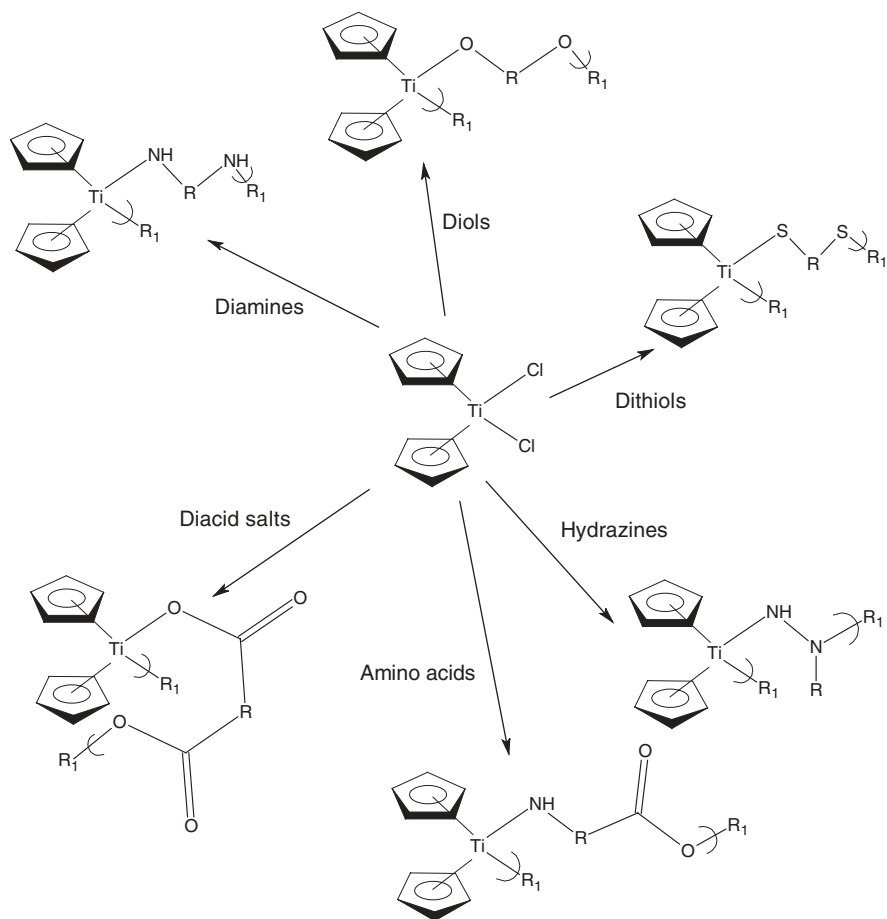


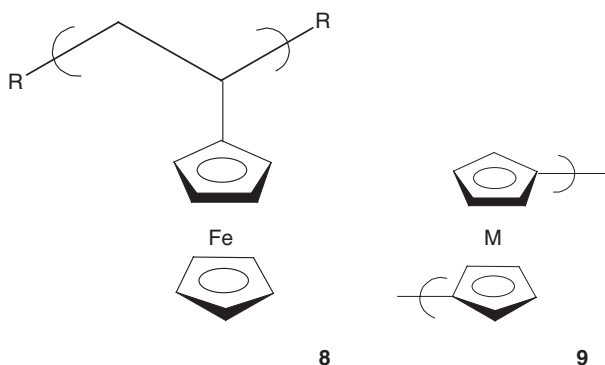
**Figure 1** Synthetic pathways for the synthesis of polymers from titanocene dichloride.

### III. HISTORICAL

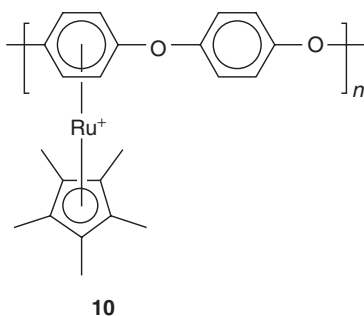
Since the first example of a metallocene based polymer was reported in 1955 by Arimoto and Haven, just a few years after the discovery of ferrocene, there has been an ever increasing interest in the development of organometallic polymers.<sup>14-18</sup> This

interest stems from the electrical, magnetic, optical, biological, thermal or catalytic properties that this class of polymers possess. Organometallic polymers have found applications in the coating, colorant, pharmaceutical, and aerospace industries. Organometallic polymers encompass many different classes of macromolecules. Due to the nature of the organic ligands, the metal and the type of M–C bond, a great variety of structures exist within each class. Transition metals can be either  $\sigma$ - or  $\pi$ -bonded to the carbon skeleton of the backbone or side chains. The first half of the 20th century saw many advances in organic and inorganic polymer chemistry, but it was not until the 1950s that organometallic polymers were identified as a new class of polymeric materials.<sup>19,20</sup>

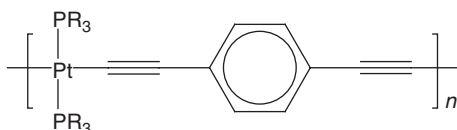
The formation of polymetalloenes through homoannular or heteroannular substitution is not the only method for obtaining the polymers; they can also be formed by polymerization via the metal. The metallocene can be attached to the polymer chain as in poly(vinyl ferrocene) (**8**), or it can be an integral part of the polymer backbone (**9**).<sup>19</sup>



Arene cyclopentadienylmetal and arene metal carbonyl complexes are two other classes of materials that are metallocene-like in structure. The first report of the synthesis of the  $\eta^6$ -mesitylene- $\eta^5$ -cyclopentadienyliron cation in 1957 by Coffield et al.<sup>21</sup> was a seminal event in this research field. However, it was the 1985 report on the polymerization of  $\eta^6$ -dichlorobenzene- $\eta^5$ -cyclopentadienylruthenium with diphenolic compounds, forming compounds such as **10**, by Segal<sup>22</sup> that caused research in this area to expand.



Research in poly(metal acetylides) such as structure **11**, dominates the area of transition metals  $\sigma$ -bonded to organic moieties.<sup>23,24</sup> Since the first report of these polymers in the 1970s, many researchers have described the incorporation of various types of transition metals into this class of materials. This class of organometallic polymers contains rigid-rod structures, making these polymers ideal for electrical and optical applications.



**11**

This chapter presents an overview of the chemistry of organometallic polymers, with emphasis on recent advances in this field.

#### **IV. POLYMERS CONTAINING BIS-(CYCLOPENTADIENYL) METAL COMPLEXES**

As noted earlier, a number of cyclopentadienyl metal-containing polymers have been synthesized. In some cases, the Cp has been substituted. In general when the substitution is “organic,” such as replacing the five Cp-hydrogens with methyl groups, the resulting products possess increased steric bulk; more electron-donating ability; and have more “organic-like” properties, including greater solubility in organic solvents. The electron donating nature of the methyl group makes the resulting pentamethyl-Cp a stronger-field ligand than Cp itself. Thus  $(\text{Me}_5\text{Cp})_2\text{Mn}$  is low spin in contrast to  $\text{Cp}_2\text{Mn}$ . The visible spectra of most  $(\text{Me}_5\text{Cp})_2\text{M}$  compounds show greater splitting between the  $2a_{1g}$  and  $2e_{1g}$  orbitals. Physical constants related to the electron density on the metal are also generally greater for the substituted Cp complexes. This electron buildup makes the substituted-Cp compound easier to oxidize than the corresponding nonsubstituted Cp. The reduction potential is often shifted by  $-0.5\text{ V}$  for such compounds.<sup>25</sup> The combination of steric hindrance and a greater gap between HOMOs and LUMOs gives organic-substituted Cp-compounds greater kinetic and thermal stability relative to Cp itself.

$\text{C}_5\text{H}_5^{-1}$  is essentially an  $\eta^5$  ligand donating six electrons. The general term *metallocene* is used to describe these bis(cyclopentadienyl) metal complexes. The most heavily studied metallocene is ferrocene.

In the MO treatment of ferrocene, the  $a'_1$  frontier orbital and all lower orbitals are full, but the  $e'_2$  and all higher orbitals are empty. These frontier orbitals are considered to be neither strongly bonding nor strongly antibonding. This characteristic

permits metallocenes that diverge from the so-called 18-electron rule. Examples include the 17-electron complex  $[\text{FeCp}_2]^{+1}$  and the 20-electron  $\text{NiCp}_2$  complex. Redox potential can also be understood in terms of the MO treatment. Oxidation of 18-electron metallocene compounds corresponds to the removal of an electron from the nonbonding  $a_1'$  orbital. Thus the 19-electron complex  $\text{CoCp}_2$  is more easily oxidized than ferrocene because the lost electron is from the antibonding  $e_1'$  orbital gives the 18-electron  $[\text{CoCp}_2]^{+1}$ . Along with ferrocene-like sandwich complexes, the so-called bent-sandwich compounds are known. The initial structure shows the general form for these bent-sandwich structures. The most studied of these are the Group IVB metallocenes. As pictured in Figure 2 for  $M = \text{Zr}, \text{V}, \text{Cr},$  and  $\text{Mn}$ , these are distorted tetrahedral compounds with one vacant orbital that is employed in complexation of electron-rich vinyl sites, forming the basis for a variety of soluble stereoregulating polymerization systems. Additional examples of distorted tetrahedral metallocenes are also given in Figure 2.

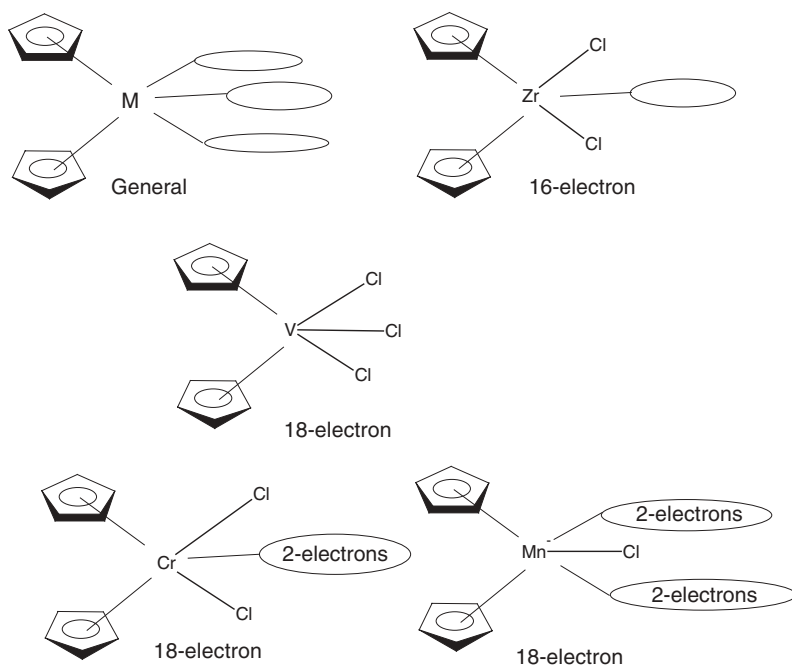
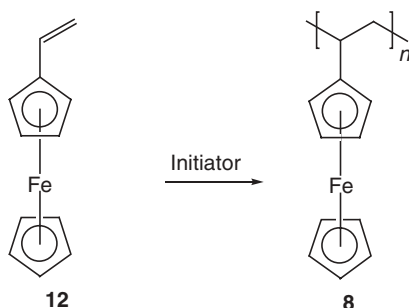


**Figure 2** Examples of distorted tetrahedral metallocenes.

### A. Polymerization of Olefin-Functionalized Metallocenes

Shortly after the first synthesis of ferrocene by Kealy and Pauson,<sup>26</sup> Arimoto and Haven<sup>27</sup> reported the homopolymerization and copolymerization of vinylferrocene.

The organometallic polymer shown in scheme 3 was synthesized using phosphoric acid, persulfate, or azobisisobutyronitrile (AIBN) as catalyst.<sup>27</sup> Copolymers prepared with methyl methacrylate, styrene, and chloroprene as well as the homopolymer were crosslinked with formaldehyde. These polymers underwent reversible chemical oxidation with ceric sulfate.



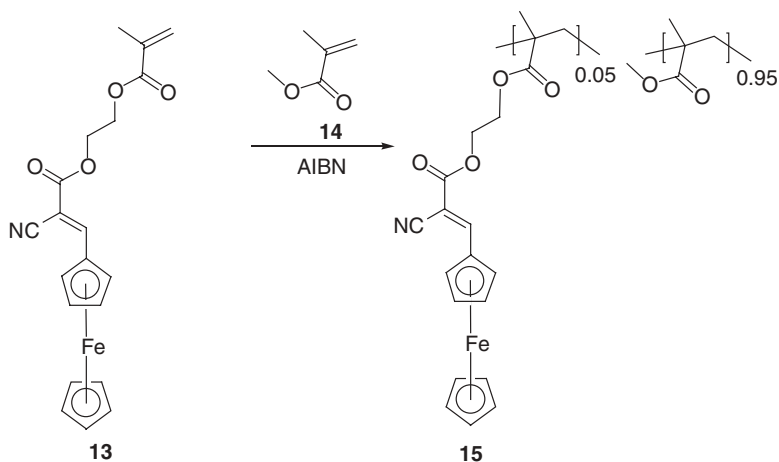
**Scheme 3**

Pittman and coworkers reported a number of ferrocene-functionalized polymers in the 1960s and 1970s that not only included the synthesis but also the properties of these polymers.<sup>29–34</sup> In particular, the bulk and solution polymerization of vinylferrocene along with the physical, chemical, and electrical properties of many polymers and copolymers were studied.<sup>29–37</sup> The copolymerization of vinylferrocene with styrene was reported by Frey and co-workers in 1999, using “living” radical initiator 2,2,6,6-tetramethyl-1-piperidinyl-1-oxy (TEMPO).<sup>38</sup> The polymers obtained by this method were block copolymers with narrow polydispersities.

Organoiron polymers have also been obtained through the homopolymerization and copolymerization of acrylate and methacrylate ferrocene monomers.<sup>39–43</sup> Such polymers have shown many interesting physical and chemical properties. For example, polymers containing ferrocene units in the side chains exhibit increased glass-transition temperatures.<sup>39</sup> A report by Wrighton’s group noted that electrodes that were modified with polymers containing ferrocene or cobaltocene groups photoelectrochemically reduce halocarbons.<sup>44</sup>

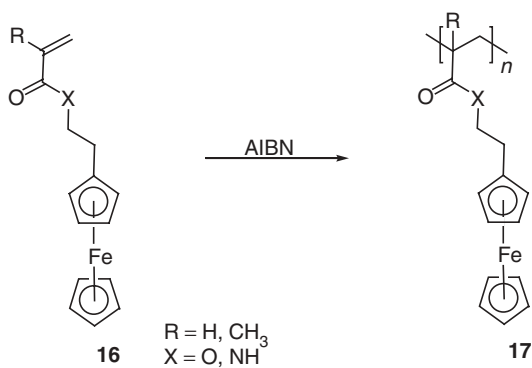
There have also been many studies of the polymerization kinetics of organoiron monomers; these have shown that such polymerizations often do not follow the same rate laws as organic monomers. Ferrocene-substituted polymethacrylates possessing nonlinear optical (NLO) properties were reported by Wright and coworkers.<sup>45–47</sup> The copolymerization of the ferrocenyl-functionalized monomer (5 mol%) **14** with methyl methacrylate **15** yielded the organometallic polymer **16**, as shown in scheme 4.<sup>47</sup> This polymer displayed second-harmonic-generation activity and possessed

a number average molecular weight of 43,000 and a glass-transition temperature of 100°C.<sup>47</sup> NLO properties have also been exhibited by polymers with cyanoester groups attached to the other cyclopentadienyl ring.<sup>47</sup>



Scheme 4

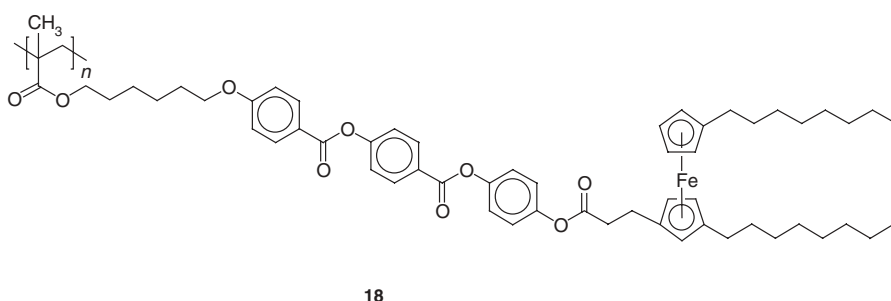
A method for the preparation of ferrocene-functionalized acrylate and methacrylate monomers as well as their homopolymerization and copolymerization reactions<sup>39–42</sup> was repeated in 2002.<sup>48</sup> Using AIBN as a radical initiator, polyferrocenylethyl acrylate, methacrylate, acrylamide, and methacrylamide were synthesized, as shown in scheme 5.



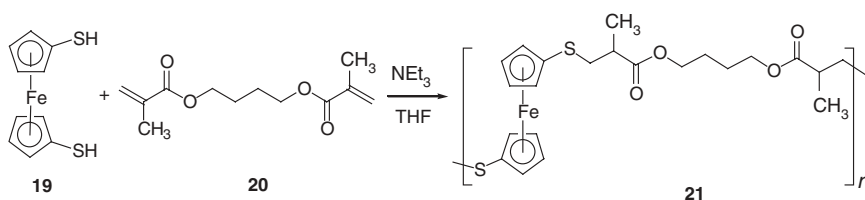
Scheme 5

The organometallic copolymer of ferrocenylethylacrylamide and isopropylacrylamide was prepared and was found to be soluble in water due to the minimal incorporation of the organometallic monomer. These polymers exhibited low critical solution temperatures (LCSTs) ranging from 26–29°C when compared to the LCST of 32°C for poly(*N*-isopropylacrylamide).<sup>49</sup>

Research into liquid-crystalline ferrocene sidechain polymers has been conducted by the research groups of Zentel<sup>50</sup> and Deschenaux.<sup>51</sup> One such liquid-crystalline polymer, polymethacrylate (**18**) and its monomer, showed enantiotropic smectic C and smectic A phases. This polymer also exhibited a weight average molecular weight of 100,000.<sup>51</sup>



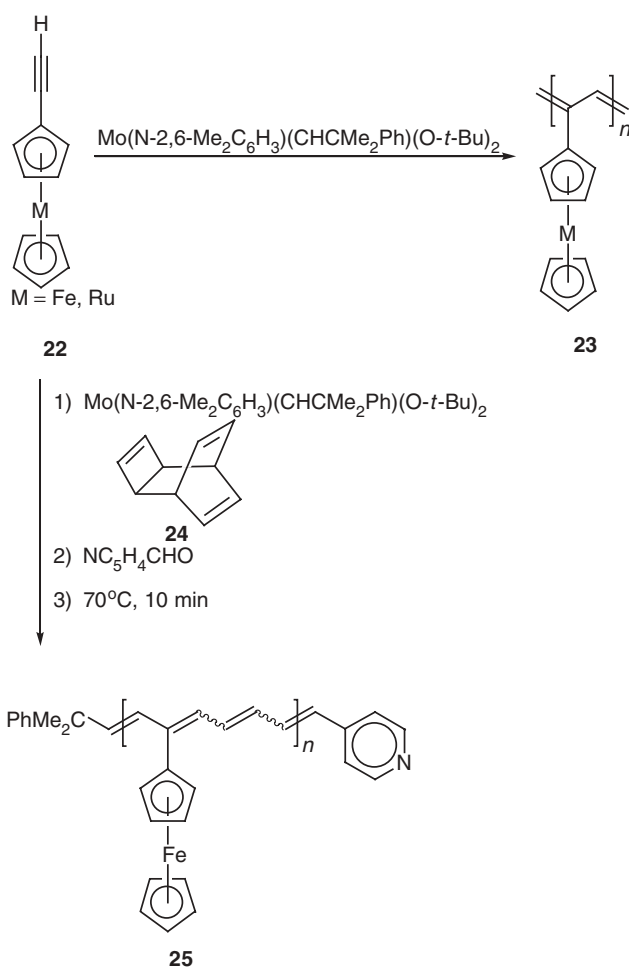
The reaction of olefinic monomers with organoiron complexes has allowed the synthesis of mainchain ferrocene-containing polymers.<sup>52</sup> This new class of organometallic polymers was formed through the reaction of various diolefins with 1,1'-dimercaptoferrocene **19** or 1,1'-bis(2-mercaptoethyl)ferrocene. The reaction of 1,1'-dimercaptoferrocene with 1,4-butandiol dimethacrylate (scheme 6) produced polymer **21** via base-catalyzed polyaddition.



## B. Alkyne Metathesis Polymerization of Substituted Metallocenes

Buchmeiser and coworkers reported the synthesis of metallocenes functionalized with alkyne groups.<sup>53–56</sup> Polyacetylenes with ferrocene or ruthenocene groups

in their sidechains were synthesized using a Schrock molybdenum catalyst on the organometallic monomers. The homopolymerization and copolymerization of ethynylferrocene and the homopolymerization of ethynylruthenocene, shown in scheme 7, produced soluble organometallic polyacetylenes with up to 50 double bonds in their backbones.<sup>53</sup> This synthetic method was determined to be a “living” polymerization and found to produce head-to-tail polymers in the trans configuration. A recent report described the grafting of a “living” polyacetylene, with pendent ferrocene, to a norbornene-functionalized silica support.<sup>56</sup> This polymer was then oxidized with iodine to yield a ferricinium-substituted polymer that can be used in anion-exchange chromatography for the separation of oligonucleotides.

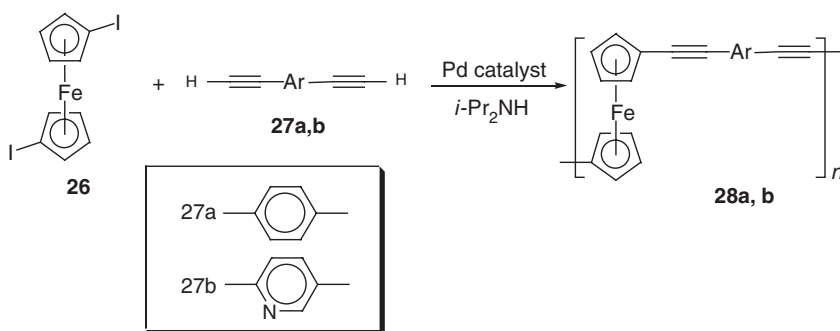


Scheme 7

### C. Polycondensation of Metallocenes

The polycondensation of acetylene-substituted metallocenes has yielded polymers containing backbone alkyne bridges. The synthesis of 1-iodo-2-methoxy-methyl-3-ethynylferrocene and 1-iodo-2-(*N,N*-dimethylamino methyl)-3-ethynylferrocene was reported by Plenio and coworkers.<sup>57,58</sup> Polymerization of these ferrocene-based complexes gave rise to soluble bimodal 1,3-linked ferrocene-acetylene polymers. Polymers exhibiting optical activity<sup>57</sup> or functionalized sidechains<sup>58</sup> were produced via Sonogashira coupling reactions.

Polymetallocenes with acetylene units in their backbones have been synthesized through reactions of diiodoferrocenes with diethynyl monomers, as shown in scheme 8.<sup>59,60</sup> These polymers, formed through palladium-catalyzed reactions, displayed semiconducting properties upon doping with iodine. The iodine adduct of polymer **28a** exhibited an electrical conductivity of  $1.3 \times 10^{-4}$  S/cm, while **28b** was resistant to oxidation.<sup>59</sup>

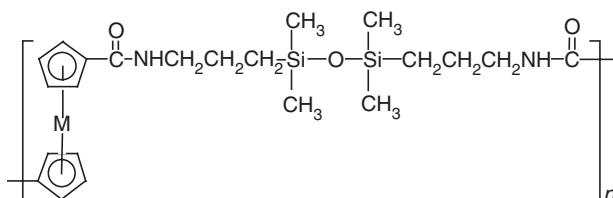


Scheme 8

One of the most important methods for obtaining organometallic polymers is polycondensation. In 1961 Knobloch and Rauscher<sup>62</sup> reported the synthesis of polyesters and polyamides with ferrocene groups in their backbones using interfacial polymerization.

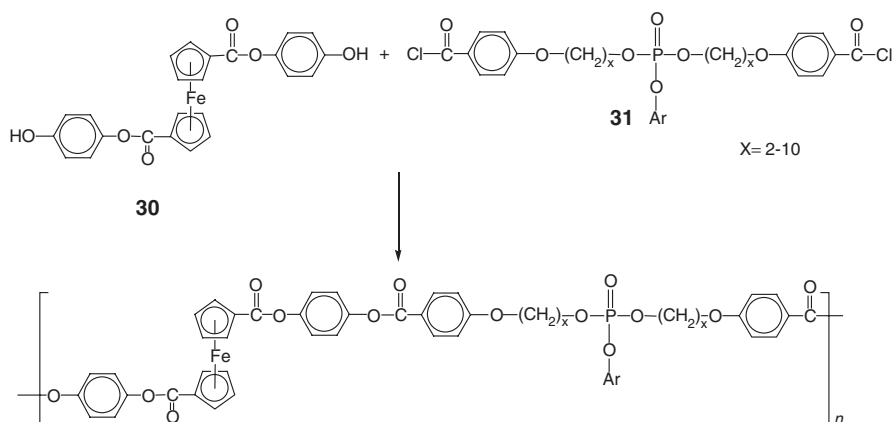
The polycondensation of ferrocene derivatives continues to give new classes of ferrocene-based polymers, beginning with the work of Pittman and coworkers, who also reported the polycondensation of disilanol with bis(dimethylamino-dimethylsilyl)ferrocene in the 1970s.<sup>63</sup> Since that time, ferrocene-based polymers containing silicon units in their backbones have received a great deal of study. The polymers Pittman and coworkers produced possessed high molecular weights and good thermal stability. The synthesis of polysiloxanes with ferrocene and cobalt-cerium groups in their backbones have been examined more recently by Cuadrado and coworkers.<sup>64,65</sup> Reaction of 1,3-bis(3-aminopropyl)-1,1,3,3-tetramethyldisiloxane

with 1,1'-bis(chlorocarbonyl)ferrocene or 1,1'-bis(chlorocarbonyl)cobalticinium hexafluorophosphate gave polymetalocene **29**. The reaction of 1,1'-bis( $\beta$ -aminoethyl)ferrocene with dimethylbis(4-chlorocarbonylphenyl)silane provides an alternative method of producing the ferrocene-based polymers.<sup>64</sup>



29

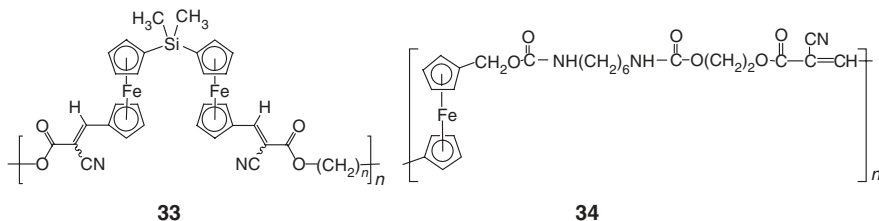
Research in metallocene-containing polyamides, polyureas, polyurethanes, and polyesters continued to be conducted in the 1980s,<sup>66-70</sup> and since that time, research into these classes of materials has continued to grow.<sup>71-75</sup> Homoannular and heteroannular liquid-crystalline polymetalloenes have been prepared by Zentel and coworkers through condensation reactions.<sup>73,74</sup> Ferrocene-based liquid-crystalline polymers have also been reported by Senthil and Kannan.<sup>75</sup> The synthesis of ferrocene polymers containing backbone organophosphorus moieties **32** is shown in scheme 9.



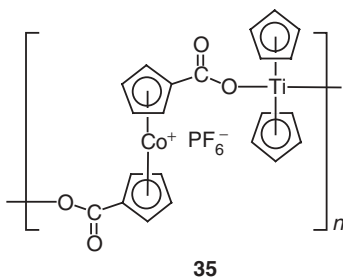
Scheme 9

Wright and coworkers examined the NLO properties of some mainchain ferrocene-based polymers.<sup>46,47,76,77</sup> The polymers **33** and **34** were formed by

polymerizing monomers containing NLO-phores. Polymer **34** was found to align by corona poling at 150°C and exhibited a stable second harmonic generation signal.<sup>47</sup>



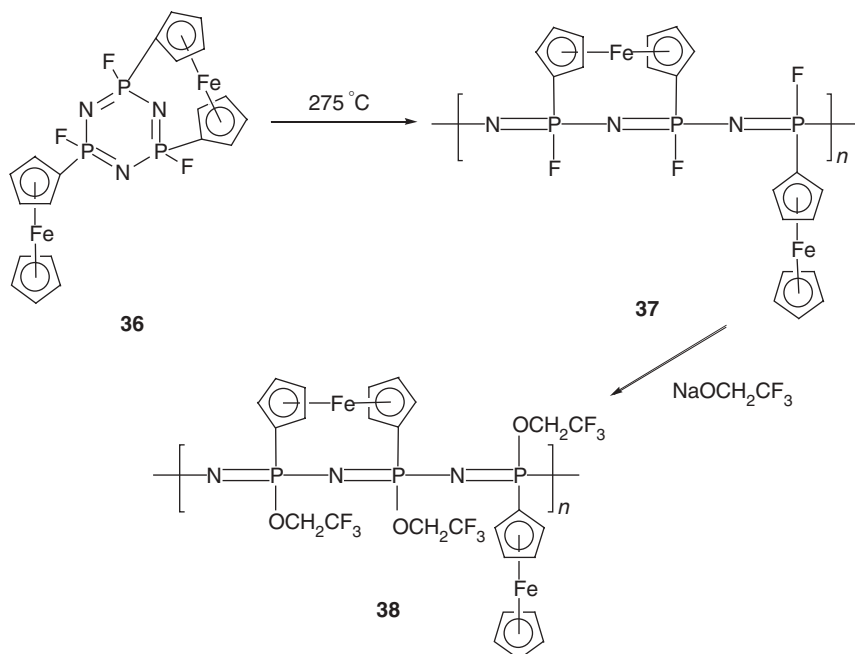
Although ferrocene-based materials have dominated the field of metallocene polymers, they are not the only metal-containing polymers studied. The polymerization of cobalticinium complexes and its copolymers with other metal complexes have also been studied, beginning in the 1970s.<sup>81–85</sup> Low molecular weight polymers formed by the reaction of 1,1'-bis(chlorocarbonyl)cobalticinium with diols have been reported by Pittman and coworkers.<sup>85</sup> High molecular weight polyesters were reported by Carraher and Sheats by reaction of 1,1'-dicarboxycobalticinium hexafluorophosphate with dicyclopentadienyltitanium hexafluorophosphate, giving **35**.<sup>83</sup> Reacting dicyclopentadienylmetal dichloride complexes with disodium dicarboxylates in either aqueous or organic solvents to yield titanium, zirconium, and hafnium polyesters have also been described.<sup>84</sup>



## D. Ring-Opening Polymerization

The ease at which ring-opening polymerization (ROP) reactions produce high molecular weight polymers makes the design of cyclic organometallic (metallocenophanes) and the functionalization of cyclic organic and inorganic monomers with metallocenes important topics in organometallic polymer chemistry. The polymerization of metallocene-functionalized trimeric cyclic phosphazenes through ROP was reported by Allcock and coworkers.<sup>86–88</sup> Backbone ferrocene and ruthenocene

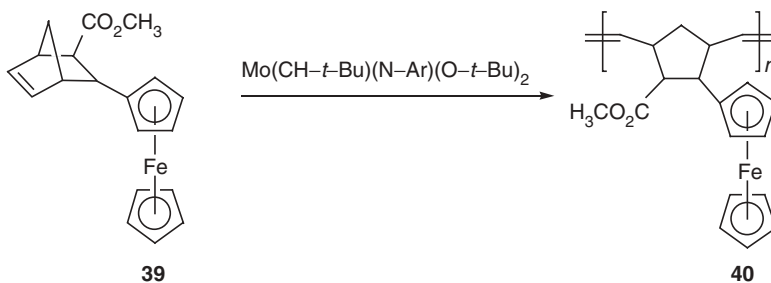
polymers and a copolymer containing both of these organometallic groups were also synthesized.<sup>86</sup> The incorporation of the metallocenes occurred through the phosphorous atoms located to either side of the cyclopentadienyl rings, as shown in scheme 10.<sup>87</sup>



Scheme 10

Ferrocenyl-functionalized polynorbornenes were synthesized by Schrock and Wrighton via ring-opening metathesis polymerization (ROMP).<sup>89,90</sup> Redox-active polynorbornenes functionalized with ferrocene were prepared with norbornene monomers functionalized with ferrocene groups or catalysts containing ferrocenyl moieties in their structures. The ROMP of organometallic monomer **39** to produce the ferrocene-substituted polymer **40** is shown in Scheme 11.<sup>89</sup>

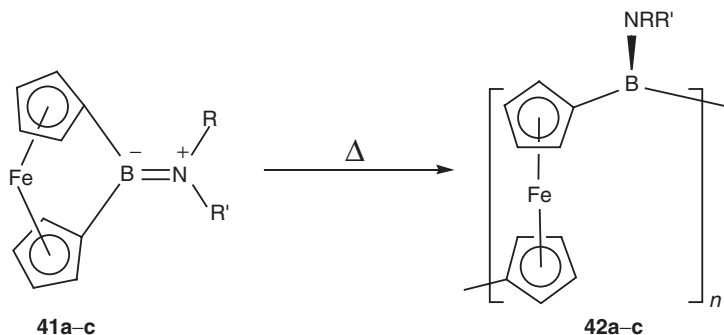
High molecular weight organometallic polymers have also been produced through the ROP of ferrocenophanes.<sup>91–93</sup> Lee and coworkers reported the incorporation of tert-butyl groups onto the backbones of the polymers.<sup>93</sup> This led to the isolation of soluble high molecular weight polymers.<sup>93</sup> The synthesis of homopolymerized and copolymerized ansa-(vinylene)ferrocene was reported by Buretea and Tilley.<sup>92</sup> The homopolymer was found to be insoluble and displayed a conductivity of  $10^{-3} \Omega^{-1}\text{cm}^{-1}$ , while the copolymer prepared with norbornene had weight = average molecular weight ( $M_w$ ) and number = average molecular weight ( $M_n$ ) values of 21,000 and 11,000, respectively.<sup>92</sup>



Scheme 11

Manners and coworkers reported the synthesis and ring opening of unsymmetrical [2]ferrocenophanes.<sup>94,95</sup> Cationic initiators could be used for the polymerization of the [2]carbathioferrocenophane.<sup>94,95</sup> Furthermore, thermal and anionic ROP have been useful for the polymerization of [1]thiaferrocenophane and [1]selenaferrocenophanes.<sup>94</sup> Poly(ferrocenyl sulfides) have been found to possess strong metal-metal interactions, as indicated by the presence of two reversible oxidation processes observed in their cyclic voltammograms.

Scheme 12 shows the thermally initiated ROP of boron bridge containing [1]ferrocenophanes.<sup>95,96</sup> Due to the high strain of these molecules from the large ring tilts, the ROP reaction was able to proceed at temperatures of 180–200°C. All the poly(ferrocenylboranes) formed were found to be insoluble except for polymer **42c**.



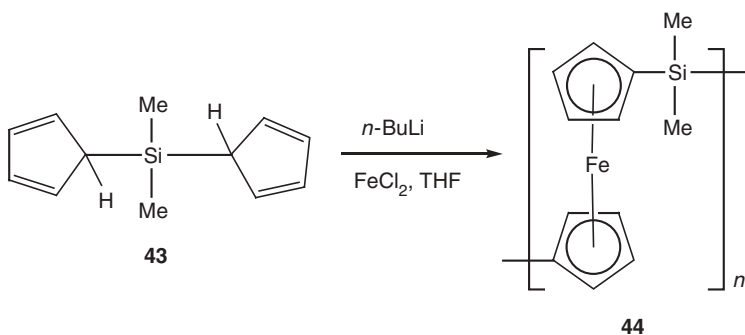
- a: R = R' = SiMe<sub>3</sub>
- b: R = <sup>t</sup>Bu, R' = SiMe<sub>3</sub>
- c: R = R' = <sup>i</sup>Pr

Scheme 12

The research groups of Manners and Pannell reported the ROP of ferrocenophanes with tin bridges.<sup>96–98</sup> High molecular weight polymers could be isolated through thermal ROP, and the ferrocenophanes could be opened in solution at room temperature.<sup>95–98</sup>

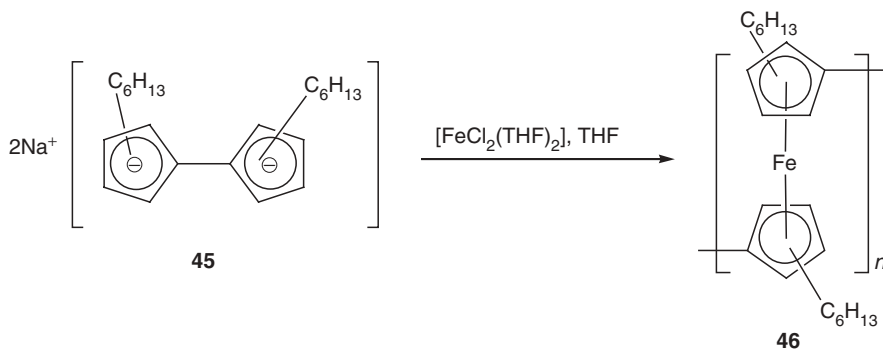
### E. Coordination of Metals to Cyclopentadienyl Rings

Scheme 13 shows the preparation of a poly(ferrocenylsilane) via the reaction of the dilithium salt of dicyclopentadienyldimethylsilane with ferrous chloride.<sup>99</sup> This reaction yielded both low molecular weight polymers, and a cyclic [1.1]ferrocenophane.



Scheme 13

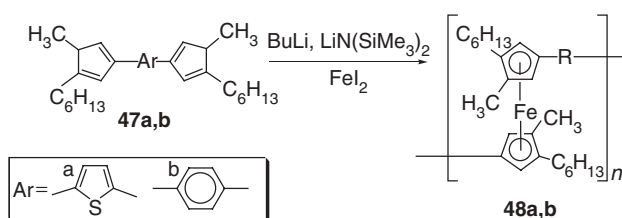
The reaction of dihexylfulvalene dianion with [FeCl<sub>2</sub>(THF)<sub>2</sub>] has reportedly produced oligomeric and polymeric polyferrocenylenes substituted with hexyl groups, as shown in scheme 14.<sup>100</sup> High molecular weight polymers could not be



Scheme 14

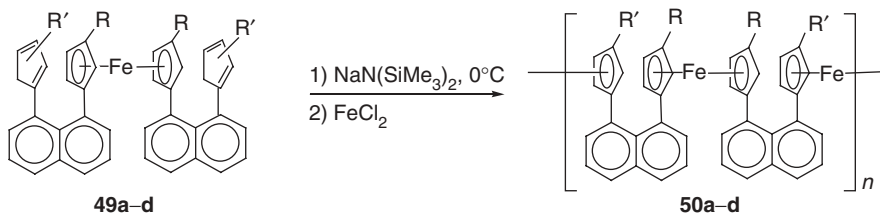
obtained in this reaction due to the steric bulk of the hexyl groups; however, the presence of the alkyl groups greatly improved the solubility of the polymers. It was also found through electrochemical studies that there were interactions between the iron centers.

Using an isomeric mixture of bis(alkylcyclopentadienyl)arenes with ferrous iodide, Southard and Curtis reported the synthesis of conjugated polymers, as shown in scheme 15.<sup>101-103</sup> Polymers **48a,b** were high molecular weight with high polydispersity. Oxidized polymers displayed electrical conductivities ranging from  $10^{-10}$  to  $10^{-7}$  S/cm.



Scheme 15

Rosenblum and coworkers reported the synthesis of face-to-face poly-metalloenes via the methodology described in scheme 16.<sup>104-106</sup> Paramagnetic mixed-metal polymers containing nickel and iron or cobalt and iron were also synthesized. The magnetic moments of these polymers were 5.3 and 5.2  $\mu_B$ , respectively.

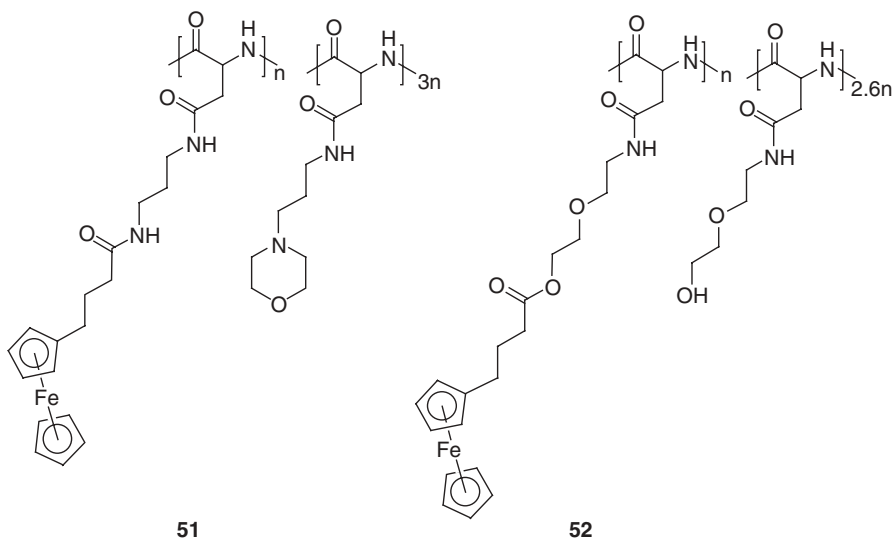


- R = 2-octyl, R' = 2-octyl,
- R = 2-octyl, R' = H
- R = 3,7-dimethyloctyl, R' = H
- R = decyl, R' = H

Scheme 16

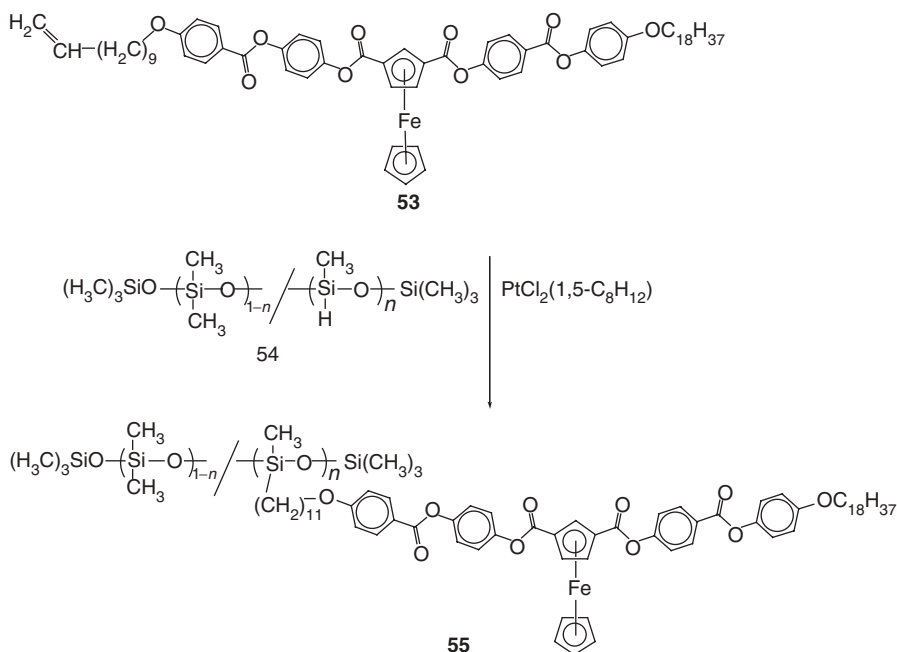
## F. Introduction of Metallocenes into Preformed Polymers

Neuse and coworkers have been investigating the biological antiproliferative activity of polymers containing ferrocene groups in their sidechains.<sup>107–110</sup> Reacting organic polymers with 4-ferrocenylbutanoic acid resulted in the formation of the corresponding organometallic polyaspartamides **51** and **52**. Polymer **51** was water soluble and possessed some anticancer properties. It was found to be more active than the platinum-based conjugates for the cancer cells that were tested.<sup>107</sup> The ferrocene-based polymers exhibited a lower activity (10–20 times) than the activity of cisplatin. However, the toxicity of the polymer bound complexes were approximately 10 times lower than the toxicity for the unbound molecules. One can't help wondering if the administration of both ferrocene-based polymer **51** and cisplatin would produce synergistic anticancer activity. Such organometallic “drug cocktails” have never been reported.



The synthesis of poly(methylsiloxanes) containing sidechain ferrocene or cobalticene groups has been studied by Cuadrado and coworkers.<sup>64,65</sup> An amperometric glucose electrode was recently created with a sidechain ferrocene containing poly(methylsiloxane).<sup>64</sup>

Liquid-crystalline polysiloxanes containing 1,3- or 1,1'-disubstituted ferrocene moieties in their sidechains were also synthesized through a reaction of vinyl organometallic monomers with preformed polysiloxanes.<sup>111</sup> The synthesis of one such liquid-crystalline metal-containing polysiloxane **55** is shown in scheme 17.



Scheme 17

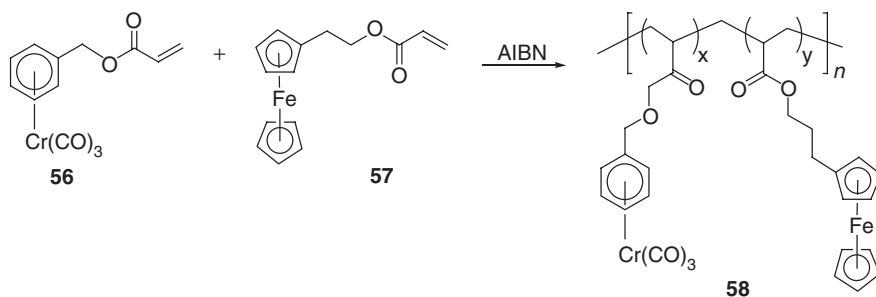
## V. ARENE-TRANSITION METAL POLYMERS

### A. Polymerization of Olefin-Containing Arenes

Arene compounds were initially prepared in 1919 by Hein who treated  $\text{CrCl}_3$  with  $\text{PhMgBr}$ . The reaction mixture included a variety of  $\pi$ -complexed  $\text{C}_6\text{H}_6\text{Cr}$  products. However, these were not recognized as  $\pi$ -complexes until 1954.<sup>112</sup> Bis(benzene) complexes generally have eclipsed rings with a  $D_{6h}$  symmetry. Arene ligands behave as six-electron donors with each occupying three coordination positions. Most of the products obey the 18-electron rule, though there are exceptions. As a general rule, bis(arylene) compounds are somewhat less reactive than mono(arylene) compounds. As will be seen repeatedly, the division between polymers designated as transition versus coordination polymers is not always clear.

The first examples of organometallic polymers where an arene was coordinated to the transition metal appeared in the early 1970s. These were reported by Pittman and coworkers.<sup>113-115</sup> The homopolymerizations and copolymerizations of many acrylate-, methacrylate-, and styrene-substituted arene monomers coordinated to chromium tricarbonyl. The copolymerization of the acrylate monomer **56** with 2-ferrocenylethyl acrylate **57** is shown in scheme 18. With the exception

of monomer **57**, which could be homopolymerized or copolymerized with AIBN, most other organometallic monomers require the incorporation of an organic comonomer to produce high polymers.<sup>113–116</sup> The determination of the reactivity ratios of the homopolymerized and copolymerized  $\pi$ -(benzylacrylate)chromium tricarbonyl **56** helped generate a greater understanding of this class of organometallic polymer.<sup>113</sup> Insoluble materials with disperse chromium oxide particles resulted from the thermal decomposition of the  $\eta^6$ -(aryl)tricarbonylchromium functions in the obtained polymers. Thermal and photodecompositions of crosslinked polymers containing  $\eta^6$ -phenyltricarbonylchromium moieties generated nano-sized metal oxide disperisons, which could not be well characterized at the time. This represented a novel “top–down” approach to nanocomposite formation. This approach presents a method of achieving, on a molecular level, single metal atom dispersion throughout a matrix.



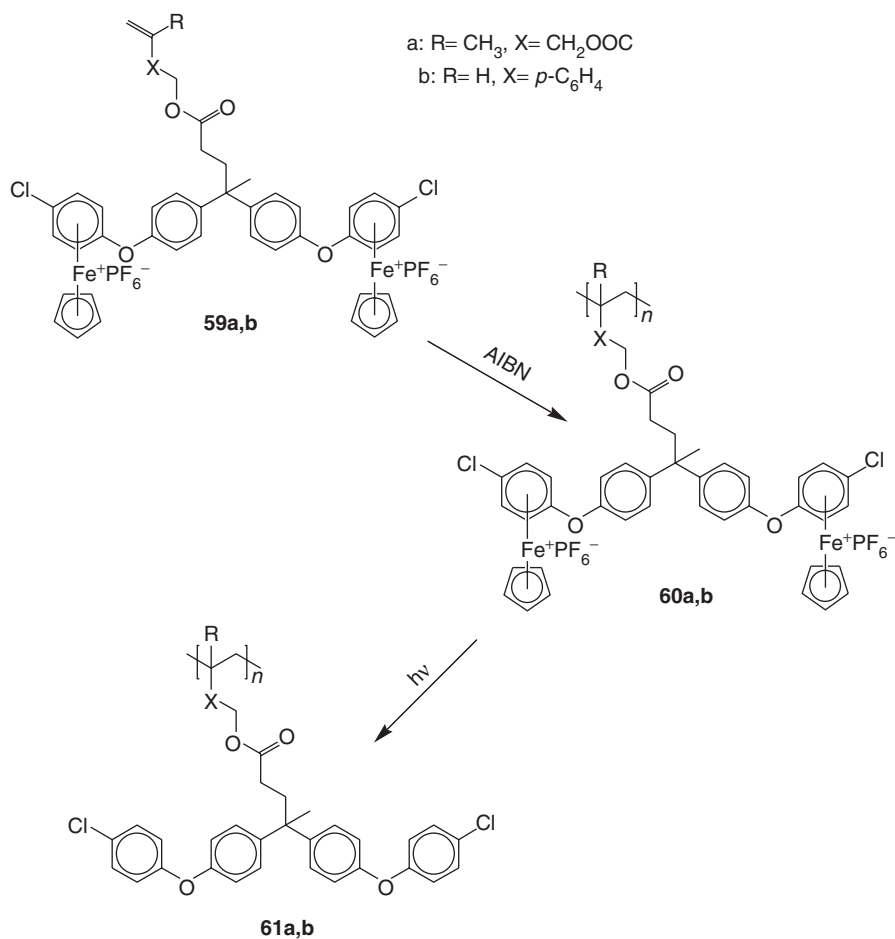
Scheme 18

In instances where the metal atom is connected to CO, the polymers are both organometallic polymers, because of the metallocene connection, and coordination polymers, because of the metal–CO connection.

The synthesis of polymethacrylates and polystyrenes with cationic cyclopentadienyliron moieties coordinated to their sidechains was recently reported.<sup>117,118</sup> The synthesis of cyclopentadienyliron-coordinated polymethacrylates by radical polymerization initiated with AIBN is shown in scheme 19.<sup>117</sup> Organic polymethacrylates **61a,b** were isolated through photolysis of the organometallic polymers **60**. The  $M_w$  of the organometallic polymer **60** was 22,500, with a polydispersity of 1.4. Electrochemical studies indicated that the metallated polymethacrylates exhibited reversible reduction of the iron centers occurring between  $E_{1/2} = -1.1$  and  $-1.2$  V.

## B. Ring-Opening Metathesis Polymerization of Substituted Norbornenes

Cationic cyclopentadienyliron-coordinated aryl ethers have been functionalized with norbornenes **62–66** through the condensation reaction of

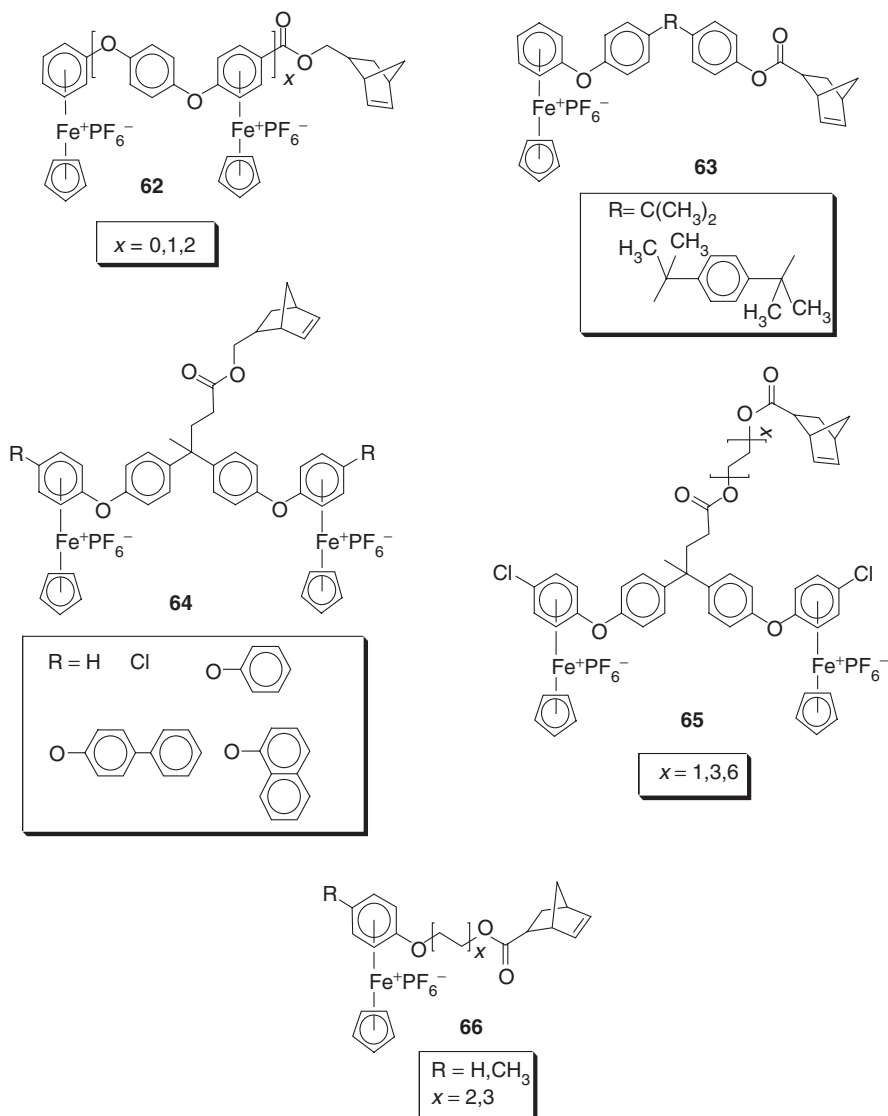


Scheme 19

5-norbornene-2-carboxylic acid or 5-norbornene-2-methanol, with many different arene complexes containing hydroxyl or carboxylic acid functions.<sup>119-122</sup>

### C. Nucleophilic Aromatic Substitution Polymerization of Chloroarene Complexes

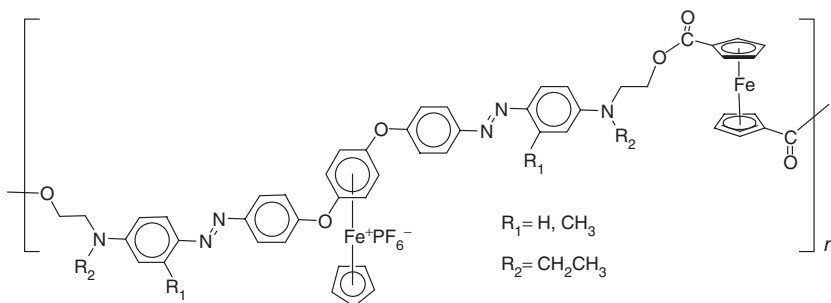
The synthesis of poly(phenylene oxides) and poly(phenylene sulfides) coordinated to pentamethylcyclopentadienylruthenium cations was described by Segal and Dembek.<sup>123,124</sup> Dembek and coworkers found that these polymers behaved like polyelectrolytes in polar organic solvents.<sup>123</sup> The trichlorobenzene and tetrachlorobenzene complexes were useful in the preparation in highly branched organometallic complexes.<sup>124</sup>



The synthesis and characterization of cyclopentadienyliron-coordinated polymers containing aromatic ether and thioether bridges have been reported.<sup>125,126</sup> These polymers were synthesized via the reaction of 1,4-dichlorobenzene-cyclopentadienyliron complex with different oxygen- and sulfur-containing dinucleophiles. This class of organoiron polymers exhibited excellent solubility in polar organic solvents, and upon photolysis, the organic analogues were isolated. The solubility of the organic analogues was affected by the bridging aromatic groups.<sup>125,126</sup> After cleavage of the cyclopentadienyliron moieties, the organic polymers containing the alkyl bridges were soluble in organic solvents, whereas the polymers containing aromatic and

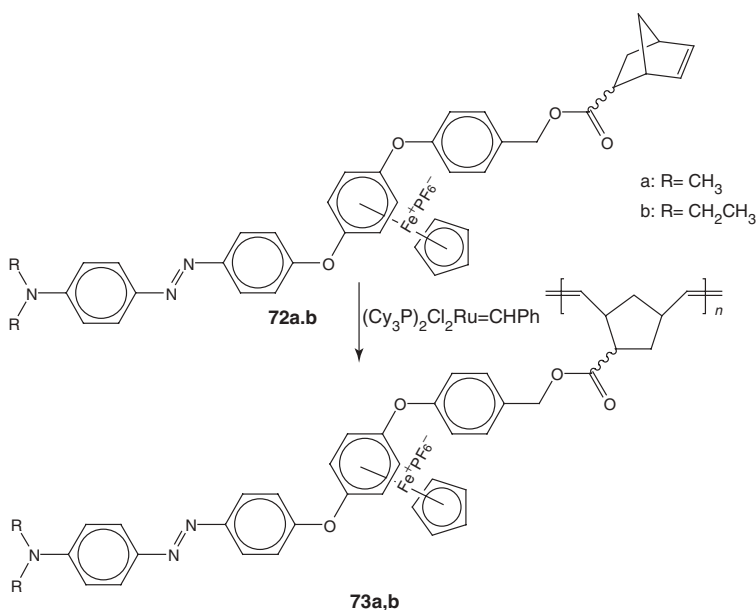


colored polymers displayed excellent solubility in organic solvent and exhibited a  $\lambda_{\text{max}} = 419 \text{ nm}$ , which was similar to that of the free azo dye. Cyclic voltammetry showed that these polymers undergo two different electrochemical processes corresponding to the two types of iron centres. The oxidation of the neutral ferrocene occurred at 0.89 V and the reversible reduction of the cationic iron center occurred at  $-1.42 \text{ V}$ .



71

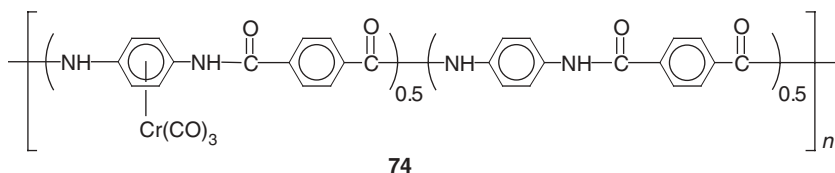
Organoiron polynorbornenes containing azo dyes have been synthesized through ROP of azo dye functionalized organoiron monomers (scheme 21). Polymers **73a** and **73b** displayed molecular weights of approximately 31,600, and cyclic voltammetry showed reversible reductions of the iron centers between  $-1.2$  to  $-1.4 \text{ V}$ .<sup>130</sup>



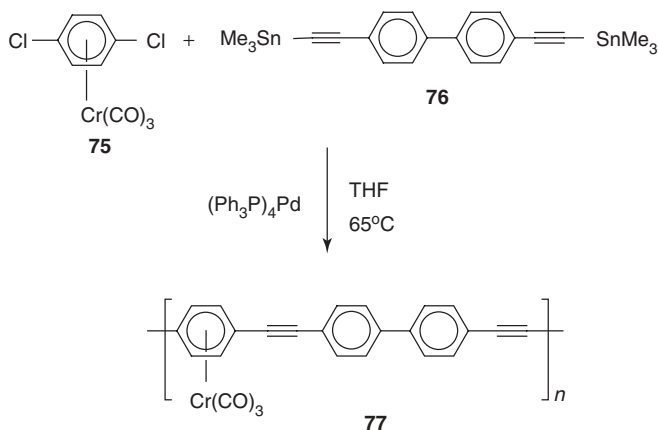
Scheme 21

## D. Polycondensation of Arene Complexes

Two research groups have reported the synthesis of polyamides, such as poly(*p*-phenylene terephthalamide) (PPTA), coordinated to chromium tricarbonyl ( $\text{Cr}(\text{CO})_3$ ).<sup>131–133</sup> These compounds are interesting due to the ability of PPTA to form a lyotropic liquid crystal in strong acids. Regular PPTA displays low solubility in organic solvents, but the coordination of the chromium tricarbonyl groups to the arene group increased the solubility of these polymers. To compare the solubilities of the metallated and organic polyamides, an organic polyamide was prepared using similar conditions. The organometallic polyamide remained in solution during polymerization, while the organic polyamide formed gels or precipitates. The organometallic polymers also showed higher viscosities in concentrated sulfuric acid than the nonmetallic products. When using concentrations of high molecular weight organometallic polyamides greater than 4–6% in DMAc, nematic liquid-crystalline formations appeared.<sup>132,133</sup> This lyotropic behavior suggests that its rigid-rod nature was retained, although the solubility of the polymer increased dramatically upon metal coordination. The copolymer **74** also displayed enhanced solubility and liquid-crystalline properties.<sup>132</sup>

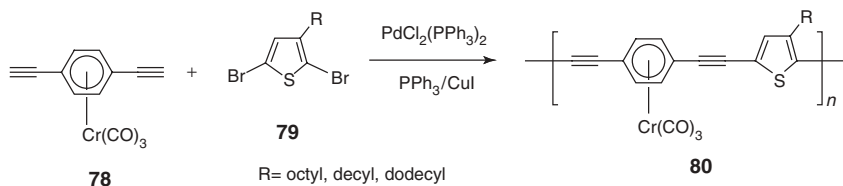


Conjugated polymers coordinated to chromium tricarbonyl were reported in 1989.<sup>134</sup> These polymers were formed through a palladium-catalyzed cross-coupling reaction of  $\eta^6$ -dichloroarene chromium tricarbonyl complexes with organostannane reagents, as shown in scheme 22.



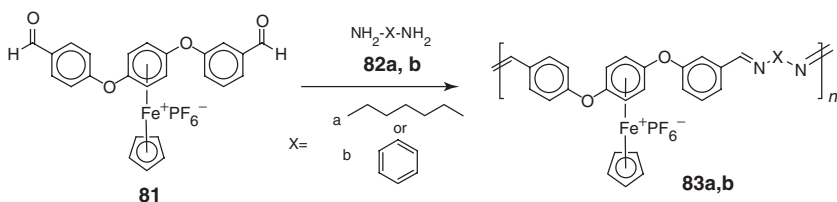
Scheme 22

The palladium-catalyzed polycondensation of 1,4-diethynylbenzene complex with 3-alkyl-2,5-dibromothiophenes (scheme 23) was recently reported.<sup>135</sup> These polymers displayed number-average molecular weights ranging from 13,000 to 24,400, with PDI ranging from 3.2 to 3.6. These organometallic polymers **80** exhibited a red shift of approximately 50 nm, indicating the  $\pi$ -delocalization in the backbone. The undoped polymer displayed semiconductor properties with a conductivity of  $8.1 \times 10^{-6}$  S/cm.



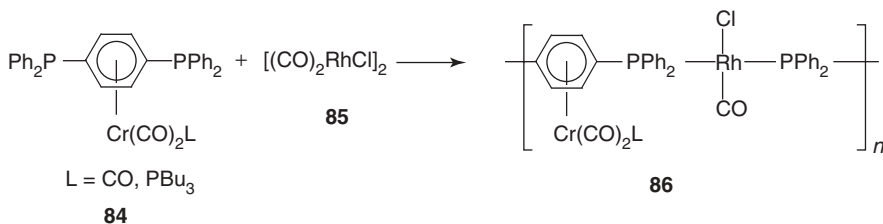
Scheme 23

Coordination of cyclopentadienyliron moieties to polyether/imines was achieved via reactions of a cyclopentadienyliron dialdehyde complex with various aliphatic and aromatic diamines (scheme 24).<sup>136</sup>



Scheme 24

Coordination of a phosphine complex **84** to Rh has resulted in the synthesis of polymers containing rhodium in their backbones as well as chromium tricarbonyl groups as pendent groups (scheme 25).<sup>137</sup> These polymers were very air and thermally sensitive; therefore, the molecular weights were not determined.

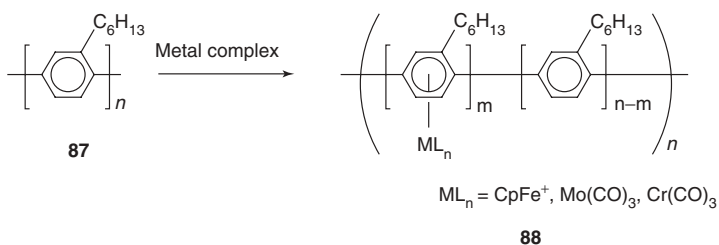


Scheme 25

## E. Coordination of Organometallic Moieties to Arenes

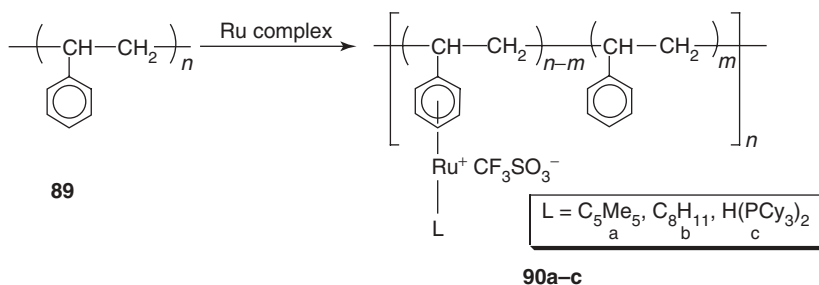
Complexation of metals to preformed polymers is a useful methodology for the synthesis of polymers incorporating metals into their backbones or sidechains.<sup>138,139</sup> In 1984 the complexation of a molybdenum tricarbonyl complex to approximately 25% of the arenes in polyparaphenylene (PPP), was reported.<sup>138,139</sup> This polymer displayed shifts in its IR spectrum similar to that of potassium-doped PPP.

Soluble conjugated polymers, synthesized by coordinating metals to poly(*n*-hexylphenylene) (PHP), were reported by Nishihara and coworkers.<sup>140-142</sup> The synthesis of mixed metal organometallic polymers **88** is shown in scheme 26. A Mo(CO)<sub>3</sub> group was coordinated to every 1 in 4.8 rings and a CpFe<sup>+</sup> coordinated to every 1 in 1.6 rings in **88**. Electrochemical studies indicated that the band gap in the organic polymer was not affected by coordination of the Mo(CO)<sub>3</sub> moiety. Spectroelectrochemical measurements indicated that the π-coordination of metallic moieties to the arene rings altered the electronic structures of these polymers.



Scheme 26

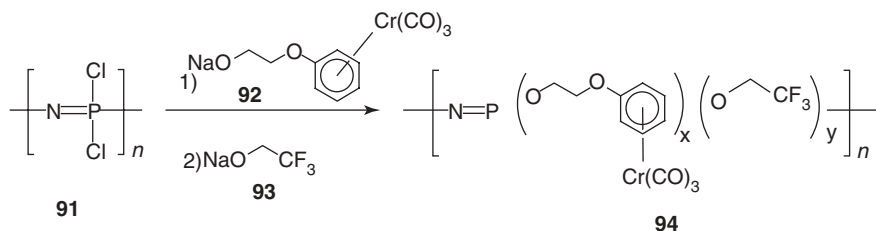
Chaudret reported the coordination of organoruthenium groups to the aromatic rings of polystyrene for use as potential transition metal catalysts incorporated to polymer supports.<sup>143</sup> Scheme 27 shows the suggested structures of polymers



Scheme 27

**90a–c.** These polymers contained ruthenium moieties ( $\text{Ru}^+\text{Cp}^*$ ,  $\text{Ru}^+\text{C}_8\text{H}_{11}$ , or  $\text{Ru}^+\text{H}(\text{PCy}_3)_2$ ) as sidechains. These polymers were the first reported polymer-supported hydrido transition metal complexes. The success of the complexation of the arene rings ranged from 25% to 100%, depending on the size of the ligand bound to the ruthenium.

Polyphosphazenes containing arene chromium tricarbonyl moieties in their sidechains (scheme 28) were reported in 1991.<sup>144</sup> Two methods of incorporation of chromium carbonyl into premade polyphosphazenes were discussed. The most successful method used the displacement of the chloro groups of the polyphosphazene with the aryloxy or arylalkoxy ligands of the  $\text{Cr}(\text{CO})_3$ . For complete displacement of the Cl groups, alkyl spacers were used on the organometallic nucleophiles to lower the steric bulk around the polymer backbone. The second method used the reaction of an aryl-functionalized polyphosphazene with  $\text{Cr}(\text{CO})_6$ . DSC studies showed that these polymers exhibited  $T_g$  values 50°C higher than those of their organic analogues.

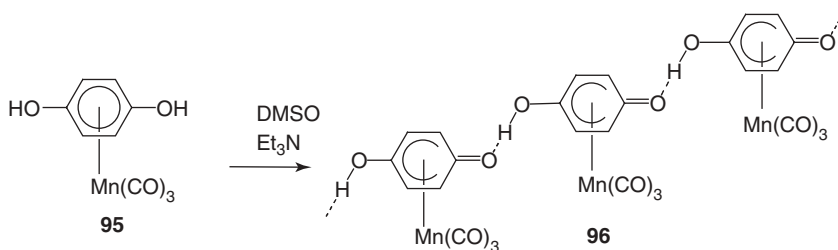


Scheme 28

## F. Supramolecular Assembly of Polymers

Numerous examples of metal-containing supramolecular assemblies were cited in Volume 1 and later volumes of this series. The areas of biomedical (generally drug delivery) studies and both single-batch and multibatch catalysis are actively studied. An example of the supramolecular assembly of polymers is the use of chromium tricarbonyl complexes as building blocks for supramolecular assemblies.<sup>145,146</sup> This was accomplished by hydrogen bonding the carboxylate-functionalized arenes that were coordinated to chromium tricarbonyl groups through 1–3 arene carboxyl substituents. Extended supramolecular structures were formed when using difunctionalized and trifunctionalized complexes, whereas dimers were formed from the complex functionalized with a single carboxylic acid group. In addition to hydrogen bonding through the carboxylic acid groups, the carbonyl carbons also behaved as hydrogen bond acceptors for the C–H donors in the 2- and 5- positions.

Articles by Sweigart and coworkers have shown that manganese tricarbonyl complexes of  $\eta^6$ -hydroquinone deprotonate to give  $\eta^5$ -semiquinone and  $\eta^4$ -quinone complexes.<sup>147,148</sup> Solution NMR analysis and crystal structures of the  $\eta^5$ -semiquinone complex indicated that this complex was polymeric due to strong intermolecular hydrogen bonding, as shown in scheme 29.<sup>147</sup> Reaction of the  $\eta^5$ -semiquinone and the  $\eta^4$ -quinone complexes allowed the production of one-, two- and three-dimensional polymers. These complexes have also been shown to self-assemble by complexation of the oxygen atoms with transition metal ions.

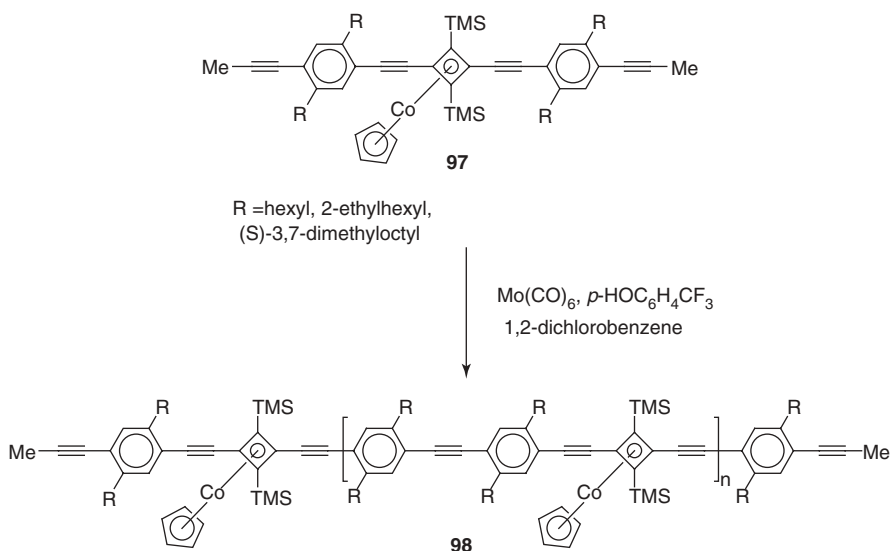


Scheme 29

## VI. POLYMERS WITH METAL-COORDINATED CYCLOBUTADIENES

Butadienes and substituted butadienes are four-electron donor ligands. They are conjugated with alternating double and single bonds. Most metal complexes are formed through interaction between the two  $\pi$ -bonds and the metal atom. Here, we will focus on polymers derived from cyclobutadiene. Unlike the straight-chain butadiene, cyclobutadienes are not stable in the free state because the four pi-electrons make them “anti-aromatic.” Calculations in the mid-1950s predicted that cyclobutadiene would be stabilized by coordination to a metal. Organometallic monomeric derivatives have been formed since the late 1950s.

Bunz and coworkers reported the synthesis of polymers containing cyclopentadienylcobalt moieties coordinated to cyclobutadiene rings.<sup>149–152</sup> These polymers were synthesized using diethynyl and dipropynyl complexes of cyclobutadiene.<sup>149–152</sup> The conjugated polymers **98** were synthesized by acyclic alkyne metathesis polymerization of monomer **97** (scheme 30).<sup>153</sup> Bunz and coworkers also studied some organocobalt polymers that exhibited liquid crystalline behavior. The cyclopentadienylcobalt groups were also found to quench fluorescence.<sup>152–154</sup> Liquid-crystalline polymers synthesized with monomers containing cyclopentadienylcobalt groups coordinated to cyclobutadiene rings have been reported by Tomita and coworkers.<sup>153,154</sup>



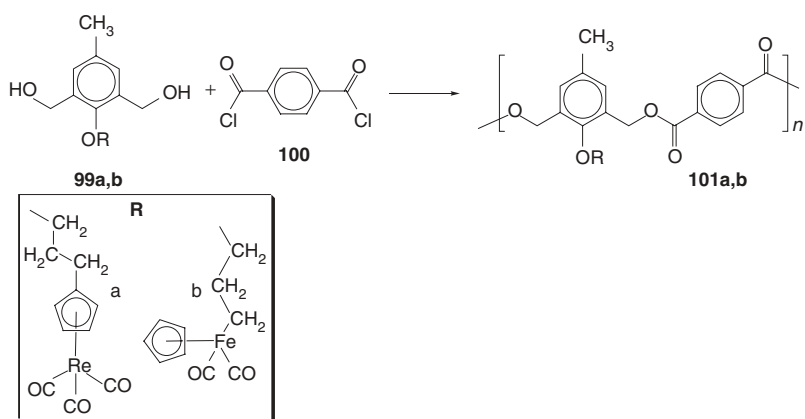
Scheme 30

## VII. POLYMERS CONTAINING METAL CARBONYL COMPLEXES

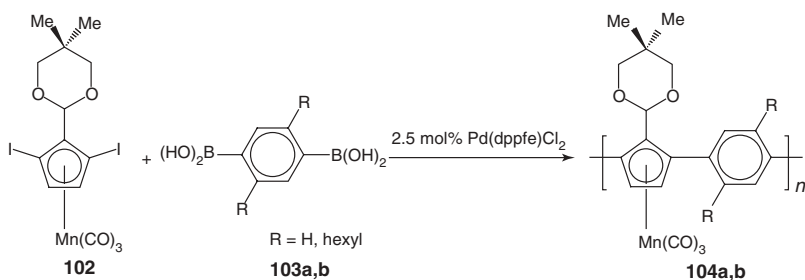
Research on polymers containing cyclopentadienylmetal moieties has been continuing since the 1970s.<sup>155–158</sup> Ferrocene-containing monomers and polymers have by far received the greatest amount of study, but there have been many other types of cyclopentadienylmetal complexes studied. Pittman and coworkers have studied the free-radical homopolymerization and copolymerization of vinylcyclopentadienylmanganese tricarbonyl.<sup>155</sup> Biological activity studies on these polymers indicated antifungal properties. The early progress on  $\eta^6$ -vinylcyclopentadienyl monomers of Mn, Cr, Ir, Ti, Co, Mo, W, and Rh by Pittman and Rausch was reviewed in Volume 1 of this series.

Bifunctional hydroxyl monomers functionalized with rhenium or iron complexes were reacted with terephthaloyl chloride to produce polymers containing metal-carbon  $\sigma$ - or  $\pi$ -bonds (scheme 31).<sup>159, 160</sup>

Polymers containing silole units will react with iron pentacarbonyl in the presence of UV light to give polymers containing iron tricarbonyl coordinated to some of the silole units.<sup>161</sup> Manganese tricarbonyl coordinated polymers have been synthesized through coupling reactions of substituted cyclopentadienylmanganese tricarbonyl complexes.<sup>162,163</sup> Scheme 32 shows the reactions of the diiodide monomer **102** with the diboronic acid monomer **103** via the Suzuki coupling reaction.<sup>163</sup>

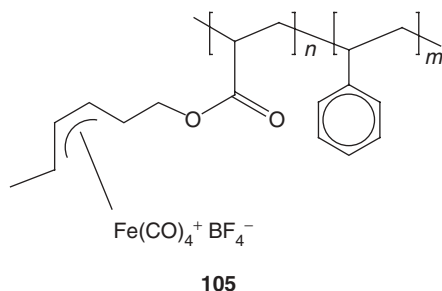


Scheme 31



Scheme 32

The synthesis of homopolymers and copolymers of  $\pi$ -(2,4-hexadienyl acrylate)tricarbonyliron with styrene, methyl acrylate, acrylonitrile, and vinyl acetate were first reported in 1973.<sup>164</sup> These polymers could undergo protonation to yield the  $\pi$ -allyliron polysalts **105**.<sup>165</sup> These compounds were easily transformed into new types of functional materials due to the ease of nucleophilic attack on the positively

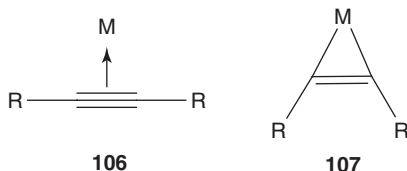


polarized  $\pi$ -allyl group. A decade later, the synthesis and electrochemical properties were reported of some polymers containing iron and ruthenium tricarbonyl groups coordinated to the dienes in the polymer as pendent groups.<sup>166</sup>

## VIII. POLYMERS WITH METAL–CARBON $\sigma$ -BONDS

### A. Transition Metal Polyynes

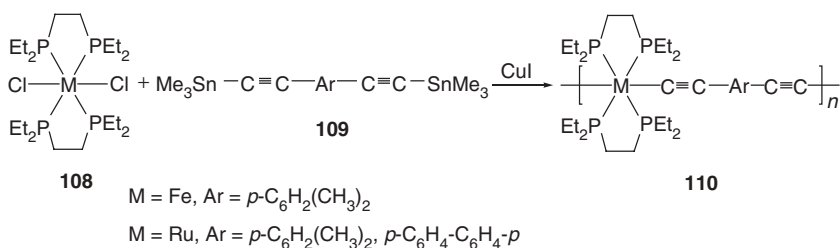
Alkynes have two mutually perpendicular sets of  $\pi$  orbitals. In mononuclear complexes, alkynes often coordinate like olefins.<sup>167</sup> Bonding is typically best represented as direct  $\pi$ -bonding to the metal. This forms a  $\pi$ -bonded alkyne (**106**), rather than as a metallocyclopropene (**107**).



Even so, there are examples that are consistent with the structure being of the metallocyclopropane variety. One ready measure of the amount of each type of bonding is the location of the alkyne stretching frequency in the IR. This absorption appears about  $2200\text{ cm}^{-1}$  in alkyne complexes while the band appears about  $1750\text{ cm}^{-1}$  for the metallocyclopropene complexes. Alkyne complexes can also act as four-electron donors.<sup>168</sup> Back-donation into the metallic  $\pi$  orbitals is negligible in these cases, but sigma-donation occurs. Furthermore, alkynes form a number of dinuclear complexes where each perpendicular  $\pi$  system can be considered to formally bond to a separate metal atom.<sup>169</sup> Thus care must be exercised in assigning the type of bonding present.

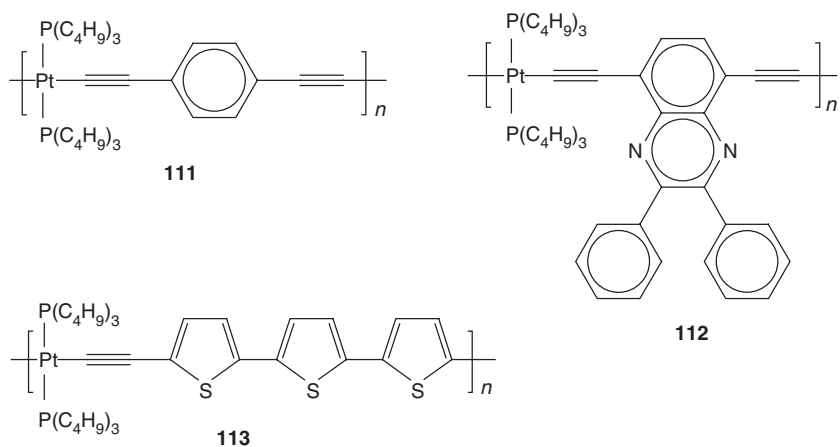
Since the first examples of metal-containing rigid rod polyynes was reported in the 1970s by a Japanese group, these polymers have remained a very interesting area of research.<sup>170–173</sup> The main interest in this class of compounds arises from their unique optical properties. Lewis and coworkers have reported many rigid-rod metal-containing polyynes via reaction with bis-trimethylstannylacetylides.<sup>174–181</sup> High molecular weight polyynes containing different kinds of metals have been reported through the reaction of a metal dihalide complex with a bis-trimethylstannyl-alkynyl compound with a catalytic amount of CuI (scheme 33).<sup>181</sup>

Current research includes the incorporation of thiophene and pyridine rings into transition metal-containing acetylide polymers.<sup>182–190</sup> Kohler and coworkers have studied the photoluminescence of various platinum polyacetylides.<sup>185</sup> Altering the conjugation of the spacers between the acetylide units in polymers **111–113**

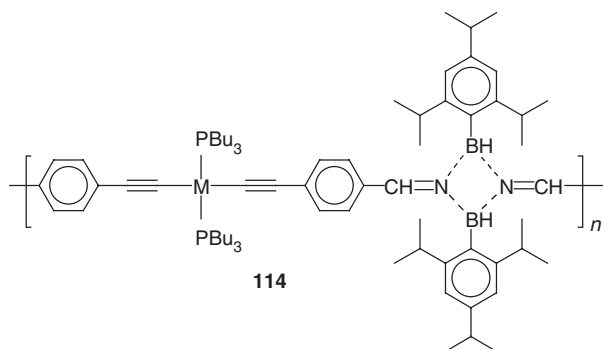


Scheme 33

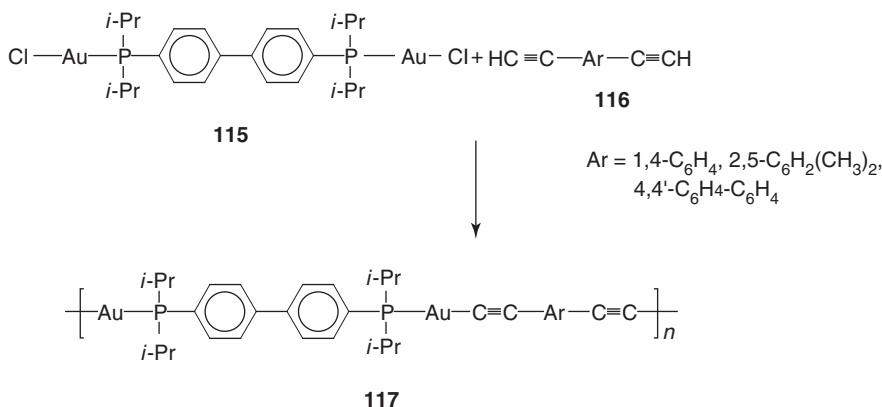
altered the triplet energies. These varied between 1.3 and 2.5 eV. The polymers exhibited a lower quantum yield than that of their monomers.



Polymers containing cyclodiborazane groups in their backbones have been synthesized via hydroboration of monomers of platinum and palladium acetylides functionalized with cyano groups.<sup>191</sup> These polymers (**114**) showed good solubility in organic solvents and possessed  $M_w$  values between 6000 and 6300.

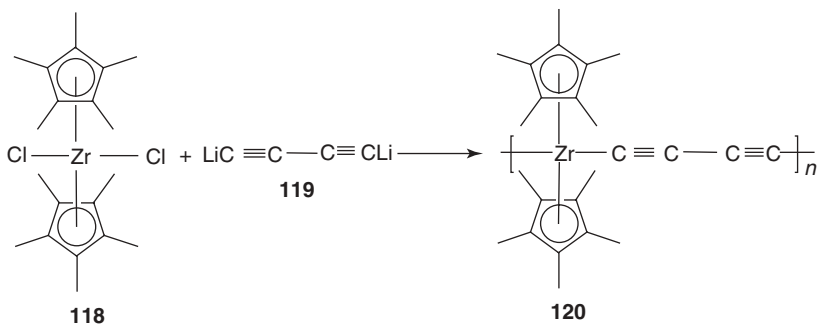


Gold acetylide polymers have been synthesized by two different methods. The first method was a reaction of diacetylide gold complexes with diphosphines. The second was a reaction of diethynylarenes with a diphosphine gold complex.<sup>192</sup> Scheme 34 shows the reaction of the gold-containing monomer **115** with the dialkyne monomers **116** to produce polymers **117**. These polymers displayed molecular weights of approximately 18,000.



Scheme 34

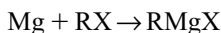
Scheme 35 shows the formation of zirconocene acetylene polymers from the reaction of bis(pentamethylcyclopentadienyl)zirconium (IV) dichloride **118** with dilithiodiacetylene **119**.<sup>193</sup> Polymer **120** displayed a weight-average molecular weight of 68,000.



Scheme 35

## B. Metal-Aryl and Metal-Alkyl Systems

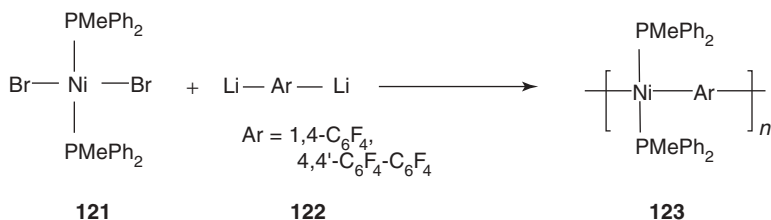
Metal-aryl and metal-alkyl compounds are generally synthesized through what is referred to as a direct route or direct method.<sup>194</sup> Here, metal atoms react with alkyl or aryl halides. The best-known direct route involves the formation of the Grignard reagent.



The reactivity order for metals approximates the electropositive character of the metal with the more active metals displacing the less active metals—that is transmetallation occurs. For alkyl and aryl halides, the reaction order is  $\text{RI} \rightarrow \text{RBr} \rightarrow \text{RCl} \rightarrow \text{RF}$ , and alkyl  $\rightarrow$  aryl. These trends reflect the decrease in C–X bond strengths.

While main group organometallics are thermodynamically unstable with respect to oxidation, their kinetic stabilities vary widely. Transition metal organometallics generally offer a greater thermodynamic stability because the transition metals are less electropositive, but kinetic stabilities still vary widely, particularly due to the tendency toward metal hydride elimination. Transition metal polymer systems can be made by the direct route. As expected, high bond polarity promotes attack by reagents. Also, compounds with empty or half-filled orbitals will be more reactive than those with filled orbitals.

Thermochemical data indicate that transition metal–carbon bonds are stronger (100–200 kJ/mol) than previously expected, though they are weaker than many other metal bonds such as M–O, M–N, and M–X (300–400 kJ/mol). The instability often found with transition metal alkyls is of kinetic rather than of thermodynamic nature. Thus stabilities can be improved by blocking reaction pathways.  $\beta$ -Elimination is a major decomposition pathway requiring a vacant metal orbital and a vacant coordination site to form a hydride-olefin complex from the metal alkyl function.  $\beta$ -Elimination can be prevented by the use of ligands that are strongly bonded and occupy all the coordination sites to stabilize metal alkyl compounds. The use of alkyl groups that contain no  $\beta$ -hydrogens—such as methyl, benzyl, neopentyl, and trimethylsilylmethyl—is a second approach to control  $\beta$ -elimination. The other three alkyls also offer some steric bulk that help block entering reagents. Aryls tend to help against  $\beta$ -elimination since there are no easily removable  $\beta$ -hydrogens. Since alkyls



Scheme 36

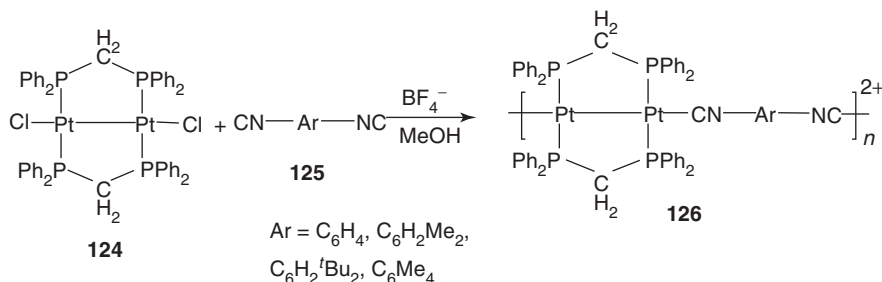
are good  $\sigma$ -electron donors, they help stabilize high oxidation states.<sup>195</sup> When these considerations are taken into account, dilithium reagents and transition metal dihalide complexes can generate polymers directly. Scheme 36 describes the synthesis developed by Hunter and coworkers for organometallic polymers containing nickel–carbon  $\sigma$ -bonds in their backbones.<sup>196,197</sup> These polymers were found to possess molecular weights ranging from 1,800 to 11,100.

## IX. METAL–METAL BONDED SYSTEMS

A number of metal–metal and metal cluster compounds are known. Metal clusters are defined as structures that form triangular or larger closed structures. There is often confusion over the identity of the actual bonding sites in metal–metal bonded systems. Thus care should be taken to determine the actual bonding sites. Bond lengths are of some help here. Therefore, if the metal–metal (M–M) bonding length is over twice that of the single metal–bonding radius, then the M–M bonding must be either quite weak or not a principle site of bonding.

Metal–metal bond strength is difficult to determine with precision. M–M interactions are evaluated from their stabilities and force constants. In general, there is an increase in the transition M–M bond strengths down a group in the periodic table. This trend is opposite that found for the main group elements where the element–element bonding generally decreases as one progresses from top to bottom in a group. Thus transition metal M–M bonds are more common for period 4 and 5 metals and for the inner transition metals.

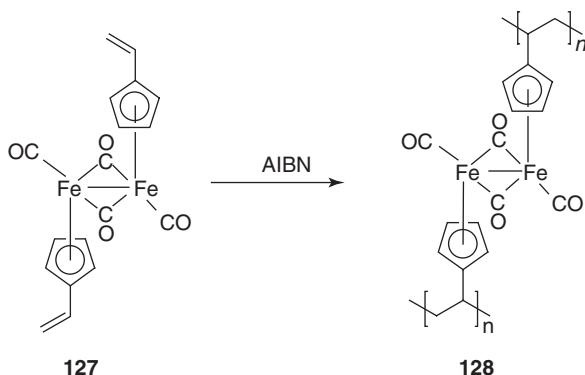
Oligomers and polymers containing backbone Pt–Pt bonds have been reported via reactions of a platinum complex with diacetylides and diisocyanides (scheme 37).<sup>198</sup> Oligomers with low solubility were formed in the reactions with diacetylides. IR studies on the polymers formed with reaction of diisocyanides did not exhibit uncoordinated isocyanide groups.



Scheme 37

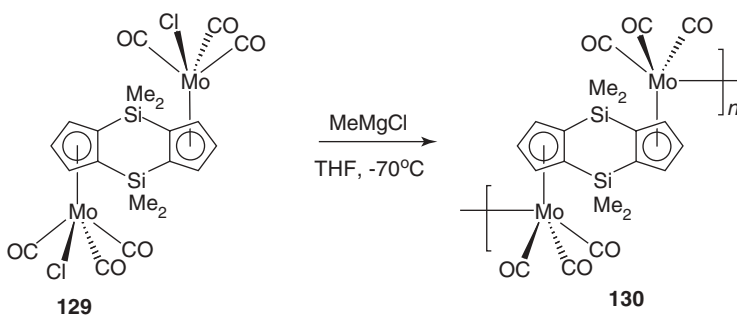
Polyurethanes, amides, and ureas containing photodegradable metal–metal bonds in the backbones were reported by Tenhaedd and Tyler in the early

1990s.<sup>199–203</sup> These polymers were formed via AIBN-initiated radical polymerization of vinyl monomers, yielding the polymers with backbone Fe–Fe bonds (scheme 38). Various polymerizations with monomer **127** and organic monomers have also been reported. Pittman and Felis did similar work in the 1970s synthesizing polymer-bound  $(\eta^1\text{-Benzyl})(\eta^5\text{-cyclopentadienyl})\text{dicarbonyliron}$ ,  $(\eta^1\text{-benzyl})(\eta^5\text{-cyclopentadienyl})\text{tricarbonylmolybdenum}$ , and its tungsten analog.<sup>204,205</sup> The thermal decompositions and rearrangements of all of the complexes were studied.



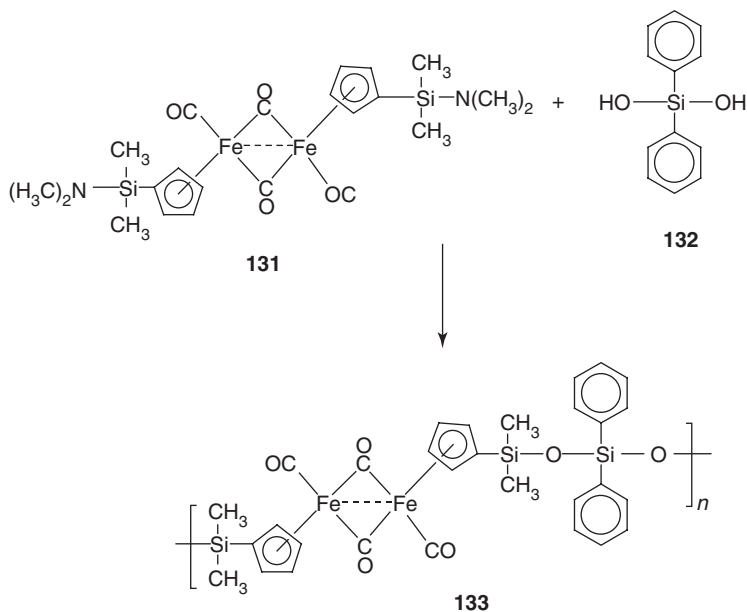
Scheme 38

Royo and coworkers reported the synthesis of polymers containing bridging molybdenum bonds (scheme 39).<sup>206</sup> Complexes containing *trans*- $\text{Mo}(\text{CO})_3\text{Cl}$  moieties were used in the reaction with  $\text{MeMgCl}$  to give the Mo–Mo bonds. Polymer **130** exhibited poor solubility in organic solvents.



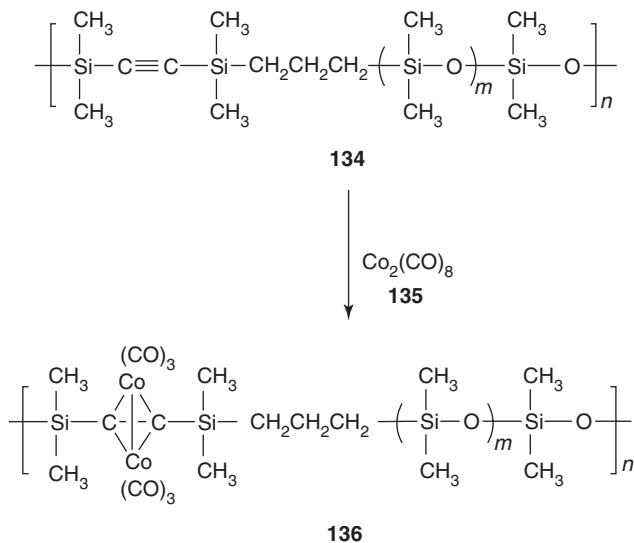
Scheme 39

Polysiloxanes containing Fe–Fe bonds have been reported using two methodologies. The first methodology reacted the polysiloxanes with  $\text{Fe}(\text{CO})_5$  and the second reacted a diiron  $\text{Cp}_2\text{Fe}_2(\text{CO})_4$  complex, containing  $\text{SiMe}_2\text{NMe}_2$  functions with disilanol.<sup>207</sup> The second method is shown in scheme 40.



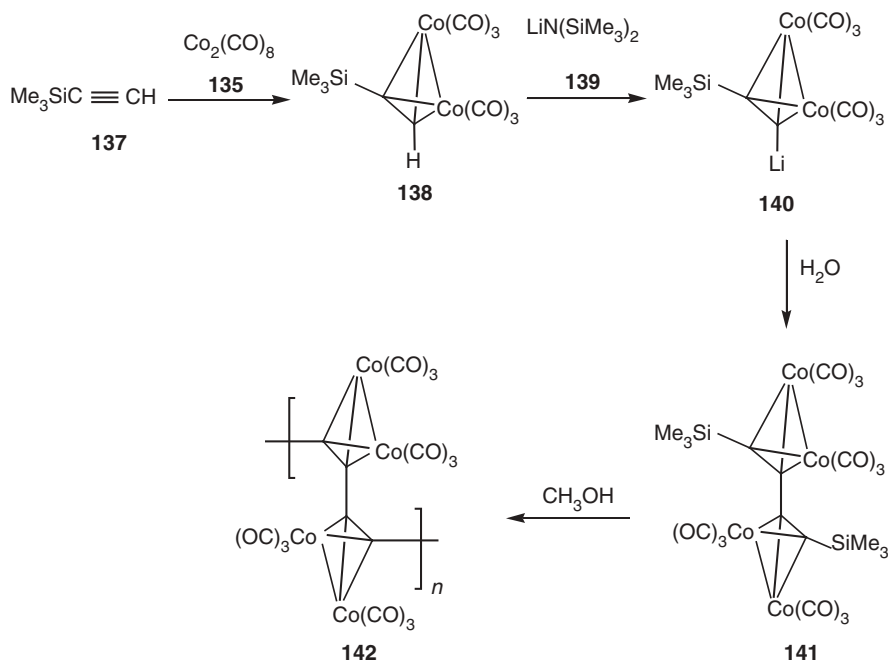
Scheme 40

Reactions of dicobaltoctacarbonyl with a silicon-based polymer with alkyne units in the backbone have led to the isolation of polymers containing Co–Co bonds (scheme 41).<sup>208</sup>



Scheme 41

An electrically conductive Co–Co bond-containing polymer was isolated from a reaction of  $\text{Co}_2(\text{CO})_8$  with alkynes (scheme 42).<sup>20</sup>



Scheme 42

## X. CONCLUSION

Although there were a few articles dealing with the synthesis of transition metal-containing polymers before 1966–1968, it was not until after this period that well-characterized organometallic polymers were described. The past two decades have seen an ever-increasing interest in these polymers, especially in light of their important electrical, optical, catalytic, biomedical, magnetic, and pharmacological properties. Synthetic strategies used to prepare these materials range from olefin and alkyne polymerization to condensation, substitution, ring opening, and coordination polymerizations. The wide range of methodologies that can be used in the production of organometallic polymers, and their remarkable applications is the reasons for the rapid developments in this field.

## XI. REFERENCES

1. C. Carraher, J. Scott, D. Schroeder, J. Giron, *J. Macromol. Sci. Chem.*, **A15**(4), 625 (1981).
2. C. Carraher, J. Scott, J. Giron, in *Bioactive Polymeric Systems*, C. Gebelein, C. Carraher, eds., Plenum, New York, 1985.

3. C. Carraher, S. Jorgenson, *J. Polym. Sci., Polym. Chem. Ed.*, **16**, 2965 (1978).
4. C. Carraher, P. Lessek, *Eur. Polym. J.*, **8**, 1339 (1972).
5. C. Carraher, S. Bajah, *Polymer (Br.)*, **14**, 42 (1973) and **15**, 9 (1974).
6. C. Carraher, G. Burrish, *J. Macromol. Sci. Chem.*, **A10**, 1457 (1976).
7. C. Carraher, S. Jorgensen, *J. Polym. Sci.*, **16**, 2965 (1978).
8. C. Carraher, P. Lessek, *Eur. Polym. J.*, **8**, 1339 (1972).
9. C. Carraher, L. Tisinger, W. Tisinger, in *Renewable Resource Materials*, C. Carraher, L. Sperling, eds., Plenum, New York, 1986.
10. C. Carraher, R. Nordin, *Makromolekular Chem.*, **164**, 87 (1973).
11. C. Carraher, R. Nordin, *J. Polym. Sci. A-1*, **10**, 521 (1972).
12. C. Carraher, S. Bajah, *Br. Polym. J.*, **7**, 155 (1975).
13. C. Carraher, L. Lanz, *PMSE*, **87**, 243 (2002).
14. A. S. Abd-El-Aziz, in: *Encyclopedia of Polymer Science and Technology*, 3rd ed., J. I. Kroschwitz, ed., John Wiley & Sons, New York, 2002.
15. A. S. Abd-El-Aziz, *Coord. Chem. Rev.*, **233–234**, 177 (2002).
16. A. S. Abd-El-Aziz, E. K. Todd, *Polym. News*, **26**, 5 (2001).
17. A. S. Abd-El-Aziz, S. Bernardin, *Coord. Chem. Rev.*, **203**, 219 (2000).
18. A. Togni, T. Hayashi, eds., *Ferrocenes: Homogeneous Catalysis, Organic Synthesis, Materials Science*, VCH, Weinheim, 1995.
19. E. W. Neuse, H. Rosenburg, *Metallocene Polymers*, Marcel Dekker, New York, 1970.
20. K. A. Andrianov, *Metallorganic Polymers*, John Wiley & Sons, New York, 1965.
21. T. H. Coffield, V. Sandel, R. D. Closson, *J. Am. Chem. Soc.*, **79**, 5826 (1957).
22. J. A. Segal, *J. Chem. Soc. Chem. Commun*, 1338 (1985).
23. R. J. Puddephatt, *Chem. Commun*, 1055 (1998).
24. M. H. Chisholm, *Angew. Chem. Int. Ed. Engl.*, **30**, 673 (1991).
25. J. L. Robbins, N. Edelstein, B. Spencer, J. C. Smark., *J. Am. Chem. Soc.*, **104**, 188 (1982).
26. T. J. Kealy, P. L. Pauson, *Nature*, **168**, 1039 (1951).
27. F. S. Arimoto, A. C. Haven Jr., *J. Am. Chem. Soc.*, **77**, 6295 (1955).
28. D. O. Cowan, J. Park, C. U. Pittman Jr., Y. Sasaki, T. K. Mukherjee, N. A. Diamond, *J. Am. Chem. Soc.*, **94**, 5110 (1972).
29. C. U. Pittman Jr., B. Suryanarayanan, *J. Am. Chem. Soc.*, **96**, 7916 (1974).
30. Y. Sasaki, L. L. Walker, E. L. Hurst, C. U. Pittman Jr., *J. Poly. Sci., Polym. Chem. Ed.*, **11**, 1213 (1973).
31. J. C. Lai, T. Rounsefell, C. U. Pittman Jr., *J. Polm. Sci. A-1*, **9**, 651 (1971).
32. C. U. Pittman Jr., R. L. Voges, J. Elder, *Polym. Lett.*, **9**, 191 (1971).
33. C. U. Pittman Jr., P. Grube, *J. Polym. Sci. A-1*, **9**, 3175 (1971).
34. C. U. Pittman Jr., P. Grube, *J. Appl. Polym. Sci.*, **18**, 2269 (1974).
35. M. George, G. Hayes, *Polymer*, **15**, 397 (1974).
36. M. George, G. Hayes, *J. Polym. Sci. Chem. Ed.*, **13**, 1049 (1975).
37. M. George, G. Hayes, *J. Polym. Sci. Chem. Ed.*, **14**, 475 (1976).
38. M. Baumert, J. Frohlich, M. Stieger, H. Frey, R. Mulhaupt, H. Plenio, *Macromol. Rapid Commun.*, **20**, 203 (1999).
39. C. U. Pittman Jr., J. C. Lai, D. P. Vanderpool, M. Good, R. Prado, *Macromolecules*, **3**, 746 (1970).
40. C. U. Pittman, Jr., J. C. Lai, D. P. Vanderpool, *Macromolecules*, **3**, 105 (1970).
41. J. C. Lai, T. D. Rounsefell, C. U. Pittman Jr., *Macromolecules*, **4**, 155 (1971).
42. C. U. Pittman Jr., R. L. Voges, W. R. Jones, *Macromolecules*, **4**, 291 (1971).

43. C. U. Pittman Jr., R. L. Voges, W. R. Jones, *Macromolecules*, **4**, 298 (1971).
44. H. B. Tatistcheff, L. F. Hancock, M. S. Wrighton, *J. Phys. Chem.*, **99**, 7689 (1995).
45. M. E. Wright, E. G. Toplikar, R. F. Kubin, M. D. Seltzer, *Macromolecules*, **25**, 1838 (1992).
46. M. E. Wright, B. B. Cochran, E. G. Toplikar, H. S. Lackritz, J. T. Kerney, in *Inorganic and Organometallic Polymers II*, P. Wisian-Neilson, H. R. Allcock, K. J. Wynne, eds., ACS Symposium Series **572**, American Chemical Society, Washington, DC, 1994.
47. M. E. Wright, E. G. Toplikar, *Macromolecules* **1994**, *27*, 3016.
48. Y. Yang, Z. Xie, C. Wu, *Macromolecules*, **35**, 3426 (2002).
49. N. Kuramoto, Y. Shishido, K. Nagai, *J. Polym. Sci. Part A Polym. Chem.*, **35**, 1967 (1997).
50. A. Wiesemann, R. Zentel, G. Lieser, *Acta Polym.*, **46**, 25 (1995).
51. R. Deschenaux, F. Turpin, D. Guillon, *Macromolecules*, **30**, 3759 (1997).
52. O. Nuyken, T. Pohlmann, M. Herberhold, *Macromol. Chem. Phys.*, **197**, 3343 (1996).
53. M. Buchmeiser, R. R. Schrock, *Macromolecules*, **28**, 6642 (1995).
54. M. R. Buchmeiser, *Macromolecules*, **30**, 2274 (1997).
55. M. R. Buchmeiser, N. Schuler, G. Kaltenhauser, K.-H. Ongania, I. Lagola, K. Wurst, H. Scottenberger, *Macromolecules*, **31**, 3175 (1998).
56. K. Eder, E. Reichel, H. Scottenberger, C. G. Huber, M. R. Buchmeiser, *Macromolecules*, **34**, 4334 (2001).
57. H. Plenio, J. Hermann, A. Sehring, *Chem. Eur. J.*, **6**, 1820 (2000).
58. H. Plenio, J. Hermann, J. Leukel, *Eur. J. Inorg. Chem.*, **12**, 2063 (1998).
59. T. Morikita, T. Mauyama, T. Yamamoto, K. Kubota, M. Katada, *Inorg. Chim. Acta*, **269**, 310 (1998).
60. T. Yamamoto, T. Morikita, T. Maruyama, K. Kubota, M. Katada, *Macromolecules*, **30**, 5390 (1997).
61. S. L. Ingham, M. S. Khan, J. Lewis, N. J. Long, P. R. Raithby, *J. Organomet. Chem.*, **470**, 153 (1994).
62. F. W. Knobloch, W. H. Rauscher, *J. Polym. Sci.*, **54**, 651 (1961).
63. W. J. Patterson, S. P. McManus, C. U. Pittman Jr., *J. Polym. Sci. Polym. Chem.*, **12**, 837 (1974).
64. C. M. Casado, M. Moran, J. Losada, I. Cuadrado, *Inorg. Chem.*, **34**, 1668 (1995).
65. I. Cuadrado, C. M. Casado, F. Lobete, B. Alonso, B. Gonzalez, J. Losada, U. Amador, *Organometallics*, **18**, 4960 (1999).
66. K. Gonzalves, L. Zhan-ru, M. D. Rausch, *J. Am. Chem. Soc.*, **106**, 3862 (1984).
67. C. U. Pittman Jr., M. D. Rausch, *Pure Appl. Chem.*, **58**, 617 (1986).
68. K. E. Gonzalves, M. D. Rausch in *Inorganic and Organometallic Polymers*, M. Zeldin, K. J. Wynne, H. R. Allcock, eds., ACS Symposium Series **360**, Washington, DC, 1988.
69. K. E. Gonzalves, M. D. Rausch, *J. Polym. Sci. Part A Polym. Chem.*, **24**, 1599 (1986).
70. K. E. Gonzalves, M. D. Rausch, *J. Polym. Sci. Part A Polym. Chem.*, **26**, 2769 (1988).
71. M. M. Abd-Alla, M. F. El-Zohry, K. I. Aly, M. M. M. Abd-El-Wahab, *J. Appl. Polym. Sci.*, **47**, 323 (1993).
72. N. Najafi-Mohajeri, G. L. Nelson, R. Benrashid, *J. Appl. Polym. Sci.*, **76**, 1847 (2000).
73. G. Wilbert, A. Wiesemann, R. Zentel, *Macromol. Chem. Phys.*, **196**, 3771 (1995).
74. G. Wilbert, R. Zentel, *Macromol. Chem. Phys.*, **197**, 3259 (1996).
75. S. Senthil, P. Kannan, *J. Appl. Polym. Sci.*, **85**, 831 (2002).
76. M. E. Wright, E. G. Toplikar, *Macromolecules*, **25**, 6050 (1992).
77. M. E. Wright, M. S. Sigman, *Macromolecules*, **25**, 6055 (1992).
78. I. Yamaguchi, K. Osakada, T. Yamamoto, M. Katada, *Bull. Chem. Soc. Jpn.*, **72**, 2557 (1999).
79. M. Bochmann, J. Lu, R. D. Cannon, *J. Organomet. Chem.*, **518**, 97 (1996).

80. R. Knapp, U. Velten, M. Rehahn, *Polymer*, **39**, 5827 (1998).
81. C. U. Pittman Jr., O. E. Ayers, S. P. McManus, J. E. Sheats, C. E. Whitten, *Macromolecules*, **4**, 360 (1971).
82. C. U. Pittman Jr., O. E. Ayers, B. Suryanarayanan, S. P. McManus, J. E. Sheats, *Makromol. Chem.*, **175**, 1427 (1974).
83. C. E. Carraher Jr., J. E. Sheats, *Makromol. Chem.*, **166**, 23 (1973).
84. C. E. Carraher Jr., *Makromol. Chem.*, **166**, 31 (1973).
85. J. E. Sheats in *Organometallic Polymers*; C. E. Carraher Jr., J. E. Sheats, C. U. Pittman Jr., eds., Academic Press, New York, 1978.
86. H. R. Allcock, K. D. Lavin, G. H. Riding, *Macromolecules*, **18**, 1340 (1985).
87. H. R. Allcock, G. H. Riding, K. D. Lavin, *Macromolecules*, **20**, 6 (1987).
88. I. Manners, G. H. Riding, J. A. Dodge, H. R. Allcock, *J. Am. Chem. Soc.*, **111**, 3067 (1989).
89. D. Albagli, G. Bazan, M. S. Wrighton, R. R. Schrock, *J. Am. Chem. Soc.*, **114**, 4150 (1992).
90. D. Albagli, G. Bazan, R. R. Schrock, M. S. Wrighton, *J. Am. Chem. Soc.*, **115**, 7328 (1993).
91. C. E. Stanton, T. R. Lee, H. R. Grubbs, N. S. Lewis, J. K. Pudelski, M. R. Callstrom, M. S. Erickson, M. L. McLaughlin, *Macromolecules*, **28**, 8713 (1995).
92. M. A. Buretea, T. D. Tilley, *Organometallics*, **16**, 1507 (1997).
93. R. W. Heo, F. B. Somoza, T. R. Lee, *J. Am. Chem. Soc.*, **120**, 1621 (1998).
94. R. Resendes, P. Nguyen, A. J. Lough, I. Manners, *Chem. Commun.*, **1998**, 1001.
95. F. Jakle, R. Rulkens, G. Zech, J. A. Massey, I. Manners, *J. Am. Chem. Soc.*, **122**, 4231 (2000).
96. H. K. Sharma, F. Cervantes-Lee, J. S. Mahmoud, K. H. Pannell, *Organometallics*, **18**, 399 (1999).
97. F. Jakle, R. Rulkens, G. Zech, D. A. Foucher, A. J. Lough, I. Manners, *Chem. Eur. J.*, **4**, 2117 (1998).
98. R. Resendes, J. M. Nelson, A. Fischer, F. Jakle, A. Bartole, A. J. Lough, I. Manners, *J. Am. Chem. Soc.*, **123**, 2116 (2001).
99. J. Park, Y. Seo, S. Cho, D. Whang, K. Kim, T. Chang, *J. Organomet. Chem.*, **489**, 23 (1995).
100. T. Hirao, M. Kurashina, K. Aramaki, H. Nishihara, *J. Chem. Soc. Dalton Trans.*, 2929 (1996).
101. G. E. Southard, M. D. Curtis, *Organometallics*, **16**, 5618 (1997).
102. G. E. Southard, M. D. Curtis, *Organometallics*, **20**, 508 (2001).
103. G. E. Southard, M. D. Curtis, *Synthesis*, **9**, 1177 (2002).
104. H. M. Nugent, M. Rosenblum, P. Klemarczyk, *J. Am. Chem. Soc.*, **115**, 3848 (1993).
105. M. Rosenblum, H. M. Nugent, K.-S. Jang, M. M. Labes, W. Cahalane, P. Klemarczyk, W. M. Reiff, *Macromolecules*, **28**, 6330 (1995).
106. R. D. A. Hudson, B. M. Foxman, M. Rosenblum, *Organometallics*, **18**, 4098 (1999).
107. G. Caldwell, M. C. Meirim, E. W. Neuse, K. Beloussow, W.-C. Shen, *J. Inorg. Organomet. Polym.*, **10**, 93 (2000).
108. E. W. Neuse, M. C. Meirim, D. D. N'Da, G. Caldwell, *J. Inorg. Organomet. Polym.*, **9**, 221 (1999).
109. B. Schechter, G. Caldwell, E. W. Neuse, *J. Inorg. Organomet. Polym.*, **10**, 177 (2000).
110. E. W. Neuse, *Macromol. Symp.*, **172**, 127 (2001).
111. R. Deschenaux, I. Jauslin, U. Scholten, F. Turpin, D. Guillon, B. Heinrich, *Macromolecules*, **31**, 5647 (1998).
112. E. Muetterties, J. Bleeke, J. Wucherer, T. A. Albright, *Chem. Rev.*, **82**, 49 (1982).
113. C. U. Pittman Jr., R. L. Voges, J. Elder, *Macromolecules*, **4**, 302 (1971).
114. C. U. Pittman Jr., P. L. Grube, O. E. Ayers, S. P. McManus, M. D. Rausch, G. A. Moser, *J. Polym. Sci. Part A-1*, **10**, 379 (1972).
115. C. U. Pittman Jr., G. V. Marlin, *J. Polym. Sci. Part A-1*, **11**, 2753 (1973).

116. C. U. Pittman Jr., O. E. Ayers, S. P. McManus, M. D. Rausch, G. A. Moser *Macromolecules*, **7**, 737 (1974).
117. A. S. Abd-El-Aziz, E. K. Todd, G. Z. Ma, J. DiMartino, *J. Inorg. Organomet. Polym.*, **10**, 265 (2000).
118. A. S. Abd-El-Aziz, E. K. Todd, *Polym. Mater. Sci. Eng.*, **86(1)**, 103 (2002).
119. A. S. Abd-El-Aziz, L. May, A. L. Edell, *Macromol. Rapid Commun.*, **21**, 598 (2000).
120. A. S. Abd-El-Aziz, A. L. Edell, L. May, K. M. Epp, H. M. Hutton, *Can. J. Chem.*, **77**, 1797 (1999).
121. A. S. Abd-El-Aziz, L. J. May, J. A. Hurd, R. M. Okasha, *J. Polym. Sci. Part A Polym. Chem.*, **39**, 2716 (2001).
122. A. S. Abd-El-Aziz, R. M. Okasha, J. Hurd, E. K. Todd, *Polym. Mater. Sci. Eng.*, **86(1)**, 91 (2002).
123. A. A. Dembek, P. J. Fagan, M. Marsi, *Macromolecules*, **26**, 2992 (1993).
124. A. A. Dembek, P. J. Fagan, M. Marsi, *Polym. Mater. Sci. Eng.*, **71**, 158 (1994).
125. A. S. Abd-El-Aziz, E. K. Todd, K. M. Epp, *J. Inorg. Organomet. Polym.*, **8**, 127 (1998).
126. A. S. Abd-El-Aziz, E. K. Todd, G. Z. Ma, *J. Polym. Sci., Part A Polym. Chem.*, **39**, 1216 (2001).
127. A. S. Abd-El-Aziz, E. K. Todd, R. M. Okasha, T. E. Wood, *Macromol. Rapid Commun.*, **23**, 743 (2002).
128. A. S. Abd-El-Aziz, T. H. Afifi, W. R. Budakowski, K. J. Friesen, E. K. Todd, *Macromolecules*, **35**, 8929 (2002).
129. A. S. Abd-El-Aziz, R. M. Okasha, P. O. Shipman, T. H. Afifi, *Macromol. Rapid Commun.*, **25**, 1497 (2004).
130. A. S. Abd-El-Aziz, R. M. Okasha, T. H. Afifi, E. K. Todd, *Macromol. Chem. Phys.*, **2004**, 555 (2003).
131. J.-I. Jin, R. Kim, *Polym. J.*, **19**, 977 (1987).
132. A. A. Dembek, R. R. Burch, A. E. Feiring, *J. Am. Chem. Soc.*, **115**, 2087 (1993).
133. A. A. Dembek, M. Marsi, U.S. Pat. 5,350,832, (1994).
134. M. E. Wright, *Macromolecules*, **22**, 3256 (1989).
135. Y. Morisaki, H. Chen, Y. Chujo, *Polym. Bull.*, **48**, 243 (2002).
136. A. S. Abd-El-Aziz, T. H. Afifi, E. K. Todd, G. Z. Ma, *Polym. Prepr. (Am. Chem. Soc., Div. Polym. Chem.)*, **42(2)** 450 (2001).
137. M. E. Wright, L. Lawson, R. T. Baker, D. C. Roe, *Polyhedron*, **11**, 323 (1992).
138. S. I. Yaniger, D. J. Rose, W. P. McKenna, E. M. Eyring, *Appl. Spectrosc.*, **38**, 7 (1984).
139. S. I. Yaniger, D. J. Rose, W. P. McKenna, E. M. Eyring, *Macromolecules*, **17**, 2579 (1984).
140. H. Funaki, K. Aramaki, H. Nishihara, *Chem. Lett.*, 2065 (1992).
141. H. Funaki, K. Aramaki, H. Nishihara, *Synth. Met.*, **74**, 59 (1995).
142. H. Nishihara, H. Funaki, T. Shimura, K. Aramaki, *Synth. Met.*, **55–57**, 942 (1993).
143. B. Chaudret, G. Chung, Y.-S. Huang, *J. Chem. Soc., Chem. Commun.*, 749 (1990).
144. H. R. Allcock, A. A. Dembek, E. H. Klingenberg, *Macromolecules*, **24**, 5208 (1991).
145. R. Atencio, L. Brammer, S. Fang, F. C. Pigge, *New J. Chem.*, **23**, 461 (1999).
146. L. Brammer, J. C. Mareque Rivas, R. Atencio, S. Fang, F. C. Pigge, *J. Chem. Soc., Dalton Trans.*, 3855 (2000).
147. M. Oh, G. B. Carpenter, D. A. Sweigart, *Angew. Chem. Int. Ed.*, **40**, 3191 (2001).
148. M. Oh, G. B. Carpenter, D. A. Sweigart, *Organometallics*, **21**, 1290 (2002).
149. M. Altmann, V. Enkelmann, F. Beer, U. H. F. Bunz, *Organometallics*, **15**, 394 (1996).
150. M. Altmann, U. H. F. Bunz, *Angew. Chem. Int. Ed. Engl.*, **34**, 569 (1995).

151. W. Steffen, B. Kohler, M. Altmann, U. Scherf, K. Stitzer, H.-C. zur Loye, U. H. F. Bunz, *Chem. Eur. J.*, **7**, 117 (2001).
152. W. Steffen, U. H. F. Bunz, *Macromolecules*, **33**, 9518 (2000).
153. Y. Sawada, I. Tomita, T. Endo, *Polym. Bull.*, **43**, 165 (1999).
154. Y. Sawada, I. Tomita, I. L. Rozhanskii, T. Endo, *J. Inorg. Organomet. Polym.*, **10**, 221 (2000).
155. C. U. Pittman Jr., G. V. Marlin, T. D. Rounsefell, *Macromolecules*, **6**, 1 (1973).
156. C. U. Pittman Jr., T. D. Rounsefell, E. A. Lewis, J. E. Sheats, B. H. Edwards, M. D. Rausch, E. A. Mintz, *Macromolecules*, **11**, 560 (1978).
157. D. W. Macomber, W. P. Hart, M. D. Rausch, *J. Am. Chem. Soc.*, **104**, 884 (1982).
158. C. U. Pittman Jr., T. V. Jayaraman, R. D. Priestler Jr., S. Spencer, M. D. Rausch, D. Macomber, *Macromolecules*, **14**, 237 (1981).
159. S. F. Mapolie, J. R. Moss, G. S. Smith, *J. Inorg. Organomet. Polym.*, **7**, 233 (1997).
160. S. F. Mapolie, I. J. Mavunkal, J. R. Moss, G. S. Smith, *Appl. Organomet. Chem.*, **16**, 307 (2002).
161. J. Ohshita, T. Hamaguchi, E. Toyoda, A. Kunai, K. Komaguchi, M. Shiotani, M. Ishikawa, A. Naka, *Organometallics*, **18**, 1717 (1999).
162. U. H. F. Bunz, V. Enkleman, F. Beer, *Organometallics*, **14**, 2490 (1995).
163. S. Setayesh, U. H. F. Bunz, *Organometallics*, **15**, 5470 (1996).
164. C. U. Pittman Jr., O. E. Ayers, S. P. McManus, *J. Macromol. Sci.-Chem.*, **A7**, **8**, 1563 (1973).
165. C. U. Pittman Jr., *Macromolecules*, **7**, 396 (1974).
166. H. Yasuda, I. Noda, S. Miyanaga, A. Nakamura, *Macromolecules*, **17**, 2453 (1984).
167. S. Otsuka, A. Nakamura, *Adv. Organometal. Chem.*, **14**, 245 (1976).
168. J. L. Templeton, *Adv. Organomet. Chem.*, **1**, 29 (1989).
169. E. L. Muetteries, *J. Amer. Chem. Soc.*, **100**, 2090 (1978).
170. K. Sonogashira, S. Takahashi, N. Hagihara, *Macromolecules*, **10**, 879 (1977).
171. S. Takahashi, M. Kariya, T. Yatake, K. Sonogashira, N. Hagihara, *Macromolecules*, **11**, 1063 (1978).
172. K. Sonogashira, S. Kataoka, S. Takahashi, N. Hagihara, *J. Organomet. Chem.*, **160**, 319 (1978).
173. S. Takahashi, H. Morimoto, E. Murata, S. Kataoka, K. Sonogashira, N. Hagihara, *J. Polym. Sci. Polym. Chem. Ed.*, **20**, 565 (1982).
174. S. J. Davies, B. F. G. Johnson, M. S. Khan, J. Lewis, *J. Chem. Soc., Chem. Commun.*, 187 (1991).
175. B. F. G. Johnson, A. K. Kakkar, M. S. Khan, J. Lewis, *J. Organomet. Chem.*, **409**, C12 (1991).
176. S. J. Davies, B. F. G. Johnson, J. Lewis, P. R. Raithby, *J. Organomet. Chem.*, **414**, C51 (1991).
177. A. E. Dray, R. Rachel, W. O. Saxton, J. Lewis, M. S. Khan, A. M. Donald, R. H. Friend, *Macromolecules*, **25**, 3473 (1992).
178. N. Chawdhury, A. Kohler, R. R. Friend, M. Younus, N. J. Long, P. R. Raithby, J. Lewis, *Macromolecules*, **31**, 722 (1998).
179. R. D. Markwell, I. S. Butler, A. K. Kakkar, M. S. Khan, Z. H. Al-Zakwani, J. Lewis, *Organometallics*, **15**, 2331 (1996).
180. M. S. Khan, S. J. Davies, A. K. Kakkar, D. Schwartz, B. Lin, B. F. G. Johnson, J. Lewis, *J. Organomet. Chem.*, **424**, 87 (1992).
181. Z. Atherton, C. W. Faulkner, S. L. Ingham, A. A. Kakkar, M. S. Khan, J. Lewis, N. J. Long, P. R. Raithby, *J. Organomet. Chem.*, **462**, 265 (1993).
182. M. Younus, A. Kohler, S. Cron, N. Chawdhury, M. R. A. Al-Mandhary, M. S. Khan, J. Lewis, N. J. Long, R. H. Friend, P. R. Raithby, *Angew. Chem. Int. Ed.*, **37**, 3036 (1998).
183. M. S. Khan, M. R. A. Al-Mandhary, M. K. Al-Suti, A. K. Hisahm, P. R. Raithby, B. Ahrens, M. F. Mahon, L. Male, E. A. Marseglia, E. Tedesco, R. H. Friend, A. Kohler, N. Feeder, S. J. Teat, *J. Chem. Soc., Dalton Trans.*, 1358 (2002).

184. M. S. Khan, M. R. A. Al-Mandhary, M. K. Al-Suti, N. Feeder, S. Nahar, A. Kohler, R. H. Friend, P. J. Wilson, P. R. Raithby, *J. Chem. Soc., Dalton Trans.*, 2441 (2002).
185. J. S. Wilson, N. Chawdhury, M. R. A. Al-Mandhary, M. Younus, M. S. Khan, P. R. Raithby, A. Kohler, R. H. Friend, *J. Am. Chem. Soc.*, **123**, 9412 (2001).
186. G. Polzonetti, G. Lucci, P. Altamura, A. Ferri, G. Paolucci, A. Goldoni, P. Parent, C. Laffon, M. V. Russo, *Surf. Interface Anal.*, **34**, 588 (2002).
187. A. Buttinelli, E. Viola, E. Antonelli, C. Lo Sterzo, *Organometallics*, **17**, 2574 (1998).
188. P. Altamura, G. Giardina, C. Lo Sterzo, M. V. Russo, *Organometallics*, **20**, 4360 (2001).
189. M. Yang, L. Zhang, Z. Lei, P. Ye, J. Si, Q. Yang, Y. Wang, *J. Appl. Polym. Sci.*, **70**, 1165 (1998).
190. W.-Y. Wong, S.-M. Chan, K.-H. Choi, K.-W. Cheah, W.-K. Chan, *Macromol. Rapid Commun.*, **21**, 453 (2000).
191. F. Matsumoto, N. Matsumi, Y. Chujo, *Polym. Bull.*, **48**, 119 (2002).
192. G. Jia, R. J. Puddephatt, J. D. Scott, J. J. Vittal, *Organometallics*, **12**, 3565 (1993).
193. P. K. Sahoo, S. K. Swain, *J. Polym. Sci. Part A Polym. Chem.*, **37**, 3899 (1999).
194. E. G. Rochow, *J. Chem. Ed.*, **43**, 58 (1966).
195. F. Cotton, G. Wilkinson, *Advanced Inorganic Chemistry*, 5th ed., John Wiley & Sons, New York, 1988.
196. K. G. Sturge, A. D. Hunter, R. McDonald, B. D. Santarsiero, *Organometallics*, **11**, 3056 (1992).
197. X. A. Guo, K. G. Sturge, A. D. Hunter, M. C. Williams, *Macromolecules*, **27**, 7825 (1994).
198. M. J. Irwin, G. Jia, J. J. Vittal, R. J. Puddephatt, *Organometallics*, **15**, 5321 (1996).
199. S. C. Tenhaeff, D. R. Tyler, *Organometallics*, **10**, 1116 (1991).
200. S. C. Tenhaeff, D. R. Tyler, *Organometallics*, **10**, 473 (1991).
201. S. C. Tenhaeff, D. R. Tyler, *Organometallics*, **11**, 1466 (1992).
202. J. L. Male, M. Yoon, A. G. Glenn, T. J. R. Weakley, D. R. Tyler, *Macromolecules*, **32**, 3898 (1999).
203. D. R. Tyler, J. J. Wolcott, G. W. Nieckarz, S. C. Tenhaeff, in *Inorganic and Organometallic Polymers II*, P. Wisian-Neilson, H. R. Allcock, K. J. Wynne, eds., ACS Symposium Series **572**, American Chemical Society: Washington, DC, 1994.
204. C. U. Pittman Jr., R. F. Felis, *J. Organometallic Chem.*, **72**, 389 (1974).
205. C. U. Pittman Jr., R. F. Felis, *J. Organometallic Chem.*, **72**, 399 (1974).
206. F. Amor, E. de Jesus, A. I. Perez, P. Royo, A. V. de Miguel, *Organometallics*, **15**, 365 (1996).
207. M. Moran, M.C. Pascual, I. Cuadrado, J. Losada, *Organometallics*, **12**, 811 (1993).
208. T. Kuhnen, M. Stradiotto, R. Ruffolo, D. Ulbrich, M. J. McGlinchey, M. A. Brook, *Organometallics*, **16**, 5048 (1997).
209. P. Magnus, D. P. Becker, *J. Chem. Soc. Commun.*, 640 (1985).



---

## CHAPTER 2

# Lithographic Applications of Highly Metallized Polyferrocenyilsilanes

**Alison Y. Cheng, Scott B. Clendenning, and  
Ian Manners**

*Department of Chemistry, University of Toronto, Toronto,  
Ontario, Canada*

### CONTENTS

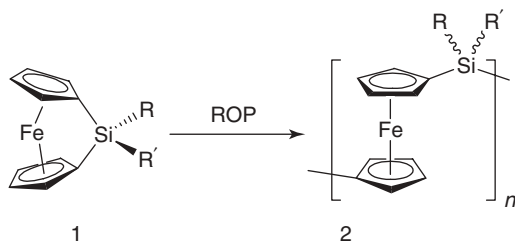
I. INTRODUCTION	50
II. POLYFERROCENYLSILANES AS ELECTRON BEAM LITHOGRAPHY RESISTS	52
III. POLYFERROCENYLSILANES AS REACTIVE ION ETCH RESISTS	53
IV. POLYFERROCENYLSILANES AS UV PHOTORESISTS	55
V. CONCLUSIONS	56
VI. ACKNOWLEDGMENTS	56
VII. REFERENCES	57

*Macromolecules Containing Metal and Metal-Like Elements,  
Volume 6: Transition Metal-Containing Polymers*, edited by Alaa S. Abd-El-Aziz,  
Charles E. Carraher Jr., Charles U. Pittman Jr., and Martel Zeldin.  
Copyright © 2006 John Wiley & Sons, Inc.

## I. INTRODUCTION

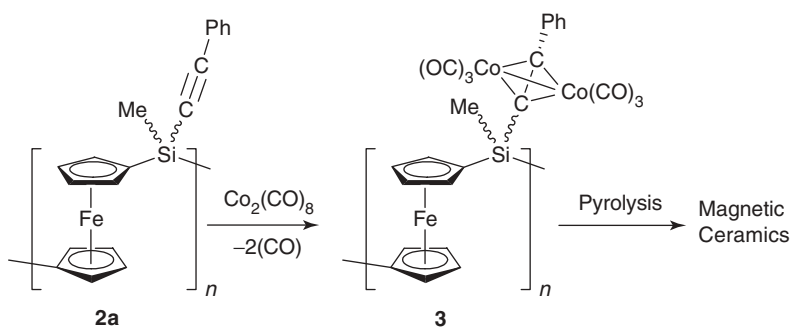
The patterning of surfaces on the nanometer scale with metals offers the possibility of fabricating materials with useful catalytic, optical, sensing, electrical and magnetic properties. Patterning methods can vary from soft lithography, scanning-probe lithography, electron-beam lithography (EBL), to photolithography. Recent reports include the use of microcontact printing ( $\mu$ CP) to order monodisperse nanoparticles of iron oxide<sup>1</sup> and nanotransfer printing (nTP) to transfer a gold pattern with 75-nm feature sizes from a gold-coated GaAs stamp to an appropriately primed PDMS substrate.<sup>2</sup> Scanning probe techniques also offer precise control of patterning. An AFM tip has been used to pen 35-nm-wide lines of MoO<sub>3</sub> through local oxidation of a Mo film,<sup>3</sup> and Pt lines 30 nm wide have been drawn via the reduction of H<sub>2</sub>PtCl<sub>6</sub> at an AFM tip, using electrochemical AFM dip-pen lithography.<sup>4</sup> It is also possible to employ a film of an organometallic polymer as a resist for electron-beam lithography. Johnson and coworkers have used thin films of the organometallic cluster polymer [Ru<sub>6</sub>C(CO)<sub>15</sub>Ph<sub>2</sub>PC<sub>2</sub>PPh<sub>2</sub>]<sub>n</sub> as a negative electron-beam resist to direct write conducting wires (ca. 100 nm wide) made up of metal nanoparticles.<sup>5</sup> This example illustrates the convenience and utility of combining conventional lithographic techniques with easily processible organometallic polymer resists. Moreover, postdevelopment treatments of the patterned organometallic resist such as pyrolysis or reactive ion etching (RIE) offer additional control over the chemical and physical properties of the surface.

The ring-opening polymerization of sila[1]ferrocenophanes (**1**) by thermal,<sup>6</sup> anionic,<sup>7</sup> and transition metal catalyzed<sup>8</sup> routes yields high-molecular weight, soluble polyferrocenylsilanes (PFSs; **2**) containing covalently bonded iron atoms in the main chain (scheme 1). The incorporation of PFS into patterned surfaces has already yielded materials with tunable magnetic properties that may find applications in protective coatings, magnetic recording media, and antistatic shielding.<sup>9</sup> Furthermore, the low plasma etch rates of polymers containing organometallic moieties in comparison to their purely organic counterparts<sup>10</sup> suggest their use as etch masks that can also deposit interesting materials.



**Scheme 1** Ring-opening polymerization of a sila[1]ferrocenophane (**1**) to afford a polyferrocenylsilane (**2**).

The introduction of additional metals into the PFS chain can increase metal loadings and allow access to binary or higher metallic alloy species. We have found in our research that PFS with acetylenic substituents at silicon<sup>11</sup> (**2a**) can be clustered by treatment with dicobalt octacarbonyl to yield the highly metallized, soluble, air-stable cobalt-clusterized polyferrocenylsilane (Co-PFS) (**3**), which contains three metal atoms per repeat unit (scheme 2).<sup>12</sup>



**Scheme 2** Cobalt clusterization of the acetylenic substituents of a polyferrocenylsilane (**2a**) to yield the highly metallized Co-PFS (**3**), a precursor to magnetic ceramics.

Pyrolysis of **3** under an  $\text{N}_2$  atmosphere at either  $600^\circ\text{C}$  or  $900^\circ\text{C}$  affords black magnetic ceramics in relatively high yield (72% and 59%, respectively). Powder X-ray diffraction (PXRD) studies revealed that the ceramic residual was composed of Fe/Co alloy particles embedded in an amorphous C/SiC matrix. Figure 1 shows the cross-sectional transmission electron micrographs (TEM) images of the ceramics prepared at  $600^\circ\text{C}$  and  $900^\circ\text{C}$ . The presence of metal nanoparticles can clearly be seen. The chemical compositions of these metal particles were determined by element-mapping electron spectroscopic imaging (ESI) experiments. The results indicated that both iron and cobalt were localized in the same nanoparticles. Superconducting quantum

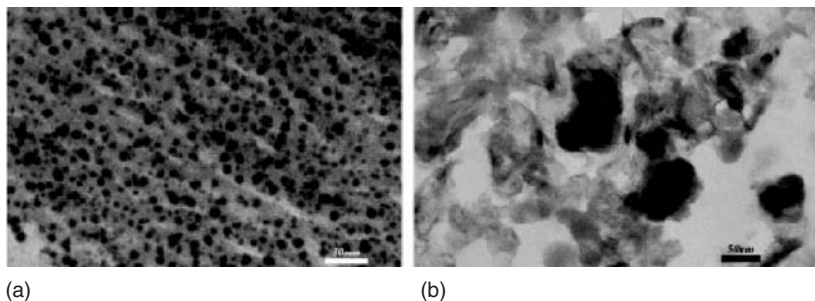


**Figure 1** Cross-sectional TEM images of ceramics resulting from pyrolysis of Co-PFS at (a)  $600^\circ\text{C}$  and (b)  $900^\circ\text{C}$ . The scale bars are 50 nm.

interference device (SQUID) magnetometry showed that ceramics formed at 900°C were ferromagnetic with no blocking temperature up to 355K.

Use of **3** as a lithographic resist offers the advantages of high metal content, ease of processability, atomic-level mixing, and stoichiometric control over composition. We recently demonstrated the use of this metallopolymer as a resist in EBL, O<sub>2</sub>- and H<sub>2</sub>-RIE, as well as UV-photolithography.<sup>14-16</sup>

## II. POLYFERROCENYLSILANES AS ELECTRON BEAM LITHOGRAPHY RESISTS

To determine whether Co-PFS could function as an electron-beam resist, uniform thin films (ca. 200 nm thick) of **3** were spin coated on to silicon substrates and EBL was carried out at varying doses and currents in a modified scanning electron microscope (SEM). The treated films were then developed in THF before to characterization. Resists of **3** were found to operate in a negative-tone fashion. Shapes such as dots and bars were successfully fabricated (Fig. 2).

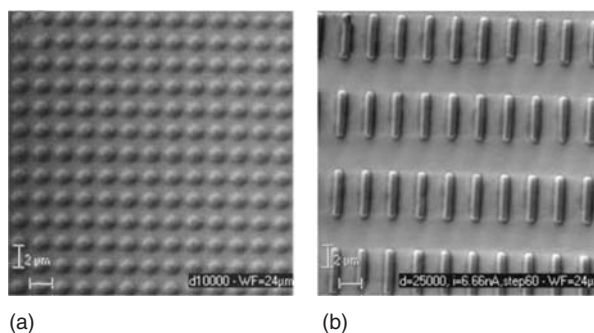


**Figure 2** SEM images of (a) dots and (b) bars fashioned by EBL using a Co-PFS resist.

The elemental composition of these patterns was investigated using time-of-flight secondary ion mass spectrometry (TOF SIMS) and X-ray photoelectron spectroscopy (XPS). Iron and cobalt elemental maps of the arrays of bars on the Si substrate were obtained using TOF SIMS. The mapping clearly revealed that Fe and Co were concentrated within the bars. Information regarding the chemical environment and distribution of Fe and Co throughout the bars was obtained via XPS and compared to data obtained from an untreated film of Co-PFS. The atomic ratio of Fe:Co for the bars is in agreement with the theoretical value of 1:2. Detailed scans for iron and cobalt revealed no change in binding energy for the elements at 3 nm and 12 nm depths, indicating uniformity in average chemical environment. Overall, XPS revealed little change in the chemical composition of the polymer resist after

EBL. Finally, magnetic force microscopy (MFM) indicated no appreciable magnetic field gradient above the bars after EBL.

To enhance the magnetism of the patterned bars, an array of bars on a Si substrate was pyrolyzed at 900°C under an N<sub>2</sub> atmosphere to promote the formation of metallic nanoclusters<sup>12,13</sup>. The same array of bars was characterized before and after pyrolysis by tapping-mode atomic force microscopy (AFM). Comparison of the images and cross-sectional profiles suggests there is excellent shape retention accompanying a decrease in the dimensions of the bars. MFM studies of the bars indicated that they consist of heterogeneous ferromagnetic clusters in which magnetic dipoles appear to be randomly oriented.

Although the aforementioned proof-of-concept experiments dealt with the formation of micron-scale objects,<sup>14</sup> EBL can be used to routinely fabricate structures down to 30–50 nm.<sup>17</sup> Indeed, this process has already been extended to the patterning of sub-500-nm bars and dots from Co-PFS.

### III. POLYFERROCENYLSILANES AS REACTIVE ION ETCH RESISTS

It has been demonstrated that polyferrocenylsilanes possess low plasma etch rates, which can be attributed to the formation of a protective layer of involatile iron and silicon compounds. This property has been exploited with PFS block copolymers self-assembled into micelles<sup>18–20</sup> or phase-separated thin films<sup>21–23</sup> to deposit patterned ceramics as well as for pattern transfer to the substrate. In our research, we are interested in the direct formation of high metal content magnetic ceramic films by RIE treatment of Co-PFS in the presence of a secondary magnetic field.<sup>15</sup>

Thin films of Co-PFS on Si substrate were treated with either H<sub>2</sub> or O<sub>2</sub> plasma. The effects of the plasmas on the chemical composition of the treated films were studied by TOF SIMS depth profiling. In both cases, by plotting the intensity of the Si<sup>+</sup>, Fe<sup>+</sup>, FeO<sup>+</sup>, Co<sup>+</sup>, and CoO<sup>+</sup> signals as a function of depth, it can be seen that the plasma affected only the top 10 nm of the films, leaving the underlying polymer untouched. The chemical compositions of the modified films were analyzed by XPS. In both cases, a Co:Fe ratio of approximately 1:1 was found at 3-nm depth. In comparison to the 2:1 ratio of Co:Fe found in the untreated polymer, this deficiency of Co in the film surface is most likely a reflection of the volatility of the cobalt carbonyl clusters during the high vacuum processing required for RIE. Formation of iron oxides (FeO and Fe<sub>2</sub>O<sub>3</sub>) as well as cobalt oxides (CoO and Co<sub>3</sub>O<sub>4</sub>) were observed at the 3-nm depth in the O<sub>2</sub>-plasma treated films. In the case of H<sub>2</sub>-RIE, small amounts of oxides were also observed at the 3 nm depth, presumably owing to the oxidation of reduced metal on exposure to atmospheric oxygen.

Morphological changes in the surface of Co-PFS films after RIE were investigated by TEM and AFM. Thin films of the polymer (ca. 50 nm thick) on a carbon-coated copper TEM grid were exposed to oxygen and hydrogen plasma. In both cases, analysis by TEM revealed the presence of electron-rich nanoworms with

widths ranging from 4 to 12 nm, which remained on the supporting carbon film. Untreated samples were featureless, supporting plasma-induced nanoworm formation. Electron energy-loss spectroscopic (EELS) elemental mapping and energy-dispersive X-ray (EDX) indicated that there was a high concentration of Fe, Co, and Si in the nanoworms. In contrast to the essentially flat and featureless surface of the untreated film, AFM images of both plasma-treated films exhibited a pervasive interconnected reticulated structure, which would appear as nanoworms in projection normal to the plane of the sample. These features are reminiscent of surface reticulations observed by Thomas et al. by AFM in organosilicon polymers after ambient-temperature O<sub>2</sub>-RIE, which were hypothesized to originate due to a polarity difference between the overlying inorganic layer and the native polymer, causing dewetting or spinodal decomposition of the strained inorganic layer.<sup>21</sup>

To access films with useful magnetic properties, plasma-induced crystallization of metallic nanoclusters was attempted by carrying out H<sub>2</sub>-RIE on a thin film of Co-PFS in a secondary magnetic field. The Co-PFS films (ca. 200 nm thick) on Si substrates were placed between two samarium-cobalt (SmCo) magnets aligned with opposite magnetic poles facing each other during H<sub>2</sub>- or O<sub>2</sub>-RIE. The magnets caused the formation of an intense plasma plume around the sample, which in turn resulted in intense etching conditions. Nanostructures obtained under these conditions were proven to be ferromagnetic by MFM. A tapping mode AFM micrograph and the corresponding magnetic force micrograph of a H<sub>2</sub> plasma-treated film are shown in Figure 3. The reticulations were much larger than those found for samples treated under similar plasma conditions in the absence of the SmCo magnets. We postulate that the secondary magnetic field concentrated the plasma, thereby accelerating nanoworm formation through more efficient removal of carbonaceous material and silicon, whereas the additional thermal energy present in the plasma plume promoted

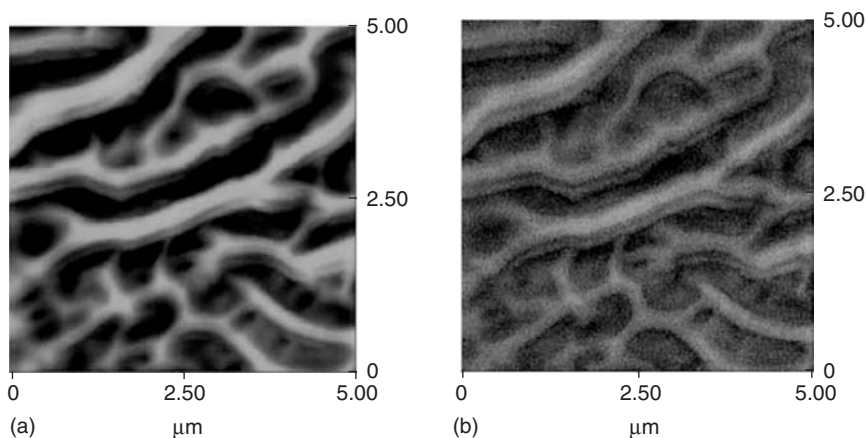


**Figure 3** Tapping-mode AFM images of thin films of Co-PFS after H<sub>2</sub>-RIE in a secondary magnetic field (a) and the corresponding MFM image (b).

metal crystallization. To the best of our knowledge this is the first example of the formation of a ferromagnetic film directly from the plasma treatment of a metallopolymer. The patterning of metallized metallopolymer resists using standard lithographic techniques such as soft lithography combined with RIE in a secondary magnetic field offers access to ordered arrays of ferromagnetic ceramics that may find applications in spintronics as an isolating, magnetic layer in a nanogranular in-gap structure<sup>25</sup> and for the formation of logic circuits using magnetic quantum cellular automata.<sup>26</sup>

#### IV. POLYFERROCENYLSILANES AS UV PHOTORESISTS

Organic polymers incorporating acetylenic moieties have been shown to be thermally crosslinkable. Upon heating, the acetylene groups from adjacent chains undergo cyclotrimerization and coupling reactions, creating crosslinks in the polymer.<sup>27</sup> In addition, photo-induced polymerization of alkyl- and aryl-substituted acetylenes are known to be catalyzed by metal carbonyls such as  $\text{Cr}(\text{CO})_6$ ,  $\text{Mo}(\text{CO})_6$ , and  $\text{W}(\text{CO})_6$ .<sup>28–30</sup> Recently, Bardarau et al. demonstrated that polyacrylates with pendent acetylenic side groups could be photocrosslinked in the presence of  $\text{W}(\text{CO})_6$  as catalyst.<sup>31</sup> In the case of Co-PFS, which inherently contains both the acetylenic unit and the metal carbonyl catalyst, is a promising candidate as a resist material for UV-photolithography.<sup>16</sup>

To study this possibility, a thin film (ca. 200 nm) of Co-PFS on Si substrate was exposed to near UV radiation ( $\lambda = 350\text{--}400\text{ nm}$ , 450 W) for 5 min. The exposed film was developed in THF before characterization. Co-PFS was found to be a negative-tone photoresist. This appears to be consistent with photo-initiated crosslinking mechanism of acetylenes in the presence of metal carbonyls. However, it is also possible to have crosslinking in Co-PFS as a result of decarbonylation of the Co-cluster. The thickness of the film before and after UV treatment was determined by ellipsometry. A 200-nm-thick film of Co-PFS had a thickness of ca. 170 nm after exposure to UV radiation and solvent development. The decrease in thickness is probably a reflection of the decreased volume of the polymer upon crosslinking.

Patterning of Co-PFS films was accomplished using a metal foil shadow mask fabricated by micromachining with features 50–300  $\mu\text{m}$ . Figure 4A is an optical micrograph of a straight line of Co-PFS patterned with the shadow mask. Smaller features (10–20  $\mu\text{m}$ ) were obtained using a chrome contact mask (Fig. 4B). In both cases, the unexposed polymer was completely removed during development with THF, leaving behind patterns with well-defined edges.

Patterned Co-PFS was pyrolyzed at 900°C under an  $\text{N}_2$  atmosphere in attempt to fabricate magnetic ceramic lines. The resulting ceramic lines have the same dimensions as the polymer precursor, showing excellent shape retention in the lateral directions. Inspection of the ceramic line at higher magnifications revealed the formation of what appeared to be Co/Fe nanoparticles throughout the line.

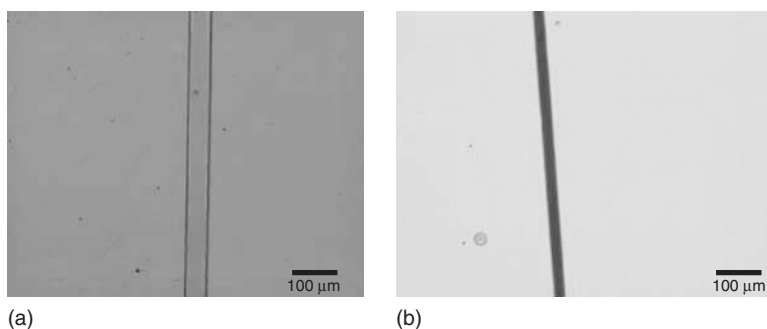


**Figure 4** Optical micrographs of Co-PFS lines fabricated by UV photolithography using (a) a shadow mask and (b) a chrome contact mask.

UV lithography using Co-PFS as a resist provides a convenient route to deposit patterned polymer and magnetic ceramic onto flat substrates. Due to the excellent RIE resistance of the polymer, Co-PFS patterned by UV photolithography can also potentially be used for pattern transfer onto the underlying substrate using conventional plasma-etching techniques. Investigations are under way to improve the resolution of this resist.

## V. CONCLUSIONS

High molecular weight Co-PFS (**3**), is readily accessible via transition metal catalyzed ROP of sila[1]ferrocenophane (**2a**) followed by clusterization of the acetylenic substituents with  $\text{Co}_2(\text{CO})_8$ . The intrinsic high metal content, air stability, and solution processability make Co-PFS an excellent candidate for lithographic resists. Fabrication of patterned arrays of polymer and magnetic ceramics on the submicron scale via EBL was made possible.<sup>14</sup> We have also demonstrated the use of this highly metallized polymer as a RIE resist. Treatment of the polymer films with either  $\text{H}_2$  or  $\text{O}_2$  plasma in the presence of a secondary magnetic field afforded ferromagnetic ceramics.<sup>15</sup> Finally, Co-PFS can also function as a negative-tone UV photoresist.<sup>16</sup> The crosslinking mechanism of this system is still under investigation.

## VI. ACKNOWLEDGMENTS

I.M. would like to thank the Canadian Government for a Canadian Research Chair. S.B.C. is grateful to NSERC for a PDF. The authors would also like to acknowledge the excellent work of our collaborators: *EBL*: Prof. Harry E. Ruda; Dr. Stephane Aouba (Center of Advanced Nanotechnology, University of Toronto); *AFM/MFM*:

Prof. Christopher M. Yip, Mandeep S. Rayat, Patrick Yang (Department of Chemical Engineering and Applied Chemistry, University of Toronto); *TEM*: Dr. Neil Coombs, *ellipsometry*: Chantal Paquet (Department of Chemistry, University of Toronto); *RIE, UV photolithography, XPS*: Prof. Zheng-Hong Lu, Dr. Sijin Han, Dr. Dan Grozea (Department of Materials Science and Engineering, University of Toronto); *TOF SIMS*: Dr. Rana N. S. Sodhi, Dr. Peter M. Brodersen (Surface Interface Ontario, Department of Chemical Engineering and Applied Chemistry, University of Toronto); *MOKE*: Prof. Mark R. Freeman, Jason B. Sorge (Department of Physics, University of Alberta).

## VII. REFERENCES

1. Q. J. Guo, X. W. Teng, S. Rahman, H. Yang, *J. Am. Chem. Soc.* **125**, 630 (2003).
2. Y. L. Loo, R. L. Willet, K. W. Baldwin, J. A. Rogers, *J. Am. Chem. Soc.* **124**, 7654 (2002).
3. M. Rolandi, C. F. Quate, H. J. Dai, *Adv. Mater.* **14**, 191 (2002).
4. Y. Li, B. W. Maynor, J. Liu, *J. Am. Chem. Soc.* **123**, 2105 (2001).
5. B. F. G. Johnson, K. M. Sanderson, D. S. Shephard, D. Ozkaya, W. Z. Zhou, H. Ahmed, M. D. R. Thomas, L. Gladden, M. Mantle, *Chem. Commun.*, 1317 (2000).
6. D. A. Foucher, B. Z. Tang, I. Manners, *J. Am. Chem. Soc.* **114**, 6246 (1992).
7. Y. Z. Ni, R. Rulkens, I. Manners, *J. Am. Chem. Soc.* **118**, 4102 (1996).
8. Y. Z. Ni, R. Rulkens, J. K. Pudelski, I. Manners, *Macromol. Rapid Comm.* **16**, 637 (1995).
9. K. Kulbaba, I. Manners, *Macromol. Rapid Comm.* **22**, 711 (2001).
10. G. N. Taylor, T. M. Wolf, L. E. Stillwagon, *Solid State Technol.* **27**, 145 (1984).
11. A. Berenbaum, A. J. Lough, I. Manners, *Organometallics* **21**, 4451 (2002).
12. A. Berenbaum, M. Ginzburg-Margau, N. Coombs; A. J. Lough, A. Safa-Safat, J. E. Greedan, G. A. Ozin, I. Manners, *Adv. Mater.* **15**, 51 (2003).
13. M. Ginzburg, M. J. MacLachlan, S. M. Yang, N. Coombs, T. W. Coyle, N. P. Raju, J. E. Greedan, R. H. Herber, G. A. Ozin, I. Manners, *J. Am. Chem. Soc.* **124**, 2625 (2002).
14. S. B. Clendenning, S. Aouba, M. S. Rayat, D. Grozea, J. B. Sorge, P. M. Brodersen, R. N. S. Sodhi, Z.-H. Lu, C. M. Yip, M. R. Freeman, H. E. Ruda, I. Manners, *Adv. Mater.* **16**, 215 (2004).
15. S. B. Clendenning, S. Han, N. Coombs, C. Paquet, M. S. Rayat, D. Grozea, P. M. Brodersen, R. N. S. Sodhi, C. M. Yip, Z.-H. Lu, I. Manners, *Adv. Mater.* **16**, 291 (2004).
16. A. Y. Cheng, S. B. Clendenning, S. Han, P. Yang, Z.-H. Lu, C. M. Yip, I. Manners, *Chem. Comm.* **16**, 780 (2004).
17. J. R. Sheat, B. W. Smith, *Microlithography*, Marcel Dekker, New York, 1998.
18. I. Manners, *Pure. Applied Chem.* **71**, 1471 (1999).
19. J. A. Massey, M. A. Winnik, I. Manners, V. Z. H. Chan, J. M. Ostermann, R. Enchlmaier, J. P. Spatz, M. Möller, *J. Am. Chem. Soc.* **123**, 3147 (2001).
20. L. Cao, J. A. Massey, M. A. Winnik, I. Manners, S. Riethmuller, F. Banhart, J. P. Spatz, M. Möller, *Adv. Funct. Mater.* **13**, 271 (2003).
21. R. G. H. Lammertink, M. A. Hempenius, J. E. van der Enk, V. Z. H. Chan, E. L. Thomas, G. J. Vancso, *Adv. Mater.* **12**, 98 (2000).
22. R. G. H. Lammertink, M. A. Hempenius, J. E. van der Enk, V. Z. H. Chan, E. L. Thomas, G. J. Vancso, *Chem. Mater.* **13**, 429 (2001).
23. I. Korczagin, S. Golze, M. A. Hempenius, G. J. Vancso, *Chem. Mater.* **15**, 3663 (2003).

24. V. Z. H. Chan, E. L. Thomas, J. Frommer, D. Sampson, R. Campbell, D. Miller, C. Hawker, V. Lee, R. D. Miller, *Chem. Mater.* **10**, 3895 (1998).
25. M. B. A. Jalil, *IEEE Tran. Magn.* **38**, 2613 (2002).
26. R. P. Cowburn, M. E. Welland, *Science* **287**, 1466 (2000).
27. S. A. Swanson, W. W. Fleming, D. C. Hofer, *Macromolecules* **25**, 582 (1992).
28. T. Masuda, K. Yamamoto, T. Higashimura, *Polymer* **23**, 1663 (1982).
29. T. Masuda, Y. Kuwane, K. Yamamoto, T. Higashimura, *Polym. Bull.* **2**, 823 (1980).
30. S. J. Landon, P. M. Shulman, G. L. Geoffroy, *J. Am. Chem. Soc.* **107**, 6739 (1985).
31. C. Bardarau, Z. Y. Wang, *Macromolecules* **36**, 6959 (2003).

---

## CHAPTER 3

# Polymers Possessing Reactive Metallacycles in the Mainchain

**Ikuyoshi Tomita**

*Department of Electronic Chemistry, Interdisciplinary Graduate School of Science and Engineering, Tokyo Institute of Technology, Yokohama, Japan*

### CONTENTS

I. INTRODUCTION	60
II. SYNTHESIS AND REACTIONS OF ORGANOMETALLIC POLYMERS POSSESSING METALLACYCLES IN THE MAINCHAIN	61
A. Cobaltacyclopentadiene-Containing Polymers	61
B. Conversion of Cobaltacyclopentadiene-Containing Polymers into Polymers Possessing Various Mainchain Structures	63
i. Conversion into Other Organometallic Polymers	63
ii. Conversion into Organic Polymers with Various Functional Groups in the Mainchain	66
C. Synthesis and Reactions of Titanacycle-Containing Polymers	69
i. Polymers Containing Titanacyclopentadiene Unit in the Mainchain	69
ii. Polymers Possessing Other Titanacycle Units	73
III. SUMMARY	74
IV. REFERENCES	75

*Macromolecules Containing Metal and Metal-Like Elements,*  
*Volume 6: Transition Metal-Containing Polymers*, edited by Alaa S. Abd-El-Aziz,  
Charles E. Carraher Jr., Charles U. Pittman Jr., and Martel Zeldin.  
Copyright © 2006 John Wiley & Sons, Inc.

## I. INTRODUCTION

Reactive polymers are important synthetic precursors for various functional materials. In general, the reactive sites in the conventional reactive polymers are not located in the mainchain. Thus their polymer reactions provide polymers with functional groups in the pendant group or the sidechain (Fig. 1). That is, it is hardly possible to functionalize the backbone of these polymers by the polymer reactions of the reactive polymers such as poly(chloromethylstyrene) and poly(glycidyl methacrylate). Because many important functions such as electrical conductivity and thermal stability originate from the mainchain structure of polymers, it is important to prepare polymers possessing various mainchain units. The synthetic methods established for the preparation of these polymers are mainly based on the polycondensation of the monomers containing the structural units to be incorporated into the mainchain. Alternatively, the incorporation of the reactive moieties into the mainchain of the polymers is potentially useful, although the insufficient efficiency of the polymer reactions might bring about the scission of the mainchain of the polymers. As the reactive sites to be incorporated into the mainchain, carbon–metal bonds are quite attractive candidates because of their versatile reactivity. That is, polymers containing organometallic components may serve as interesting reactive materials on the basis of the reactivity of the organometallic moieties. Some organometallic polymers containing carbon–metal bonds in the mainchain have been reported. However, except for the organoboron polymers reported by Chujo et al.,<sup>1</sup> they are mainly focused on their potential applications to functional materials such as electron-conductive, nonlinear optical, and liquid-crystalline materials.

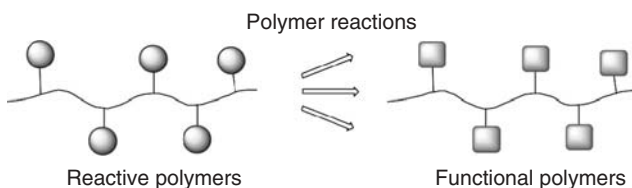


**Figure 1** Ordinary reactive polymers having reactive sites in the sidechain.

On the basis of the fact that metallacycles such as metallacyclopentadiene derivatives have unique and versatile reactivity,<sup>2,3</sup> incorporation of these units into the backbone of the polymers are quite attractive to realize mainchain reactive materials (Fig. 2). Besides, these materials are potentially attractive as novel functional materials if the unique geometry of the organometallic systems reflects the character of the polymers and/or each metal center included in the polymer chains interacts by appropriate macromolecular design.

Accordingly, this chapter deals the synthesis and the reactions of polymers containing reactive organometallics such as cobaltacyclopentadiene and titanacyclopentadiene units in the mainchain. That is, cobaltacyclopentadiene-containing polymers have been prepared by the metallacyclization process of a low-valent cobalt

complex and diyne monomers. Reactions of the polymers having cobaltacyclopentadiene moieties were performed to establish novel polymer reaction systems that involve the conversion of the functional groups in the mainchain. Also, their conversion into polymers possessing other organocobalt moieties, alternative synthetic methods for the organocobalt polymers, and the properties of the resulting organocobalt polymers were studied in detail. To seek polymers exhibiting different reactivity and to generalize the idea of the mainchain reactive polymers, polymers with other metallacycle structures (such as titanacyclopentadiene, titanacyclobutene, and diazatanacyclohexadiene) were prepared, and their polymer reactions were performed.

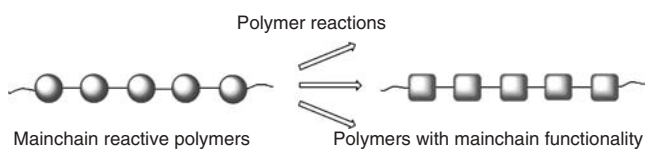


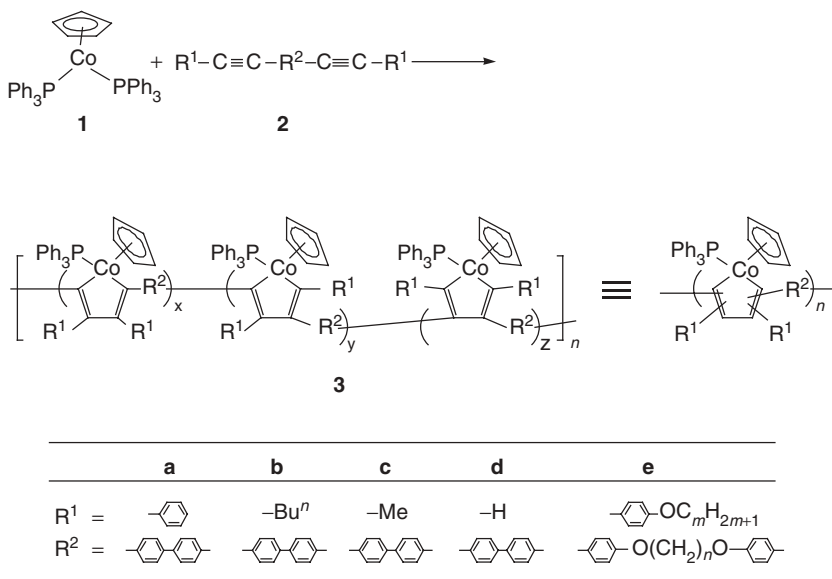
**Figure 2** General idea for mainchain reactive organometallic polymers.

## II. SYNTHESIS AND REACTIONS OF ORGANOMETALLIC POLYMERS POSSESSING METALLACYCLES IN THE MAINCHAIN

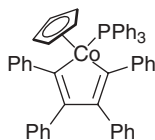
### A. Cobaltacyclopentadiene-Containing Polymers

Polymers containing cobaltacyclopentadiene moieties in the mainchain (**3**) are produced in high yields by the reaction of  $\text{CpCo}(\text{PPh}_3)_2$  (**1**) and diynes (**2**) in toluene at 50–60°C (scheme 1).<sup>4</sup> The polymerization should be carried out under the inert atmosphere because of the instability of **1** under air. The molecular weight of the resulting polymers (**3**) depends on the purity of **1**, which reached up to  $2.0 \times 10^5$ .<sup>5</sup> The brown-colored polymers (**3**) thus obtained are soluble in organic solvents such as chloroform, toluene, and tetrahydrofuran (THF); and they are stable under air and can be kept at least for a few months without any change in their molecular weight. The polymers are occasionally contaminated with cyclobutadienecobalt moieties (~10%). In terms of the regiochemistry of the mainchain connections at each cobaltacyclopentadiene unit, three regioisomers (i.e., the connections through 2,5-, 2,4-, and 3,4-positions of the metallacycles) should exist with a statistical distribution unless the character of the lateral substituents on the starting diynes are not different from that of the fragments between two acetylene moieties (e.g., **3a**).<sup>2b</sup> Namely, the regioselectivity of the mainchain connections can be controlled to some extent by the substituents on the diyne monomers. Using diynes with less sterically hindered lateral substituents such as **2b** and **2c**, the selectivity of the 2,5-linkage increased (the content of 2,5- in **3b** is ~70% and in **3c** is ~100%), but the solubility of the polymers in organic solvents decreased.

The UV–Vis spectrum of **3a** exhibited a subtle red shift compared to that of a model compound, a 2,3,4,5-tetraphenyl substituted cobaltacyclopentadiene (**4**). According to Nishihara et al., the organocobalt polymer obtained from terminal diyne (**3d**) showed a significant red shift in its UV–Vis spectrum, although the polymer is barely soluble in organic solvents.<sup>6</sup>



Scheme 1



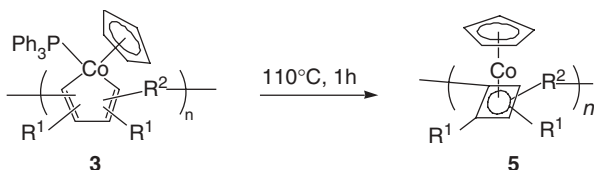
4

Thermal decomposition of the organocobalt polymers is observed at approximately 200°C by the thermogravimetric analyses (TGAs). This temperature is close to the decomposition point of a model cobaltacyclopentadiene (**4**) (193–194°C).<sup>2a</sup> The two-step decomposition was observed in all the organocobalt polymers. The first decomposition starting at 200°C can be attributed to the rearrangement of the cobaltacyclopentadiene moieties into the cyclobutadienecobalt, which accompanies the elimination of triphenylphosphine (vide infra) and the second one above 400°C to the decomposition of the organic fragments. No peak for either the glass-transition ( $T_g$ ) or the melting temperature ( $T_m$ ) is observable for **3a** in its differential scanning calorimetric (DSC) analysis. Organocobalt polymers (**3e**) that exhibit  $T_g$  and  $T_m$  points could be designed from diynes with flexible spacers (**2e**).<sup>7</sup> The polymers (**3e**) have  $T_g$  values at -20–130°C, depending on the length of the aliphatic spacers. Some of the polymers also exhibit  $T_m$  values in the range of 60–120°C.

## B. Conversion of Cobaltacyclopentadiene-Containing Polymers into Polymers Possessing Various Mainchain Structures

### i. Conversion into Other Organometallic Polymers

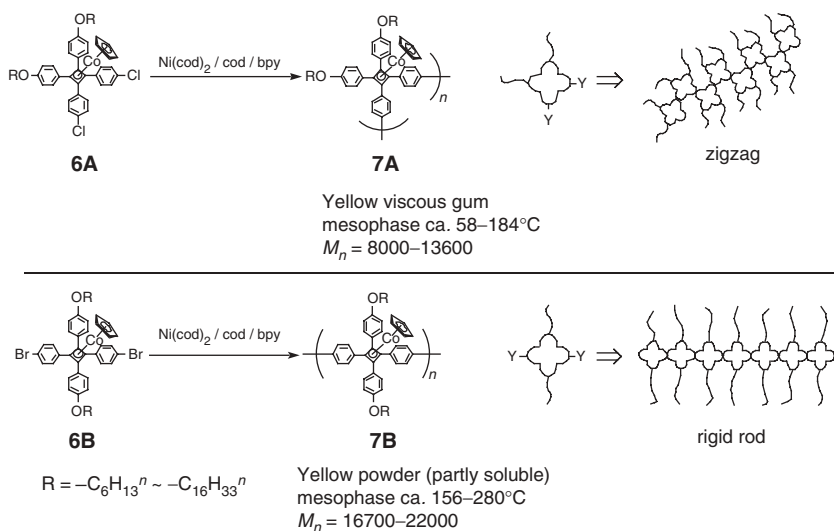
As mentioned above, organocobalt polymers are stable under air. However, they serve as novel type of reactive polymers whose mainchain can be reconstructed by polymer reactions under appropriate conditions. Yellow-colored polymers (**5**) containing  $\eta^4$ -cyclobutadienecobalt moieties are produced by the thermal rearrangement reaction of the organocobalt polymers (**3**) in a solution (scheme 2).<sup>8</sup> As can be monitored in TGA analyses of **3**, this rearrangement also takes place in bulk. However, it is preferable to carry out the reaction in the solution to avoid the formation of insoluble products. This reaction seems to proceed by the dissociation of the ligand followed by the elimination of the cobalt. The cyclobutadienecobalt-containing polymers (**5**) are also stable under air and soluble in organic solvents such as chloroform, THF, and *N,N*-dimethylformamide (DMF). The polymer (**5a**) produced from **3a** exhibited good thermal stability, and the 5%-weight loss was observed at 480°C in its TGA. The cobaltacyclopentadiene-containing polymers with flexible spaces (**3e**) also give rise to cyclobutadienecobalt-containing polymers (**5e**) by the thermal treatment. The resulting cyclobutadienecobalt-containing polymers (**5e**) also have  $T_g$  and  $T_m$  points.<sup>7</sup>



Scheme 2

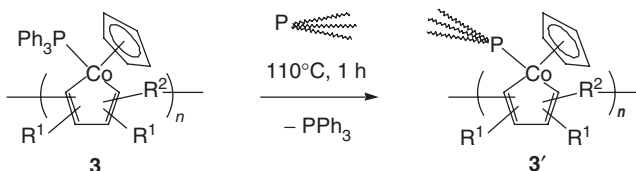
Unique functional materials might be created based on the cyclobutadienecobalt-containing polymers because of their chemical and thermal stability and of the peculiar square geometry of the cyclobutadiene ligands. Reflecting on the squarer geometry of the cyclobutadiene moieties, thermotropic liquid-crystalline polymers can be designed by the polycondensation of the regioisomerically pure organocobalt monomers.<sup>9-12</sup> As shown in scheme 3, the Ni(0)-promoted dehalogenation polycondensation of both 1,2- and 1,3- regioisomerically pure bifunctional ( $\eta^5$ -cyclopentadienyl)( $\eta^4$ -cyclobutadiene)cobalt complexes (**6A** and **6B**) yields zigzag and rigid-rod  $\pi$ -conjugated polyarylenes (**7A** and **7B**), respectively.<sup>11</sup> Both of these polymers exhibit thermotropic and, in some cases, lyotropic liquid-crystalline behavior. However the properties of these two series of the polymers are entirely different; the zigzag-type polymers (**7A**) exhibit thermotropic liquid crystals in a lower temperature range and higher solubility in organic solvents compared to the rigid-rod

type polymers (**7B**). In the case of the polymers consisting of both these two monomer units, the thermal properties of the polymers are controllable by the ratio of the 1,2- and the 1,3-isomers incorporated into the polymers, where the mesomorphic temperature rose with the increase of the rigidity of the polymer backbone by increasing the 1,3-linkage.<sup>13</sup> Likewise the polymerization using the Heck reaction of the organocobalt monomers (**6A** and **6B**) with *p*-divinylbenzene can give rise to polymers with arylene–vinylene backbones, which also exhibited the thermotropic liquid-crystalline phase.<sup>12</sup>



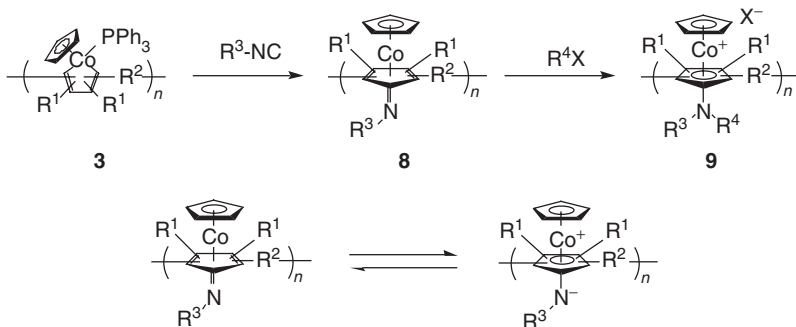
**Scheme 3**

In the presence of appropriate ligands, triphenylphosphine on the organocobalt polymers (**3**) can be replaced by the added ligands such as trialkylphosphines (scheme 4).<sup>14</sup> Because this ligand-exchange reaction takes place under the similar conditions for the rearrangement reaction to the cyclobutadienecobalt-containing polymers, the reaction should be carried out in the presence of excessive amounts of the ligands to avoid the contamination of the cyclobutadienecobalt units. For instance, the quantitative replacement reaction of **3a** takes place in the presence of 10 equiv excess of tri-*n*-alkylphosphines, while the use of a stoichiometric amount of the phosphine brought about the polymers with 30–40% of the cyclobutadienecobalt units. The solubility of the polymer **3** is affected by the coordinated phosphines. For example, a polymer (**3a**) prepared by the reaction of **3a** with tri-*n*-octylphosphine is soluble in hexane, a poor solvent for **3a**.



Scheme 4

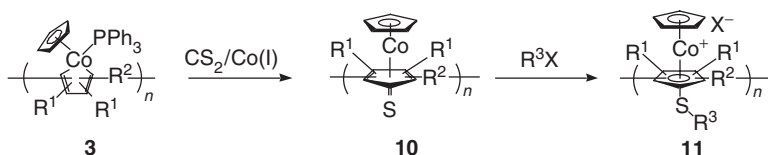
The chemical conversion of the cobaltacyclopentadiene-containing polymers (**3**) with appropriate reagents can also give rise to polymers with other organometallic moieties. On the basis of the reaction of cobaltacyclopentadiene derivatives with isocyanides that gives rise to  $(\eta^5\text{-cyclopentadienyl})(\eta^4\text{-iminocyclopentadiene})$ cobalt derivatives,<sup>2k</sup> polymers having  $(\eta^5\text{-cyclopentadienyl})(\eta^4\text{-iminocyclopentadiene})$ cobalt moieties in the mainchain (**8**) are obtained with a quantitative conversion (scheme 5).<sup>15</sup> It is of note that the polymers produced exhibit a unique solvatochromism. That is, a polymer solution exhibits a reversible color change from purple to red by varying the nature of the solvent (e.g., purple in benzene and red in methanol). This color change might be ascribable to the structural change between the neutral  $(\eta^4\text{-iminocyclopentadiene})$ cobalt unit and the zwitterionic cobalticenium unit. The subsequent polymer reaction of **8** with alkyl halides gives polymers containing cobalticenium units (**9**), although the efficiency of the alkylation was not quantitative due to the precipitation of the polymer during the reaction. The electrochemical analysis of **9** suggests the presence of the electronic interaction between the plural organometallic centers which might be of importance for applications of the polymers.



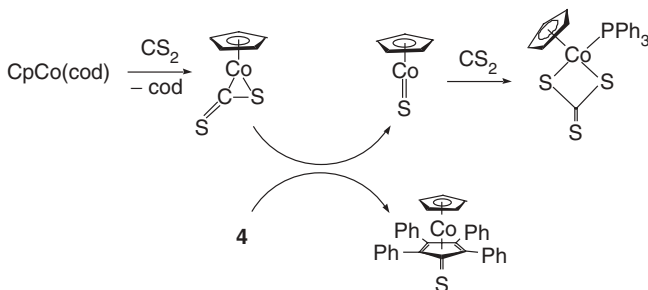
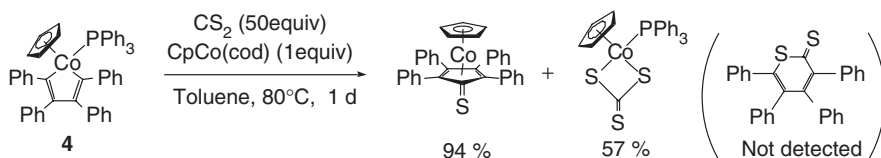
Scheme 5

Analogous cobalticenium-containing polymers (**11**) are also obtainable by the reaction of the polymers (**3**) with carbon disulfide in the presence of a Co(I) complex, followed by the S-alkylation (scheme 6).<sup>16</sup> It is reported that the reaction of **4** with carbon disulfide gives unsaturated dithiolactones in moderate yields.<sup>21</sup> On the

contrary, the addition of an equimolar amount of Co(I) complexes such as CpCo(cod) to the reaction system gives rise to an entirely different result. In this case, the dithiolactones were not detected at all and ( $\eta^4$ -cyclopentadiene)cobalt complexes are obtained in excellent yields.<sup>17</sup> This reaction is likely to proceed by the reaction of the cobaltacyclopentadiene derivative (**4**) with carbon monosulfide generated in situ by reduction of carbon disulfide with the Co(I) complexes (scheme 7).



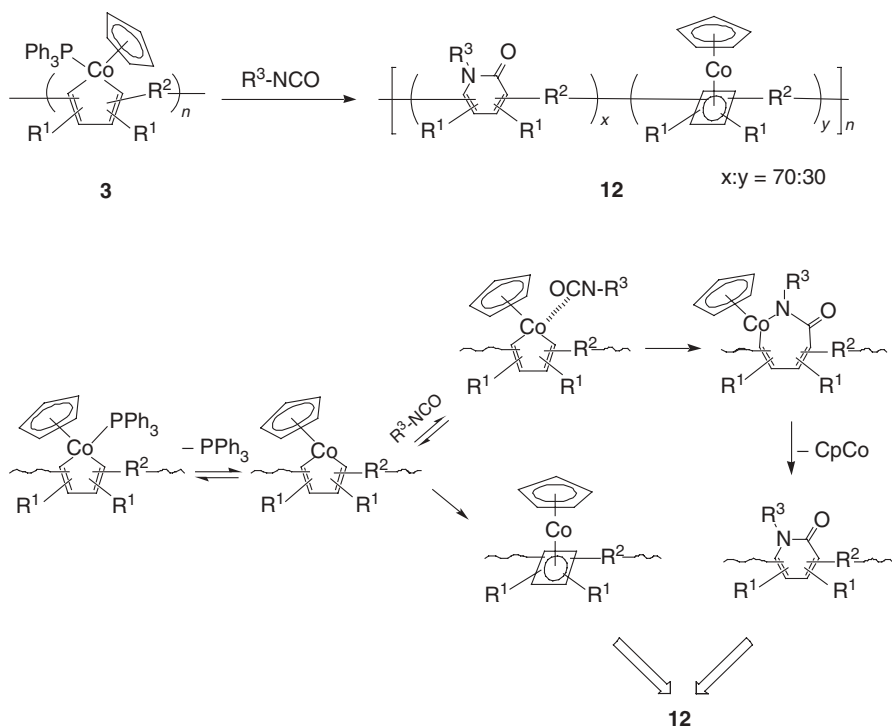
Scheme 6



Scheme 7

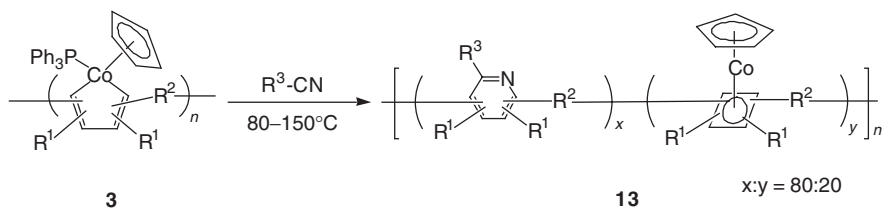
### ii Conversion into Organic Polymers with Various Functional Groups in the Mainchain

Chemical conversion of the organocobalt polymers (**3**) into functional polymers is attainable by the polymer reactions with appropriate reagents. Novel polymers having pyridone moieties in the mainchain (**12**) are produced from **3** by the reaction with isocyanates (scheme 8).<sup>18</sup> This polymer reaction proceeds smoothly at  $120^\circ\text{C}$ , and the content to the 2-pyridone moieties reaches about 70% with respect to the starting cobaltacyclopentadiene units. In this case, the remaining 30% is not the starting cobaltacyclopentadiene unit but the  $\eta^4$ -cyclobutadienecobalt moieties as a result of the rearrangement reaction.

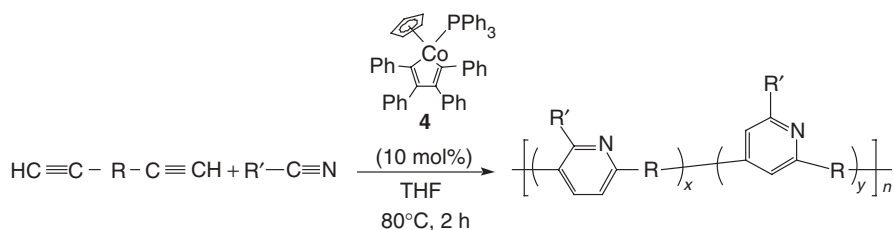


Scheme 8

Polymers containing pyridine moieties in the mainchain (**13**) are likewise obtainable by the reaction of the polymers (**3**) with nitriles (scheme 9).<sup>19</sup> In this case, polymers containing pyridine moieties (about 80%) are produced with an increase of the molecular weight of the polymers. The increase of the molecular weight is most probably due to the pyridine formation of the nitriles with the acetylene moieties at the polymer end catalyzed by the eliminated ( $\eta^5$ -cyclopentadienyl)cobalt(I).<sup>2h,2i,2m</sup> In fact, it is also possible to prepare pyridine-containing polymers directly from diynes and nitriles in the presence of catalytic amount of **4** (scheme 10).<sup>20</sup> Within the examined combinations, this catalytic polymerization by the pyridine-ring-formation process is



Scheme 9



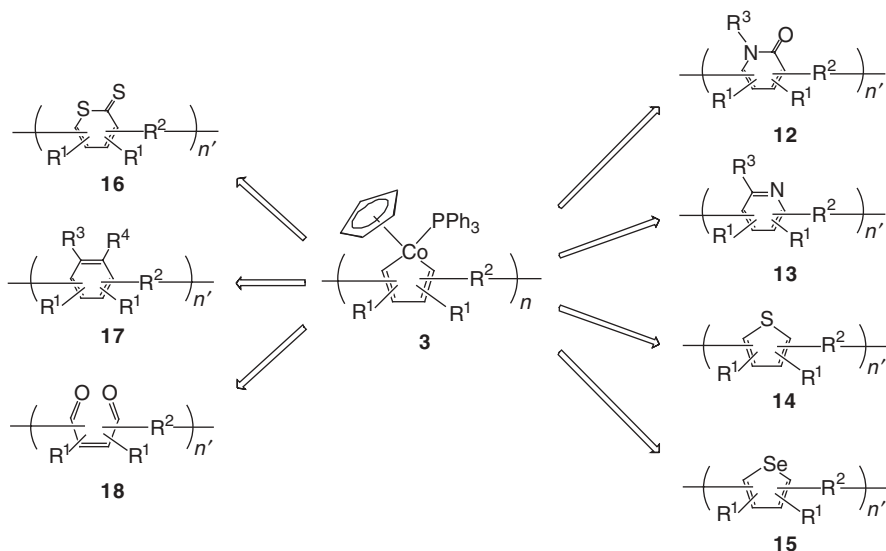
Scheme 10

limited to the terminal diynes otherwise the molecular weight of the polymers does not increase sufficiently.

As summarized in scheme 11, the organocobalt polymers can be converted into many kinds of polymers with versatile functional groups in the mainchain. Thiophene-containing polymers (**14**) can also be prepared from the organometallic polymers (**3**).<sup>21</sup> The polymer reaction takes place simply by heating a toluene solution of the polymer (**3**) with sulfur at 80°C for 1 day in which the cobaltacyclopentadiene moieties in the starting polymers are converted quantitatively to the thiophene rings. By using the polymers whose cobaltacyclopentadiene-diyl repeating units are connected through  $\pi$ -conjugated systems, such as biphenyl-4,4'-diyls (**3a-c**), the polymers produced by the polymer reaction have fully aromatic backbones (i.e., alternating units of thiophene-diyls and the  $\pi$ -conjugated systems). Due to the presence of regioisomeric connections at the produced thiophene moieties, the  $\pi$ -conjugated characters of the polymers are close to those of  $\pi$ -conjugated oligothiophenes, judging from their UV-Vis spectra and the electrochemical properties.

Likewise, the reaction of the polymers (**3**) with selenium proceeds in a quantitative fashion to give selenophene-containing polymers (**15**).<sup>22</sup> The organocobalt polymers (**3**) can be converted to polymers containing unsaturated dithiolactone moieties (**16**) by the reaction with carbon disulfide.<sup>23</sup> In this case, the content of the objective dithiolactone unit in the polymers reaches to 70%. The minor units in the polymers (~30%) are composed of both the cyclobutadienecobalt and the ( $\eta^5$ -cyclopentadienyl)( $\eta^4$ -cyclopentadiene)cobalt moieties by the thermal rearrangement and by the reaction with carbon monosulfide generated in situ from the eliminated cobalt(I) complex with carbon disulfide, respectively.<sup>16,17</sup> Polyphenylenes (**17**) are also obtainable by the reaction of the organocobalt polymers (**3**) with acetylene derivatives.<sup>24</sup> As mentioned above, the organocobalt polymers (**3**) are stable enough to be handled under air. However, on heating a solution of the organocobalt polymers under oxygen, polymers with diketone units (**18**) are produced effectively.<sup>25</sup>

The efficiency of these polymer reactions is affected by the reagents and the reaction conditions, which ranged from 70 to 100%. In the cases of polymer reactions that do not proceed in a quantitative fashion, no distinct decrease of the molecular weight of the produced polymers were observed because the lower efficiency of the polymer reactions does not mean the scission of the mainchain of the polymers but the conversion into other structures such as the cyclobutadienecobalt unit.



Scheme 11

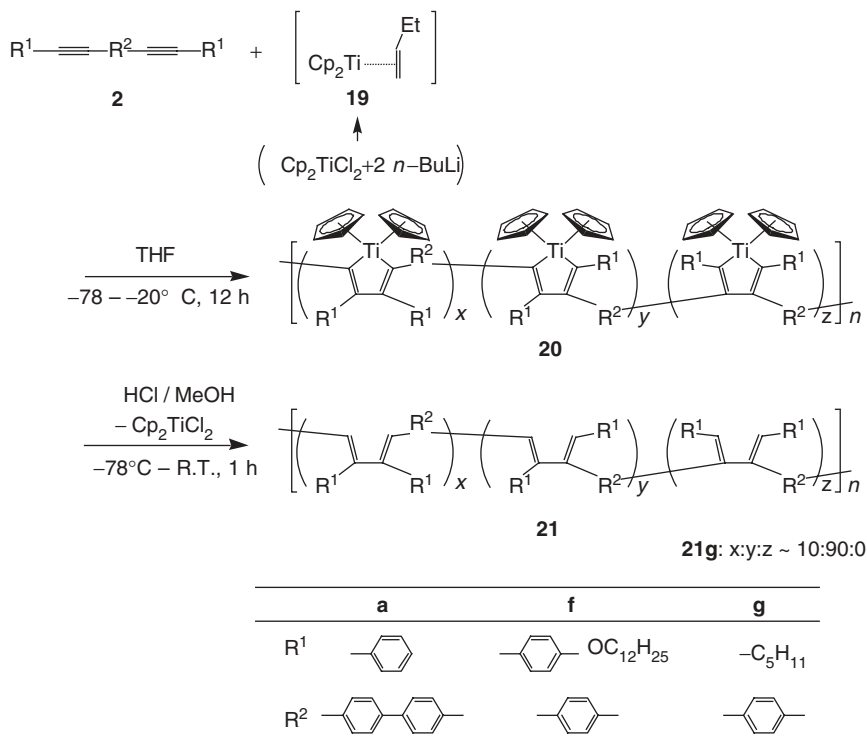
## C. Synthesis and Reactions of Titanacycle-Containing Polymers

### *i. Polymers Containing Titanacyclopentadiene Unit in the Mainchain*

Polymers containing various metallacycle units are attractive synthetic targets for creation of novel polymers with much versatile mainchain reactivity. As described by Tilley et al., zirconacyclopentadiene-containing polymers can be prepared by means of the analogous metallacyclization process between a low-valent bis(cyclopentadienyl)zirconium and diynes, and the resulting zirconium-containing polymers also reveal interesting reactivity.<sup>26</sup>

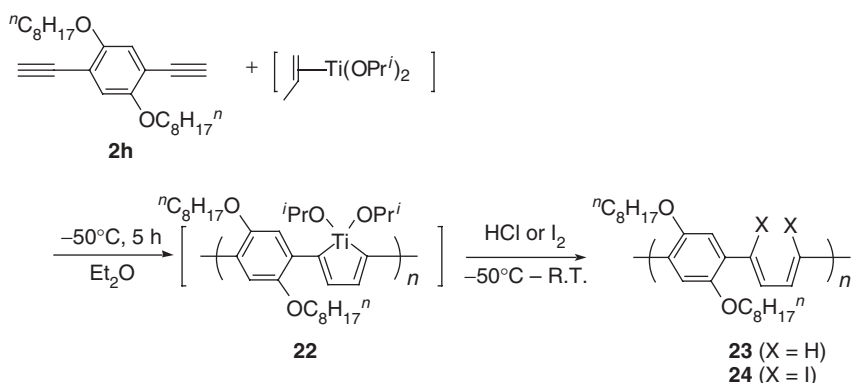
Owing to the recent progress of the chemistry of titanacycles,<sup>3</sup> polymers possessing titanacyclopentadiene units are also potentially attractive for the creation of mainchain reactive materials. On the basis of the titanacyclization process described recently by Takahashi et al.,<sup>3a</sup> it is possible to prepare titanacyclopentadiene-containing polymers.<sup>27</sup> That is, the polymerization of diynes (**2**) and a low-valent titanocene derivative (**19**) generated from bis(cyclopentadienyl)titanium dichloride gives the objective polymers (**20**), which are stable at ambient temperature under argon atmosphere (scheme 12).

The hydrolytic workup of the polymers (**20**) gives rise to diene-containing polymers (**21**) in moderate yields ( $M_n \sim 4000$ ). The regioisomeric linkage of the mainchain of **20** at the titanacycle moieties must depend on the diynes used and the polymers (**20a** and **20f**) may have statistical distribution of 2,5-, 2,4-, and 3,4-linkages, although these units are difficult to be distinguished by the spectroscopic methods. In the case of the polymer (**20g**), the regiochemistry could be determined by the model experiment. In the case of the titanacycles obtained from 1-heptynylbenzene, two phenyl

**Scheme 12**

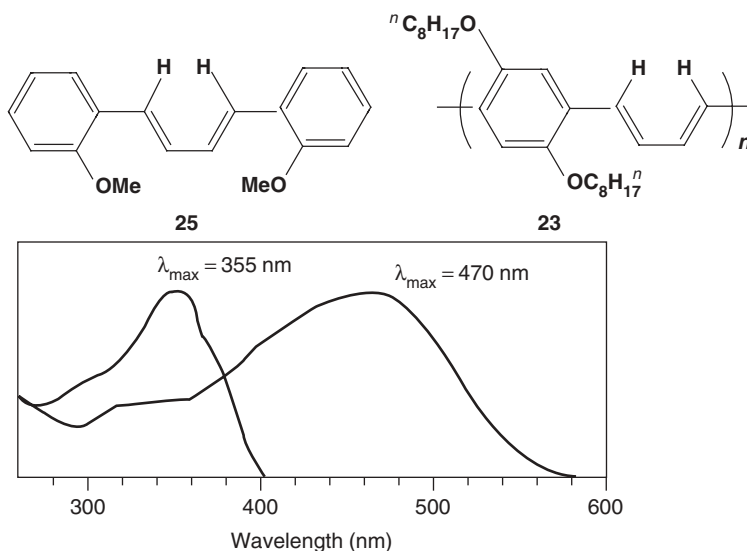
substituents are located at the 2,4- and the 2,5-positions (2,4-:2,5- = 90:10), judging from their hydrolysis products. Accordingly, the mainchain of the polymer (**20g**) is supposed to be connected through the 2,4- and the 2,5-positions of the metallacycle moieties. Because of the rather low content of the 2,5-connection, an effective linkage for  $\pi$ -conjugation, the polymer (**21g**) produced exhibited a relatively small red shift in the UV-Vis spectrum in comparison with the model dienes. The result also supports that the polymer (**20g**) produced from the low-valent titanocene derivative and diyne (**2g**) has the major 2,4- and the minor 2,5-connections through the titanacycle units.

As shown in scheme 13, titanacyclopentadiene-containing polymers with a regiospecific mainchain connection could be obtained by the polymerization of terminal diynes (**2h**) and a low-valent titanium generated from titanium(IV) isopropoxide.<sup>28</sup> The polymerization proceeds at  $-78^\circ\text{C}$  to  $-50^\circ\text{C}$ , and the polymers produced should be converted into other polymers without isolation because they are not stable at ambient temperature. According to the report of Yamaguchi et al.,<sup>3b</sup> 1,4-disubstituted dienes are produced in the reaction of terminal acetylenes such as phenylacetylene followed by the hydrolysis. In accordance with their report, the polymerization of terminal diynes such as 1,4-diethynyl-2,5-dioctyloxybenzene (**2h**) gives rise to polymers with regioregular backbone (**22**). The hydrolysis or the iodination of the titanacycle unit

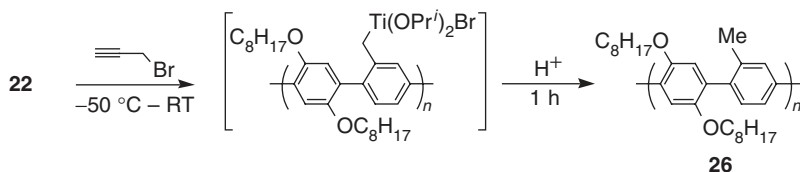


Scheme 13

gave rise to polymers with diene units (**23** and **24**, respectively). For example, the treatment of the polymer (**22**) with iodine provided an iodinated diene-containing polymer (**24**) in 81% yield ( $M_n = 7700$ ). Owing to the alkoxy substituents, both the polymers (**23** and **24**) are soluble in organic solvents. The regioregularity of the mainchain affects largely on the properties of the diene-containing polymers. The polymer (**23**) produced by the hydrolysis of the titanacyclopentadiene-containing polymer exhibits a clear bathochromic shift of the UV–Vis absorption compared to that of a model compound (**25**) (Fig. 3). That is, the absorption maximum ( $\lambda_{\max}$ ) of the polymer ( $\lambda_{\max} = 470$  nm) appeared at longer wavelength by 115 nm than that of the model compound ( $\lambda_{\max} = 355$  nm). The polymers also exhibit luminescence upon irradiation of the UV–Vis light.

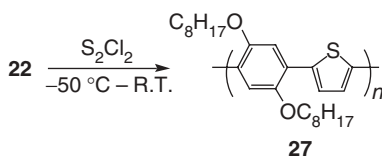

 Figure 3 UV–Vis spectra of polymer **23** and its model compound (**25**) (measured in  $\text{CHCl}_3$ ).

Derivatives of poly(*p*-phenylene) (**26**) are produced by the reaction of the titanacyclopentadiene-containing polymers (**22**) with propargyl bromide (scheme 14).<sup>29</sup> Similar to the case of the chemical conversion into diene-containing polymers, the polymer reaction proceeds under mild conditions, and the yellow powdery polymers produced are soluble in organic solvents (~80% yield,  $M_n \sim 5000$ ). Because of the  $\pi$ -conjugated backbone, the poly(*p*-phenylene) derivatives (**26**) obtained in this study have the UV–Vis absorption in a longer wavelength range ( $\lambda_{\max} = 329$  nm) than that of model compounds ( $\lambda_{\max} = 276$  nm), *p*-terphenyl derivatives produced from phenylacetylene derivatives via the titanacyclopentadiene. The polymers also exhibited photoluminescence whose emission maximum also shifts to the longer wavelength region with respect to that of the model compounds.



Scheme 14

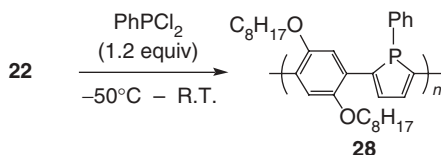
Thiophene-containing polymers (**27**) are likewise produced by the reaction of the titanacyclopentadiene-containing polymers (**22**) with sulfur monochloride under mild conditions (scheme 15).<sup>30</sup> The yield of the soluble fraction was a little lower (~50%) because the produced polymers are partially insoluble in organic solvents. The brown powdery polymers thus obtained exhibit a substantial bathochromic shift in the UV–Vis and photoluminescence spectra compared to those of the corresponding model compounds, 2,5-diarylthiophenes.



Scheme 15

The titanacyclopentadiene-containing polymers (**22**) can be converted into  $\pi$ -conjugated phosphole-containing polymers (**28**) by the reaction with dichlorophenylphosphine (scheme 16).<sup>31</sup> Similar to the case of the above-mentioned conversion reaction into thiophene-containing polymers, the produced polymers are partially

insoluble in organic solvents. The polymers thus obtained revealed  $\lambda_{\max}$  at about 500 nm in the UV–Vis spectra and the emission maximum at 600 nm, supporting the  $\pi$ -conjugated character of the resulting phosphole-containing polymers.

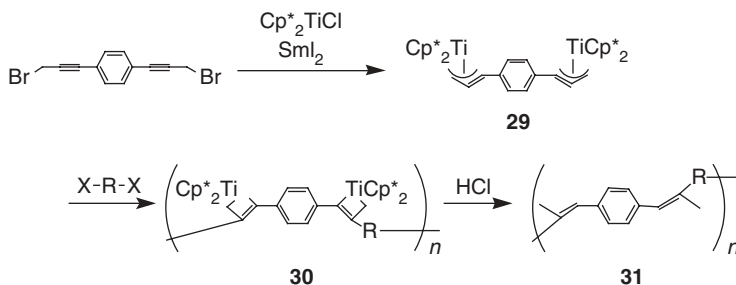


Scheme 16

### ii. Polymers Possessing Other Titanacycle Units

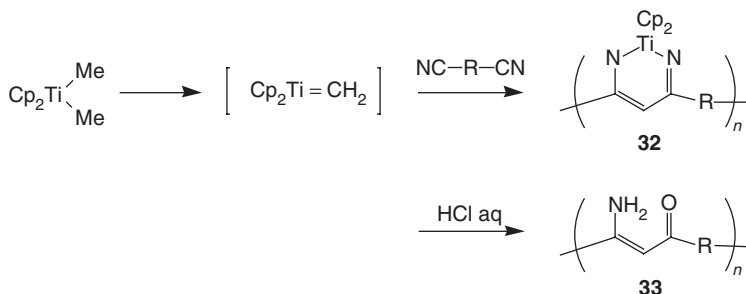
On the basis of the fact that not only the titanacyclopentadienes but also many kind of titanacycles are important intermediates of the organic reactions as well as the catalytic cycles,<sup>3F-31</sup> the synthesis and the reactions of polymers containing other titanacycle systems, such as titanacyclobutene and diazatitanacyclohexadiene moieties, were also studied.

Metallacyclobutenes are regarded as intermediates of metathesis reactions of acetylene derivatives. Incorporation of metallecyclobutene units might realize polymers with unique reactivity and/or catalytic activity. Thus, as a preliminary example, titanacyclobutene-containing polymers (**30**) were prepared by the reaction of bis(pentamethylcyclopentadienyl)propargyltitaniums (**29**) with organic dihalides (scheme 17).<sup>32</sup> The polymers (**30**) are soluble in organic solvents and stable at ambient temperature under argon atmosphere. Under the hydrolytic workup conditions, these polymers can be converted into polymers with unsaturated systems (**31**). Although we do not have sufficient results to support the reactivity and/or the catalytic activity of these polymers yet, these polymers are potentially useful as synthetic precursors of organic polymers with unique functionality and as macroinitiators for the polymerization of unsaturated monomers.



Scheme 17

Polymers with diazatitanacyclohexadiene units (**32**) could be prepared by the reaction of bis(cyclopentadienyl)dimethyltitanium and dicyano compounds (scheme 18).<sup>33</sup> Protonation of the polymers gave rise to polymers with  $\beta$ -amino- $\alpha,\beta$ -unsaturated ketone-repeating units (**33**). Judging from the versatile reactivity of the diazatitanacyclohexadiene derivatives, the polymers (**32**) might also serve as attractive reactive materials.



**Scheme 18**

### III. SUMMARY

Novel polymers possessing reactive sites in the mainchain have been successfully prepared by the reactions of diynes with low-valent transition metal complexes such as cobalt(I) and titanium(II). The cobaltacyclopentadiene-containing polymers are stable under air and can be handled like common organic polymers. However, they exhibit versatile reactivity under appropriate reaction conditions. That is, the organocobalt polymers serve as reactive precursors for a variety of polymers containing functional groups such as heterocycles, benzene rings, and unsaturated ketones in their repeating unit. The organocobalt polymers can also be converted to other organocobalt polymers with unique repeating units such as cyclobutadienecobalt and cobalticenium moieties. The titanacyclopentadiene-containing polymers are likewise obtained by the metallacyclization process of diynes with low-valent titanium complexes. Although the two series of the titanacyclopentadiene-containing polymers are not stable under air, they serve as reactive precursors giving rise to organic polymers with versatile mainchain structures.

In both cases, the structure of the organometallic polymers can be designed by the diyne monomers. The regiochemistry of the mainchain connections at each metallacycle unit is affected by the nature of the substituents on diynes and/or the ligands on the low-valent transition metal complexes. It was also demonstrated that the regioselectivity of the mainchain connections reflects directly on the character of the functional polymers obtained by the polymer reactions. That is, the organotitanium polymers with regiospecific mainchain connections obtained from titanium

isopropoxide and terminal diynes can yield organic polymers with excellent  $\pi$ -conjugated characters, whereas the regio-irregular organometallic polymers provides organic polymers with irregular mainchain connections.

Further studies on the synthesis and the reactions of reactive organometallic polymers might be an effective approach to establish a new polymer synthetic route for organic functional polymers with well-defined structures. It might also be possible that the polymer reaction routes give organic polymers whose structural units are difficult to be designed by the conventional polycondensation routes. Further studies are in progress to expand the scope of the main chain reactive organometallic polymers.

## REFERENCES

1. See, for example, Y. Chujo, I. Tomita, T. Saegusa, *Makromol. Chem. Symp.*, **70/71**, 47 (1993).
2. For the chemistry of cobaltacyclopentadiene derivatives, see (a) H. Yamazaki, Y. Wakatsuki, *J. Organomet. Chem.*, **139**, 157 (1977). (b) Y. Wakatsuki, O. Nomura, K. Kitaura, K. Morokuma, H. Yamazaki *J. Am. Chem. Soc.*, **105**, 1907 (1983). (c) Y. Wakatsuki, H. Yamazaki, *J. Chem. Soc., Dalton Trans.*, 1923 (1982). (d) P. Hong, H. Yamazaki, *Synthesis*, 50 (1977). (e) Y. Wakatsuki, H. Yamazaki, *J. Chem. Soc., Dalton Trans.*, 1923 (1982). (f) K. Yasufuku, A. Hamada, K. Aoki, H. Yamazaki, *J. Am. Chem. Soc.*, **102**, 4363 (1980). (g) H. Yamazaki, N. Hagihara, *J. Organomet. Chem.*, **7**, P22 (1967). (h) Y. Wakatsuki, H. Yamazaki, *Tetrahedron Lett.*, 3383 (1973). (i) Y. Wakatsuki, H. Yamazaki, *Synthesis*, 26 (1976). (j) Y. Wakatsuki, H. Yamazaki, *J. Chem. Soc., Dalton Trans.*, 1278 (1978). (k) H. Yamazaki, Y. Wakatsuki, *Bull. Chem. Soc. Jpn.*, **52**, 1239 (1979). (l) Y. Wakatsuki, H. Yamazaki, *J. Chem. Soc., Chem. Commun.*, 280 (1973). (m) D. J. Brien, A. Naiman, K. P. C. Volhardt, *J. Chem. Soc., Chem. Commun.*, 133 (1982).
3. For the chemistry of titanacycles related to this chapter, see (a) K. Sato, Y. Nishihara, S. Huo, Z. Xi, T. Takahashi, *J. Organomet. Chem.*, **633**, 18 (2001). (b) S. Yamaguchi, R. Z. Jin, K. Tamao, F. Sato, *J. Org. Chem.*, **63**, 10060 (1998). (c) E. Block, M. Birringer, C. He, *Angew. Chem. Int. Ed. Engl.*, **38**, 1604 (1999). (d) D. Suzuki, R. Tanaka, H. Urabe, F. Sato, *J. Am. Chem. Soc.*, **124**, 3518 (2002). (e) R. Tanaka, S. Hirano, H. Urabe, F. Sato, *Org. Lett.*, **5**, 67 (2003). (f) S. Ogoshi, J. M. Stryker, *J. Am. Chem. Soc.*, **120**, 3514 (1998). (g) J. D. Mainhart, R. H. Grubbs, *Bull. Chem. Soc. Jpn.*, **61**, 171 (1988). (h) K. M. Doxsee, J. K. M. Mouser, *Tetrahedron Lett.*, **32**, 1687 (1991). (i) K. M. Doxsee, G. S. Shen, C. B. J. Knobler, *J. Am. Chem. Soc.*, **111**, 9129 (1989). (j) K. M. Doxsee, J. K. M. Mouser, *Organometallics*, **9**, 3012 (1990). (k) K. M. Doxsee, J. B. Farahi, *J. Am. Chem. Soc.*, **110**, 7239 (1988). (l) J. Barluenga, C. P. Losada, *Tetrahedron Lett.*, **33**, 7579 (1992).
4. I. Tomita, A. Nishio, T. Igarashi, T. Endo, *Polym. Bull.*, **30**, 179 (1993).
5. J.-C. Lee, A. Nishio, I. Tomita, T. Endo, *Macromolecules*, **30**, 5205 (1997).
6. A. Ohkubo, K. Aramaki, H. Nishihara, *Chem. Lett.*, 271 (1993).
7. I. L. Rozhanskii, I. Tomita, T. Endo, *Macromolecules*, **29**, 1934 (1996).
8. I. Tomita, A. Nishio, T. Endo, *Macromolecules*, **27**, 7009 (1994).
9. Buntz et al. reported the synthesis of arylene-ethynylene type polymers from regioisomerically pure cyclobutadienecobalt derivatives. See (a) M. Altmann, U. H. F. Bunz, *Macromol. Rapid Commun.*, **15**, 785 (1994). (b) M. Altmann, U. H. F. Bunz, *Angew. Chem., Int. Ed. Engl.*, **34**, 569 (1995).
10. (a) I. L. Rozhanskii, I. Tomita, T. Endo, *Macromolecules*, **30**, 1222 (1997). (b) I. L. Rozhanskii, I. Tomita, T. Endo, *Polymer*, **40**, 1581 (1999).
11. (a) I. L. Rozhanskii, I. Tomita, T. Endo, *Chem. Lett.*, 477 (1997). (b) Y. Sawada, I. Tomita, I. L. Rozhanskii, T. Endo, *J. Inorg. Organomet. Polym.*, **10**, 221 (2000). (c) Y. Sawada, I. Tomita, T. Endo, *Makromol. Chem. Phys.*, **201**, 510 (2000).

12. Y. Sawada, I. Tomita, T. Endo, *Polym. Bull.*, **43**, 165 (1999).
13. (a) Y. Sawada, I. Tomita, T. Endo, unpublished data. (b) Y. Sawada, I. Tomita, and T. Endo, *Polym. Prepr. Jpn.*, **47**, 1445 (1998).
14. I. Tomita, A. Nishio, T. Endo, *Appl. Organometal. Chem.*, **12**, 735 (1998).
15. I. Tomita, J.-C. Lee, T. Endo, *J. Organomet. Chem.*, **611**, 570 (2000).
16. (a) J.-C. Lee, I. Tomita, T. Endo, unpublished data. (b) J.-C. Lee, I. Tomita, T. Endo, *Polym. Prepr. Jpn.*, **46**, 1617 (1997).
17. J.-C. Lee, I. Tomita, T. Endo, *Chem. Lett.*, 121 (1998).
18. I. Tomita, A. Nishio, T. Endo, *Macromolecules*, **28**, 3042 (1995).
19. J.-C. Lee, I. Tomita, T. Endo, *Polym. Bull.*, **39**, 415 (1997).
20. (a) I. Tomita, J.-C. Lee, T. Endo, *Macromolecules*, **28**, 5688 (1995). (b) J.-C. Lee, I. Tomita, T. Endo, *J. Polym. Sci. Part A Polym. Chem.*, **37**, 1979 (1999).
21. J.-C. Lee, I. Tomita, T. Endo, *Macromolecules*, **31**, 5916 (1998).
22. (a) J.-C. Lee, I. Tomita, T. Endo, unpublished data. (b) J.-C. Lee, I. Tomita, T. Endo, *Polym. Prepr. Jpn.*, **45**, 1463 (1996).
23. (a) I. Tomita, J.-C. Lee, A. Nishio, T. Endo, unpublished data. (b) I. Tomita, A. Nishio, T. Endo, *Pacific Polym. Prepr.*, **3**, 661 (1993). (c) J.-C. Lee, I. Tomita, T. Endo, *Polym. Prepr. Jpn.*, **46**, 1617 (1997).
24. (a) J.-C. Lee, I. Tomita, T. Endo, unpublished data. (b) J.-C. Lee, I. Tomita, T. Endo, *Polym. Prepr. Jpn.*, **47**, 1760 (1998).
25. (a) J.-C. Lee, I. Tomita, T. Endo, unpublished data. (b) J.-C. Lee, I. Tomita, T. Endo, *Polym. Prepr. Jpn.*, **46**, 1619 (1997).
26. (a) S. S. H. Mao, T. D. Tilley, *J. Am. Chem. Soc.*, **117**, 5365 (1995). (b) S. S. H. Mao, T. D. Tilley, *Macromolecules*, **30**, 5566 (1997).
27. (a) M. Ueda, I. Tomita, unpublished data. (b) M. Ueda, I. Tomita, *Polym. Prepr. Jpn.*, **51**, 1259 (2002).
28. (a) I. Tomita, K. Atami, T. Endo, M. Ueda, T. Utsumi, unpublished data. (b) I. Tomita, K. Atami, T. Endo, *Polym. Prepr. Jpn.*, **48**, 341 (1999). (c) I. Tomita, K. Atami, T. Endo, *Polym. Prepr. Jpn.*, **49**, 1641 (2000).
29. (a) T. Utsumi, I. Tomita, unpublished data. (b) T. Utsumi, I. Tomita, *Polym. Prepr. Jpn.*, **51**, 267 (2002).
30. (a) T. Utsumi, I. Tomita, unpublished data. (b) T. Utsumi, I. Tomita, *Polym. Prepr. Jpn.*, **51**, 1323 (2002).
31. (a) M. Ueda, I. Tomita, unpublished data. (b) M. Ueda, I. Tomita, *Polym. Prepr. Jpn.*, **52**, 1255 (2003).
32. (a) M. Ueda, I. Tomita, unpublished data. (b) M. Ueda, I. Tomita, *Polym. Prepr. Jpn.*, **50**, 1291 (2001).
33. (a) M. Ueda, I. Tomita, unpublished data. (b) M. Ueda, I. Tomita, *Polym. Prepr. Jpn.*, **51**, 1437 (2002).

---

## CHAPTER 4

# Mechanistic Aspects of the Photodegradation of Polymers Containing Metal–Metal Bonds Along Their Backbones

**David R. Tyler**

*Department of Chemistry, University of Oregon, Eugene, Oregon*

### CONTENTS

I. INTRODUCTION	78
II. GENERAL OVERVIEW OF POLYMER PHOTODEGRADATION	79
A. The Auto-Oxidation Mechanism	79
B. Reactions of Hydroperoxide Species That Lead to Backbone Degradation	80
C. Other Photochemical Degradation Mechanisms	82
D. Methods for Intentionally Making Polymers Photodegradable	83
III. METAL–METAL BOND-CONTAINING POLYMERS	85
A. Synthesis and Characterization	85
B. Synthesis of the Difunctional Dimers	86
C. Synthesis of the Polymers	88
D. Characterization of the Polymers	90
E. Photochemical Reactions in Solution	91
F. Photochemistry in the Solid State	94

*Macromolecules Containing Metal and Metal-Like Elements,*  
*Volume 6: Transition Metal-Containing Polymers*, edited by Alaa S. Abd-El-Aziz,  
Charles E. Carraher Jr., Charles U. Pittman Jr., and Martel Zeldin.  
Copyright © 2006 John Wiley & Sons, Inc.

IV. FACTORS CONTROLLING THE RATE OF PHOTOCHEMICAL DEGRADATION	95
A. Cage Effects	95
B. The Effect of Tensile Stress on Photodegradation	98
i. Theories of Stress-Induced Photodegradation	98
ii. Stress-Induced Changes in $\phi_{\text{homolysis}}$ ; the Plotnikov Hypothesis	99
iii. Stress-Induced Changes in $k_{\text{recombination}}$ ; the Decreased Radical Recombination Efficiency Hypothesis	100
iv. Stress-Induced Changes in the Rates of Radical Reactions Subsequent to Radical Formation	100
v. The Zhurkov Equation	100
vi. Quantum Yields as a Function of Stress for Polymer 3	101
C. Other Factors Affecting Photochemical Degradation Rates of Polymers	102
i. Absorbed Light Intensity	103
ii. Polymer Morphology	104
iii. Oxygen Diffusion	105
iv. Chromophore Concentration	106
V. ACKNOWLEDGMENTS	106
VI. REFERENCES	106

## I. INTRODUCTION

It is well-known that many polymers are susceptible to photodegradation when exposed to ultraviolet radiation.<sup>1-6</sup> In most instances, degradation is not wanted, and polymer chemists have consequently gone to great lengths to stabilize their materials to the effects of UV radiation. There are an increasing number of applications, however, for polymers that are intended to degrade when exposed to light. For example, photochemically reactive polymers have practical uses as photodegradable plastics, photoresists, biomedical materials, and precursors to ceramic materials.<sup>7</sup> In regard to photochemically degradable plastics, the biggest use is in agriculture, specifically in the burgeoning practice called plasticulture. In plasticulture, the ground is covered with plastic sheeting (typically a polyolefin), which acts as a mulch to (1) prevent the growth of weeds (thus requiring the use of fewer herbicides), (2) decrease water demand, and (3) extend the growing season. By making these agricultural films out of degradable plastics, considerable labor and money can be saved in the plastics-recovery phase of the technique. In the environmental area, photodegradable plastics are finding increased use as packaging materials in items that have a high probability of becoming litter. The idea is that if such materials should end up as litter they will degrade rather quickly and not be an eyesore.

To improve the performance of photodegradable plastics, it is necessary to understand the photochemical decomposition mechanisms so that appropriate features and properties can be incorporated into the polymers to make them suitable as photodegradable materials. In this regard, it is noted that the ideal photodegradable polymer has (at least) two essential properties. First, the polymer will degrade completely and quickly once degradation starts (Fig. 1). This characteristic makes practical sense, but it is also important for structural reasons because most polymer mechanical properties are related to molecular weight.<sup>8</sup> Small amounts of degradation can drastically decrease the molecular weight (and thus the mechanical properties) of a plastic, yet to all appearances the plastic piece is visually unchanged. In essence, the plastic is still present but it is not structurally sound—and hence useless and perhaps dangerous. Under such circumstances, it may as well be completely degraded. The second essential property is that the onset of degradation should be tunable. Again, this property makes practical sense, but it is difficult to achieve in practice because light intensities vary, as do temperatures and a host of other mechanistic variables.

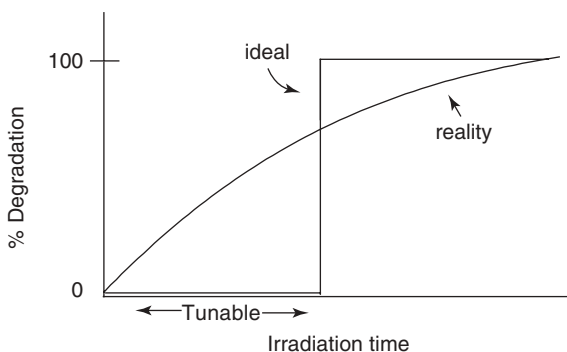


**Figure 1** The properties of an ideal photochemically degradable polymer—namely, tunable onset of degradation and rapid degradation.

This review presents an overview of the mechanistic aspects of polymer photodegradation, with a primary emphasis on a special class of photodegradable polymer that has metal–metal bonds along the polymer backbones. Throughout the review, the major emphasis is on degradation pathways and the parameters that control the rates of degradation.

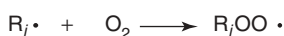
## II. GENERAL OVERVIEW OF POLYMER PHOTODEGRADATION

### A. The Auto-Oxidation Mechanism

In the absence of an intentionally added chromophore, most polymers photochemically degrade by the so-called photo-oxidative mechanism.<sup>1–6,9</sup> Practically

speaking, photo-oxidative degradation refers to reactions initiated by UV radiation because few commodity polymers absorb visible light when they are first manufactured (unless they are specifically designed to degrade in visible light or unless they contain impurities). The photo-oxidative degradation mechanism has been extensively investigated<sup>1-6,9</sup> for polyolefins and selected other polymers, and there is general agreement that the initial phase in the degradation is an auto-oxidation cycle, shown in its most general form in scheme 1. Of course, some polymers degrade by photoreactions that occur in addition to oxidative degradation. PVC, for example, reacts photochemically to eliminate HCl and form C=C bonds.<sup>10,11</sup> Even in these cases, however, oxidative degradation of the polymer still occurs.

*Initiation*



*Propagation*



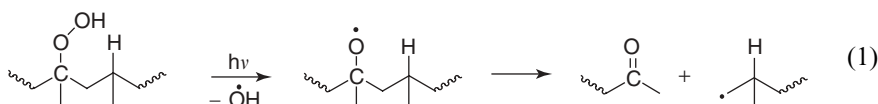
*Termination*

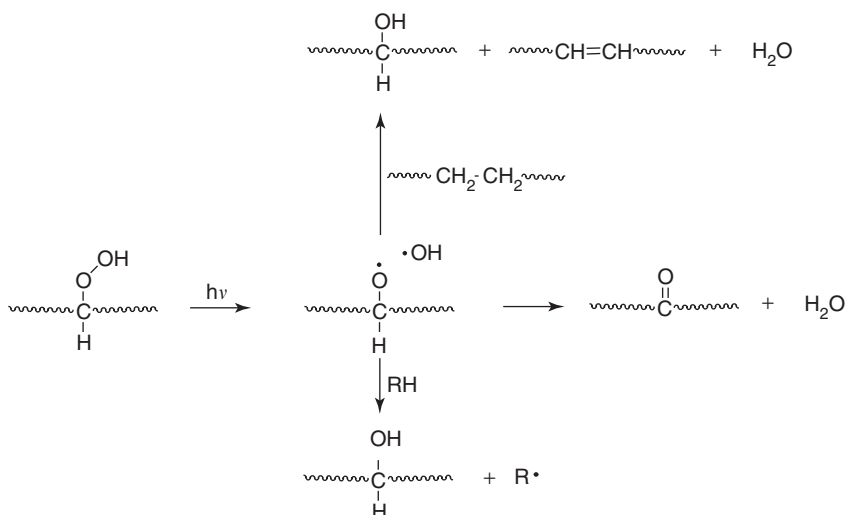
Various radical-radical coupling or disproportionation reactions

**Scheme 1** The autooxidation mechanism for hydrocarbon materials.

## B. Reactions of Hydroperoxide Species That Lead to Backbone Degradation

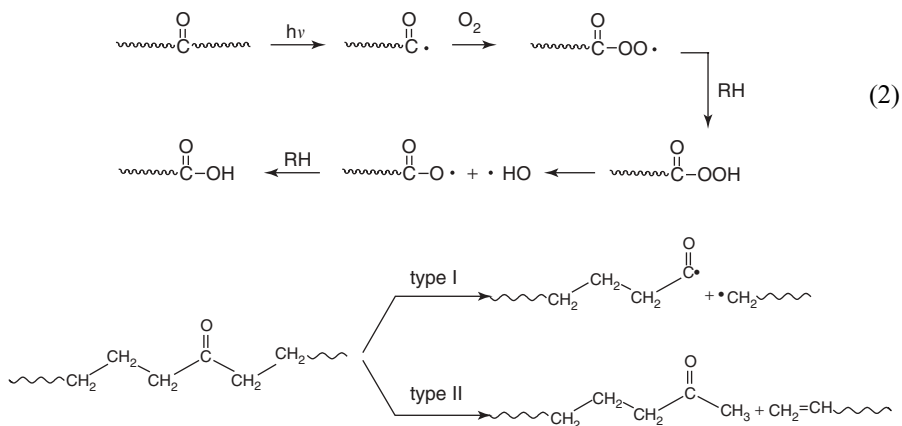
The propagating reactions of the autooxidation cycle (scheme 1) are common to all carbon-backbone polymers and, indeed, to many organic and biochemically relevant molecules. Note, however, that these reactions do not lead to backbone cleavage but rather to a hydroperoxide species. It is the backbone cleavage reactions that are primarily responsible for diminishing the mechanical properties of weathered/photodegraded polymers. Subsequent to hydroperoxide formation, polymer backbone cleavage generally occurs by one of two pathways: (1) Cleavage of the hydroperoxide O—O bond occurs, followed by scission of a  $\beta$ -bond ( $\beta$ -scission) in the alkoxy radical (Eq. 1). (2) The hydroperoxide species react to form new





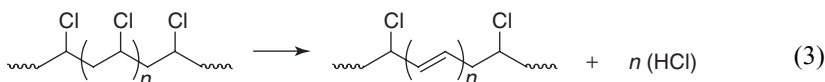
**Scheme 2** Formation of new functional groups and color centers from a hydroperoxide species in a degrading polymer.

functional groups (typically carbonyls, alcohols, carboxylic acids, and olefins) and other chromophores. The most important of these latter reactions are compiled in scheme 2 and equation 2, but not all of these reactions occur in every system. Polymer backbone cleavage then occurs by subsequent irradiation or thermal reactions of these functional groups and chromophores. For example, carbonyl formation leads to backbone cleavage by the Norrish type I and II reactions (scheme 3). It is generally agreed that the  $\beta$ -scission route (Eq. 1) is the prevailing pathway for backbone degradation in the photo-oxidative degradation of most polymers.<sup>5</sup>

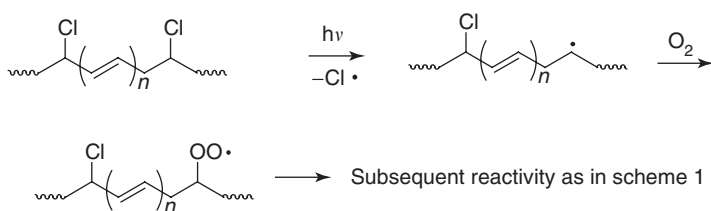


**Scheme 3** Photochemical degradation pathways for polymers containing carbonyl groups along the backbone.

The short polyenes that occur in PVC by elimination of HCl (Eq. 3) are another example of chromophore formation.<sup>10,11</sup>

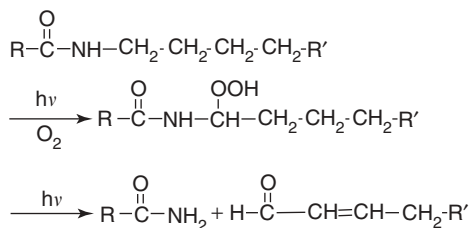


These polyenes readily absorb near-UV and visible light, which is why unstabilized PVC tends to yellow on exposure to UV radiation. Subsequent photochemical reactions with oxygen to form hydroperoxy species then occur as shown in scheme 4.



**Scheme 4** Radical formation in a polyene segment of degraded PVC.

One final example serves to illustrate that backbone cleavage can occur directly from the hydroperoxy species itself. On the basis of resonance Raman studies with polyamides, Valentini et al. proposed the chain scission sequence involving the hydroperoxide species shown in scheme 5.<sup>12</sup>



**Scheme 5** Chain scission in the photo-oxidative degradation of polyamides.

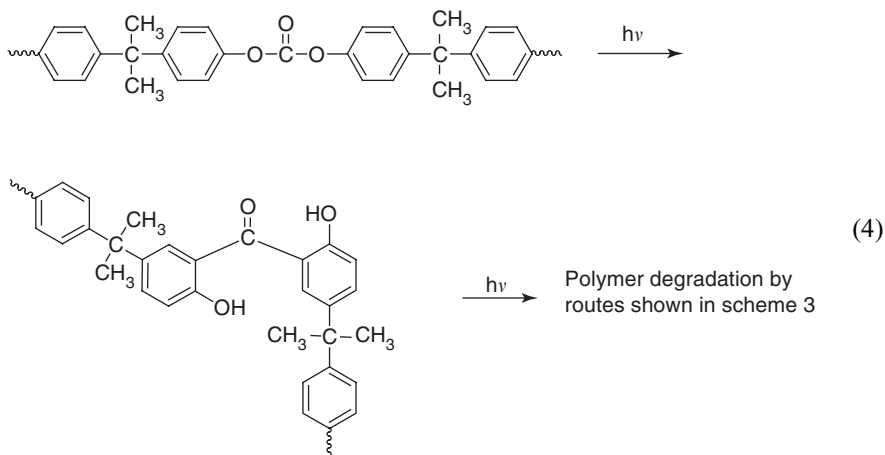
### C. Other Photochemical Degradation Mechanisms

In addition to autocatalytic oxidative degradation, selected polymers undergo additional photochemical reactions, depending on their structure and environment:

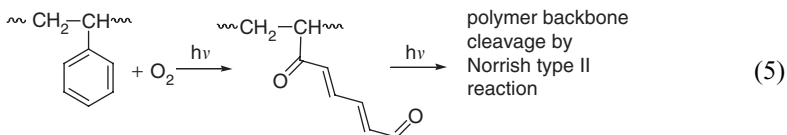
1. As mentioned above, PVC degrades to form polyenes (Eq. 3), which subsequently undergo backbone degradation (scheme 4).<sup>10,11</sup>

2. The photochemical Fries rearrangement can occur in polycarbonates, polyurethanes, epoxies, and other polymers with suitable structures.<sup>13</sup> An example is shown

in equation 4. Note that the net effect of the photochemical Fries rearrangement is to introduce ketone carbonyl groups into the polymer chain. Subsequent degradation of the polymer backbone then occurs according to the reactions in scheme 3.



3. Pendant phenyl rings along polymer backbones (in polystyrene, for example) can undergo photochemical ring-opening reactions, which leads to backbone cleavage by subsequent Norrish type II reactivity (Eq. 5).<sup>6</sup> Again, the introduction of carbonyl groups makes these polymers photochemically degradable.

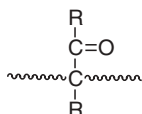


A more complete listing of polymer photochemical reactions can be found in many of the excellent monographs that describe the photochemistry of polymers.<sup>1-6,14-19</sup>

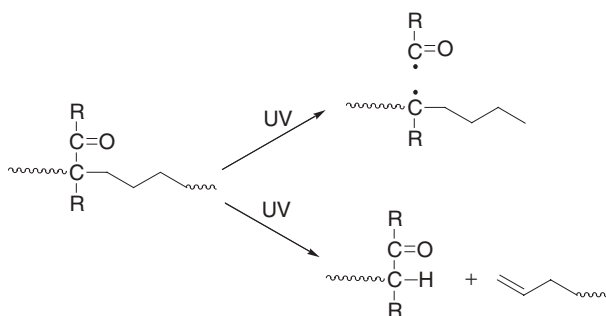
#### D. Methods for Intentionally Making Polymers Photodegradable

Some polymers are intentionally designed to degrade when exposed to light. There are two basic methods for doing this.<sup>1,2</sup> One method is to incorporate a chromophore into the polymer chains. For example, deliberate incorporation of carbonyl groups leads to light-sensitive polymers, as in the commercial Ecolyte polymers.<sup>2,20</sup> These polymers are made by copolymerizing vinyl ketones with vinyl monomers

such as ethylene or styrene to give polymers with the following structural unit interspersed along the backbone:<sup>21</sup>



Radical production and/or backbone degradation occurs by the Norrish types I and II routes in these polymers (scheme 6).



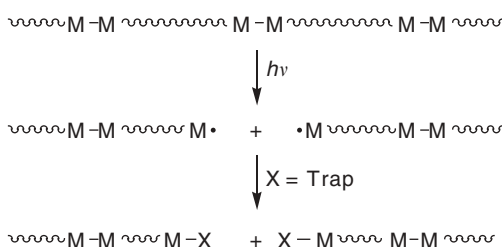
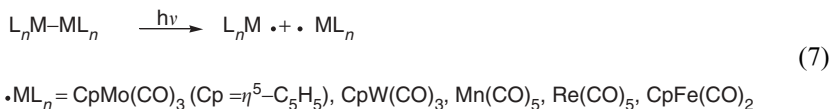
**Scheme 6** Photochemical degradation of a polymer backbone with pendant carbonyl groups.

An alternative strategy for incorporating CO into vinyl polymers is to copolymerize vinyl monomers with CO, thereby incorporating the CO directly into the polymer backbone. This approach, used commercially with ethylene,<sup>2,20</sup> yields polymers with structures like that shown in scheme 3. Degradation is by the pathways indicated in that scheme. Note that once radicals are introduced into the system, chain degradation can occur by the auto-oxidation pathway and the subsequent backbone cleavage reactions.

The second general method for making polymer materials photochemically degradable is to mix a radical initiator into the polymer. Again, once carbon-based radicals have formed, the chains degrade by the auto-oxidation cycle. Numerous radical initiators have been investigated, and a partial list includes metal oxides (e.g., TiO<sub>2</sub>, ZnO, CuO) (Eq. 6), metal chlorides (e.g., LiCl, FeCl<sub>3</sub>), M(acac)<sub>n</sub> complexes, M(stearate)<sub>n</sub> complexes, benzophenone, quinones, and peroxides.<sup>1,2</sup> Note that both the carbonyl-containing- and the radical initiator-containing types of degradable polymers require ultraviolet light for degradation.



Finally, it is noted that chromophores other than CO have been incorporated into polymer backbones to make the polymers photodegradable. An example is the class of polymers with metal–metal bonds along the polymer backbones.<sup>22–27</sup> Photochemical degradation occurs with these polymers because metal–metal bonds cleave homolytically when irradiated with visible light (Eq. 7; scheme 7).<sup>28</sup> The remainder of this review focuses on these materials.

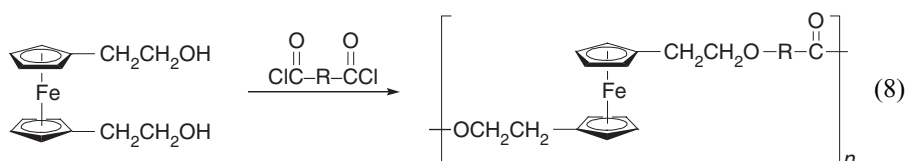


**Scheme 7** Photochemical degradation of a polymer with metal–metal bonds along its backbone.

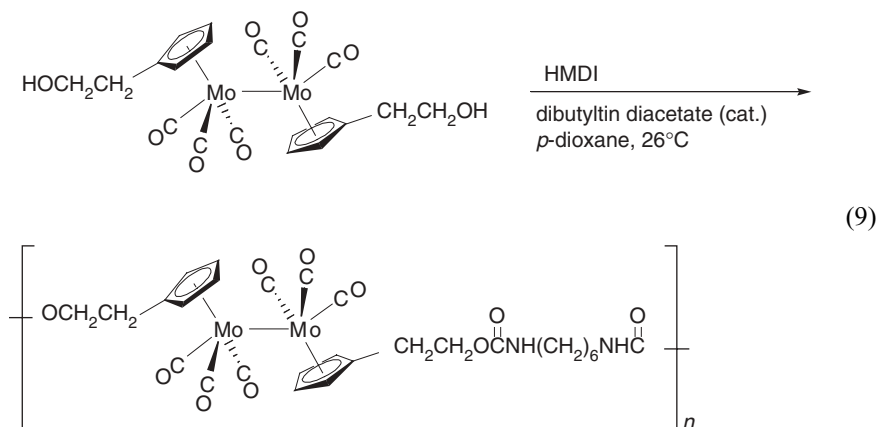
### III. METAL–METAL BOND-CONTAINING POLYMERS

#### A. Synthesis and Characterization

A general synthetic route for incorporating metal–metal bonds into polymer backbones is based on the step polymerization techniques for incorporating ferrocene into polymer backbones.<sup>29–35</sup> Step polymers of ferrocene can be made by substituting the Cp ( $\eta^5\text{-C}_5\text{H}_5$ ) rings with appropriate functional groups, followed by reaction with appropriate difunctional organic monomers (e.g., Eq. 8).<sup>36–38</sup>



The analogous strategy for synthesizing metal–metal bond-containing polymers also uses difunctional, cyclopentadienyl-substituted metal dimers. A sample polymerization reaction is shown in equation 9, which illustrates the reaction of a metal–metal bonded “diol” with hexamethylene diisocyanate (HMDI) to form a polyurethane.<sup>23</sup>

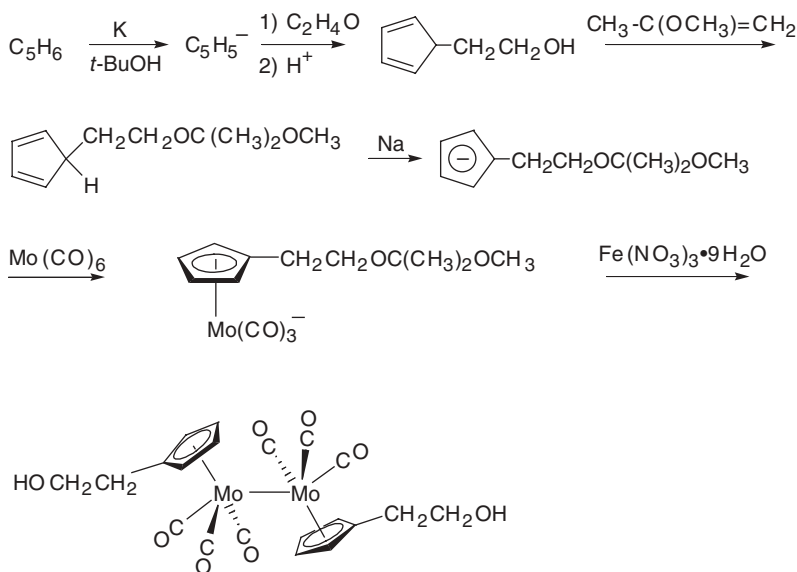


This step polymerization strategy is quite general, and a number of metal–metal bond-containing polymers have been made from monomers containing functionalized Cp ligands.<sup>27,39</sup>

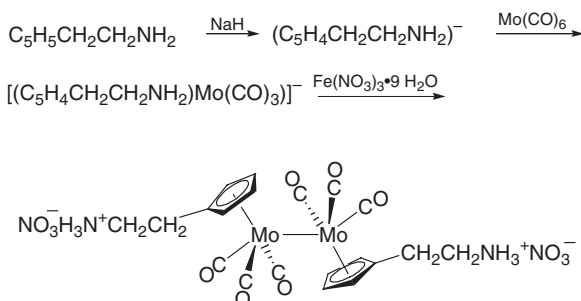
## B. Synthesis of the Difunctional Dimers

The synthesis of metal–metal bonded dimers with functional groups substituted on the Cp rings is a synthetic challenge. The reason lies in the relative weakness of the metal–metal bonds ( $D_{W-W} \approx 56 \text{ kcal mol}^{-1}$ ;  $D_{Mo-Mo} \approx 32 \text{ kcal mol}^{-1}$ ).<sup>40–42</sup> Because they are relatively weak, the metal–metal bonds will not stand up to the harsh synthetic conditions typically required for the substitution of metal-coordinated Cp rings. For this reason, it is necessary to synthesize first the substituted Cp molecules and then coordinate these rings to the metals. High-yield synthetic routes to alcohol- and amine-substituted Cp rings are incorporated in schemes 8 and 9.<sup>23–25</sup> (The vinyl-substituted  $\text{Cp}_2\text{Fe}_2(\text{CO})_4$  dimer is an exception to this general synthetic strategy. The synthesis of  $(\text{Cp-CH}=\text{CH}_2)_2\text{Fe}_2(\text{CO})_4$  is discussed in the following section.) The routes to the difunctional dimer molecules are also shown in schemes 8 and 9. (The analogous synthesis of a diacid functionalized W-W dimer is found in Ref. 43) Note that the general route shown for the Mo-containing dimers (involving  $\text{Fe}^{3+}$  oxidation of the anionic species) was developed by Birdwhistell.<sup>44</sup> The difunctional metal complex dimers were characterized by the usual spectroscopic methods, and it is worth noting that the electronic absorption spectra and infrared spectra in

the  $\nu(\text{C}\equiv\text{O})$  region are virtually identical to those of the unsubstituted dimers. The  $(\text{CpCH}_2\text{CH}_2\text{OH})_2\text{Mo}_2(\text{CO})_6$  dimer was further structurally characterized by x-ray crystallography.<sup>45</sup>

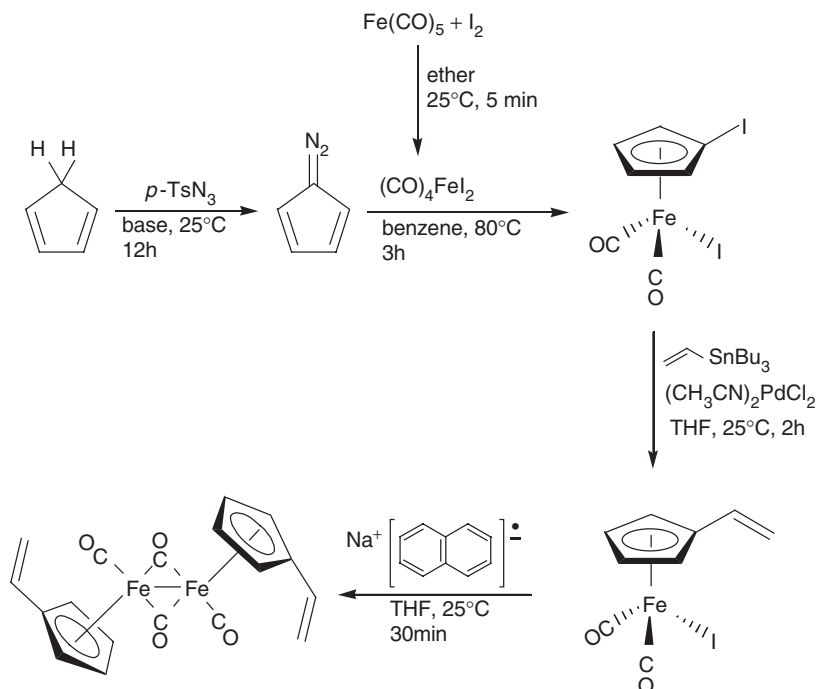


**Scheme 8** Synthesis of an organometallic diol used in the polymer syntheses.



**Scheme 9** Synthesis of an organometallic diamine used in the polymer syntheses.

The synthesis of  $(\text{Cp-CH}=\text{CH}_2)_2\text{Fe}_2(\text{CO})_4$  is outlined in scheme 10. The method involves the synthesis of the iodocyclopentadiene iron complex as outlined by Herrmann.<sup>46</sup> The vinyl group is then attached to the Cp by a palladium-catalyzed cross-coupling reaction,<sup>47</sup> and finally the dimer is made by treatment with sodium naphthalide.



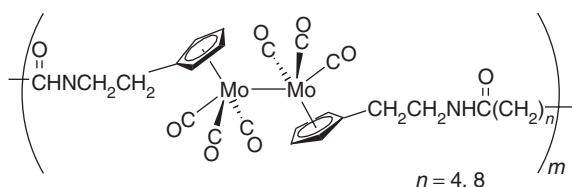
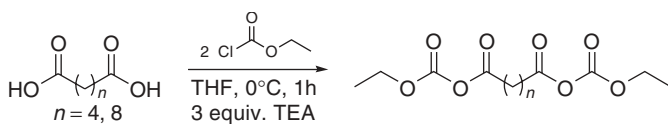
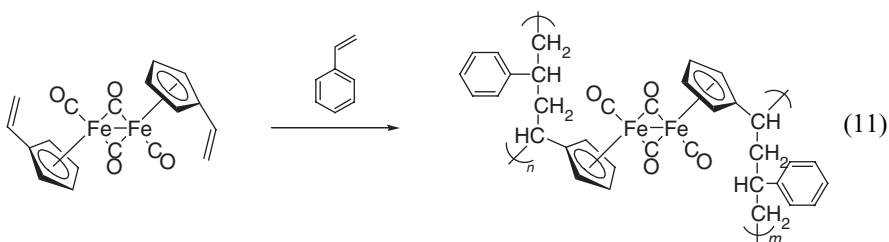
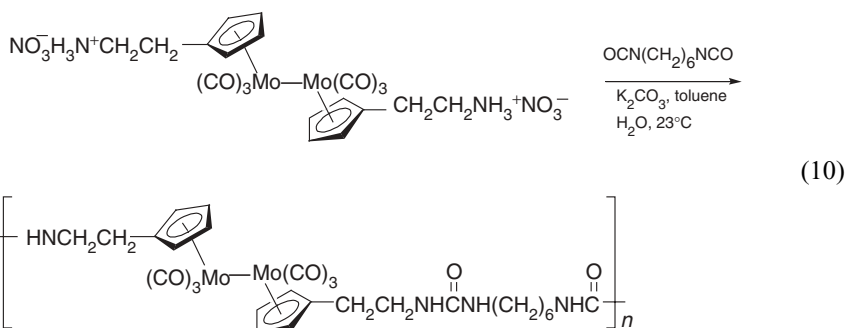
**Scheme 10** Synthesis of an organometallic divinyl molecule used in the polymer syntheses.

### C. Synthesis of the Polymers

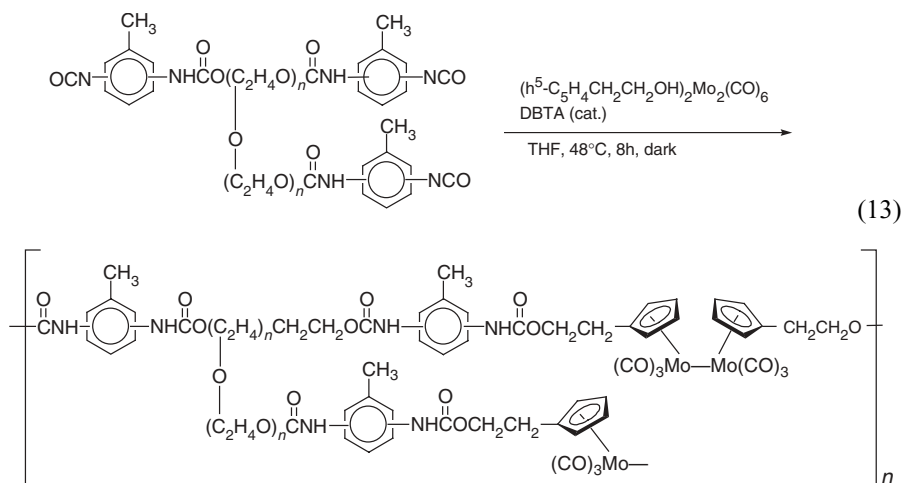
Just as the comparatively weak metal–metal bonds pose problems for the synthesis of the difunctional dimers, they cause similar problems in the synthesis of the polymers. The relative weakness of the metal–metal bonds makes them more reactive than the bonds found in standard organic polymers; thus under many standard polymerization reaction conditions, metal–metal bond cleavage would result. For example, metal–metal bonds react with acyl halides to form metal halide complexes. Therefore, the synthesis of polyamides using metal–metal bonded “diamines” and diacyl chlorides would simply lead to metal–metal bond cleavage rather than polymerization. Likewise, metal–metal bonded complexes are incompatible with many Lewis bases because the Lewis bases cleave the metal–metal bonds in disproportionation reactions.<sup>48</sup> This type of reactivity rules out many standard condensation polymerization reactions in which bases are used to neutralize any acids produced. All of the polymerization strategies are thus carefully designed to avoid cleaving the metal–metal bond during the polymerization process.

A sample polymerization reaction, showing the synthesis of a polyurethane, was shown in equation 9. Using similar synthetic strategies, various polyurethanes, polyureas (e.g., Eq. 10), polyvinyls (e.g., Eq. 11), and polyamides (e.g., Eq. 12) were

synthesized.<sup>23–25,49</sup> Note that the step polymers in the various equations have a metal–metal bond in every repeat unit. Experiments showed that it was not necessary to have a metal–metal bond in every repeat unit to photochemically degrade the polymers.<sup>25</sup> Copolymers are straightforwardly synthesized by adding appropriate difunctional organic molecules into the reaction mixture.

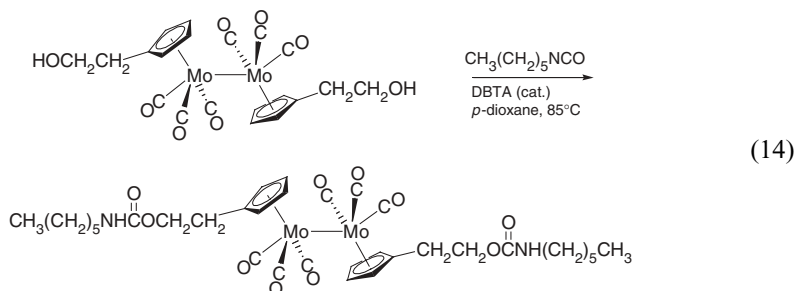


Yet another polymer synthesis strategy is to react the difunctional dimer molecules with prepolymers. Equation 13 shows an example of this technique.<sup>25</sup> (In this instance, the prepolymer is one of the Hypol polymers sold by W. R. Grace. Analysis of the sample showed it to contain, on average, three tolyl isocyanate end groups; number = average molecular weight was about 2000.)



#### D. Characterization of the Polymers

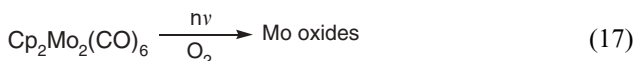
The polymers were spectroscopically characterized by comparison of their infrared, electronic, and NMR spectra to model complexes.<sup>23-25,49</sup> For example, the product shown in equation 14, a model complex for the polymer in equation 9, was synthesized by reaction of  $(\text{CpCH}_2\text{CH}_2\text{OH})_2\text{Mo}_2(\text{CO})_6$  with a monoisocyanate (Eq. 14).



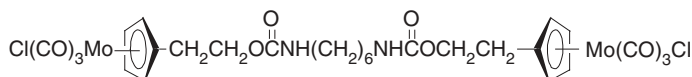
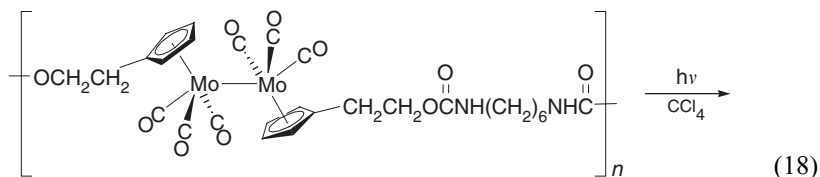
Typical number = average molecular weight values, as measured by VPO or GPC, are between 5,000 and 20,000 ( $n = 7-25$ ). Thus in many cases, the polymers are best described as oligomers. However, it is important to note that no effort was made to maximize the molecular weights.

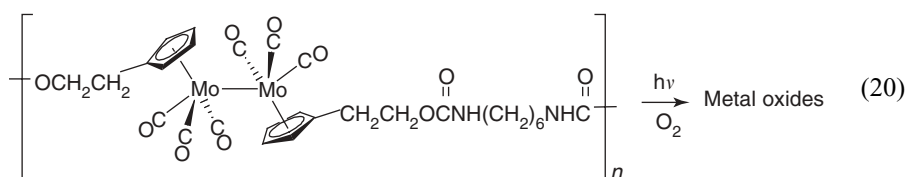
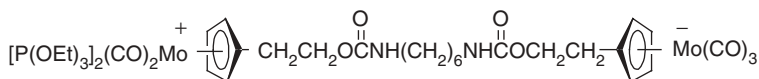
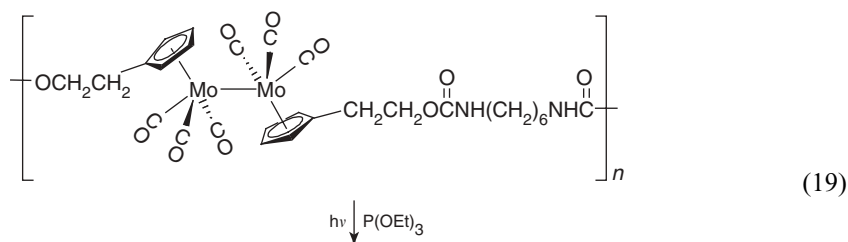
### E. Photochemical Reactions in Solution

Irradiation of metal–metal bonded complexes into their lowest energy absorption band ( $\approx 500$  nm) generally leads to one of three fundamental types of reactivity:<sup>23,28,50</sup> (1) The metal radicals produced by photolysis react with radical traps to form monomeric complexes (e.g., Eq. 15). (2) The complexes react photochemically with ligands to form ionic disproportionation products (e.g., Eq. 16). (3) The complexes react with oxygen to form metal oxides (Eq. 17). (The latter reaction is likely a radical trapping reaction but may involve excited state electron transfer.) Note that higher energy excitation leads to M–CO bond dissociation. This type of reactivity is discussed below.

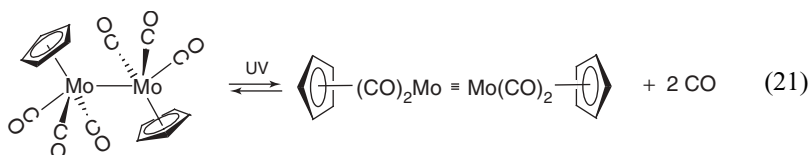


The qualitative photochemistry of the polymers in solution is analogous to the reactions of the discrete metal–metal bonded dimers in solution.<sup>23–25,49</sup> As in the photochemical reactions of the dimers, the photochemical reactions of the polymers can be conveniently monitored by electronic absorption spectroscopy. The quantum yields for the reactions are in the range  $\approx 0.1$  to 0.6, depending on the specific polymer and the M–M bond.<sup>24</sup> Sample reactions of the polymers showing the three types of reactivity are shown in eqs. 18–20.

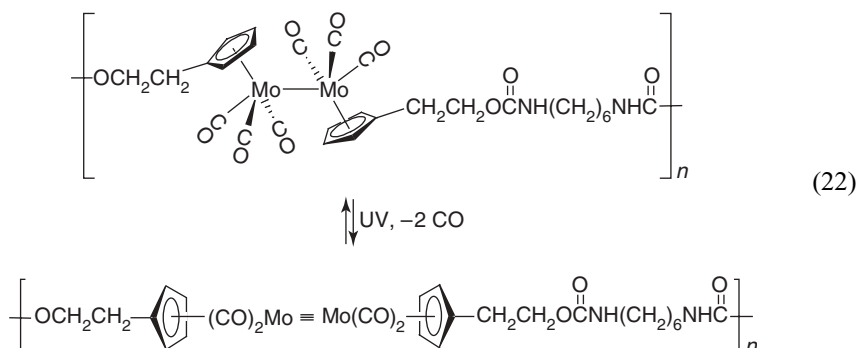




As mentioned, a fourth type of dimer reactivity is dissociation of a CO ligand from the dimer. Generally, this type of reactivity increases in efficiency relative to M–M photolysis as the radiation energy increases.<sup>28</sup> In solution, this type of reactivity generally leads to substitution. However, in the case of the  $\text{Cp}_2\text{Mo}_2(\text{CO})_6$  molecule, the reaction in equation 21 occurs.<sup>24</sup> (Among the dimers, this reaction to form a triply bonded product is unique to the Mo and W species.)

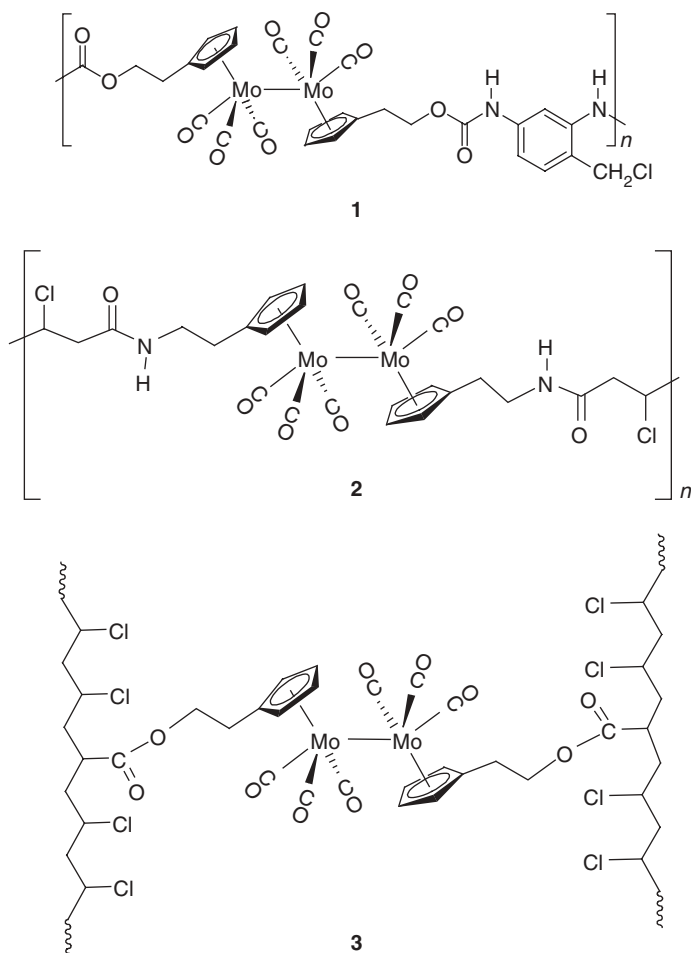


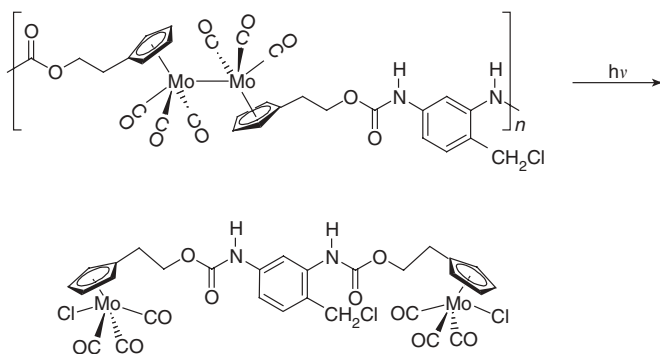
An analogous photoreaction occurs with polymers containing the Mo–Mo unit (Eq. 22).



In both equations 21 and 22, addition of CO to the product solution causes the system to back-react to reform the starting materials. Once again, the main point to be made is that the solution photochemistry of the polymers is analogous to the solution photochemistry of the discrete metal–metal bonded dimers.

Photochemical reactivity in the absence of exogenous radical traps is possible in the case of polymers that have carbon–halogen bonds along their backbones. For example, irradiation of polymers **1–3** in solution in the absence of  $\text{CCl}_4$  or  $\text{O}_2$  led to net metal–metal bond cleavage.<sup>51</sup> Spectroscopic monitoring of the reaction showed that metal–metal bond cleavage is accompanied by an increase in the concentration of  $\text{CpMo(CO)}_3\text{Cl}$  units. Photochemical reactions analogous to that in scheme 11 were proposed.





**Scheme 11** Photochemical reaction of polymer 3 in the absence of an external trapping reagent.

## F. Photochemistry in the Solid State

Thin films of the polymers ( $\approx 0.05$  mm in thickness) reacted when they were exposed to visible light, whether from the overhead fluorescent lights in the laboratory, from sunlight, or from the filtered output of a high pressure Hg arc lamp.<sup>23–25,49</sup> All of the films were irradiated both in the presence and absence of oxygen. For each film and its dark reaction control, the absorbance of the  $d\pi \rightarrow \sigma^*$  transition near 500 nm was monitored periodically over a period of several months. Only the polymer films that were exposed to sunlight in air completely degraded, while thin films stored in the dark in air or irradiated under nitrogen showed only slight degradation over a 1-year period. From these results, it was concluded that the decomposition of the polymers requires both light and air (oxygen). Infrared spectra of the decomposition products showed the absence of products with CO ligands, as indicated by the absence of any stretches in the region  $1600\text{--}2200\text{ cm}^{-1}$ . As mentioned previously, oxide complexes form in the solution phase reactions of  $\text{Cp}_2\text{Mo}_2(\text{CO})_6$  with  $\text{O}_2$ , and it was proposed that the metal-containing decomposition product of the polymer is a metal oxide. These data suggest that oxygen is necessary for the solid-state photochemical reaction to occur. It was proposed that oxygen traps the metal radicals produced in the photolysis of the metal–metal bonds, thereby preventing radical recombination (Eq. 23). If oxygen diffusion is rate limiting then the relative rates of polymer photochemical decomposition in the solid-state will reflect the oxygen diffusion rate.

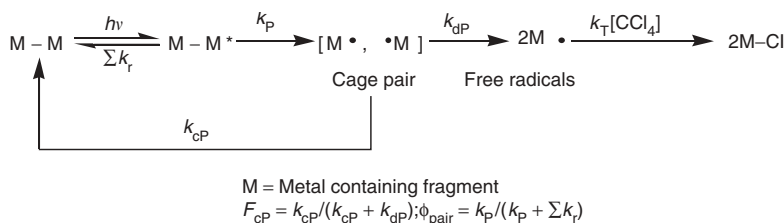


As described in the previous section, polymers 1–3 were designed to degrade in the absence of exogenous radical traps by building in carbon–chlorine bonds along their backbones. As indicated, all of these polymers did degrade in the absence of oxygen when dissolved in solution, but only polymer 3 degraded in the solid state when irradiated in the absence of oxygen.<sup>51</sup> Apparently, only polymer 3 has a sufficiently high concentration of carbon–chlorine bonds to overcome the slow rate of diffusion in the solid state.

## IV. FACTORS CONTROLLING THE RATE OF PHOTOCHEMICAL DEGRADATION

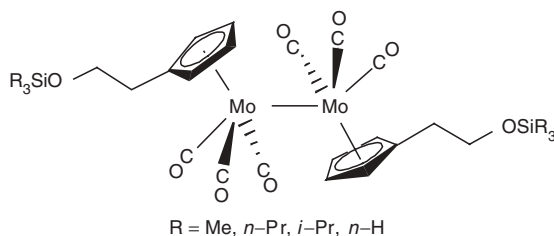
### A. Cage Effects

In a series of recent papers, we showed that the overall quantum yields for the degradation of metal–metal bond-containing polymers and their model complexes varied as a function of molecular weight and size.<sup>25</sup> The dependence on molecular weight and size was shown to be attributable to the radical cage effect, specifically to changes in the “cage recombination efficiency” as the chain length is varied (scheme 12).<sup>52,53</sup> The cage recombination efficiency (denoted as  $F_c$  and colloquially known as the *cage effect*) is defined as the ratio of the rate constant for cage recombination to the sum of the rate constants for all competing cage processes. (The  $F_c$  value for a photochemically formed cage pair does not necessarily equal  $F_c$  for the same cage pair formed by thermolysis or by diffusional collision of two free radicals.<sup>54</sup> To differentiate these cases, the photochemical cage efficiency is denoted  $F_{cP}$  and the associated rate constants as  $k_{cP}$  and  $k_{dP}$ . In the photolysis reaction in scheme 12,  $F_{cP} = k_{cP}/(k_{cP} + k_{dP})$ .)

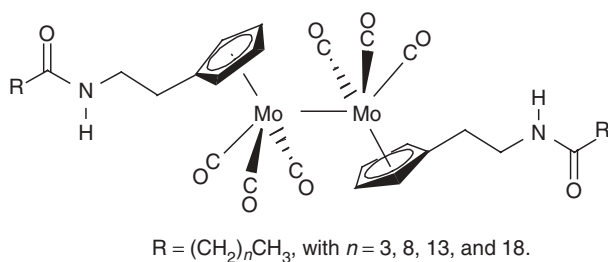


**Scheme 12** Reaction scheme for metal–metal bond photolysis.

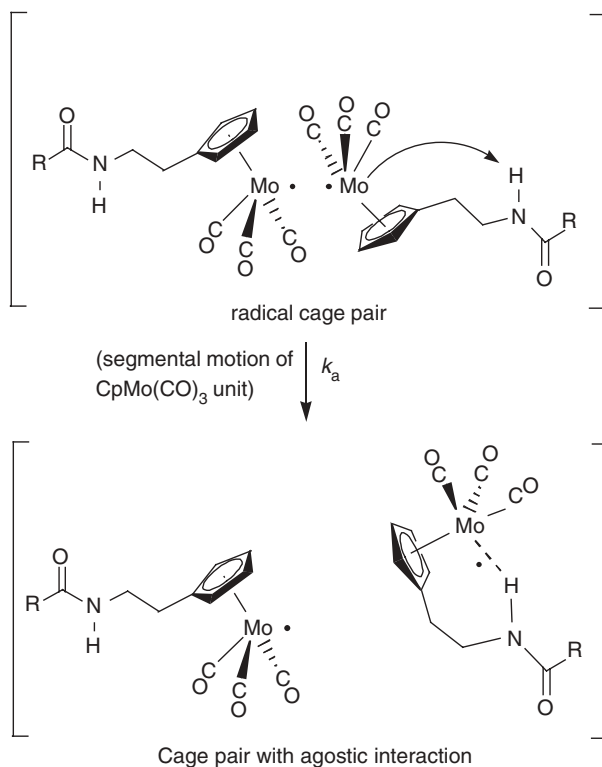
To gain greater insight into the role that  $F_{cP}$  plays in controlling the degradation of polymers, we synthesized and studied the series of model complexes  $(CpCH_2CH_2OSiR_3)_2Mo_2(CO)_6$  ( $R = Me, i-Pr, n-Pr, n-Hx$ ) and determined that the ratio  $k_d/k_c$  was linearly proportional to  $m^{1/2}/r^2$  (where  $m$  is the mass of the radical, and  $r$  its radius). This result represented the first experimental verification of Noyes’s prediction concerning the relationship of particle mass and size to the cage effect.<sup>55–58</sup>



To study the generality of this result, we next synthesized and studied the cage effects in the model complexes  $(CH_3(CH_2)_nC(O)NHCH_2CH_2Cp)_2Mo_2(CO)_6$  ( $n = 3, 8, 13, 18$ ).<sup>59</sup>

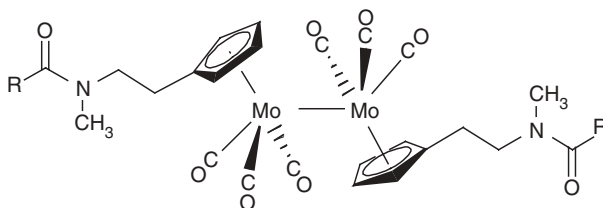


To our initial surprise, the  $F_{CP}$  values for the four radical cage pairs formed by photolysis of these complexes were essentially identical—that is, there was no dependence of  $F_{CP}$  on the value of  $n$ . To explain this result, we hypothesized that, while still in the cage, the Mo radicals interacted with an H atom on the sidechain to form a six-membered ring (scheme 13). In effect, the metal radicals were captured in the cage. The cage recombination efficiencies were thus independent of  $n$  because the segmental motion of the Mo radical to form the agostic interaction is independent of the chain length.



**Scheme 13** In-cage trapping of the Mo-centered radical.

To test the in-cage trapping hypothesis and to further explore the dependence of  $F_{\text{CP}}$  on mass and chain length, we synthesized molecules 4–6 in which methyl groups replace the H atoms of the model complexes discussed above. No Mo···H agostic interactions are possible with these new complexes.



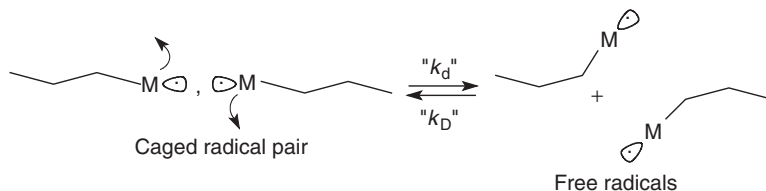
4 – 6; R =  $(\text{CH}_2)_n\text{CH}_3$ , with  $n = 3, 8, \text{ and } 18$

As was the case for the silylated molecules,  $F_{\text{CP}}$  increased as the length of the chain increased, and again  $k_c/k_d$  was linearly proportional to  $m^{1/2}/r^2$ .<sup>53</sup> Although this is just the second experimental verification of Noyes's prediction, the Noyes relationship is emerging as a rather general expression for predicting (or at least comparing)  $F_{\text{CP}}$  values.

The interesting feature about the reasonably good linear fit between  $k_d/k_c$  and  $m^{1/2}/r^2$  for the radical cage pairs derived from the model complexes in the preceding paragraph is that Noyes derived his expression for spherical particles,<sup>55–58</sup> yet the various radicals discussed above are decidedly not spherical. The explanation for the good fit lies in the reason for the dependence of  $F_{\text{CP}}$  on  $r^2$ . The parameter  $r^2$  is proportional to the surface area of a particle, which in turn is proportional to the number of interactions a particle has with solvent molecules. The more interactions a particle has with the solvent, the greater the viscous drag and consequently the slower the rate of diffusion (and hence the inverse dependence of  $k_d/k_c$  on  $r^2$ ). This analysis suggests that Noyes's expression can be modified by replacing  $r^2$  with the particle's surface area—that is,  $k_d/k_c \propto m^{1/2}/\text{radical surface area}$ . In fact, plots of  $k_d/k_c$  vs.  $m^{1/2}/\text{surface area}$  were linear.<sup>53</sup> As a further test, plots of  $k_d/k_c$  vs.  $m^{1/2}/\text{surface area}$  were also linear for the  $(\text{CpCH}_2\text{CH}_2\text{OSiR}_3)_2\text{Mo}_2(\text{CO})_6$  molecules (R = Me, i-Pr, n-Pr, n-Hx). This result provided further support for the modified Noyes expression. The significance of being able to use a particle's surface area in the Noyes expression is that the expression becomes useful for nonspherical particles—that is, it becomes possible to use the Noyes expression for virtually all radicals, not just spherical ones.

These results show that  $F_{\text{CP}}$  increases as the length of the chain on a radical center increases. In turn, this explains why the quantum yields for the photochemical degradation of polymers (and long-chain molecules, in general) decrease as the chains get longer. Undoubtedly, after a certain chain length is reached, no changes in  $F_{\text{CP}}$  will likely be observed due to the considerable inertia of the radicals. In such cases, the chain movements will be local—that is, radical diffusion out of the cage or recombination in the cage will occur by segmental motion of the chain end and

not by movement of the center of mass of the entire chain (scheme 14). If such is the case then once a certain chain length is reached, additional chain length will not impact the segmental motion of the radical end.<sup>60</sup>



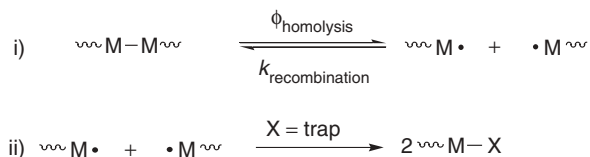
**Scheme 14** Segmental motion leading to separation of two radicals in a radical cage pair.

## B. The Effect of Tensile Stress on Photodegradation

An interesting outcome of photodegradation studies on polymers is the finding that tensile and shear stress can accelerate the rate of photochemical degradation. For example, recent studies of this phenomenon have shown that tensile stress will accelerate the photodegradation of numerous polyolefins<sup>61–76</sup> as well as polycarbonates,<sup>67</sup> nylon,<sup>12,77</sup> and acrylic-melamine coatings.<sup>78,79</sup> Conversely, compressive stress will generally retard photodegradation reactions.<sup>63</sup> These observations are of enormous practical importance because most polymers are subjected to light and some form of temporary or permanent stress during their lifetime. To control the onset of degradation and the rate of degradation in polymers, it is important to understand the mechanistic origin of the synergism between light and stress in these systems.<sup>27</sup>

### i. Theories of Stress-Induced Photodegradation

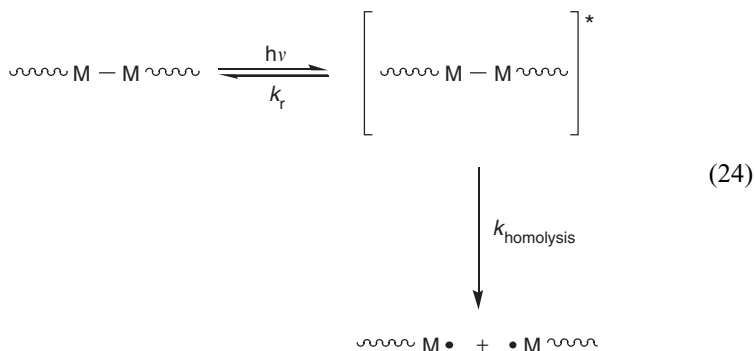
Mechanistic hypotheses to explain stress-accelerated photodegradation fall into three main categories. In one category, it is proposed that stress leads to an increase in the quantum yields for bond photolysis—that is, it is proposed that  $\phi_{\text{homolysis}}$  increases with stress (scheme 15). The second category attributes the increased degradation rates to a decrease in the efficiency of radical recombination following homolysis;  $k_{\text{recombination}}$  is proposed to decrease as stress increases. The third category attributes the effects of stress to changes in the rates of reactions that occur subsequent to formation of the radicals, or to changes in the rate of the radical trapping reactions. The salient points of these theories are outlined in the following sections.



**Scheme 15** A generalized reaction scheme showing photolysis of a metal–metal bond along the backbone in a polymer.

**ii. Stress-Induced Changes in  $\phi_{\text{homolysis}}$ ; the Plotnikov Hypothesis**

For a direct photochemical bond cleavage, the photochemical step in scheme 15 labeled “ $\phi_{\text{homolysis}}$ ” can be broken down into the elementary steps shown in equation 24. (The asterisk in Eq. 24 is used to indicate an excited state of the molecule.)



Equation 25 shows the value of  $\phi_{\text{homolysis}}$  in terms of the rate constants in equation 24.

$$\phi_{\text{homolysis}} = \frac{k_{\text{homolysis}}}{k_{\text{homolysis}} + k_r} \tag{25}$$

Clearly, if stress affects either  $k_r$  or  $k_{\text{homolysis}}$  then  $\phi_{\text{homolysis}}$  will vary with stress. No studies have investigated the effect of stress on  $k_r$ , but Plotnikov derived a theory for the stress dependence of  $k_{\text{homolysis}}$ .<sup>80</sup> His quantitative hypothesis attributes the increase in degradation rates with applied stress to a decrease in the activation barrier for bond dissociation in the excited state. The predicted relationship of quantum yield to stress is shown in Figure 2A.

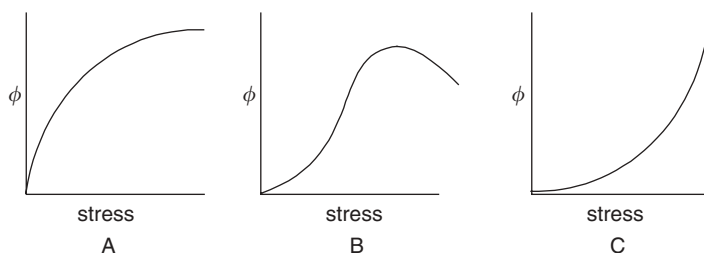


**Figure 2** A plot of quantum yield for degradation vs. stress according to (A) the Plotnikov equation, (B) the DRRE hypothesis, and (C) the Zhurkov equation.

### *iii. Stress-Induced Changes in $k_{\text{recombination}}$ : the Decreased Radical Recombination Efficiency Hypothesis*

Busfield,<sup>70</sup> Rogers,<sup>71,81</sup> Baimuratov,<sup>82</sup> and others<sup>83</sup> proposed explanations for stress effects that are based decreased radical recombination efficiencies (DRREs) in stressed systems. In their models (which are reasonably similar so they are combined here for ease of discussion), the effect of stress is divided into four stages. Stage one represents the low stress domain. In this stage, there is only slight deformation of the original polymer structure and the rate of photodegradation is not greatly affected. In stage two, higher stress causes significant morphological changes, including the straightening of the polymer chains in the amorphous regions. When bonds in the taut tie molecules are cleaved by light, the probability of radical recombination is decreased relative to nonstressed samples because entropic relaxation drives the radicals apart and prevents their efficient recombination. At slightly higher stresses (stage three), the chains are not only straightened but “stretched,” and recoil aids in their separation. According to this model, the diminished ability of the radicals to recombine is the primary reason that tensile stress will increase the rate of photodegradation. An increased separation leads to slower radical–radical recombination, which increases the probability of radical trapping and thus of degradation. Finally, in stage four, a strong stress is present that gives the polymer a fibrillar structure with a higher degree of orientation and crystallinity. Diffusion in a crystalline structure is retarded relative to the amorphous material, and the rate of degradation is expected to decrease because of decreased movement apart of the radicals. In summary, the DRRE hypothesis predicts that tensile stress will initially increase the quantum yield of degradation and then further increases in stress will decrease the quantum yield (Fig. 2B).

### *iv. Stress-Induced Changes in the Rates of Radical Reactions Subsequent to Radical Formation*

The effect of stress on the rates and efficiencies of reactions that occur subsequent to radical formation is complicated. Examples have been noted in which the rates decrease because of decreased oxygen diffusion<sup>64,65</sup> in the stressed (more ordered) sample.<sup>84</sup> In other systems, it has been suggested that the important point is that stress changes the conformations of the C–C bonds in the polymer chains;<sup>85–87</sup> depending on the system either a rate decrease<sup>85–87</sup> or a rate increase<sup>88</sup> can occur. The quantitative relationship of quantum yields to stress in such cases is generally considered to be given by the so-called Zhurkov equation, as discussed in the next section.

### *v. The Zhurkov Equation*

The effect of stress on the thermal degradation rates of polymers can be fitted to an empirical Arrhenius-like equation that is attributed to Zhurkov:<sup>89</sup> rate =  $A \exp[-(\Delta G - B\sigma)/RT]$ , where  $\Delta G$  is an “apparent” activation energy,  $\sigma$  is the stress, and  $A$  and  $B$  are constants. It has been suggested<sup>90</sup> that an equation similar to the Zhurkov equation might apply in photodegradation:  $\phi_{\text{obs}} = A \exp[-(\Delta G - B\sigma)/RT]$ . The Zhurkov equation is empirical and does not fall strictly into any of the three

mechanistic categories discussed above because it deals with an “effective” activation energy, which (in the case of a photochemical reaction) is a composite of the activation barriers for the  $k_{\text{homolysis}}$ ,  $k_{\text{recombination}}$ , and  $k_{\text{trapping}}$  steps. The relationship of quantum yield to stress for a system that follows the Zhurkov hypothesis is shown in Figure 2C.

#### vi. Quantum Yields as a Function of Stress for Polymer 3

Thin films of the polymer **3** were stressed by hanging weights of known mass from one end of the film. The stress was varied from 0 to 10 MPa. The maximum at 10 MPa is about 20% of the yield stress in commercial PVC, as indicated by the stress–strain curve. At each stress, the quantum yield of Mo–Mo disappearance was calculated. Figure 3 is a plot of the quantum yield for the degradation of **3** as a function of stress. Note that the quantum yields increased with increasing stress, reached a maximum, and then decreased. As discussed above, such a plot is predicted by the DRRE hypothesis (Fig. 2b).

A key tenet of the DRRE hypothesis is that stress eventually causes ordering of the amorphous polymer chains, and this ordering causes a decrease in the quantum yields (or rates) of the polymer decomposition. X-ray scattering and IR spectroscopy are both commonly used to assess crystallinity in PVC,<sup>91–95</sup> and both techniques clearly showed that stress increased the chain ordering in polymer **3**. In the case of IR spectroscopy, an increase in the absorbance ratio of the infrared peak at 635–638 to that at 610–615  $\text{cm}^{-1}$  indicates an increase in crystallinity,<sup>94,95</sup> and this ratio did, in fact, increase with increasing stress. In the case of wide-angle x-ray diffraction, an increase in intensity of the (200) and (110) reflections (in the 16–18°  $2\theta$  region<sup>91–93</sup>) has been shown to correlate with an increase in crystallinity in PVC. Experiments showed that these peaks grew in and increased in intensity with increasing stress, again consistent with the conclusion that stress is increasing the chain ordering in polymer **3**.

Additional mechanistic evidence consistent with the DRRE hypothesis was sought to confirm this interpretation on the role of stress, and for that reason the experiments described above were repeated with plasticized polymer **3**. Because chain movements are more facile in plasticized polymer, it was predicted that, at any given stress, the quantum yields for degradation should be higher (because it is easier for the radicals to separate from each other, which lowers their probability of recombination). In addition, the maximum in the curve shown in Figure 3 should occur at a lower stress because chain alignment is easier.

Polymer **3** was plasticized by blending it with dioctyl phthalate (DOP). As expected, the presence of the plasticizer decreased the glass transition temperature ( $T_g$ ) of the polymer to  $<25^\circ\text{C}$  from  $65^\circ\text{C}$ . As likewise expected, the DOP plasticizer resulted in a decrease in the tensile strength and yield stress of the polymer and a longer elongation. A plot of quantum yield for degradation vs. tensile stress for plasticized polymer **3** matched the predictions of the DRRE hypothesis—that is, stress initially caused an increase in degradation efficiency to some maximum value, at which point the quantum yields started to decrease. Thus, for a given stress, the quantum yields of degradation were higher for plasticized polymer than for **3**. In addition, the maximum in the curve occurred at a lower stress compared to that in

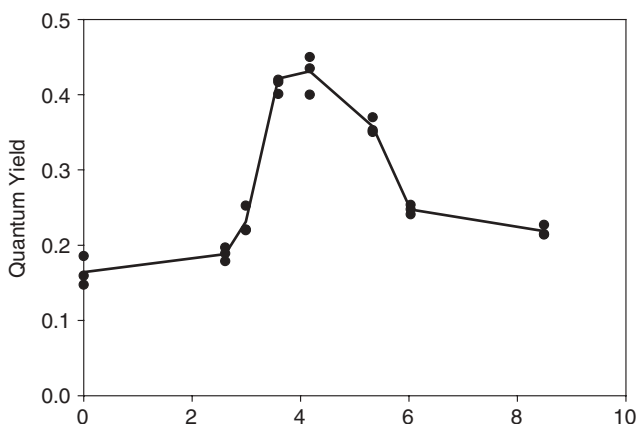


**Figure 3** Quantum yields for degradation of 3 vs. applied tensile stress. The results of three independent measurements at each stress are shown.

the plot in Figure 3 for polymer 3. Both of these results are consistent with the predictions made in earlier concerning the effect of plasticizer, and this was taken as additional evidence in support of the DRRE hypothesis. Infrared spectroscopy and x-ray diffraction again provided evidence for increased crystallinity with increasing stress in the plasticized polymer.

In summary of this section, the results presented above are consistent with the predictions of the DRRE hypothesis. According to this hypothesis, the initial effect of stress on the degradation efficiency is to separate the photogenerated radicals further from each other than in the absence of stress and thereby lower their recombination efficiency. At higher stresses, however, the stress induces enough order in the polymer chains to inhibit radical separation, which increases their recombination efficiency and lowers the degradation efficiency. Although it is tempting to generalize these results to other polymers and to other degradation mechanisms (photooxidative degradations, in particular), it is prudent to be cautious. For example, in a photooxidation reaction, the downturn in efficiency with higher stress may be caused by the development of microcracks and fissures, which act to release the stress. Or, perhaps the  $k_r$  term in equation 25, generally assumed to be stress independent, is in fact stress dependent, and this is what causes the downturn. Further study is required before the generality of these results can be established.

### C. Other Factors Affecting Photochemical Degradation Rates of Polymers

The early studies of stress effects on photodegradation rates were often contradictory in the sense that tensile stress sometimes seemed to cause a rate acceleration and other times a rate decrease. It was speculated that this inconsistency might be attributable to changes in reaction parameters other than stress that were not recognized

at the time as being an influence on the photochemical reaction rates. Some of the experimental parameters that affect the rates of photochemical reactions include light intensity,<sup>96</sup> temperature,<sup>97</sup> and chromophore concentration.<sup>97</sup> In addition, several additional factors unique to polymer systems (such as polymer morphology) will also affect the photodegradation rates of polymers. The way in which these additional experimental factors affect photochemical rates is discussed briefly below.

*i. Absorbed Light Intensity*

Light intensity effects are generally analogous to the “dose rate” effects seen in  $\gamma$  irradiation experiments.<sup>98</sup> In general, an increase in the absorbed light intensity will increase the rate of a photochemical reaction. To visualize why this is so, consider the photon as a reagent.<sup>13</sup> An increase in the number of photons striking the polymer per unit time (i.e., an increase in the absorbed intensity) will increase the rate of the photochemical step in the same way that increasing the concentration of a reagent will increase the rate of an elementary step. Although saturation can occur with chemical reagents, saturation rarely occurs with photons unless lasers or exceptionally high-intensity lamps are used as the light source. Note that only “absorbed” photons can cause photochemical reactions.<sup>99</sup> Hence, rate laws and quantum yield expressions use the absorbed intensity (generally abbreviated  $I_a$ ) and not merely the intensity ( $I$ ). To normalize for the effect of the absorbed light intensity, photochemists use the concept of the quantum yield, which is defined as the rate of the reaction divided by the absorbed light intensity.<sup>13,99</sup> Thus, although light intensity will generally affect the rate of polymer degradation, the quantum yield (also called the quantum efficiency) will generally not be affected by intensity.

$$\phi = \frac{\text{number of reactions}}{\text{number of photons absorbed}} = \frac{\text{rate of the reaction}}{\text{absorbed light intensity}} \quad (26)$$

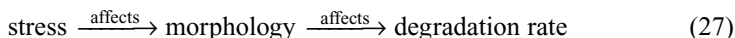
There are well-established instances, however, in which the quantum yield of a photochemical reaction can be affected by the light intensity. A specific case in point relevant to polymer degradations occurs in those pathways where two photochemically generated intermediates, such as radicals, can react. In such instances, the rate of the elementary reaction involving the two intermediates will be proportional to the square of the intermediate’s concentration (i.e.,  $\text{rate} \propto [\text{intermediate}]^2$ ). Such bimolecular reactions would typically be termination steps in, say, a radical polymerization reaction. If this reaction is in competition with other reactions of the intermediates involving rates that are first-order in intermediate concentration, then the second-order reaction will increase in rate relative to the first-order reactions as the concentration of the intermediate increases. In general, intermediates increase in concentration as the light intensity increases. Thus, in this example, the quantum yield would drop as the light intensity increased because the termination step increases in efficiency relative to the propagating steps. Note, however, that the rate of the overall reaction would likely still increase as the light intensity increased.

The metal–metal bond containing polymers (generically shown in scheme 7) photolyze according to the mechanism in scheme 12, and it is expected that the

quantum yields will decrease as the light intensity increases. (Note in scheme 12 that two competing reactions of the radicals occur; one is a first-order trapping reaction and the other is a second-order radical-radical recombination.) In fact, a study showed that the quantum yields for disappearance of the metal-metal bonded dimers are intensity dependent.<sup>96</sup> A complete analysis of light intensity effects in metal-metal bonded systems is found in Ref. 96.

### *ii. Polymer Morphology*

Despite early claims to the contrary, there is now general agreement that polymer morphology is a parameter that has an extremely important influence on the rate of polymer photochemical degradation reactions.<sup>84,100-102</sup> In fact, polymer morphology is one of the keys to interpreting the effect of stress on degradation rates because stress affects the morphology and morphology affects the degradation rates. The equation 27 shows the relationship between stress, polymer morphology, and degradation rates:



Recall that increasing the tensile or shear stress will (1) first stretch the chains in an amorphous region of a polymer sample, (2) then order the polymer chains, and (3) then induce crystallinity in regions of the polymer. These changes will affect chemical reactivity because molecular diffusion is slower in ordered and crystalline phases compared to amorphous phases,<sup>103</sup> consequently, intermolecular reaction rates, such as those in the autooxidation cycle, will be slower in ordered polymers.

The sections above contained numerous examples that demonstrated how the relationship between stress and morphology affects polymer degradation reaction rates. For example, the interplay is exploited in the decreased radical recombination hypothesis. The key tenet of this hypothesis is that stress causes increased order in a polymer, which in turn affects the efficiency of degradation because radical-radical recombination is less likely in a stretched chain because recoil has separated them further relative to an unstressed sample. Eventually, however, the polymer chains become ordered and recoil is inhibited, which facilitates recombination and lowers the rate. Another example of the stress/morphology/degradation-rate interplay is Rapoport's study of polypropylene,<sup>86,87</sup> which showed that oriented chains of this polymer were less susceptible to oxidation because they had an unfavorable conformation for participation in the autooxidation reaction relative to amorphous chains. Stress and chain-orientation-effects work both ways, however. The work of Bellinger on PVC is frequently cited as an example where stress induces a chain orientation that is more favorable for degradation, apparently because of a chain conformation that is more susceptible to hydrogen abstraction.<sup>85</sup> Finally, the definitive work of Rabello and White is noted on the role of morphology in the photochemical degradation of polypropylene.<sup>84</sup> These authors found that samples with higher fractions of crystallinity degraded slower than samples with less crystallinity (for sample exposure times of at least 12 weeks; for short exposure times there was no correlation between fractional crystallinity and extent of degradation). Their explanation was that oxygen diffusion is slower in the crystalline regions.

Crosslinking can also affect photodegradation rates by “locking” the polymer structure and preventing lamellar unfolding. The consequence is to prevent separation of photoproduct radicals, which favors radical–radical combination. Crosslinked systems therefore generally have smaller quantum yields of degradation relative to non-crosslinked systems.<sup>64</sup>

Finally, it has been noted several times above that the rate of oxygen diffusion is morphology dependent.<sup>65</sup> The consequences of this fact are discussed in the next section.

### *iii. Oxygen Diffusion*

Oxygen diffusion is the rate-limiting step in many photo-oxidative degradation reactions.<sup>104–107</sup> (One would expect rate-limiting oxygen diffusion under experimental conditions where the light intensity is high relative to the rate at which oxygen is available to capture radicals.) A specific example of rate-limiting oxygen diffusion comes from O’Donnell and White’s study of photochemically degraded polystyrene.<sup>61</sup> By sampling molecular weight as a function of depth (“depth profiling”), they found that the variation in degradation with depth could not be explained by the difference in light intensity at the various depths or by variations in the stress at the various depths. They concluded, rather, that oxygen depletion was responsible for the variation in degradation with depth (i.e., oxygen diffusion was rate limiting). Their data showed that the degradation rate was oxygen limited even at a depth of 100  $\mu\text{m}$  from the surface. Using the Zhurkov equation, they were able to estimate an activation free energy for the degradation process of 4.2  $\text{kJ mol}^{-1}$ , a value consistent with the activation energy for small particle diffusion in a polymer matrix (i.e., a value consistent with rate-limiting oxygen diffusion). It is interesting that O’Donnell and White found that oxidative degradation is more prevalent at the corners of a sample. They hypothesized that oxygen has easier access to these regions of the sample because two surfaces are present rather than just one.

For applications to kinetics, the general premise is that molecular diffusion is slower in crystalline regions than through amorphous regions; therefore, samples with high fractional crystallinity should degrade slower than samples with smaller fractional crystallinity. Rabello and White<sup>84</sup> showed that fractional crystallinity was the main structural factor controlling the rate of polypropylene degradation for this very reason. An interesting point, however, is that the diffusion of all molecules, not just oxygen, is hindered in crystalline material. By inhibiting the diffusion of the radical species involved in the termination steps of the autooxidation cycle, the kinetic chain length of the cycle will increase, with a resulting increase in the amount of oxidative degradation. Thus as the fractional crystallization increases two outcomes are possible: If oxygen diffusion is affected the most and is rate limiting, then the rate of photo-oxidative degradation will decrease. If changes in the rate of the termination steps dominate, then the rate of degradation will increase. Both cases have been observed experimentally. For a summary of examples where an increase in crystallinity leads to a decrease in degradation, see Ref. 84. Increases in degradation rates are found for the systems cited in Refs. 100, 101, and 108–110.

As a matter of practical application, the effect of decreased oxygen diffusion (caused by an increase in chain order or crystallinity) is not always to decrease the rate of oxidative degradation. Most commercial polymers contain antioxidants, and the diffusion of these species will also decrease as ordering increases in the polymer. Their ability to act as antioxidants will thus also decrease. The net effect on the autooxidation process in these systems will be determined by which species, oxygen or antioxidant, is more affected by the decrease in diffusion.

The availability of oxygen in the interior of a polymer sample is also influenced by macroscopic structural features of the polymer. As a polymer degrades, cracks and fissures generally develop (initially on the surface), and their presence will facilitate penetration of oxygen into the interior.<sup>66</sup> And, as discussed, the presence of corners will increase oxygen diffusion into a sample.<sup>61</sup> Finally, it is noted that oxygen diffusion rates will be dependent on the oxygen partial pressure.

#### *iv. Chromophore Concentration*

As the final point for discussion, it is noted that chromophore concentration can affect the rate of a photochemical reaction.<sup>111,112</sup> (As used here and in the literature, *chromophore* refers to any functional group, whether intentionally present or not, that absorbs light. Examples of adventitious chromophores include the hydroperoxy, carbonyl, and hydroxy groups that form in the autooxidation cycle.) If a polymer has a higher concentration of chromophores, its degradation rate will be faster simply because more sites are available to absorb photons and initiate a reaction. The quantum yield of the reaction will not change, however, because the quantum yield is the reaction rate normalized by the intensity of the absorbed light (Eq. 26). (As discussed, the quantum yield can be intensity dependent if the reaction mechanism involves first-order propagating steps in competition with second-order termination steps.)

## V. ACKNOWLEDGMENTS

The National Science Foundation (CHE-0093869 and DMR-0096606) and the Donors of the Petroleum Research Fund, administered by the American Chemical Society, are acknowledged for support of the work in the author's laboratory.

## VI. REFERENCES

1. N. Grassie, G. Scott, *Polymer Degradation and Stabilization*, Cambridge University Press, New York, 1985.
2. J. Guillet, *Polymer Photophysics and Photochemistry: An Introduction to the Study of Photoprocesses in Macromolecules*, Cambridge University Press, New York, 1985.
3. J. F. Rabek, *Mechanisms of Photophysical Processes and Photochemical Reactions in Polymers*, Wiley, New York, 1987.

4. G. Geuskens, *Compr. Chem. Kinet.*, **14**, 333 (1975).
5. J. F. Rabek, *Photodegradation of Polymers Physical Characteristics and Applications*, Springer, New York, 1996.
6. S. H. Hamid, et al., *Environ. Sci. Pollut. Control Ser.* 2000, **21** (2000).
7. J. E. Guillet, in *Degradable Materials*, S. A. Barenberg, J. G. Brash, R. Narayan, A. E. Redpath, eds., CRC Press, Boston, 1990.
8. G. Odian, *Principles of Polymerization*. 3rd ed., 1991.
9. G. Scott, D. Gilead, et al., *Degradable Polymers: Principles and Applications*, 1995.
10. S. Cho, W. Choi, *J. Photochem. Photobiol., A*, **143**, 221 (2001).
11. H. Zweifel, et al., *Plastics Additives Handbook*, 5th ed., Hanser, Cincinnati, OH 2001.
12. H. Matsui, S. M. Arrivo, J. J. Valentini, J. N. Weber, *Macromolecules*, **33**, 5655 (2000).
13. N. J. Turro, *Modern Molecular Photochemistry*, Addison-Wesley, Reading, MA, 1978.
14. F. Gugumus, in *Plastics Additives Handbook*, H. Zweifel, ed., Hanser, Cincinnati, OH 2001.
15. M. Shirai, K. Suyama, H. Okamura, M. Tsunooka, *J. Photopolym. Sci. Tech.*, **15**, 715 (2002).
16. B. Ranby, paper presented at Recent Advances in Environmentally Compatible Polymers, International Cellucon Conference, 11th, Tsukuba, Japan, Mar. 24–26, 1999.
17. D. Feldman, *J. Polym. Environ.*, **10**, 163 (2002).
18. N. C. Billingham, D. M. Wiles, B. E. Cermak, J. G. Gho, C. W. J. Hare, J. F. Tung, paper presented at Addcon World 2000, Two-Day Conference, 6th, Basel, Switzerland, Oct. 25–26, 2000.
19. M. Shirai, *Kemikaru Enjinyaringu*, **47**, 657 (2002).
20. P. J. Hocking, *J. Macromol. Sci., Rev. Macromol. Chem. Phys.*, **C32**, 35 (1992).
21. Blending these copolymers with homopolymer resins leads to the final commercial product. Radical production and/or backbone degradation occurs by the Norrish type I and II routes in these polymers (scheme 6).
22. S. C. Tenhaeff, D. R. Tyler, *J. Chem. Soc., Chem. Commun.*, 1459 (1989).
23. S. C. Tenhaeff, D. R. Tyler, *Organometallics*, **10**, 473 (1991).
24. S. C. Tenhaeff, D. R. Tyler, *Organometallics*, **10**, 1116 (1991).
25. S. C. Tenhaeff, D. R. Tyler, *Organometallics*, **11**, 1466 (1992).
26. S. C. Tenhaeff, J. J. Wolcott, D. R. Tyler, *Polym. Prepr. Am. Chem. Soc., Div. Polym. Chem.*, **34**, 354 (1993).
27. D. R. Tyler, *Coord. Chem. Rev.*, **246**, 291 (2003).
28. T. J. Meyer, J. V. Caspar, *Chem. Rev.*, **85**, 187 (1985).
29. C. U. Pittman Jr., M. D. Rausch, *Pure Appl. Chem.*, **58**, 617 (1986).
30. K. Gonsalves, L. Zhan-Ru, M. D. Rausch, *J. Am. Chem. Soc.*, **106**, 3862 (1984).
31. K. E. Gonsalves, R. W. Lenz, M. D. Rausch, *Appl. Organomet. Chem.*, **1**, 81 (1987).
32. F. W. Knobloch, W. H. Rauscher, *J. Polym. Sci.*, **54**, 651 (1961).
33. C. U. Pittman Jr., *J. Polym. Sci., Polym. Chem. Ed.*, **6**, 1687 (1968).
34. K. E. Gonsalves, M. D. Rausch, *J. Polym. Sci., Part A Polym. Chem.*, **26**, 2769 (1988).
35. W. J. Patterson, S. P. McManus, C. U. Pittman Jr., *J. Polym. Sci., Polym. Chem. Ed.*, **12**, 837 (1974).
36. P. Nguyen, P. Gomez-Elipse, I. Manners, *Chem. Rev.*, **99**, 1515 (1999).
37. I. Manners, *Adv. Organomet. Chem.*, **37**, 131 (1995).
38. I. Manners, *Coord. Chem. Rev.*, **137**, 109 (1994).
39. M. Moran, M. C. Pascual, I. Cuadrado, J. Losada, *Organometallics*, **12**, 811 (1993).
40. S. Amer, G. Kramer, A. Poe, *J. Organomet. Chem.*, **209**, C28 (1981).
41. J. R. Krause, D. R. Bidinosti, *Can. J. Chem.*, **53**, 628 (1975).

42. J. T. Landrum, C. D. Hoff, *J. Organomet. Chem.*, **282**, 215 (1985).
43. A. Avey, S. C. Tenhaeff, T. J. R. Weakley, D. R. Tyler, *Organometallics*, **10**, 3607 (1991).
44. R. Birdwhistell, P. Hackett, A. R. Manning, *J. Organomet. Chem.*, **157**, 239 (1978).
45. S. C. Tenhaeff, D. R. Tyler, T. J. R. Weakley, *Acta Crystallogr., Sect. C: Cryst. Struct. Commun.*, **C47**, 303 (1991).
46. W. A. Herrmann, M. Huber, *Chem. Ber.*, **111**, 3124 (1978).
47. E. C. Brehm, J. K. Stille, A. I. Meyers, *Organometallics*, **11**, 938 (1992).
48. A. E. Stiegman, D. R. Tyler, *Coord. Chem. Rev.*, **63**, 217 (1985).
49. G. F. Nieckarz, D. R. Tyler, *Inorg. Chim. Acta*, **242**, 303 (1996).
50. G. L. Geoffroy, M. S. Wrighton, *Organometallic Photochemistry*, Academic Press, New York, 1979.
51. M. Yoon, D. R. Tyler, unpublished data.
52. J. L. Male, B. E. Lindfors, K. J. Covert, D. R. Tyler, *J. Am. Chem. Soc.*, **120**, 13176 (1998).
53. E. Schutte, T. J. R. Weakley, D. R. Tyler, *J. Am. Chem. Soc.*, **125**, 10319 (2003).
54. T. Koenig, H. Fischer, in *Free Radicals*, vol. 1, J. Kochi, ed., Wiley, New York, 1973.
55. R. M. Noyes, *J. Chem. Phys.*, **22**, 1349 (1954).
56. R. M. Noyes, *J. Am. Chem. Soc.*, **77**, 2042 (1955).
57. R. M. Noyes, *J. Am. Chem. Soc.*, **78**, 5486 (1956).
58. R. M. Noyes, *Progr. Reaction Kinetics*, **1**, 129 (1961).
59. J. L. Male, M. Yoon, A. G. Glenn, T. J. R. Weakley, D. R. Tyler, *Macromolecules*, **32**, 3898 (1999).
60. J. Guillet, *Adv. Photochem.*, **14**, 91 (1988).
61. B. O'Donnell, J. R. White, *J. Mater. Sci.*, **29**, 3955 (1994).
62. B. O'Donnell, J. R. White, *Polym. Prepr. Am. Chem. Soc., Div. Polym. Chem.*, **34**, 137 (1993).
63. L. Tong, J. R. White, *Polym. Degrad. Stab.*, **53**, 381 (1996).
64. R. Baumhardt-Neto, M. A. De Paoli, *Polym. Degrad. Stab.*, **40**, 59 (1993).
65. R. Baumhardt-Neto, M. A. De Paoli, *Polym. Degrad. Stab.*, **40**, 53 (1993).
66. G. E. Schoolenberg, P. Vink, *Polymer*, **32**, 432 (1991).
67. C. T. Kelly, L. Tong, J. R. White, *J. Mater. Sci.*, **32**, 851 (1997).
68. B. O'Donnell, M. M. Qayyum, L. Tong, J. R. White, *Polym. Prepr. Am. Chem. Soc., Div. Polym. Chem.*, **34**, 211 (1993).
69. C. T. Kelly, J. R. White, *Polym. Degrad. Stab.*, **56**, 367 (1997).
70. W. K. Busfield, M. J. Monteiro, *Mat. Forum*, **14**, 218 (1990).
71. D. Benachour, C. E. Rogers, *ACS Symp. Series*, **151**, 263 (1981).
72. M. Igarashi, K. L. DeVries, *Polymer*, **24**, 1035 (1983).
73. A. Huvet, J. Philippe, J. Verdu, *Eur. Polym. J.*, **14**, 709 (1978).
74. W. K. Busfield, P. Taba, *Polym. Degrad. Stab.*, **51**, 185 (1996).
75. F. ThomINETTE, J. Verdu, *Polym. Prepr. Am. Chem. Soc., Div. Polym. Chem.*, **35**, 971 (1994).
76. V. I. Tupikov, S. A. Khatipov, V. F. Stepanov, *Phys. Chem. Mat. Treatment*, **31**, 32 (1997).
77. M. Igarashi, K. L. DeVries, *Polymer*, **24**, 769 (1983).
78. M. E. Nichols, J. L. Gerlock, C. A. Smith, *Polym. Degrad. Stab.*, **56**, 81 (1997).
79. H. Nguyen Truc Lam, C. E. Rogers, *Polym. Mater. Sci. Eng.*, **56**, 589 (1987).
80. V. G. Plotnikov, *Dok. Akad. Nauk SSSR*, **301**, 376 (1988).
81. T. L. Nguyen, C. E. Rogers, *Polym. Mater. Sci. Eng.*, **53**, 292 (1985).
82. E. Baimuratov, D. S. Saidov, I. Y. Kalontarov, *Polym. Degrad. Stab.*, **39**, 35 (1993).

83. Y. A. Shlyapikov, S. G. Kiryushkin, A. P. Marin, *Antioxidative Stabilization of Polymers*, Taylor & Francis, Bristol, PA, 1996.
84. M. S. Rabello, J. R. White, *Polym. Degrad. Stab.*, **56**, 55 (1997).
85. V. Bellenger, J. Verdu, G. Martinez, J. Millan, *Polym. Degrad. Stab.*, **28**, 53 (1990).
86. N. Y. Rapoport, G. E. Zaikov, *Eur. Polym. J.*, **20**, 409 (1984).
87. N. Y. Rapoport, L. S. Shibryaeva, V. E. Zaikov, M. Iring, Z. Fodor, F. Tudos, *Polym. Degrad. Stab.*, **12**, 191 (1985).
88. F. Castillo, G. Martinez, R. Sastre, J. Millan, V. Bellenger, B. D. Gupta, J. Verdu, *Polym. Degrad. Stab.*, **27**, 1 (1990).
89. S. N. Zhurkov, V. A. Zakrevskii, V. E. Korsukov, V. S. Kuksenko, *J. Polym. Sci. Polym. Phys. Ed.*, **10**, 1509 (1972).
90. J. R. White, N. Y. Rapoport, *Trends Polym. Sci.* **2**, 197 (1994).
91. P. C. Dawson, M. Gilbert, W. F. Maddams, *J. Polym. Sci. Part B Polym. Phys.*, **29**, 1407 (1991).
92. S. J. Guerrero, H. Veloso, E. Randon, *Polymer*, **31**, 1615 (1990).
93. C. Baker, W. F. Maddams, J. E. Preedy, *J. Polym. Sci. Polym. Phys. Ed.*, **15**, 1041 (1977).
94. J. A. Kwon, R. W. Truss, *J. Mater. Sci.*, **37**, 1675 (2002).
95. R. P. Chartoff, T. S. K. Lo, E. R. Harrell Jr., R. J. Roe, *J. Macromol. Sci., Phys.*, **B20**, 287 (1981).
96. A. S. Goldman, D. R. Tyler, *Inorg. Chem.*, **25**, 706 (1986).
97. V. Balzani, V. Carassiti, *Photochemistry of Coordination Compounds*, Academic Press, New York, 1970.
98. P. F. Barron, W. K. Busfield, J. V. Hanna, *Polym. Commun.*, **29**, 70 (1988).
99. J. G. Calvert, J. N. Pitts, *Photochemistry*, Wiley, New York, 1966.
100. L. J. Dogue, N. Mermilliod, F. Genoud, *J. Polym. Sci. Part A Polym. Chem.*, **32**, 2193 (1994).
101. N. C. Billingham, P. Prentice, T. J. Walker, *J. Polym. Sci. Polym. Symp.*, **57**, 287 (1977).
102. L. Ogier, M. S. Rabello, J. R. White, *J. Mater. Sci.*, **30**, 2364 (1995).
103. A. Popov, N. Rapoport, G. Zaikov, *Oxidation of Stressed Polymers*, Gordon & Breach, New York, 1991.
104. L. Audouin, V. Langlois, J. Verdu, J. C. M. de Bruijn, *J. Mater. Sci.*, **29**, 569 (1994).
105. A. V. Cunliffe, A. Davis, *Polym. Degrad. Stab.*, **4**, 17 (1982).
106. C. R. Boss, J. C. W. Chien, *J. Polym. Sci. Polym. Chem. Ed.*, **4**, 1543 (1966).
107. H. H. G. Jellinek, S. N. Lipovac, *Macromolecules*, **3**, 237 (1970).
108. N. Y. Rapoport, S. I. Berulava, A. L. Kovarskii, I. N. Musaelyan, Y. A. Ershov, V. B. Miller, *Vysokomolekulyarnye Soedineniya, Seriya A*, **17**, 2521 (1975).
109. G. Akay, T. Tincer, E. Aydin, *Eur. Polym. J.*, **16**, 597 (1980).
110. E. M. Slobodetskaya, *Uspekhi Khimii*, **49**, 1594 (1980).
111. D. J. Carlsson, D. M. Wiles, *J. Macromol. Sci. Rev. Macromol. Chem.*, **C14**, 65 (1976).
112. A. Garton, D. J. Carlsson, D. M. Wiles, *J. Polym. Sci. Polym. Chem. Ed.*, **16**, 33 (1978).



---

## CHAPTER 5

# Zirconocene and Hafnocene-Containing Macromolecules

**Charles E. Carraher Jr.**

*Florida Atlantic University, Department of Chemistry and Biochemistry, Boca Raton, Florida, and Florida Center for Environmental Studies, Palm Beach Gardens, Florida*

### CONTENTS

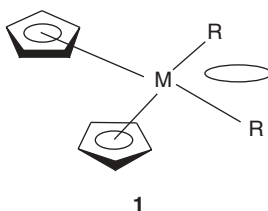
I. GENERAL	112
II. INTRODUCTION	113
III. INORGANIC SUPPORTED ZIRCONOCENE AND HAFNOCENE CATALYSTS	116
IV. OTHER SUPPORTS	119
V. CONDENSATION REACTIONS WITH MONOMERIC LEWIS BASES	121
VI. ZIRCONOCENE AND HAFNOCENE REACTIONS WITH ALREADY EXISTING POLYMERS	137
VII. MISCELLANEOUS	139
VIII. SUMMARY	143
IX. REFERENCES	143

*Macromolecules Containing Metal and Metal-Like Elements,*  
*Volume 6: Transition Metal-Containing Polymers*, edited by Alaa S. Abd-El-Aziz,  
Charles E. Carraher Jr., Charles U. Pittman Jr., and Martel Zeldin.  
Copyright © 2006 John Wiley & Sons, Inc.

## I. GENERAL

Interest in the metallocenes began in the 1950s when two independent groups (Pauson is often credited as the first) prepared ferrocene by reaction of iron II chloride with cyclopentadienyl magnesium bromide and by reaction of reduced iron with cyclopentadiene in the presence of potassium oxide.<sup>1,2</sup> Ferrocene is a true sandwich compound with the iron resting between two planer and parallel cyclopentadiene groups.

By comparison the Group IV B metallocene have the cyclopentadiene groups facing the metal atom but present in a distorted tetrahedral arrangement as **1**. Here, the empty SP orbital is indicated by the open ellipse.



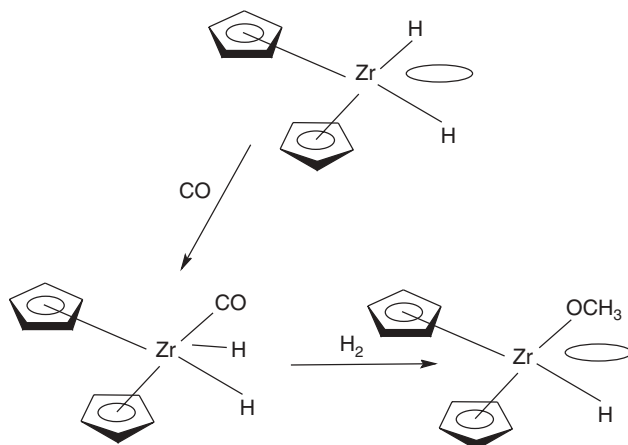
In fact, the tetrahalides of zirconium IV and hafnium IV are all tetrahedral monomers in the gas phase (but as solids they are polymeric with halide bridging). Organozirconium and organohafnium chemistry resembles organotitanium chemistry. The best studied of the Group IVB products are the cyclopentadienyl products with the general form  $Cp_2MX_2$  where X can be any of the halides, hydrogen, alkyl and aryl groups. In all cases, the four ligands are mainly present in a distorted tetrahedral arrangement about the metal atom.

Cotton and Wilkinson<sup>3</sup> described Group IVB metallocene compounds as 9-coordinate bonding with the hybrid orbitals being derived from one-s, three-p, and five-d orbitals. Each pi-Cp ring interacts with three hybrid orbitals. The remaining three orbitals consist of two equivalent  $spdx^2-y^2$ ,  $d_z^2$  orbitals (overlapping the halides, oxygen, nitrogen, etc.) and one sp vacant orbital as shown above.

In reaction with carbon monoxide, as well as many other Lewis acid–base type reactions, the “vacant” orbital is often the initial site of reaction. Thus the reaction between zirconium dihydride and carbon monoxide initially forms a carbonyl metal dihydride complex about the zirconium metal atom concluding in the formation of the ethoxide derivative after hydrogenation as shown in scheme 1.<sup>4</sup> This reaction is important because it leads to the formation of a variety of compounds that have M–O bonds. But, it is also important because it signals a probable mechanistic mode for attack by a Lewis base.

The metallocenes of the early d-elements, including zirconocene and hafnocene, are viewed as being hard because of this strong affinity for oxygen.

The atomic radii (in picometers) for Ti, Zr, and Hf are 147, 160, and 159.<sup>5</sup> The reversal of the typical trend where the members of a family increase in atomic radii as one goes down the column is only violated here although the atomic radii for most



Scheme 1

of the 5- and 6-row transition elements are similar due to the lanthanide effect. This results in zirconium and hafnium-containing compounds having similar properties and in the difficulty in separating mixtures containing compounds that differ only in whether the metal is zirconium or hafnium. The chemistry of organometallic zirconium and hafnium compounds has been reviewed.<sup>6,7</sup> Reviews of metallocenes and metallocene polymers have appeared.<sup>8-12</sup>

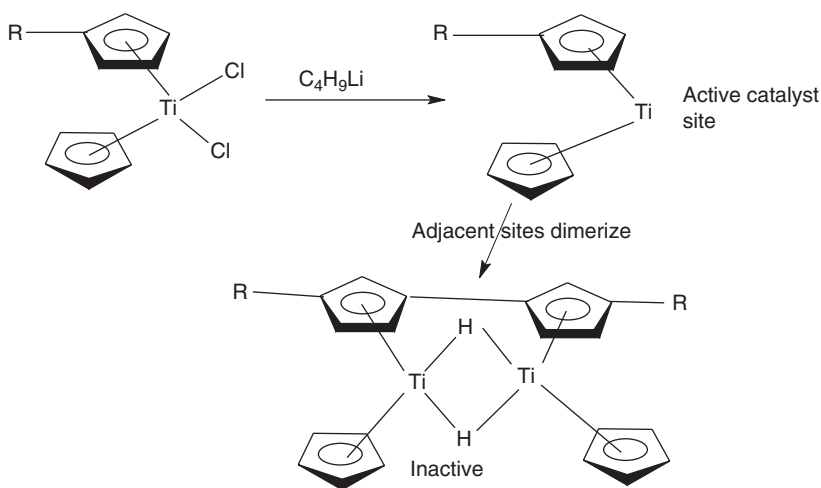
Unlike titanocene dichloride, which contains two visual color sites, the Ti-Cp yellow and the Ti-Cl red, zirconocene dichloride and hafnocene dichloride are white. Thus products derived from them are ordinarily white unless the other reactant contains its own color sites.

## II. INTRODUCTION

More than 2 million entries are given when searching the general topics and entering the terms *hafnocene* and *polymers*. Almost all of entries for both hafnocene and zirconocene connected with polymers are associated with their use as stereoregulating catalysts. These metallocenes are important Ziegler-Natta catalysts and are also important catalysts in the current generation of so-called soluble single site stereoregulating catalysts.

While the amount of interest in these two groups of metallocenes is great, the amount of work involving their incorporation into polymers is small. Much of it involves the metallocenes serving as supported catalysts. The mechanism of activity involves having at least one unoccupied orbital available about the metal atom. For instance Grubbs and coworkers in 1977 suggested, based on work done with olefin hydrogenations, that the two chlorides in titanocene dichloride are absent in the active catalyst, as shown in scheme 2.<sup>12,13</sup>

Many Natta-Ziegler mechanisms require the adduct and active species to contain at least two participating orbitals, the unfilled orbital of the Group IVB metals and one additional orbital.<sup>15</sup> If the metallocene is tied into a polymer through its noncyclopentadienyl groups, then the only way two vacate sites are available is to break the polymer chain. If however, the metallocene portion is present as a sidechain, then open sites can be made available without scission from the polymer chain. There has been a great deal of work on creating immobilized metallocene-containing catalysts.

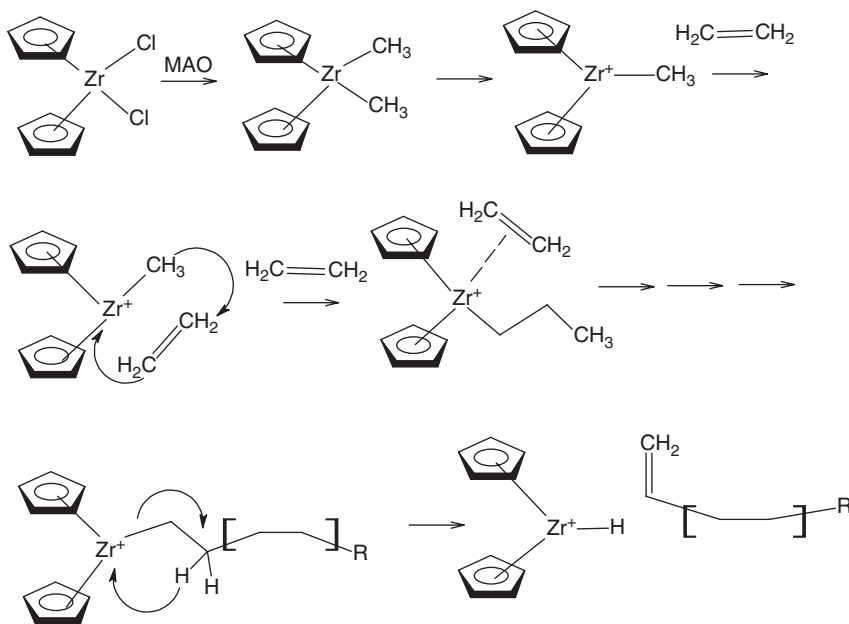


**Scheme 2**

It is not clear if more than one site always needs to be available for some catalytic activity. In this case the metallocenes already have one open site, as noted above. Thus polymers with the metallocene in the backbone connected through the metal atom might be active for these systems.

Much of the recent work with zirconocene and hafnocene derivatives involves their use as catalysts in soluble stereoregulating polymerizations. The active site is a cationic metallocene-alkyl generated by reaction of a neutral metallocene formed from reaction with excess methylalumoxane (MAO) or other suitable cocatalysts such as a borane Lewis acid. This sequence is shown below employing MAO with ethylene to form polyethylene. Initiation and propagation occur through precoordination and insertion of the ethylene into the alkyl group-polymer chain. Here termination occurs through beta-hydride elimination, producing a zirconium hydride and a long-chain alpha-olefin. Slowing  $\beta$ -elimination leads to linear high-density polyethylene or when used with comonomers such as 1-propylene, 1-hexene, or 1,5-hexadiene a variety of branched and linear polymers can be made. The general series of reaction steps is described in scheme 3. The Group IVB metallocene catalysts are active, producing yields in excess of 1 ton of polyethylene per gram of catalyst per hour with a total efficiency on the order of 25 tons of PE per gram of catalyst. These

catalysis systems are also used to form a variety of polyethylenes and other vinyl-derived polymers and copolymers.



Scheme 3

A major limitation of such Group IVB metallocene catalysts is that they are air and moisture sensitive and not tolerant of heteroatom-containing monomers. The unbonded electron pairs on heteroatom-containing monomers, such as oxygen, preferentially coordinate to the Lewis acid metal center in place of the carbon-carbon double bond. Some middle and late transition metal organometallics are more tolerant to the presence of such heteroatoms and can be used as effective cocatalysts. These include some palladium, iron, cobalt, and nickel initiators. Even so, the current major interest involves the Group IVB metallocenes. The proposed mechanism involves the metal atoms' open coordination sites being free to act as the catalytic site. This does not eliminate the potential use of Group IVB metallocene polymers, that have the metallocene metal as part of the polymer backbone as being catalysts, but it does demonstrate why the current interest is on free (monomeric) metallocenes and anchored metallocenes where the nonmetallocene portion is free and available to be converted into the active catalytic site.

While most studies use hafnocene and zirconocene, many of their derivatives have been reported. Furthermore, most of the activity has involved the dichlorides of these two metallocenes. This is probably largely due to the fact that the zirconocene and hafnocene dichlorides are commercially available.

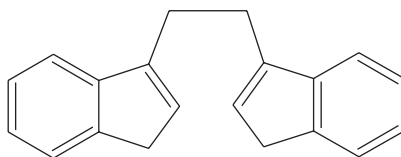
### III. INORGANIC SUPPORTED ZIRCONOCENE AND HAFNOCENE CATALYSTS

Chien<sup>16</sup> recently reviewed supported metallocene polymerization catalysts. Here, we will indicate more recent efforts and trends. Many of the support systems are polymers being derived from silicon dioxide. Thus it is appropriate to consider this topic within this chapter.

Supported catalysts are employed industrially to produce a wide range of stereoregular polymers. Supported metallocene/MAO catalysts were first suggested by Sinn and coworkers<sup>17</sup> and Kaminsky and coworkers.<sup>18</sup> Supported metallocene catalysts were recently reviewed by Ribeiro and coworkers.<sup>19</sup>

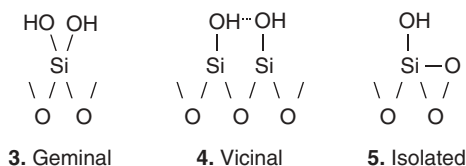
The advantages and disadvantages of supported metallocene polymerization catalysts versus the analogous homogeneous catalysts are well known.<sup>16</sup>

The two most widely used inorganic supports are silica (SiO<sub>2</sub>) and alumina (Al<sub>2</sub>O<sub>3</sub>). Typical reactive surface functionality requirements include an acidic OH group, Lewis base oxide groups, and a Lewis acidic metal center. A zirconocene and hafnocene precursor of the general formula L<sub>2</sub>MX<sub>2</sub>, where M=Zr or Hf, L=cyclopentadiene (Cp), indenyl, or bis(indenyl)ethane, **2**, and surface hydroxyl groups (Si-O-H and Al-O-H) fulfill this requirement.



**2** Bis(indenyl)ethane, Et(THI)<sub>2</sub>

Silicas and aluminas with a wide variety of surface areas, pore volumes, and porosities are available. These surfaces will have different groupings of surface hydroxyl groups including geminal, **3**, vicinal, **4**, and isolated, **5**, as shown for silanols.



The interaction of Lewis acid metal centers in alumina has been studied using Cp<sub>2</sub>Zr(<sup>13</sup>CH<sub>3</sub>)<sub>2</sub>.<sup>20</sup> This study was consistent with a methide anion being transferred from Zr to a Lewis acid site on the surface forming a “cation-like” zirconium or zirconocenium surface species, Cp<sub>2</sub>Zr<sup>+</sup>(CH<sub>3</sub>) with the formation of an Al-CH<sub>3</sub><sup>-</sup> anionic complex.

A number of MAO-free cocatalysts containing trimethylaluminum, TMA, have been studied. Soga and coworkers<sup>21–23</sup> prepared a number of catalytic systems. Using supported zirconocene dichloride catalysts, productivities were close to those found for the simple solution systems. Greater stereospecificity was achieved using bridged zirconocene systems, where the bridges included ethylenediindenyl systems, supported on alumina. It is believed that the support enhances the profacial monomer selection by the  $Zr^+$  center and at the same time renders more favorable the beta-agostic interaction between it and the hydrogen atom on the beta-carbon atom of the growing chain.

The variation in results found for such systems is consistent with the need for precise structural control to achieve good polymerization and reproducible polymerization results.

The molecular weight distributions (MWD),  $M_w/M_n$ , for polypropylene, PP, obtained from alumina supported catalysts are less than two.

For ansa (meaning “bent handle”) bridged systems, such as  $Et(THI)_2ZrCl_2$ , the polypropylene polymerization activities are only 10–20% those of the same zirconocene complexes in solution. However, supported  $Cp_2ZrCl_2$  catalysts exhibit productivities closer to those when the zirconocene is in solution. Furthermore, the supported systems on alumina are more stereospecific than corresponding soluble systems. The supported symmetric zirconocenes give *i*-PP and *s*-PP with higher melting points and greater homosteric pentad populations. It is believed that the supports enhance the profacial monomer selection by the  $Zr^+$  center and at the same time renders the beta-agostic interaction between it and atomic hydrogen on the beta carbon atom of the growing chain more favorable, as evidenced by a significantly lower molecular weight for the PP obtained with the heterogenized zirconocenes. The molecular weight distributions of the alumina supported PP are less than 2.

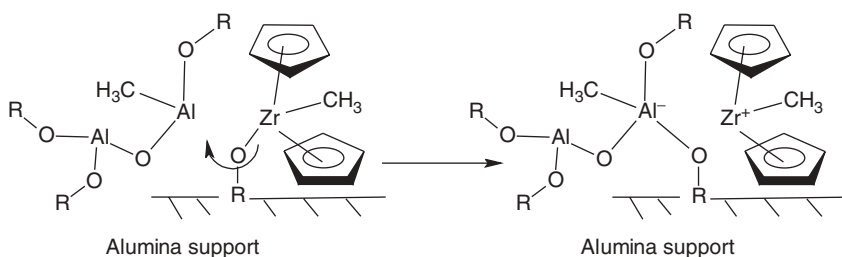
Earlier, Kaminsky and Renner<sup>24</sup> supported zirconocene derivatives on dehydroxylated silica and studied the polymerization of propylene. The catalysts had an activity of  $1 \times 10^4$  g PP/mol Zr h. This PP has a high stereoregularity and high melting point. In solution, the same zirconocene catalyst has a much greater activity ( $4 \times 10^6$  g PP/mol Zr h) but the stereoregularity was less and the melting point of the PP lowered from 160° to 128°C.

Sacchi and coworkers<sup>25</sup> found that even an aspecific zirconocene catalyst can become isospecific when bound. Thus  $(Ind)_2ZrCl_2$  in solution with MAO gave PP as a waxy product with an activity of  $1.5 \times 10^5$  g PP/mol Zr h. The PP had a  $[mm]=0.18$ ,  $[mr]=0.46$ , and  $[rr]=0.36$  ( $m$ =meso;  $r$ =racemic). When the zirconocene was supported on dehydroxylated silica it gave high molecular weight ( $2 \times 10^5$ ) *i*-PP ( $[mm]=0.71$ ,  $[mr]=0.15$ , and  $[rr]=0.14$ ) but with poor activity ( $4 \times 10^3$  g PP/Zr h). In solution, the various conformations of the zirconocene compound are in rapid equilibrium. If the rate of conformational transition is more rapid than the formation of the PP molecule, then only atactic PP is formed. But when the catalyst is immobilized on a support, conformational equilibration is slow on this time scale. Thus such supported catalysts can give greater stereospecificity, but the yields and rates of polymerization are generally less than for the soluble catalysts.

Sacchi and coworkers<sup>25</sup> found that zirconocene complexes react with silica through reaction with surface hydroxyl groups.

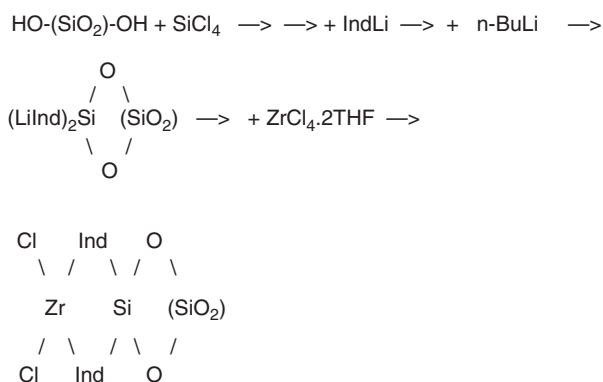
The cocatalysts containing MAO has been studied. Chen et al.<sup>26</sup> studied the immobilization of diindenyl zirconium dichloride on alumina. The activity of partially dehydroxylated silica, PDA, supported catalysts is nine times greater than that of dehydroxylated silica, DA. This is contrary to what was expected because the DA supported catalyst is more Lewis acidic and more active in promoting the formation of the  $Cp_2Zr^+$  species. Apparently, MAO is able to activate oxo-bonded zirconocenes, as shown in scheme 4.

Chien and He<sup>27</sup> used a  $Et(Ind)_2ZrCl_2$  supported catalysts to produce a number of copolymers. The reactivity ratios were the same as those found for the analogous homogeneous systems. By comparison, Soga and Kaminaka<sup>28</sup> found that the comparative homogeneous reactivity systems varied with the particular support system utilized. In general, alumina supported catalysts produced copolymers with narrow molecular weight ratios.



Scheme 4

Metallocenes have been connected by spacers to silica. Soga and coworkers<sup>29</sup> prepared extended catalysts, as shown in scheme 5.



Scheme 5

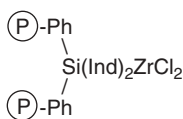
Addition of an aluminum-ether catalyst, TIBA, polymerizes propylene at a low activity (10 g PP/mol Zr h). The reaction of TIBA with the zirconocene does not generate the  $3d^0 14e^- Zr^+$  catalytic site. Even so, the PP that is produced contains 98%

[mmmm] tetrads, is high molecular weight ( $7 \times 10^5$ ), and high melting ( $158.6^\circ\text{C}$ ). This system does not improve using MAO instead of TIBA as a cocatalyst. The activity is increased but to only 20 g PP/Zr h. A slightly higher melting point ( $159.2^\circ\text{C}$ ), slightly lower [mmmm] of 94%, and a lower molecular weight ( $3.4 \times 10^5$ ) are obtained.

#### IV. OTHER SUPPORTS

Grubbs and others<sup>30–32</sup> have reported the use of metallocenes attached to crosslinked styrene-divinylbenzene (20%) copolymers. These systems catalyze a wide variety of reactions, including reduction of dinitrogen, isomerization of olefins, hydrogenation of olefins and acetylenes, epoxidation of olefins, and isomerization of cyclo-dienes.

Nishida and coworkers<sup>33,34</sup> lithiated styrene-divinylbenzene (2%) beads with *n*-BuLi. This product was then reacted with  $\text{Cl}_2\text{Si}(\text{Ind})_2$  followed by metallation to give an attachment described by structure 6.



6

This system produced PP with an activity of  $5 \times 10^5$  g PP/mol Zr h. The product was 62% *i*-PP which had a melting point of  $140^\circ\text{C}$ , [mmmm]=90%, a molecular weight of  $2.5 \times 10^4$ , and a molecular weight distribution ratio of 3.1.

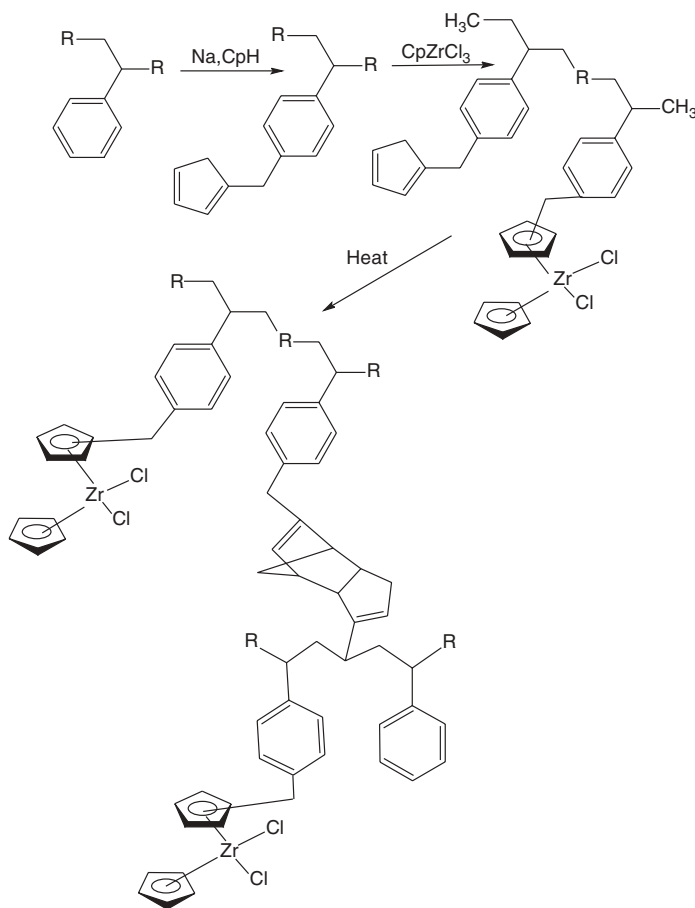
Soga and coworkers<sup>29</sup> created polydimethylsiloxane-supported systems containing zirconocene derivatives. These systems polymerized ethylene with activities of 2 to  $4 \times 10^6$  g PE/mol Zr h. The same system was used to polymerize propylene. The activities were lower than those of the analogous homogeneous systems. The systems produced 40–60% PP with a [mmmm] of about 90% and melting points in the range of  $142^\circ$  to  $154^\circ\text{C}$ . A juxtaposition of the bridging backbone atoms occurs to arrange the zirconocene in some “rac-like” and “meso-like” structures that are believed to produce isotactic and atactic PP stereochemistries.

Other inorganic polymer supports have been used. Zeolites have large surface areas, narrow pore-size distributions, and well defined structures. Woo and coworkers<sup>35,36</sup> studied the catalytic activity of bound zirconocenes on several zeolites. Little or no activity was found when the zeolite cage size was too small to readily accommodate the catalyst, monomer, and growing chain. Two zeolite-like supports with larger pore sizes, 130 nm and 400 nm, were studied. These supported catalysts polymerized propylene much like the same catalyst in solution with respect to activity, molecular weight, and homosteric pentad population.

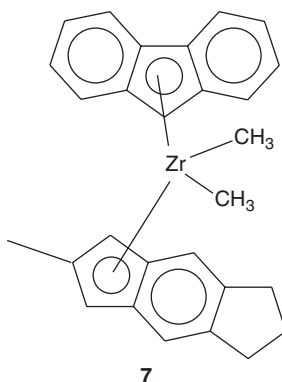
Stork and coworkers<sup>37</sup> constructed a zirconocene dichloride catalysts system supported on a crosslinked polystyrene as described in scheme 6. The crosslinking

is achieved using a Diels-Alder reaction of cyclopentadiene functions. This approach provides polymer supported zirconocene with a homogeneous distribution of active sites. The zirconocene-containing supported catalyst forms spherical beads and is active when combined with MAO at promoting PE formation. The polymerization activity was 5–30% that of the homogeneous catalyst, producing 5 to  $66 \times 10^5$  g PE/Zr h. The molecular weight of the PE prepared was  $6 \times 10^6$ , and the molecular weight distribution ratio was 2.9–3.4.

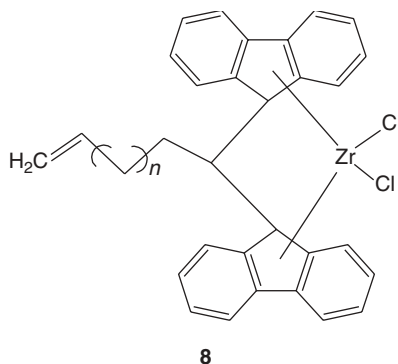
Rietmuller and coworkers<sup>38</sup> recently reported locating zirconocene-containing groups on hyperbranched polysilanes for the purpose of producing stereoregular polymers. The polycarbosilane dendrite is hydroborated at the terminal vinyl groups and then the zirconocene moiety is attached. PP was produced using this dendrite in toluene at a propylene pressure of 5 bar yielding PP in moderate yields with [mmmm] values about 35%. The proposed zirconocene site is pictured in structure 7.



Scheme 6



Alt and Jung<sup>39</sup> synthesized a wide variety of bridged metallocene dichloride complexes where the metal is Zr or Hf. These metallocene-containing units had a vinyl group appended to the bridging carbon that has subsequently polymerized giving a polymer with metallocene arms radiating from the central carbon-backbone core. One such structure is **8**, where  $M = \text{Zr}$  and  $n = 1, 3, 5$ .



The polymers containing this type of metallocene were activated with MAO and the PE polymerized. The general melting points for the PEs obtained ranged from a low of about 132°C to a high of about 140°C. Activities ranged from about  $9 \times 10^3$  to  $3 \times 10^5$  g PE/mmol Zr h for the catalyst systems.

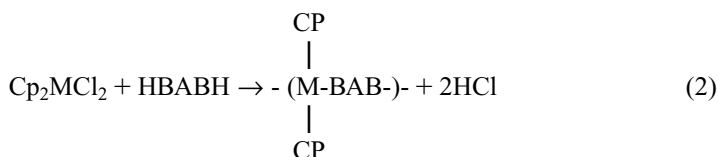
## V. CONDENSATION REACTIONS WITH MONOMERIC LEWIS BASES

Electronegative halides attached to the  $\text{Cp}_2\text{M}$  metal centers can undergo condensation reactions. The metallocene dihalide acts as the Lewis acid. When the

Lewis base is monofunctional the products will be monomeric, as shown later for a metallocene dichloride.



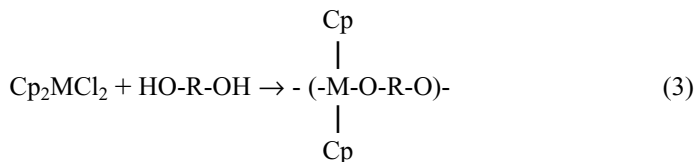
But when the Lewis base is difunctional a polymer chain is formed.



Finally, when the Lewis base's functionality is greater than two, crosslinking occurs.

These are rapid reactions for the Group IVB metallocene dichlorides, generally being over in less than 5 s. Therefore, the yield is a direct measure of the polymer forming step(s) relative to all other competing steps. This is consistent with observations made studying the color changes in titanocene-containing reactions. Titanocene dichloride has two color sites, the Cp-Ti is a mild yellow to orange, whereas the Ti-Cl is an intense off red color. As the titanocene dichloride loses the chloride color sites becoming another species either through inclusion into the polymer or hydrolyzes, the color of the reaction changes from red to yellow. This color change is related to product formation and is a valid indicator to measure the progress (polymerization rate) and termination of the reaction.<sup>40-44</sup> Assuming that the Group IVB metallocene dichlorides react similarly, product yield has been used as a direct measure of reaction rate.

A number of zirconocene and hafnocene polyethers (Eq. 3) have been synthesized using both the classical and inverse interfacial systems as well as a totally aqueous system.<sup>40-44</sup> In the inverse system, the metallocene is contained in water and the diol contained in the organic liquid such as chloroform. Product yields were in the range of 30 to above 60% for the inverse interfacial systems. In the classical (aqueous-containing) interfacial system, the metallocene is contained in the organic liquid and the diol and added base are present in an aqueous phase. For analogous diols, product yields were from about 15 to over 60%, similar to that of the inverse interfacial systems.



An entirely aqueous medium also proved successful in the synthesis of polyethers. Both the diol, with added base, and metallocene dichloride are dissolved in two separate aqueous solutions. The two solutions are then brought together and the

polyether formed. Product yield from the aqueous solution systems varied from 5 to over 50%. These yields were lower than for the interfacial system, in every instance, when compared with the same diol. No product was formed using a simple organic system, where both the metallocene and diol along with added organic base, triethylamine, were mixed.

The inverse interfacial and aqueous systems are possible because the Group IVB metallocene dichlorides hydrolyze rapidly forming various products. These products are mainly hydroxyl-related and undergo polycondensation in the same manner as the metallocene halides.

An extensive study was made employing zirconocene dichloride. Product yield was studied as a function of stirring rate. It increased steadily from 13,000 to 24,500 rpm, the highest stirring rate studied for both the classical interfacial and aqueous solution systems. Smirhoya et al.<sup>45</sup> refer to such situations as indicating of diffusion-controlled processes (i.e., differences in the diffusion rates of reactants are responsible for the variations in yield with stirring rate). Diffusion effects are generally apparent only for systems in which the activation energy for reaction is in the low to medium range (generally 20 kcal/mol or 80 kJ/mol and less). While the activation energies for these reactions are unknown, it is reasonable to assume that they are in the low to medium range since many Schotten-Baumann reactions exhibit activation energies in this range.<sup>46-48</sup>

The exact form of the reacting metallocene species is unknown. Aqueous solutions of the zirconocene dichloride are acidic, exhibiting a pH in the range of 1-3. This is consistent with the formation of species such as  $\text{Cp}_2\text{ZrOH}^+$ . Other studies have shown that the dihydroxylated species,  $\text{Cp}_2\text{Zr}(\text{OH})_2$  is insoluble in water.

A 0.1 M aqueous solution of  $\text{Cp}_2\text{ZrCl}_2$  gives a pH of 1.4. Assuming the two most prevalent species are  $\text{Cp}_2\text{Zr}^{+2}$  and  $\text{Cp}_2\text{ZrOH}^+$ , this would indicate a ratio of these two species to be 1.5:1. In fact, with the exception of products synthesized using such organic bases as triethylamine, the products have no detectable Zr-Cl end groups and only R-OH and Zr-OH end groups are found. When triethylamine is used, most of the end groups are R-OH with small amounts of Zr-OH found.

Synthesis of zirconocene polyethers was general for the interfacial systems but was effected only with aromatic diols using the aqueous systems.<sup>49</sup> This suggests that the active form(s) of reactants may be different for the two synthetic systems. The lack of polymer formation in aqueous solution systems with aliphatic diols may be due to the difference in acidity between aromatic and aliphatic diols. For instance, hydroquinone is 99% monoionized at pH's >12 and over 99% diionized at pH's >13.8. Aliphatic diols remain largely unionized even at a pH of about 14. It is possible that polycondensation is only effected in aqueous solutions containing deprotonated diols whereas other criteria and/or active species are critical for the interfacial systems.

To help evaluate this, yield was studied as a function of pH using buffered aqueous systems with hydroquinone over a pH range of 8 to 13. There is a direct correlation between pH and product yield and between product yield and the percentage of monoionized and diionized hydroquinone. Product was formed only when a large amount of the hydroquinone is at least monoionized. This is consistent with the active diol species being the deprotonated diol in the aqueous solution systems.

A similar pH profile study was made for the interfacial condensation of hydroquinone and  $\text{Cp}_2\text{ZrCl}_2$ . There is an obvious difference in the pH-yield trend results in comparison to the aqueous solution systems. Medium product yields are achieved even at low pH's. In fact, better yields are achieved in the pH ranges where little or no diol is deprotonated in comparison to pH's where the hydroquinone is deprotonated. The results are consistent with the diol being in its nondeprotonated form in interfacial systems.

Further evidence was sought by comparing the relative reactivity trends for the interfacial and aqueous solution systems. If the reactive species in both systems are the same, then the orders and/or general dependencies should be the same for both systems. The only difference is the presence of an organic layer which supplies a somewhat constant supply of the metallocene reactant. Furthermore, the active diol species would be the same with reaction occurring in the aqueous layer for the interfacial system.

The trends are dissimilar for the aqueous solution and interfacial systems using sodium hydroxide as the added base. Solubilities were unrelated to the observed relative reactivity trends. Thus the reactive species are probably not the same for the two systems. Several observations are apparent. First, steric hindrance appears to be less important for the aqueous system. This is expected if the active species are the highly energetic  $\text{Cp}_2\text{Zr}^{+2}$  and  $\text{R-O}^-$  which would be more solvated and stable in the aqueous solution system. This is consistent with the active species being the less energetic forms in the interfacial system where the reactive species were  $\text{Cp}_2\text{ZrCl}_2$  and  $\text{R-OH}$ . Second, the electronic nature of the substituted hydroquinones appears to be of secondary importance for both the aqueous solution and interfacial systems.

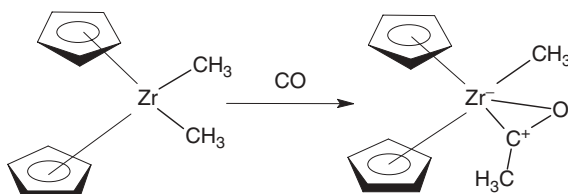
An analogous study, using the aqueous solution and interfacial systems, was carried out using triethylamine as the added base in place of sodium hydroxide. The reaction trends for the aqueous system are essentially the same as those obtained when using sodium hydroxide as the added base. Several differences in the trends are found for the interfacial system when compared with the trends found for the sodium hydroxide systems. These differences do not appear to be related to such criteria as bond polarity and steric requirements. The differences may be due to the fact that unlike sodium hydroxide which is not soluble in the organic layer, triethylamine is soluble in the organic layer.

The overall order of polyester yields for both the aqueous solution and interfacial systems is  $\text{Hf} > \text{Zr} > \text{Ti}$ . The lanthanide contraction causes the sizes, physical properties, and chemical properties of Zr and Hf to be similar, more so than for any other pair of congeneric elements.<sup>3</sup> It is difficult to separate one of these from the other. Most of the work with Zr and Hf has been done with ionic compounds. The current synthetic polymer studies involve largely covalently bonded products with the reaction involving the breakage and formation of covalent bonds.

Since the sizes and properties of Zr and Hf are so similar, subtle arguments probably need to be invoked to explain the observed polymerization trends. Hard-soft acid-base (HSAB) arguments have been used to explain some of the polymerization rate trends. The outer orbitals of Hf have one additional "node" with the center of electron density further from the metal nucleus than for Zr. This presents

a more disperse (or softer acid) outer shell for Hf in comparison to Zr. Thus the somewhat hard Lewis base, R-OH or R-O<sup>-</sup> is able to distort Hf at a longer distance consistent with the observed trend.

Zirconocene and hafnocene are generally considered as hard because of their affinity for hard ligands like O and Cl. Thus Cp<sub>2</sub>Zr(CH<sub>3</sub>)<sub>2</sub> when reacted with carbon monoxide gives the C- and O-bonded product rather than simply the C-bonded product (scheme 7).



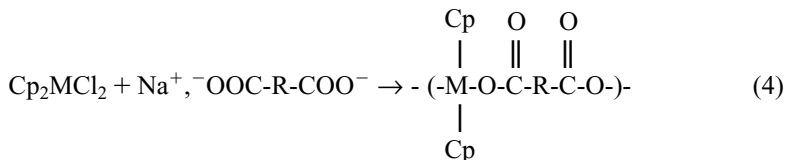
Scheme 7

Reactions on already existing polymers will be covered later. Nevertheless, it is instructive to note that for the interfacial modification of dextran through reaction with alcohol functional groups. The overall percentage yield is quite variable and depends on the ratio of each reactant. As expected, this is similar to what occurs for the more simple diol situations.<sup>50</sup>

The order of stability in air or nitrogen, for products derived from the same alcohol, is Hf > Zr > Ti.<sup>51</sup> The weight retention trend may simply be a result of the greater proportion of metal. The trend with respect to inception of degradation is more subtle. The initiation of degradation for titanocene-containing polymers occurs with the removal of small amounts of the cyclopentadiene rings. It is possible that the Cp-M bond strength is Hf-Cp > Zr-Cp > Ti-Cp. As noted elsewhere, the order of long-range interaction is Hf > Zr > Ti. This may translate into the order of Cp-group retention.

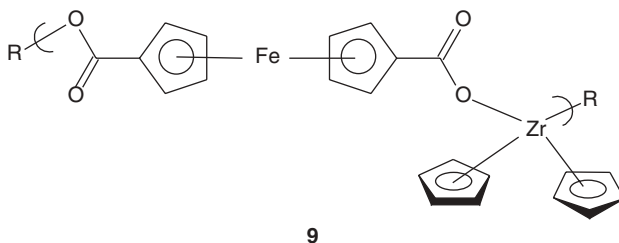
The analogous Group IVB-containing polyesters were synthesized using salts of dicarboxylic acids employing both the interfacial and aqueous solution systems (Eq. 4).<sup>52-55</sup> Reaction was general for both systems and for both aliphatic and aromatic diacids. Weight-average molecular weights were in the range of 10<sup>4</sup> to 10<sup>6</sup>. Over a short time span, yield increases with increase in stirring time. The aqueous solution syntheses were faster than the interfacial syntheses. The active metallocene form is believed to be, or act like, Cp<sub>2</sub>M<sup>+2</sup> for the aqueous solution system. A white precipitate, AgCl, is formed on addition of silver nitrate to an aqueous solution of zirconocene dichloride. When an equivalent (based on chloride content) of silver nitrate was added to an aqueous solution of zirconocene dichloride and the precipitated silver chloride was removed, the metallocene solution reacted with a dicarboxylate salt in the usual manner. Product yield was similar to that obtained using untreated zirconocene dichloride. Thus reaction rate is independent of the identity of the anion associated with the metallocene.

For Zr or Hf, it is reasonable to assume that the reactive Lewis base species in both the interfacial and aqueous solution systems was  $\text{RC(O)O}^-$  as found for the analogous titanocene reactions. It is not clear if the metallocene active species, in aqueous media, is the  $\text{M-Cl}$  or some form of  $\text{M-OH}$ . Even so, it is evident that the reaction occurs near the interface for the interfacial reactions because the active Lewis base reactant is fully charged and should have a low solubility in the organic layer, much lower than for the systems employing diols.



For the aqueous solution systems, the trend in yield is generally  $\text{Ti} > \text{Zr} > \text{Hf}$ .<sup>56</sup> For the interfacial system there are no clear trends with respect to yield as a function of the Group IVB metal. The lack of an overall generally trend for the interfacial system may be due to other factors being important, such as ability of the reactants to arrive at the surface and/or penetrate the interface.

Several “special” dicarboxylic acid salts were used to produce both ferrocene<sup>57,58</sup> and cobalticinium-containing<sup>59</sup> polyesters. Ferrocene reactions to produce structure **9**, were studied as a function of pH. The  $\text{pK}_{\text{eq}}$  for 1,1'-ferrocenedicarboxylic acid (FDCA) is not known but should be near 6.8.<sup>60</sup>



Yield varies greatly with pH consistent with the need to have the acid in the salt form. There is a decrease in product yield at high pH. The polymer rapidly degrades at high pH. Product yield can be increased by addition of sodium chloride in the aqueous phase. The sodium chloride presumably acts to “salt out” the Lewis base. Product yield increased as the stirring rate increased to about 20,000 rpm after which it remained essentially constant.

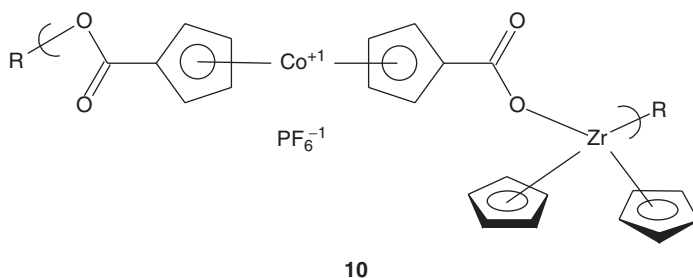
One of the few kinetic studies employing rapidly stirred interfacial systems was made using zirconocene dichloride and the salt of FDCA. The kinetic data were consistent with the reaction being zero order in the diacid salt, first order in zirconocene dichloride, and first order overall. A model based on the Langmuir adsorption isotherm is consistent with the observed kinetic data. This indicates that

a relatively high concentration of diacid salt must be present if this model is correct. Previous studies routinely use systems where the diacid salt concentration was down to  $7 \times 10^{-3}$  M. If the model is correct, then one should reach a dilution where the concentration of the diacid salt on the surface of the water droplets is no longer constant as the reaction progresses and the kinetics will no longer be zero order with respect to the diacid salt. Thus polymerizations were conducted at even lower concentrations of the reactants and these results are consistent with the kinetic rate depending on both the concentration of the diacid salt and metallocene.

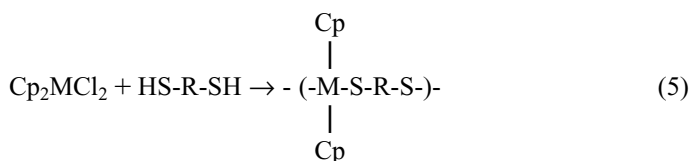
Cobalticinium-containing products, **10**, were synthesized using 1,1'-dicarboxycobalticinium salts.<sup>59</sup> The results are consistent with other studies reported above. Product yield increases to about a stirring rate of 15,700 rpm. The observed variations in where the (concentration) plateau occurs may eventually be used to better understand these rapidly stirred systems.

Product yield depends on the ratio of reactants. The reaction also depends on the nature of the counter anion. Using the hexafluorophosphate anion give much better yields than the bromide or nitrate counter anions.

Product yield also depends on the aging of the cobalticinium acid. Higher product yields are found when the cobalticinium is added just before the reaction. Thus some sort of exchange with the hexafluorophosphate appears to occur with the counter anion if the polymerization is not conducted immediately after addition of water to the cobalticinium.



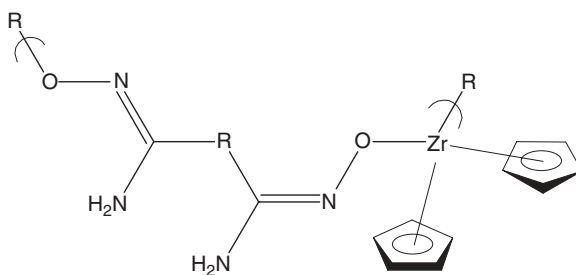
Metallocene-containing polythioethers were formed from the reaction of the metallocene dihalides with dithiols using both the interfacial and aqueous solution systems, (Eq. 5).<sup>61-64</sup> The interfacial system gave products over a wider range of dithiols in comparison to the aqueous solution systems. The products were generally produced in poor yield (1 to 30%) and were oligomeric with degrees of polymerization generally on the order of 3 to 6.



The overall yield is  $\text{Hf} > \text{Ti} > \text{Zr}$  for both aqueous solutions and interfacial systems. While the  $\text{Ti} > \text{Zr}$  portion can be rationalized using the HSAB approach, where both  $\text{R-SH}$  and  $\text{R-S}^-$  are considered soft bases, the overall trend is difficult to explain. Treating  $\text{Cp}_2\text{MCl}_2$  and  $\text{Cp}_2\text{M}^{+2}$  as intermediate bases, we would predict that the order should be  $\text{Ti} > \text{Zr} > \text{Hf}$ . Group IVB metallocenes are considered as hard bases.

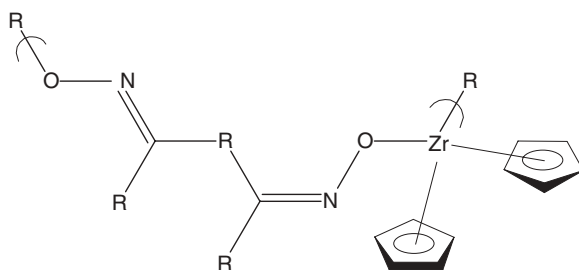
While some of the trends are consistent with the HSAB interruption, we might consider objections to applying the HSAB treatment to the present system. First, Pearson's theory applies to nucleophilic displacements reactions. In aqueous solution systems, the chemical-rate-determining step is probably the simple addition of  $\text{Cp}_2\text{M}^{+2}$  or  $\text{RCpM}^+$  to  $\text{R-S}^-$ , but for the interfacial systems (and possibly also for aqueous solution systems) the vacant metal orbital may complex forming an intermediate. The rate-determining step may be the formation of either this intermediate or its decomposition, depending on the particular complex. Second, Pearson's theory deals largely with only polarization and ionic terms. Terms such as those involving solvation and inner layer penetration may also be important for some of these systems. Third, there may be a variation in the precise mechanism of addition as one goes from the thiols to the salts of diacids (related to point one). Thus while HSAB may be useful in rationalizing much of the data, it alone is not sufficient to rationalize all of the observed trends.

Products, **11**, were also formed from the reaction of  $\text{Cp}_2\text{MCl}_2$  with amidoximes, derived from dinitriles.<sup>65,66</sup> Good to moderate product yields were found using both the interfacial and the aqueous solution systems. Yields for the reaction with the diamidoximes were greater for zirconocene than titanocene. This order is different from that found for the dithiols but is the same as that found for the diacids. In the HSAB, approach, the salts of diacids and the amidoximes (either in the deprotonated form or protonated form) are both considered hard bases, while undeprotonated diols and dithiols are soft bases. The hardness order of the Lewis acids is  $\text{Cp}_2\text{M}^{+2} > \text{Cp}_2\text{MCl}_2$  and  $\text{Cp}_2\text{TiCl}_2 > \text{Cp}_2\text{ZrCl}_2 = \text{Cp}_2\text{HfCl}_2$  which is consistent with these trends.

**11**

Ketones can be converted to oximes. This was done for a number of diketones, including biologically important ones such as vitamin  $\text{K}_3$ , progesterone, and androstaenedione. The dioximes were reacted with Group IVB metallocene dichlorides, forming products with the repeat unit shown in **12**.<sup>67,68</sup> The polyoximes, with degrees of polymerization in the general range of 20–600, are soluble in DMF and 1-methylimidazole. Solubility is largely independent of chain length. Copolymers were synthesized

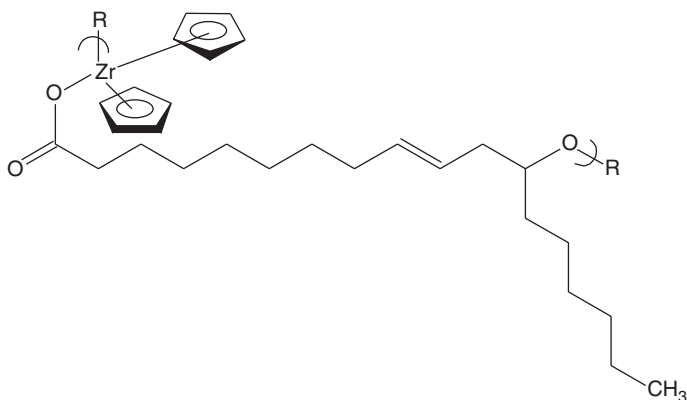
in an effort to increase the solubility of the product. In one case the copolymer showed a greater solubility but in another case the solubility was less than for one of the homopolymers.



12

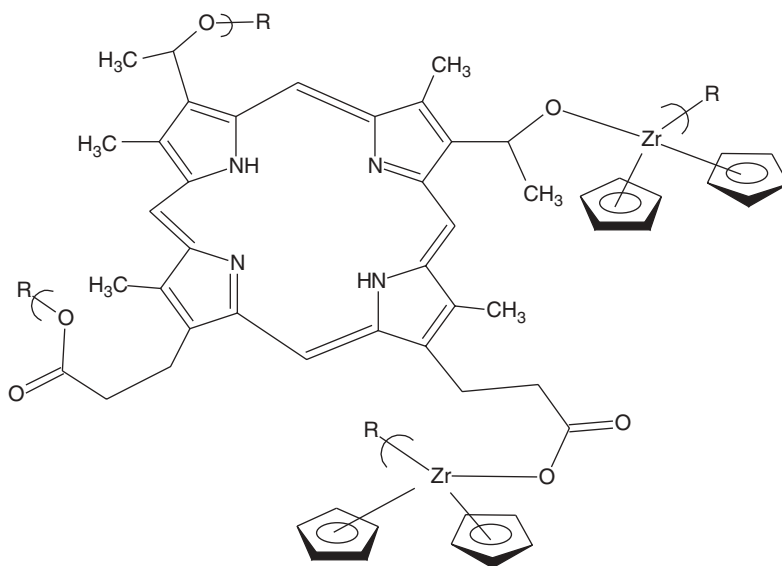
The electrical properties of a number of the polyoximes was studied.<sup>69,70</sup> All of the structures studied can offer what is referred to as “whole-chain resonance”—that is, the polymer backbone consists entirely of alternating double bonds with the exception of the metal atom. Values for the dissipation factor *D* ranged from 3 to 10 (at  $10^3$  Hz); the bulk resistivity *P*, from 0.05 to 0.6 (at  $10^3$  Hz), and the bulk capacitance from 0.2 to 0.9 K. Thus most of the materials are semiconductors. Efforts are currently under way to evaluate some of these after doping.

Several mixed functional group-containing Lewis acids have been studied. To use naturally renewable resources, the synthesis of polyester-ethers, **13**, using ricinoleic acid was studied. Ricinoleic acid is typically derived from castor oil through a crystallization of the fatty acids giving a product of about 97% purity. The salt of ricinoleic acid was reacted with zirconocene dichloride giving a product as shown in structure **13**.<sup>71</sup> The products are moderately soluble in acetone, DMF, and benzene. The product has a molecular weight of  $8 \times 10^4$  corresponding to a degree of polymerization of about 160.



13

The Group IVB metallocene derivatives of hematoporphine, IX or HPIX, were synthesized, **14**,<sup>72-74</sup> as part of an effort to synthesize new porphyrin-containing materials. IX is a macrocyclic “tetrapyrrole” with four methyl, two ethanoic, and two propionic acid side chains. The products are crosslinked because IX has four reactive functional groups, two acid groups, and two alcohol groups. The products contain a variety of repeat units, including that shown in structure **13** for M=Zr.

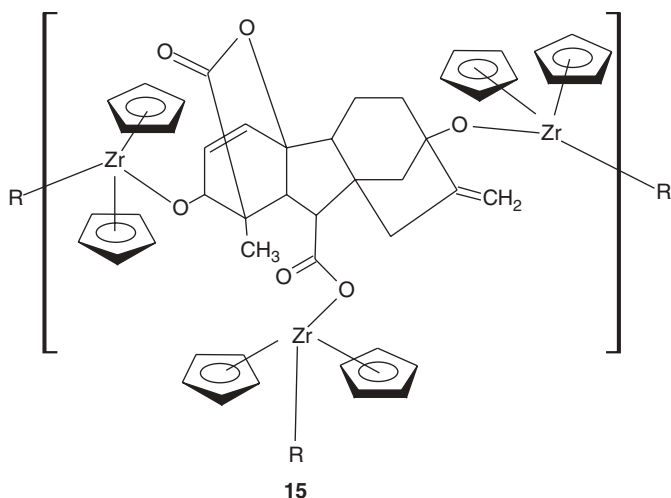


14

The adsorption of the  $\text{Ni}^{+2}$  was studied. Only the titanocene product exhibited good adsorption.<sup>75</sup>

As part of the effort to help the restoration of the Everglades and to improve the germination of seeds, Group IVB metallocene dichlorides were reacted with the plant growth hormone gibberellic acid, GA3 or GA.<sup>76</sup> Product yields for both Zr and Hf were above 90% and less than 20% for Ti. GA3 has three reactive sites, two alcohol and one acid functional group. The products are crosslinked and a representative structure is given in **15**. The polymers were tested as slow-release growth promoters.

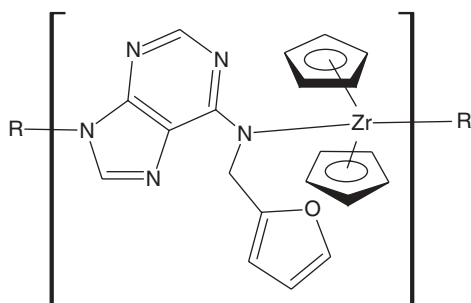
The Everglades ecosystem has two essential features—lots of water and sawgrass. A study to evaluate the effect of ppm amounts of polymers containing GA3 and GA3 itself on the germination of sawgrass and southern cattail was undertaken.<sup>77</sup> It was found that the GA3 polymers and GA3 itself decrease the germination time and increase the germination rate of sawgrass. In contrast, the germination rates of cattail seeds decreased sharply when treated with GA3 polymer and GA3 itself. There was little effect on the germination time. This is significant because the major competing plant in the Everglades is the southern cattail, and application of the polymer-containing the GA3 and GA3 itself both worked in favor of the desired sawgrass and against cattail.



In a similar study,<sup>78</sup> the GA3-containing polymers and GA3 were tested at the parts per million level for their ability to increase the germination rate of damaged and aged seeds that might be the sole seed source for third world farmers. The Group IVB–GA3 containing polymers were able to increase the germination of (Jagger) wheat seed twofold to threefold and (Little Marvel) peas to eightfold.

Another study focused on the rooting of plant cuttings.<sup>79</sup> Anderson's 'Crepe Pink', a variety of hibiscus, was used as the test root stock representing woody plants. Polymer use allowed a faster and more vigorous root formation. Red kidney beans and 'Kentucky Wonder' beans were also studied. Plant growth was so fast at high part per million application levels of polymer and GA3 that the bean and pea stocks outgrew their ability to stand on their own or to form good holds on the growing columns.

Group IVB polymers containing the plant growth hormone kinetin in the backbone were also synthesized.<sup>80</sup> The zirconocene product was a semiconductor with a (bulk) electrical conductivity of about 600 kilo-ohms, well within the range of being a semiconductor. The product yields were similar for all three Group IVB metallocene dichlorides, all within the range of 55–63%. The resulting polymers are linear as shown in **16**, because kinetin has only two functional groups.



The kinetin polymers were tested in a manner similar to the GA3 products described above.<sup>81</sup> In the wild, sawgrass seed germination efficiency is reported to be from 0 to 2%. Even in the laboratory, the percentage germination of sawgrass seeds was low before our efforts. Treatment of randomly selected sawgrass seeds for the control was 0, but when these polymers were applied, some germination efficiencies exceeded 50%. This would allow the Everglades to be reseeded using a water boat or airplane employing simple casting of treated seeds rather than the present practice of hand planting single seedlings.

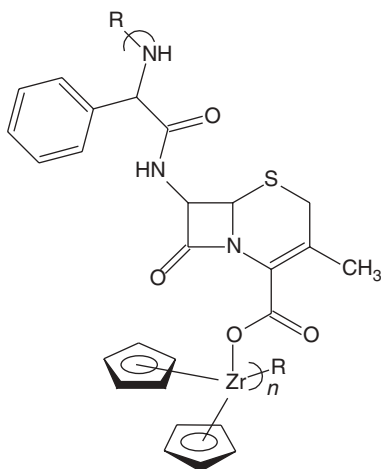
A similar study was conducted employing kinetin polymers with the focus on increasing the germination of damaged and old seeds.<sup>32</sup> The polymers generally showed increased germination rates for all seeds tested.

Thus Group IVB-containing polymers can effectively act as controlled release agents.

The synthesis of a number of drug-containing polymers derived from the reaction of the Group IVB metallocene dichlorides has been achieved.<sup>83</sup> Thus Group IVB-containing polymers were formed from the interfacial condensation with cephalixin, **17**. Yield was about the same for Zr and Hf (about 55%) but the product yield for Ti was much lower (about 5%). The products range in average chain length from a DP of 70 for Ti to 3,000 for Hf.

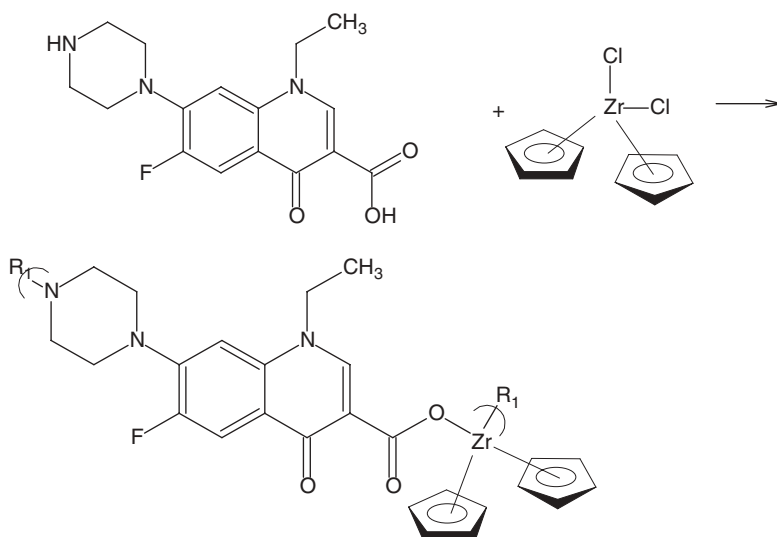
Many of the polymers reported in this section are formed from reaction with rigid and semirigid Lewis acids. Thus the resulting polymers can be rigid to semirigid because the metallocene moiety acts as a rigid moiety within polymer chains. Thus these polymers can be liquid crystals and should behave as such.

The unusual combination of polar and nonpolar units within these polymers, their stiffness, and their ability to form crystalline structures, all serve to lower solubility. The best solvents have been DMSO, HMPA, DMF, DMA, and 1-methylimidazole. These dipolar aprotic liquids appear to offer the right combination of polarity.



Most solubilities are in the range of 0.1 to 1%, sufficient for light scattering, UV, and proton NMR but not sufficient for many other desirable analysis techniques that require higher solubilities. The solubility is several fold higher just after polymer formation and before all solvent is removed. The negative factor is that there is some liquid captured in the product. This approach appears to work because the incompletely dried material includes some liquid that prevents the polymer chains from approaching one another until they are removed. Upon re-exposure to solvent, the solvent molecules are able to invade and displace the included liquid molecules thus assisting in product solubility.

Various mass spectral techniques have been used in characterizing various metal-containing macromolecules. The focus will be on two techniques. The first one is the most commonly employed mass spectrophotometer setup, called high-resolution electron impact mass spectrometry (HREI-MS). The second system is the matrix-assisted laser desorption ionization (MALDI) system. Illustrative examples of these two procedures are given for the products of Group IVB metallocene dichlorides and the antibacterial drug norfloxacin, scheme 8.



Scheme 8

There are several goals for MS studies of metal-containing polymers. First is the identification of various units present. Here, for the metal-containing moiety, isotopic abundance and identification of the organo portions are important. For polymers derived from the Group IVB metallocenes, identification that the Cp unit is present is consistent with the presence of the metallocene moiety. Also, isotopic abundance matches allows the identification that the metal is also present in the product. Second, identification of the type of linkage is also important. For the norfloxacin polymers that means location of M-O and M-N end groups. For such nonsymmetrical reactants such as norfloxacin, it is

possible to identify the type of preferred linkage, such as N-M-N, N-M-O, and O-M-O, allowing a measure of determining the initial reaction preferences. Finally, MALDI allows the identification that the products are at least oligomeric.

While we have run the corresponding Zr and Hf polymers using HREI-MS, the data from titanocene dichloride are presented because it allows a better presentation of identification by isotopic abundance.<sup>84</sup> HREI-MS data obtained as a function of the pyrolysis temperature are given in Table 1 for the product of titanocene dichloride and norfloxacin. Here the piperazinyl moiety is shorten to *Pip*, ethyl is shorten to *Et*, norfloxacin shorten to *Nor*, and one repeat unit simply referred to as *one unit*. Only ions with relative abundances of about 20% and greater are listed. Ion fragments derived from both reactants are present. Furthermore, ion fragments containing Ti-O, O-Ti-O, pip-Ti and pip-Ti-pip are all present consistent with the presence of all linkage combinations.

Titanium has five naturally occurring isotopes. Table 2 contains a listing of these isotopes and their abundances (where  $m/z$  is the mass per unit charge). It also contains a match for ions derived from  $TiO_2$  at 400°C. The match is reasonable because of the high percentage of isotope 80 in comparison with all of the other isotope abundances.

Table 3 contains a fragmentation pattern match for ions assigned as being derived from cyclopentadiene. The standard is for cyclopentadiene taken at 200°C. At 400°C the match is reasonable but by 450°C the match is not good with a reversal in the most

**Table 1** Most Abundant Ion Fragments in the HREI-MS of the Polymer of Titanocene Dichloride and Norfloxacin<sup>84</sup>

Temperature, °C			(Possible) Assignment
400	425	450	
66		67	Cp
80	80	80	TiO <sub>2</sub>
	95	94	Ph-F
	127	127	Cp-Ti-O
	144	144	O-CpTi-O
162	162	162	Nor minus Pip,CO <sub>2</sub> ,Et
181	178	181	Cp <sub>2</sub> Ti
	197	196	CpTi-Pip
204	206	205	Nor minus Pip,Et
		209	O-Cp <sub>2</sub> Ti-O
218	219	219	Nor minus Pip,F
233	233	233	Nor minus Pip
275	275	275	Nor minus CO <sub>2</sub>
319	319		Nor

**Table 2** Isotopic Abundance Match for the Ion Fragment TiO<sub>2</sub><sup>84</sup>

$m/z = 1$	46	47	48	49	50
Natural abundance (%)	8	8	74	6	5
TiO <sub>2</sub> ( $m/z$ )	78	79	80	81	82
Found (%)	17	7	61	13	4

**Table 3** Ion Fragmentation Pattern for the Most Abundant Ion Fragments Assigned to Cyclopentadiene<sup>84</sup>

Ion fragment, m/z	66	65	39	40
Relative abundance				
Standard, 200°C	100	47	32	27
400°C	100	64	64	34
450°C	26	33	100	44

abundant ion fragment from  $m/e=66$  to 39. This is consistent with other findings where good matches are obtained at low temperatures near to that where the standard pattern was obtained but as temperature increases there is a divergence away from the pattern.

MALDI MS has been also applied to Group IVB-containing polymers. MALDI works best when the material to be tested is soluble in a solvent with a high vapor pressure. Since the polymers are not appreciably soluble in such a solvent sample preparation is simply to grind together the polymer with the matrix. What are formed are degradation fragments rather than whole chain ion fragments. However, this is sufficient to assist us in the structural analysis of the product. Here we will look at the Zr and Hf product. Table 4 contains the most abundant ion fragments for the zirconocene/ norfloxacin product.

**Table 4** Most Abundant Ion Fragment Clusters (> 500 Daltons) Derived from MALDI Analysis of the Products from the Reaction of Zirconocene Dichloride and Norfloxacin<sup>84</sup>

Mass (Daltons)	(Tentative) Assignment
534	one unit
650	one unit-Zr-OH minus 2Cp
663	one unit-Zr-Cl minus 2Cp
705	one unit-Nor minus pip, 2Cp
718	one unit-Nor minus 2Cp
760	one unit-Zr
793	one unit-Zr-Cl
880	two units minus 3Cp
903	
988	two units minus pip
1004	two units minus Cp
1045	two units-Cl minus Cp
1099	two units-Zr minus 3Cp
1135	two units-Nor minus 4Cp
1221	HO-two units-Zr-Cl minus 2Cp
1243	two units-Zr-OH minus Cp
1299	two units-Zr
1386	two units-Nor
1441	three units-OH minus 3Cp
1580	three units-Cl minus Cp
1606	three units
1824	three units-Zr
2026	four units minus 2Cp
2205	four units-Nor minus 4Cp

Table 5 contains MALDI data for the hafnocene polymer with norfloxacin. Table 6 contains isotopic matches for hafnium. The matches are decent, particularly when considering the low abundance of these higher molecular weight ion fragments

Ion fragment assignment was carried out employing only bond breakages that have been found in previous MS work to be particularly susceptible to breakage. For norfloxacin, this involves cleavage to release piperazinyl. Metallocene compounds release cyclopentadiene. In comparison to HREI MS, longer intact chain segments were identified using MALDI.

**Table 5** Abundant Ion Fragments (> 500 Daltons) Obtained from the MALDI Mass Spectrometry of the Sample Derived from Reaction of Hafnocene Dichloride and Norfloxacin<sup>84</sup>

Mass (Daltons)	(Tentative) Assignment
678	one unit-Hf-OH minus 4Cp
700	one unit-pip
719	unit-Hf minus pip, 2Cp
847	one unit-Nor minus pip
904	one unit-Hf-Cl minus Cp
968	one unit-Hf-Cl
991	two units minus 4Cp
1047	two units minus 3Cp
1076	two units-OH minus 3Cp
1135	two units-OH minus 2Cp
1158	two units-Nor minus pip
1184	two units minus Cp
1201	two units-OH minus Cp
1310	two units-Nor minus 4Cp
1332	two units-Hf-Cl minus 4Cp
1377	two units-Nor minus 3Cp
1396	two units-Hf-Cl minus 3Cp
1476	HO-2Units-Hf-Cl minus 2Cp
1527	HO-2Units-Hf-Cl minus Cp
1617	Cl-3Units minus 3Cp, pip
1665	three units minus 2Cp, pip
3988	six units-Hf-pip minus 2Cp

**Table 6** Isotopic Match for Hafnium for a Two Hafnium-Containing Ion Fragment Cluster Two Units-Nor Minus Pip<sup>84</sup>

m/z	354	355	356	357	358	359	360
Calculated	6	12	16	21	22	10	13
m/z	1154	1155	1156	1157	1158	1159	1160
Found	4	9	16	22	27	11	13

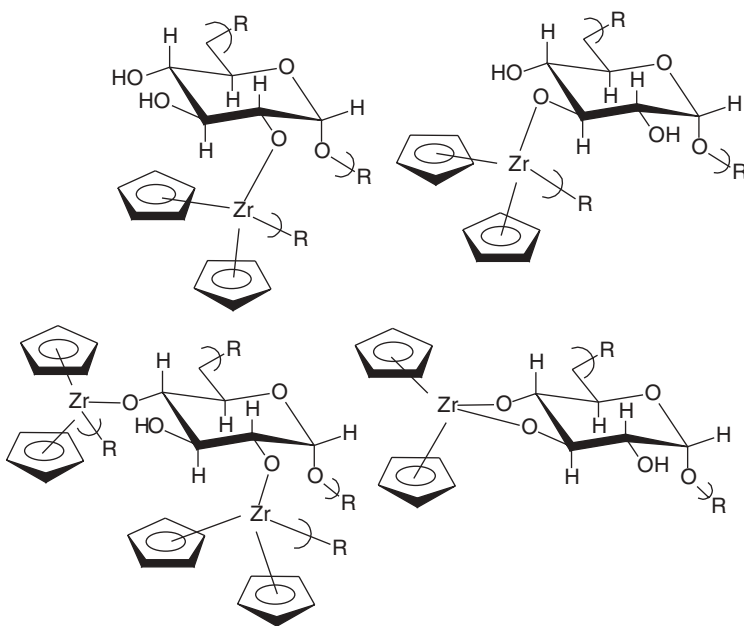
## VI. ZIRCONOCENE AND HAFNOCENE REACTIONS WITH ALREADY EXISTING POLYMERS

The formation of zirconocene and hafnocene-containing polymers by reactions with existing polymers was partially covered in the sections III and IV. Other polymers have been prepared for reasons other than for use as catalysts.

Linear and crosslinked products can be formed though addition and condensation reactions. Reactions with unsaturated sites (addition) and Lewis bases (condensation) can occur that, depending on the particular situation, may or may not increase the amount of crosslinking.

Carraher, Naoshima, and coworkers<sup>50,85-92</sup> have produced a number of products derived from the condensation reaction of natural products using Group IVB metallocene dichlorides. These natural materials include dextran and cotton. Much of this work employed the titanocene dichloride.

Scheme 9 shows possible repeat units for the reaction between zirconocene dichloride and dextran. The products will contain a mixture of monosubstituted, disubstituted, trisubstituted, and unsubstituted hydroxyl products. Unsubstituted repeat units, and those containing only cyclic zirconocene units, will not increase the amount of crosslinking or branching. However, the other repeat units shown in scheme 8 will increase the crosslinking and/or branching. Thus these products are all insoluble in all tested liquids.

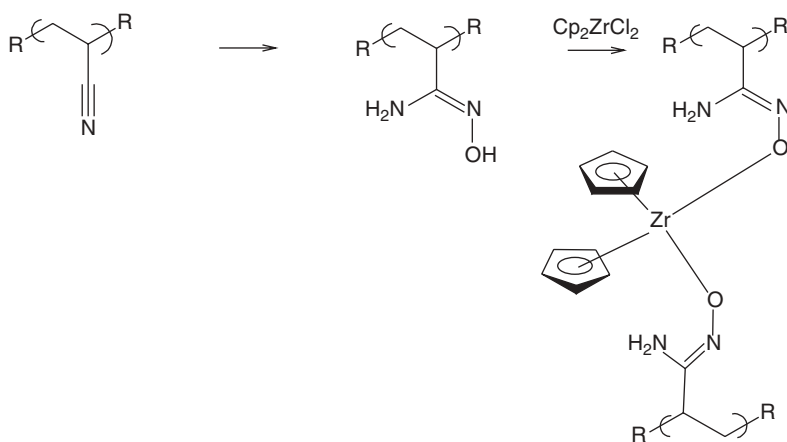


Scheme 9

To determine the percentage yield, a one metallocene to two dextran units, was chosen for the basis of percentage yield calculations. The yields of Hf and Zr were similar and were generally greater than Ti. Maximum yields for Hf and Zr substitution were 80–95% while for Ti it was about 60% with the percentage yields for Hf generally a little higher than for Zr. This trend is consistent with what would be predicted from the HSAB approach (i.e., Hf > Zr > Ti). As expected, this order is the same as that found for the polyether formation.

The modification of dextran highly depends on the nature of both the organic and aqueous phases and are consistent with the reaction occurring in the organic phase but very near the interface.

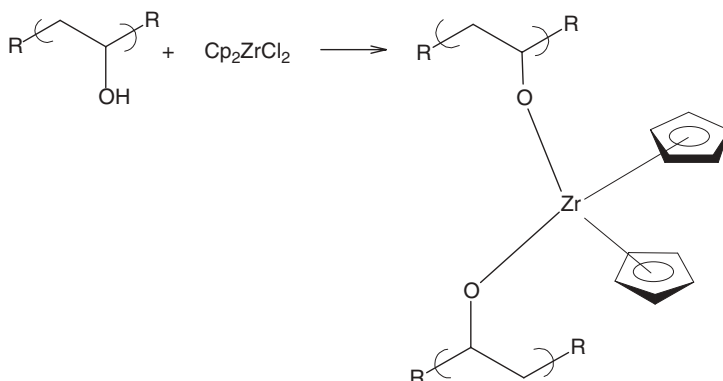
A number of Lewis base-containing synthetic polymers and copolymers should undergo similar reactions with zirconocene and hafnocene dihalides.



**Scheme 10**

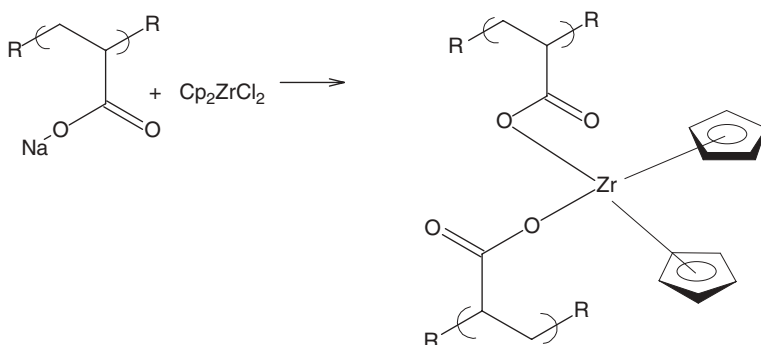
Carraher and Wang<sup>93,94</sup> reacted  $\text{Cp}^2\text{MCl}^2$  with polyacrylamide oxime, which had been prepared from polyacrylonitrile. The sequence is given in scheme 10. The -N-O-H moiety was deprotonated under the reaction conditions so it is a stronger base than the amine. Even so, there is probably a mixture of structural units, including those shown in scheme 10, including acrylamide oxime and acrylonitrile units. The products were formed in about 50% yield based on the repeat unit given in scheme 10. As with most of the Group IVB metallocene-containing products, the materials begin losing weight, mainly the Cp moieties, at about 100°C. About 50% (Hf) to 80% (Zr) remained at 900°C. in nitrogen and only 20% (Hf) and 40% (Zr) remained in air.

Similar products were synthesized from the reaction with poly(vinyl alcohol), scheme 11.<sup>95</sup> These products were produced in higher yields, about 80%, in comparison to those derived from the polyacrylamideoxime via polyacrylonitrile, probably because all of the nitrile groups were not converted to amideoxime groups.



Scheme 11

Analogous polymers were synthesized by the reaction of  $\text{Cp}_2\text{ZrCl}_2$  with the sodium salt of poly(acrylic acid) as shown in scheme 12.<sup>96</sup> Product yields for the zirconocene were in the upper 90% using a variety of reaction conditions but upon employing hafnocene dichloride, the product yield was only about 20%. The products are initially glassy and can be ground to give a powder. As in other cases, the thermal stability is greater in nitrogen than in air and the thermal stabilities of the Zr and Hf products are similar.

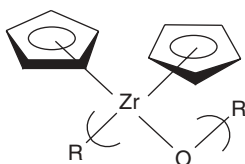


Scheme 12

## VII. MISCELLANEOUS

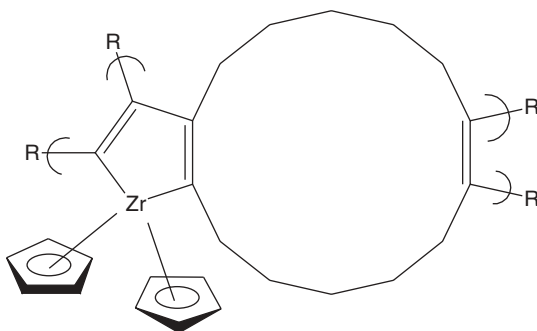
Possibly the earliest report of zirconocene-containing polymers was by Watt and Drummond.<sup>97</sup> This was the same paper in which they reported the initial synthesis of  $\text{Cp}_2\text{Zr}$ . On exposure to air,  $\text{Cp}_2\text{Zr}$  gave products that varied in color (yellow to orange) and composition, depending on conditions. The products were insoluble,

gave broad IR bands, and the x-ray diffraction lines were weak and diffuse. They believed that they had produced the polyoxide polymer shown in **18**. It is not known if this is the correct structure for the products.

**18**

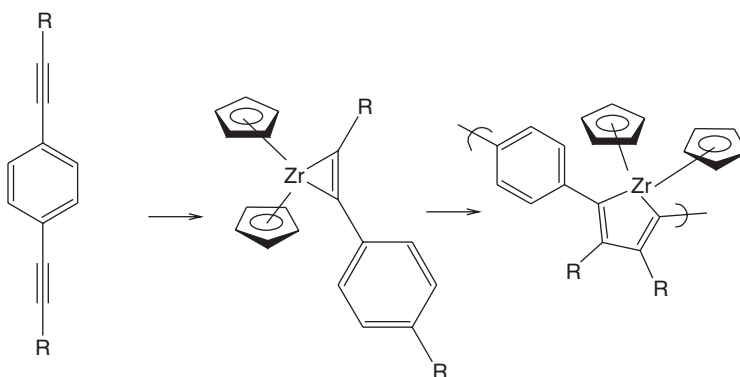
Mao, Tilley, and coworkers<sup>98–100</sup> have been investigating various ways to use versatile intermediate structures that may be derivatized in many ways. These efforts are aimed at developing new conjugated polymers with potential applications as electrically conducting materials in chemical sensors, light-emitting diodes, batteries, and nonlinear optical materials. They have been emphasizing the use of zirconacyclopentadiene units contained in polymer backbones and subsequently converting them into a variety of other conjugated materials, including butadienyl, phosphole, thiophene, and aromatic.

In one study, Mao and Tilley<sup>101</sup> produced a zirconocene-containing polymer as part of an overall scheme for producing a nonmetal containing hydrocarbon macromolecule. Zirconocene was formed in situ by the reduction of zirconocene dichloride with BuLi. This combination catalyzed the 1,8-cyclotetradecadiyne polymerization, forming a polymer containing tetradecadiene rings and zirconacyclopentadiene units in the backbone as shown in **19**. Hydrolysis of **19** gave polycyclotetradecadiene that can be hydrogenated to give polycyclotetradecane. One half of the Zr-containing polymer is given as **19**.

**19**

In related work, Tilley and coworkers<sup>102</sup> reported the synthesis of polyarylenediynes by the Heck-coupling of 1,4-diiodoaryl and diynes that had been reacted with zirconocene. The products were fully conjugated polymers with

zirconacyclopentadiene units in the backbone. Mao and Tilley also reported the formation of zirconocene-containing polymers from thermolysis as described in scheme 13.

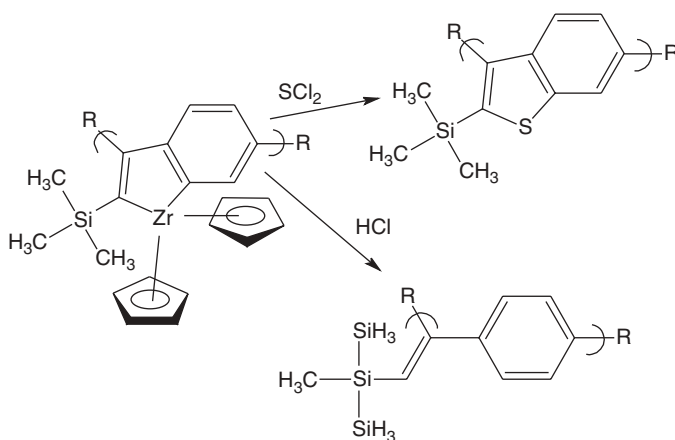


Scheme 13

Tilley also reported the formation of two conjugated polymers as shown in scheme 14.

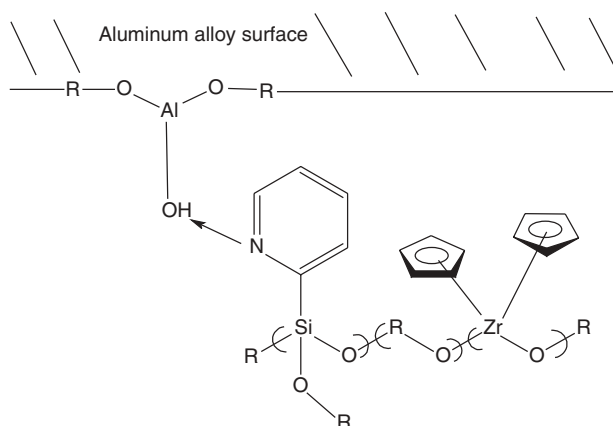
In related work, zirconocene<sup>103</sup> was coupled with (alkynyl-CH<sub>2</sub>-C(CH<sub>2</sub>-O-C<sup>6</sup>H<sup>13</sup>)<sub>2</sub>-CH<sub>2</sub>C C arylene)<sub>n</sub> in polymers; then this intermediate is used to produce diene-arylene polymers.

Platonova and coworkers<sup>104</sup> synthesized materials by the reaction of zirconocene dichloride with aromatic polymers bearing alpha-diketones and alpha-hydroxyl ketone moieties. The product was formed through reaction with the hydroxyketone functional group.



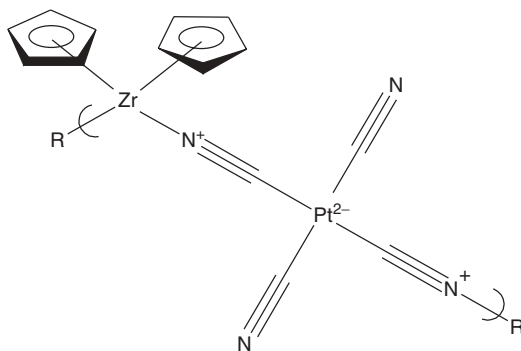
Scheme 14

Sugama and coworkers,<sup>105</sup> as part of an effort to prepare organometallic polymers as corrosion protective coatings for lightweight metals as aluminum, magnesium and zinc alloys, prepared pyridine-pendent siloxane polymers containing a backbone modified with a zirconocene moiety. These materials were prepared through the hydrolysis-condensation reaction of the mixed precursor solutions of the beta-trimethoxysilylethyl-2-pyridine solution and the zirconocene dichloride dissolved in tetrahydrofuran. The surface structure is depicted in scheme 15. The zirconocene-containing coatings applied to aluminum alloy surfaces provided excellent protection against NaCl-caused corrosion.



**Scheme 15**

It is well known that metal cyanide complexes can act as Lewis bases when the nitrogen forms C-N bridges to compounds containing Lewis acid moieties. Using this rationale, Alys, and coworkers<sup>106</sup> prepared materials in which Group IVB metallocenes are bridged to Group VIII B metals. Structure **20** is proposed where there is a tetrahedral coordination about Zr and a square-planar coordination about Pt.



**20**

## VIII. SUMMARY

Most of the effort to make Zr, and Hf metallocene polymers has focused on macromolecules containing zirconocene and hafnocene as catalysts, especially stereoregular catalysts. There are a number of other potential uses, including corrosion resistant coatings, thermally stable materials, liquid crystals, electrodes, sensors, semiconductors, and in controlled-release structures. The most widely employed Zr and Hf-containing metallocenes are zirconocene dichloride and hafnocene dichloride. Even so, there are a number of other metallocenes that have been introduced, including bridged structures. The journey has only begun and much remains to be done with these and other potentially important zirconocene and hafnocene-containing materials of the 21st century.

## IX. REFERENCES

1. T. Kealy, P. Pauson, *Nature*, **168**, 1039, (1951).
2. S. A. Miller, J. Tebboth, J. Tremaine, *J. Chem. Soc.*, 632 (1952).
3. F. A. Cotton, G. Wilkinson, *Advanced Inorganic Chemistry*, Wiley, New York, 1988.
4. G. Erker, *Acc. Chem. Res.*, **17**, 103 (1984).
5. M. Silverberg, *Chemistry*, 3rd ed., McGraw-Hill, New York, 2003.
6. D. Cardin, M. Lappert, C. Raston, *Chemistry of Organo-Zirconium and Hafnium Compounds*, Horwood, Chichester, UK, 1986.
7. R. Fay, *Coord. Chem. Rev.*, **37**, 41 (1981); **45**, 41 (1982); **52**, 285 (1983).
8. E. Neuse, H. Rosenberg, *Metallocene Polymers*, Dekker, New York, 1979.
9. P. Wailes, R. Coutts, H. Weigold, *Organometallic Chemistry of Titanium, Zirconium, and Hafnium*, Academic Press, New York, 1974.
10. G. Wilkinson, F. Stone, E. Abel, *Comprehensive Organometallic Chemistry*, Pergamon, Oxford, UK, 1982.
11. E. W. Neuse, in *Encyclopedia of Polymer Science and Technology*, vol. 8, Wiley-Interscience, New York, 1968.
12. E. Neuse, H. Rosenberg, *Metallocene Polymers*, Dekker, New York, 1970.
13. R. H. Grubbs, C. Lau, R. Curkier, C. Brubaker, *J. Amer. Chem. Soc.*, **99** (1977).
14. C. Pittman, C. Carraher, J. Reynolds, in *Encyclopedia of Polymer Science and Engineering*, vol. 10, 2nd ed., Wiley, New York, 1987.
15. C. Carraher, *Polymer Chemistry*, 6th ed., Dekker, New York, 2003.
16. J. Chien, *Topics Catalysis*, **7**, 23 (1999).
17. H. Sinn, W. Kaminsky, H. Vollmer, R. Woldt, U.S. Pat. 4,403,344, (1983) to BASF.
18. W. Kaminsky, H. Hahnsen, K. Kulper, R. Woldt, U.S. Pat. 4,542,199, (1985) to Hoechst.
19. M. Ribeiro, A. Deffieux, M. Portela, *Ind. Eng. Chem. Res.*, **36**, 1224 (1997).
20. K. Dahmen, D. Hedden, R. Burwell, T. J. Marks, *Langmuir*, **4**, 121 (1988).
21. M. Kaminaka, K. Soga, *Makromol. Chem., Rapid Comm.*, **12**, 367 (1991).
22. M. Kaminaka, K. Soga, *Polymer*, 1105 (1992).
23. K. Soga, M. Kaminaka, *Makromol. Chem.*, **194**, 1745 (1993).
24. W. Kaminsky, F. Renner, *Makromol. Chem., Rapid Com.*, **14**, 239 (1993).
25. M. Sacchi, D. Zucchi, I. Tritto, P. Locatelli, T. Dall'Occo, *Macromol. Rapid Com.*, **16**, 581 (1995).

26. Y. Chen, M. Rausch, J. Chien, *J. Polym. Sci. Part A. Polym. Chem.*, **33**, 2093 (1995).
27. J. Chien, D. He., *J. Polym. Sci. Part A. Polym. Chem.*, **29**, 1585, (1991).
28. K. Soga, M. Kaminaka, *Macromol. Chem. Phys.*, **195**, 1369 (1994).
29. K. Soga, T. Arai, B. Hoang, T. Uozumi, *Macromol. Rapid Com.*, **16**, 317 (1995).
30. W. Bonds, C. Brubaker, E. Chandrasekaran, C. Gibbons, R. Grubbs, L. Kroll, *J. Am. Chem. Soc.*, **97**, 2128 (1973).
31. R. Grubbs, C. Gibbons, L. Kroll, W. Bonds, C. Brubaker, *J. Am. Chem. Soc.*, **95**, 2373 (1973).
32. E. Chandrasekaran, R. Grubbs, C. Brubaker, *J. Organomet. Chem.*, **120**, 49 (1976).
33. H. Nishida, T. Uozumi, T. Arai, K. Soga, *Macromol. Rapid Comm.*, **16**, 821 (1995).
34. K. Pepper, H. Paisley, M. Young, *J. Chem. Soc.*, 4097 (1953).
35. D. Breck, *Zeolite Molecular Siever*, Wiley, New York, 1974.
36. S. Woo, Y. Ko, T. Han, J. Park, W. Hun, in *Proceedings Metalloenes, '96*, Houston, TX, 1996.
37. M. Stork, M. Koch, M. Klapper, K. Mullen, H. Gregorius, U. Rief, *Macromol. Rapid Commun.* **20**, 210 (1999).
38. S. Riethmuller, C. Drohmann, A. Muzafarov, M. Moller, M. Schlogl, B. Rieger, *Polymer P.*, **43**(2), 434 (2002).
39. H. Alt, M. Jung, *J. Organomet. Chem.*, **580**, 1 (1999).
40. C. Carraher, L. Jambaya, *J. Macromol. Sci.-Chem.*, **A8**(7), 1249 (9174).
41. C. Carraher, L. Jambaya, *Org. Coat. Plast. Chem.*, **34**(2), 484 (1974).
42. C. Carraher, L. Jambaya, *Angew. Makromolekulare Chem.* **39**, 69 (1974).
43. C. Carraher, L. Jambaya, *Angew. Makromolekulare Chem.*, **52**, 111 (1976).
44. C. Carraher, S. Bajah, L. Jambaya, in *Crown Ethers and Phase Transfer Catalysis in Polymer Science*, L. Mathias, C. Carraher, eds., Plenum, New York, 1984.
45. O. Smirhova, E. Ali Khasan, I. Losev, G. Kolesnikov, *Vysokomol. Soden.*, **7**, 503 (1965).
46. F. Millich, C. Carraher, *J. Polym. Sci., A1*, **7**, 2669 (1969).
47. P. Morgan, *Condensation Polymers: By Interfacial and Solution Techniques*, Wiley, New York, 1963.
48. F. Millich, C. Carraher, *Interfacial Synthesis*, Dekker, New York, 1974.
49. C. Carraher, L. Jambaya, *Angew. Makromole. Chem.*, **39**, 41 (1974).
50. Y. Naoshima, C. Carraher, K. Natsumoto, in *Renewable-Resource Materials*, C. Carraher, L. Sperling, eds., Plenum, New York, 1986.
51. C. Carraher, *Org. Coat. Plast. Chem.*, **31**(2), 338 (1971).
52. C. Carraher, *Eur. Polym. J.*, **8**, 215 (1972).
53. C. Carraher, *Eur. Polym. J.*, **8**, 215 (1972).
54. C. Carraher, *Angew. Makromolekulare Chem.* **28**, 145 (1973).
55. C. Carraher, *Chemtech*, 741 (1972).
56. C. Carraher, L. Jambaya, S. Bajah, *Polymer P.*, **18**(2), 403 (1977).
57. C. Carraher, J. Reimer, *J. Poly. Sci. Polym. Chem. Ed.*, **10**, 3367 (1972).
58. C. Carraher, J. Reimer, *Polymer* **13**, 153 (1972).
59. J. Sheats, C. Carraher, D. Bruyer, M. Cole, *Coat. Plast. Chem.*, **34**(2), 474 (1972).
60. R. Benkeser, D. Goggin, G. Schroll, *J. Am. Chem. Soc.*, **76**, 4025 (1954).
61. C. Carraher, R. Nordin, *J. Applied. Polym. Sci.*, **18**, 53 (1974).
62. C. Carraher, *Polymer*, **17**, 231 (1976).
63. C. Carraher, *Org. Coat. Plast. Chem.*, **33**(1), 629 (1973).
64. C. Carraher, R. Nordine, *J. Macromol. Sci.-Chem.*, **A15**(1), 143 (1981).
65. C. Carraher, R. Frary, *J. Polym. Sci. Polym. Chem. Ed.*, **12**, 799 (1974).

66. C. Carraher, R. Frary, *Org. Coat. Plast. Chem.*, **33**(2), 433 (1973).
67. C. Carraher, L. Torre, in *Macromolecular Solutions: Solvent-Property Relationships*, R. Seymour, G. Stahl, eds., Pergamon, New York, 1982.
68. C. Carraher, L. Torre, *Org. Coat. Plast. Chem.*, **45**, 252 (1981).
69. C. Carrher, T. Manek, R. Linville, J. R. Taylor, L. Torre, W. Venable, *Org. Coat. Plast. Chem.*, **43**, 753 (1979).
70. C. Carraher, R. Linville, T. Manek, H. Blaxall, J. R. Taylor, L. Torre, in *Conductive Polymers*, R. Seymour, ed., Plenum, New York.
71. C. Carraher, E. Frankel, *PMSE*, **73**, 396 (1995).
72. C. Carraher, A. Rivalta, J. Haky, *PMSE*, **74**, 149 (1996).
73. C. Carraher, J. Haky, A. Rivalta, D. Sterling, *PMSE*, **70**, 329 (1993).
74. C. Carraher, J. W. Louda, D. Sterling, A. Rivalta, Q. Zhang, E. Baker, *PMSE*, **71**, 386 (1994).
75. C. Carraher, J. Haky, A. Rivalta, in *Functional Condensation Polymers*, C. Carraher, G. Swift, eds., Kluwer, New York, 2002.
76. A. Salamone, C. Carraher, J. Stewart, S. Miao, J. Peterson, A-M. Francis, *PMSE*, **81**, 147 (1999).
77. A. Salamone, C. Carraher, S. Carraher, H. Stewart, S. Miao, C. Cowen, *PMSE*, **82**, 79 (2000).
78. C. Carraher, H. Stewart, S. Carraher, D. Chamely, W. Learned, J. Helmy, K. Abby, A. Salamone, in *Functional Condensation Polymers*, C. Carraher, G. Swift, eds., Kluwer, New York, 2002.
79. C. Carraher, H. Stewart, W. Soldani, J. de la Torre, B. Pandya, L. Reckleben, *PMSE*, **71**, 783 (1994).
80. C. Carraher, D. Chamely, *PMSE*, **85**, 358 (2001).
81. C. Carraher, D. Chamely, S. Carraher, H. Stewart, *PMSE*, **85**, 381 (2001).
82. C. Carraher, D. Chamely, S. Carraher, H. Stewart, W. Learned, J. Helmy, K. Abby, *PMSE*, **85**, 375 (2001).
83. J. Peterson, C. Carraher, A. Salamone, A-M Francis, *PMSE*, **81**, 149 (1999).
84. C. Carraher, L. Lanz, unpublished data.
85. Y. Naoshima, C. Carraher, in *Chemical Reactions on Polymers*, J. Benham, J. Kinstle, eds., ACS, Washington, DC., 1988.
86. Y. Naoshima, M. Kurokawa, C. Carraher, *PMSE*, **52**, 24 (1985).
87. C. Carraher, Y. Naoshima, *PMSE*, **62**, 497 (1990).
88. C. Carraher, Y. Naoshima, in *Biotechnology and Polymers*, C. Gebelein, ed., Plenum, New York, 1991.
89. Y. Naoshima, C. Carraher, G. Hess, M. Kurokawa, and S. Hirono, *Bull. Okayama Univ. Sci.*, **20**, 33 (1985).
90. Y. Naoshima, C. Carraher, *PMSE*, **50**, 403 (1984).
91. Y. Naoshima, C. Carraher, T. Gehrke, L. Tisinger, *Polymer P.*, **27**(2), 99 (1986).
92. Y. Naoshima, C. Carraher, G. Hess, M. Kurokawa, in *Metal-Containing Polymeric Systems*, J. Sheats, C. Carraher, C. Pittman, eds., Plenum, New York, 1985.
93. C. Carraher, L-S. Wang, *Angew. Makromol. Chem.*, **25**, 121 (1972).
94. C. Carraher, J. Piersma, L-S. Wang, *Org. Coat. Plast. Chem.*, **31**(2), 254 (1971).
95. C. Carraher, J. Piersma, *J. Macromol. Sci.-Chem.*, **A7**(4), 913 (1973).
96. C. Carraher, J. Piersma, *Makromol. Chem.* **152**, 49 (1972).
97. G. Watt, F. Drummond, *J. Am. Chem. Soc.*, **88**(24), 5296 (1966).
98. S. Mao, T. Tilley, *J. Am. Chem. Soc.*, 117 (1995).
99. S. Mao, T. Tilley, *J. Am. Chem. Soc.*, 7031 (1995).
100. T. Tilley, S. Mao, in *Modular Chemistry*, J. Michl, ed., Kluwer, New York, 2003.

101. S. Mao, T. Tilley, *Polymer P.* **37**(1), 443 (1996).
102. T. Tilley, B. Lucht, S. Mao, *Book of Abstracts, ACS National Meeting*, San Francisco, April 1997.
103. B. Lucht, T. Tilley, *Chem. Comm.*, **16**, 1645 (1998).
104. O. Platonova, M. Seregina, L. Bronshtein, P. Valstskii, M. Ezernitskaya, I. Yanovskaya, Y. Yygodskii, N. Brandukova, *Vysokomol. Soedin, Seriya A i Seriya B*, **38**(9), 1619 (1996).
105. T. Sugama, N. Carciello, S. Rast, *Thin Solid Films*, **258**, 174 (1995).
106. J. Abys, G. Ogar, W. Risen, *Inorg. Chem.*, **20**, 4446 (1981).

# Compositional and Structural Irregularities of Macromolecular Metal Complexes

**Anatolii D. Pomogailo and Gulzhian I. Dzhardimalieva**

*Institute of Problems of Chemical Physics, Russian Academy of Sciences, Moscow Region, Russia*

## CONTENTS

I. INTRODUCTION	148
II. BASIC TRANSFORMATIONS OF MACROLIGANDS IN BINDING $MX_n$	150
A. Conformational Changes in Polymer Chains	150
B. Macroligand Structuring Processes	152
C. Macroligand Decomposition in $MX_n$ -Polymer Systems	155
D. Changes in Origin of Functional Groups of Polymers in Their Reactions with $MX_n$	159
III. TRANSFORMATION OF TRANSITION METAL COMPOUNDS IN REACTIONS WITH POLYMERS	161
A. Oxidation-Reduction Conversion of Transition Metals	161
B. Monomerization of Transition Metal Dimer Complexes in Reactions with Polymers	162
C. Composite Inhomogeneity of Macromolecular Complexes	164

IV. PROBLEM OF TOPOCHEMISTRY OF MACROMOLECULAR COMPLEXES	166
A. Topochemistry of Polymer Macroligand Functional Layers	166
B. Topochemistry of Diamagnetic Complexes That Are Fixed to the Polymers	167
C. Topochemistry of Polymer-Bonded Paramagnetic Complexes	168
D. The Main Data on MMC Topochemistry	172
V. PROBLEMS OF UNIT VARIABILITY IN METAL-CONTAINING POLYMERS OBTAINED BY COPOLYMERIZATION OF METAL-CONTAINING MONOMERS	172
A. Unit Variability Due to Elimination of a Metal-Containing Group During Polymerization	175
B. Unit Variability Due to Different Valence States of the Transition Metal Ions	177
C. Unit Variability Due to the Presence of Stable Metal Isotopes	179
D. Anomalies in Metallopolymeric Chains Caused by the Diversity of Chemical Binding of a Metal to Polymerizable Ligands	180
E. Unit Variability Due to Qualitatively and Quantitatively Different Ligand Environments of the Metal	183
F. Extra-Coordination as a Spatial and Electronic Anomaly of the Polyhedron	186
G. Exchange Interactions Between Metal Ions Incorporated in the Chain	188
H. Change in the Nuclearity of Metal Sites as a Type of Unit Variability	190
I. Stereoregularity of Metallopolymeric Chains	192
J. Unit Variability Due to Chirality in Pendant Groups	194
K. Unsaturation and Structurization of Metallopolymers	196
L. Cyclization During Polymerization	197
VI. SOME PRACTICAL APPLICATIONS OF UNIT VARIABILITY OF METAL-CONTAINING POLYMERS	198
VII. ACKNOWLEDGMENTS	202
VIII. REFERENCES	202

## I. INTRODUCTION

Currently, two basic chemical approaches to the formation of macromolecular metal complexes (MMCs) are widely used. The first and most commonly used is based on the chemical binding of transition metal compounds ( $MX_n$ ) with macroligands

(polymer supports). This method requires that the polymers have the appropriate functional groups. The type of the bond formed (donor-acceptor, covalent, ionic, etc.) is defined by the nature of the reacting compounds. Such a bond is usually highly stable. This method of the MMC preparation is called polymer-analogous transformations.<sup>1</sup>

The structural principles of MMC formation are almost always the same: a polymer support (macroligand) → its functionalization → chemical binding → isolation of chemically unbound reagents. There are variations when a number of stages are shortened, and the MMC preparation is realized according to a short scheme. A binding ligand can either be added to a polymer and then linked to a metal complex or a metal complex can be bonded to the ligand and then added to the polymer. The stages of the metal complex synthesis with a given ligand can also be combined with its binding to the polymer.

The second method, not widely used till now, consists of polymerization transformations of metal-containing monomers (MCM) (metal complexes) whose ligand environment involves at least one group with a multiple bond that is capable of polymerization transformations. Each of two methods possesses certain advantages and shortcomings. However, a purposeful selection of ligands and an optimal synthetic technique of their binding to  $MX_n$  allow the design of metal complexes of desirable composition to be immobilized onto polymers.

It is known that the  $MX_n$  reactions with polymer reagents are essentially different from those with low-molecular-weight analogs.<sup>2</sup> These processes are accompanied by a number of transformations in reacting components. Their investigation is of particular interest for the following reasons: (1) with respect to coordination chemistry—namely, elucidation of the effect of a macromolecular chain of a reactant on the resulting coordination centers, their structures, bond nature, transition metal valency, and other aspects; and (2) with respect to the chemistry of high-molecular-weight compounds—namely, elucidation of peculiarities of the reactivity of the macromolecular functional groups, conformation and configuration transformations of the macrochain, transformations that are destructive, topochemistry and topography of the macrocomplexes that are linked to polymer chains, morphology and supramolecular structural organization of macrocomplexes, etc.

Polymerization of MCM is often accompanied by a violation of the structural homogeneity of the macrocycles that are formed. These macrocycles are similar to those occurring in the reaction of polymer-like transformations and give rise to a variety of ring sizes.

Unfortunately, the aforementioned problems have not been adequately discussed in literature,<sup>1</sup> although there is considerable interest in the preparation of structurally homogeneous macromolecular metal complexes for catalysis, photochemistry, biological applications, etc. This chapter reports on the specificity of the processes for formation of macromolecular complexes through both routes; polymer-like transformations and copolymerization of metal-containing monomers. In addition, the predictive potential of reactions and the ways of preventing some of them will be discussed.

## II. BASIC TRANSFORMATIONS OF MACROLIGANDS IN BINDING $\text{MX}_n$

This section considers the most essential transformations of polymers (macroligands) in the course of  $\text{MX}_n$  bonding. These transformations are conformational changes, macroligand structuring processes, destruction of macroligands, the nature of functional groups and so forth.

### A. Conformational Changes in Polymer Chains

Configuration changes in a spacial arrangements of a neighboring ring (neighbor effect), and conformation, macromolecular reorganizations in the course of reaction, effects are distinguished in  $\text{MX}_n$  binding. For example, changes in chain conformation that are stipulated by the magnitude and character of intermolecular interactions associated with valence-nonbonded atoms are observed in a great number of polymers. Therefore, the difference in flexibility of various conformations and a sharp increase in the equilibrium constant of a complex formation reaction in a narrow range of degree of conversion ( $\Theta$ ) is usually observed. Conformational changes can take place both in each act of  $\text{MX}_n$  binding and by attaining a certain value of  $\Theta$ , and involve a different number of monomer units. Metal ions usually form two or more bonds with the closest active centers. As a result, five- or six-membered metallocycles are formed. High energy is required to form large rings because of the growth of entropy loss.<sup>3</sup> If the neighbor of the reacted group is a conformation inactive group (the neighboring effect extends right and left units entering in the coordination sphere of the transition metal), the reaction with such a group does not occur. For example, ethylenediamine complexes of  $\text{Co}^{2+}$  are large enough ( $\sim 10 \text{ \AA}^3$ ), and upon coordination with numerous vinylpyridine (ViPy) units in poly(vinylpyridine) (PViPy), even if dense packing is assumed, a large number of ViPy units do not coordinate because of steric hindrances. The calculated maximum conversion level for PViPy is 0.63, which is close to the experimental value.<sup>4,5</sup> The changes in chain flexibility depend on the number of bonded functional groups and affect the MMC stability (i.e., the most stable complexes form at small  $\Theta$  values and the least stable complexes form at high  $\Theta$  values).

High lability of a polymer ligand usually results in the changes in its conformation in the place of binding in accordance with the electron configuration of transition metals. As a result, both a helix-ball transition characteristic of charged chains and the changes in preferable conformation of a statistical ball are possible. The presence of hydrogen bonds and steric reasons hinder bending and rotation (i.e., a conformational adaptability). This also may be why a lot of functional groups are excluded from complex formation.

It should be noted that complex formation often allows stabilization of conformational and tautomeric forms, which are not characteristic of the parent polymers. A representative example is poly(ethylene glycol) (PEG), which has a helical structure with alternating *trans*- and *gauche*-CO, OC, and C-C bonds, respectively ( $\text{T}_2\text{G}$  conformation, helix  $7_2$ ).<sup>6</sup> PEG reacts with  $\text{HgCl}_2$  to form a complex of

a regular composition,  $HgCl_2(OCH_2CH_2)_4$ , whose unit cell involves 4  $HgCl_2$  molecules and 16  $(OCH_2CH_2)$  units.<sup>7</sup> Three of every four G-forms transform to T-, T  $\bar{G}$ -forms (G and  $\bar{G}$  are dextrorotatory and sinistrorotatory *gauche*-forms); as a result, the chain in the complex has the  $T_5GT_5\bar{G}$ -conformation with an increased portion of convolute (*gauche*) configurations, and the PEG unit transforms from monoclinic to orthorhombic. Moreover, the linear shape of the  $HgCl_2$  molecule slightly distorts ( $ClHgCl$  angle =  $176^\circ$ ). The period of identity of the macromolecule changes and includes 4 monomer units instead of 7 as in the initial lattice, where each unit in the complex is more elongated (Fig. 1).

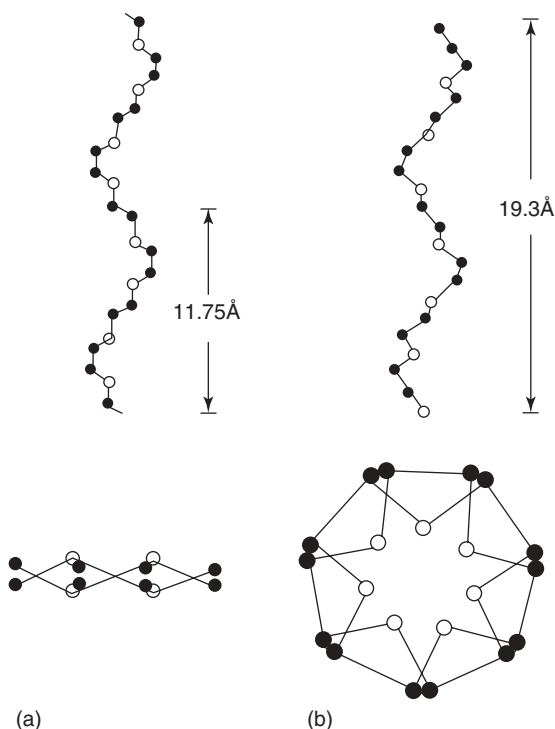


**Figure 1** (a) Helix structure of PEG and (b) its complex with  $HgCl_2$  (conformation  $T_5GT_5\bar{G}$ ).

It should be noted for comparison, however, that the structural properties of PEG-alkali metal ion macrocomplexes are better described in terms of a double helix model.<sup>8</sup>

Metal ions are usually linked to a macrochain through the formation of several bonds with one (intramolecular complexes) or more (intermolecular complexes) chains. Dilute solutions prefer intramolecular complexes and concentrated solutions and matrixes provide intermolecular complexes. In intramolecular complex formation

**Table 1** The Stepwise Constants of Formation of Macrocomplexes and Their Low-Molecular Mass Analog

Macroligand	M	lg $K_1$	lg $K_2$	lg $K_3$	lg $K_4$	lg $\bar{K}$
PAC	Sm(III)	5,7	5,4	—	—	11,1
	Eu(III)	5,7	5,2	—	—	10,9
	Pr(III)	5,6	5,2	—	—	10,8
	Cu(II)	4,8	4,2	—	—	9,0
	Ni(II)	3,9	3,4	—	—	7,2
	Co(II)	3,7	3,1	—	—	6,8
PE-gr-PAC	Sm(III)	6,2	5,9	—	—	12,1
	Tb(III)	3,86	—	—	—	—
Propionic acid	Cu(II)	5,9	5,2	2,9	—	11,1
	Sm(III)	3,9	3,2	—	—	10,0
	Eu(III)	3,8	3,2	2,9	—	9,9
	Pr(III)	3,7	3,1	2,9	—	9,7
P4ViPy (DP = 108)	Cu(II)	3,4	2,9	—	—	6,3
	Cu(II)	1,1	1,6	2,7	4,4	9,7
	Cu(II)	2,5	1,9	1,3	0,8	6,5

the first addition of the metal ion is a second-order reaction (i.e., first order in each component). All the following complexation reactions form intramolecular bonds and are first order. The overall  $MX_n$  reaction with a single chain is second order. Since complex formation reaction rates are high, it is difficult to discriminate successive stages of the process.

However, it has been found that  $K_i$ , the stability constant for the  $i$ th complex, usually increases with conversion level in contrast to the behavior of low-molecular-weight analogs (Table 1).

This is a result of a cooperative effect that occurs when the shape of the macromolecule changes in solution upon complex formation. The cooperative effect in the macroligand- $MX_n$  system is also evidenced by both the change in the macromolecule shape in solution, charge on the chain, dependency of thermodynamic parameters on molecular weight, chain-length distribution, conversion level, and chain flexibility. One should also note that poly-2-vinylpyridine (P2ViPy) undergoes conformational changes upon its interaction with  $Co^{2+}$  bis-acetylacetonate,<sup>9</sup> and linear poly(amidoamines) undergoes conformational transitions upon protonation and complex formation.<sup>10</sup> Such transitions affect the properties of the macromolecule as a whole since the binding sites of different monomer units are very rigid.

## B. Macroligand Structuring Processes

Intermolecular interactions are stronger in polymers than in similar low-molecular-weight compounds. Such interactions seem to be much stronger in macrocomplexes than in the parent polymers as a result of both lower chain flexibility upon complex formation and intermolecular interactions. The latter are significantly stronger in concentrated than dilute solutions. The intermolecular interaction parameters in

macrocomplexes are affected by (1) the donor properties of functional groups that define complex stability and the strength of intermolecular interactions between the chains, (2) the location of functional groups (i.e., anchor group length), and (3) the presence and size of other substituents not involved in complex formation. As a result, polymer complexes often form more perfect morphological structures than the parent macroligands.

The enhanced degree of crosslinking results in a lower stability of MMC due to the strain of a bent chain upon the formation of the multiple coordination centers and in changes in the character of the intermolecular interactions. Crosslinking can also increase because of enhanced chain rigidity or decrease because of the decrease of molecular weight of the chains located between the crosslinked sites. For example, an increase in the degree of PViPy crosslinking leads to a transition from stable square-planar to distorted tetrahedral complexes<sup>11</sup> with  $Cu^{2+}$ . Moreover, any disturbance affecting intermolecular processes causes changes in the chain structure and polymer morphology. For example, the storage of poly(vinyl alcohol) (PVA) complexes with  $MoOCl_3$  or  $MoOEt_3$  at 100–160°C results in chain crosslinking.<sup>1</sup>

If  $MX_n$  reacts with porous polymers, accessible pores are filled first. Such overgrown pores, which are associated with filling and shielding of the crosslinked macromolecule, is evidence for the  $MX_n$  contribution to a supramolecular buildup of macroligands. Thus it is impossible to predict the effect of a macroligand pore size on complex formation for macroreticular glycidyl methacrylate–ethylene glycol dimethacrylate copolymer (Fig. 2) since the material has a bimodal and even polymodal pore distribution in radius.<sup>12</sup> Nevertheless, it was shown that insertion of  $[RhCl(CO)_2]_2$  in a polyamide<sup>13</sup> is accompanied by a shift of the pore size to lower values; some

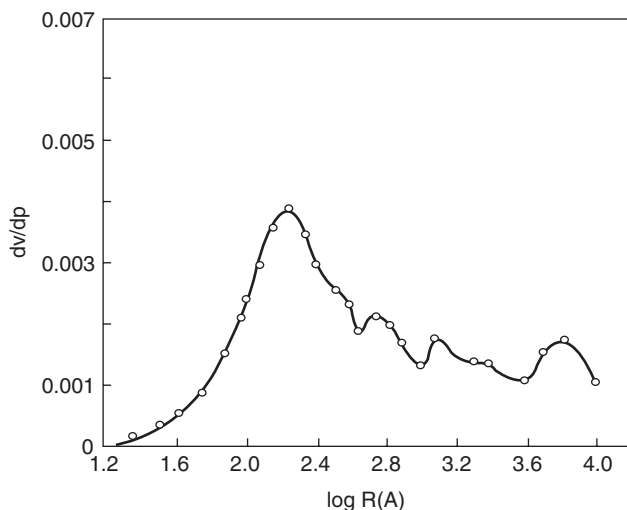


**Figure 2** Mercury porosimetry graph of the copolymer of glycidyl methacrylate–ethylene glycol dimethacrylate.

pores that are 18–22 Å in radius disappeared presumably by being blocked by the metal complex, and new pores below 10 Å were formed (Fig. 3).

Intermolecular interactions in MMC are significantly affected by molecular weight parameters of the parent microligands. If weak intermolecular interactions occur, then association in the macromolecules increases starting at a specific chain length.<sup>14</sup> Furthermore, polymers that possess strong intermolecular interactions exhibit both changes in morphologic structure and crosslinking. For example, PVA with a degree of polymerization ( $n$ ) > 60 forms stable intramolecular complexes with  $\text{Cu}^{2+}$  due to coordination with four-hydroxyl groups of the that macromolecule, whereas polymers with  $n < 160$  are intermolecular complexes due to PVA chain crosslinking with the  $\text{Cu}^{2+}$  cations.

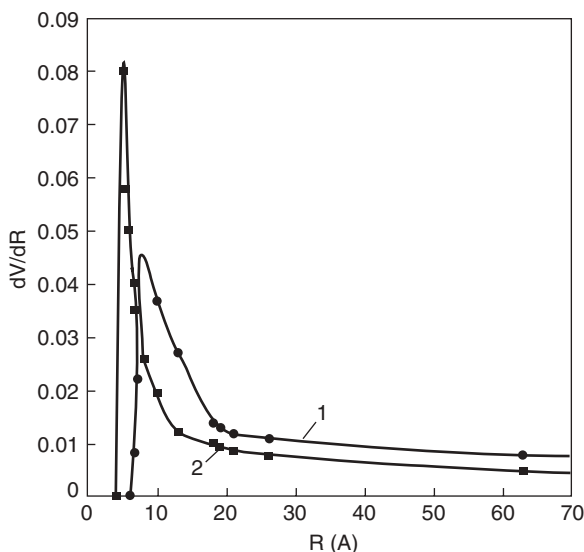


**Figure 3** The micropore size distribution of (1) polyamide and (2) polyamide/Rh systems by the BET method.

It should be noted that the changes in the supramolecular structure in the MMC formation are clearly more pronounced for crosslinked polymers than for soluble polymers. To illustrate, structural changes in the styrene copolymer with divinylbenzene is caused by alkylation with 5-chloromethyl-8-hydroquinoline in the presence of  $\text{AlCl}_3$ .<sup>15</sup> The copolymer is reorganized on covalent complexation—that is, MMC formation and simultaneous alkylation result in rearrangements and polymer bending. These processes are realized in highly flexible polymers in a swollen state at high concentrations of the complexing metal. Steric peculiarities of the latter define the structure of reacting polymer units. In all cases, the ability of the chain molecules to twist depends on the chain rigidity and the nature of the solvent. These

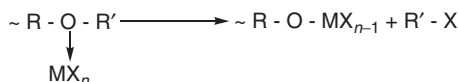
factors can enhance chain twisting or stretching. Since the MMC structure depends on synthetic conditions, thermodynamically nonequilibrium products most likely formed. The relaxation time and, therefore, the dynamically changing properties of the polymers with time should also be considered.<sup>16</sup>

Metal complexes in polymers and their segments cause higher chain rigidity that is manifested in changes in relaxation transitions. Clearly, this phenomenon relates to  $\alpha$ -relaxation, which is associated with the Brownian micromotion of long segments. At low degrees of  $\text{MX}_n$  binding by a macroligand, total chain mobility is almost unlimited; however, it also provides a greater number of bonded complexes so that the number of interchain crosslinks increases and results in higher glass-transition temperature ( $T_g$ ). For example,  $\alpha$ -relaxation remains almost unchanged in the products of an ethylene copolymer reaction with acrylic acid (9.3%) and  $\text{Ni}^{2+}$  or  $\text{Mn}^{2+}$  acetate if up to 14% of the acrylic acid units are neutralized.<sup>17</sup> The value of  $T_g$  increases with a number of reacted units as a result of an increase in rigidity of separate rings and a decrease in mobility of the chain as a whole (i.e.,  $\beta$ -relaxation is almost independent of the metal content). An increase of  $T_g$  is also observed for  $(\eta^6\text{-pentamethylbenzyl})(\eta^5\text{-cyclopentadienyl})\text{iron}$  bonding to poly(vinyl chloride) (PVC)<sup>18</sup> and in many other cases.

Interchain crosslinks, which are formed as a result of rigid-chain polymer interactions with  $\text{MX}_n$ , significantly change the supramolecular organization of the complexed polymer; both the structural elements (microfibers, fibers, etc.) and chains are linked through a metal ion inside the supramolecular structures. Thus  $\text{MX}_n$  is involved in both the molecular and the supramolecular organization of polymers.

### C. Macroligand Decomposition in $\text{MX}_n$ -Polymer Systems

One additional, nontrivial phenomenon that was observed on the MMC formation has not yet been analyzed. That is the complete decomposition of polymer chains in dilute solutions, including nonaqueous solutions. Viscosimetry, gel-permeation chromatography (GPC), and centrifugal sedimentation of parent macroligands and macrocomplexes or regenerated polymers give indisputable evidence for this. Figure 4 shows chromatograms for parent PEG isolated after the decomposition in an inert atmosphere of its complexes with  $\text{VOCl}_3$  or  $\text{VCl}_4$ . PEG decomposition is described in scheme 1.<sup>19</sup>



Scheme 1

Decomposition is initiated when the polymer has a specific molecular weight. Thermodynamic parameters that can result in initial chain scission at the minimum molecular weight require that the difference in the free energies of the decomposition

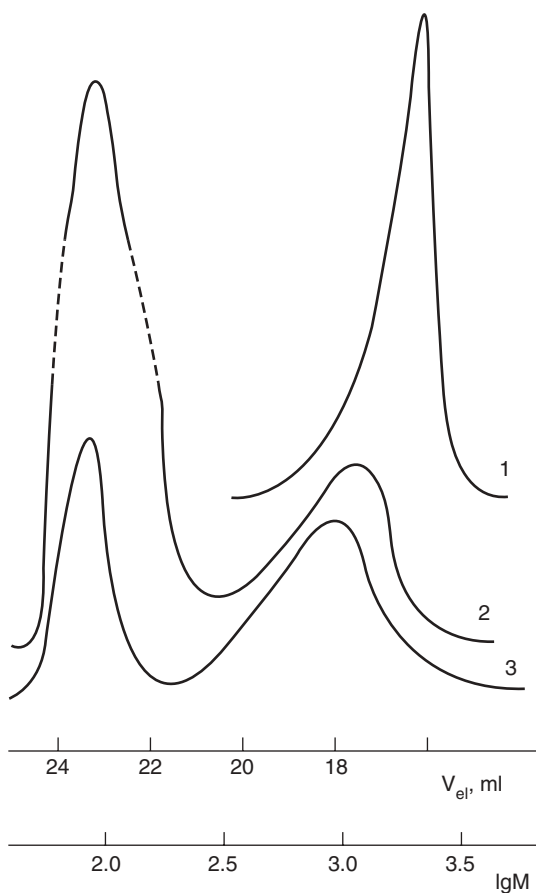


**Figure 4** Gel-penetrating chromatography for (1) polyethylene glycol ( $M_n = 2250$ ), (2) the complexes of PEG with  $\text{VOCl}_3$ , and (3)  $\text{VCl}_4$ .

products and the initial chain formation,  $\Delta G$ , is less than zero. The free energy of macrocomplex formation in dilute solution (assuming additivity of all components) is a sum of the free energies of (1) the elongated chain formation including bonded complexes; (2) solvation; (3) perfect mixing; and (4) polymer-solvent contact energy, which is stipulated by (1) the excess entropy of mixing of molecules of different size, (2) the solvent-solvent interaction close to chain molecules, and (3) the free energy of bending.

The free energy of formation of dilute solution after chain scission includes additionally the free energy of formation of decomposition products and the free energy of perfect mixing of decomposition products with a solvent. It is sometimes necessary to consider the changes in free energy as a result of changes in the conformer ratios both in the initial chains and the decomposition products. The dependency of the free energy of chain bending in solution initiates with a polymer of certain chain

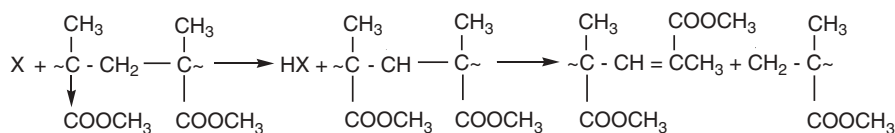
**Table 2** The Molecular-Weight Parameters of the Initial and Complex-Bonded Macroligands

Macroligand	$\text{MX}_n$	$\bar{M}_w \cdot 10^{-4}$	$\bar{M}_n \cdot 10^{-4}$	$\bar{M}_w/\bar{M}_n$	$\delta$
PMMA	—	109	60.6	1.80	—
	$\text{TiCl}_4$	10	(2.0)	5.0	30.3
	$\text{VCl}_4$	12	(2.48)	4.84	24.4
PVA	—	54	19.7	2.75	—
	$\text{VCl}_4$	17.2	(6.2)	2.78	3.2
Alternate copolymer of styrene with methylmethacrylate (50:50 mol%)	—	1.03	0.640	1.61	—
	$\text{TiCl}_4$	1.16	(0.526)	2.20	1.2
Copolymer styrene and $\alpha, \beta, \beta'$ -trifluorinestyrene	—	24	6,32	3.80	—
	$\text{TiCl}_4$	2.36	(0.96)	2.45	6.6
	$\text{VCl}_4$	18.8	(4.80)	3.90	1.3
Polyethylene glycole	—	2.25	1.98	1.14	—
	$\text{TiCl}_4$	1.6	(1.1)	1.45	1.8
	$\text{VCl}_4$	0.094	(0.067)	1.40	3.4
	$\text{VOCl}_3$	0,123	(0,094)	1,31	2,4

length and its ability to break (i.e., the chain is unstable if there is even one thermodynamically preferable break). However, the latter can be determined from reaction kinetics. Thus the decomposition of any polymer having various functional groups would occur in a similar manner to that of carbochain and heterochain macromolecules if the molecular weight exceeds a threshold value and if the process has favorable kinetics. The decomposition degree defined as the ratio of average-number molecular weight of the employed macroligand ( $\bar{M}_n$ ) to that of the obtained macroligand ( $\bar{M}'_n$ ) ( $\delta = \bar{M}_n/\bar{M}'_n$ ) can reach great values (Table 2).<sup>20,21</sup>

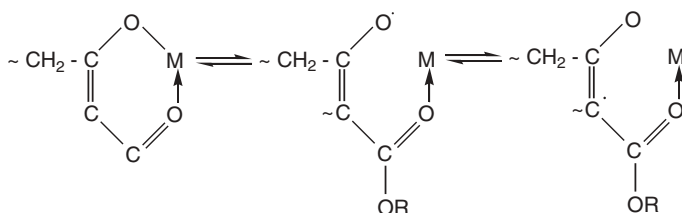
Moreover, decomposition can also occur upon macrocomplex formation at an interface. It was reported by Joppien<sup>22</sup> that PEG of  $M_n = 20,000$  dissolved in  $\text{CCl}_4$  in the presence of a  $\text{TiO}_2$  dispersion decomposes, Roman et al. also reported a decrease in intrinsic viscosity of PVC in its reaction with  $\eta^5$ -pentamethylbenzyl ferrocene in THF.<sup>23</sup> Both observations may be interpreted as decompositions that occur during the interaction with the metal moiety.

One of most probable destruction mechanisms may be related to radical formation in the reaction system; as illustrated in the reduction of PMMA (scheme 2).

**Scheme 2**

A radical mechanism has been supported by the fact that the  $\delta$  value decreases significantly on PMMA interaction with  $\text{MX}_n$  in radical entrapping solvents or by the insertion of radical acceptors in the reaction system. On the contrary,  $\delta$  increases on the addition or generation of radicals in a reaction zone.

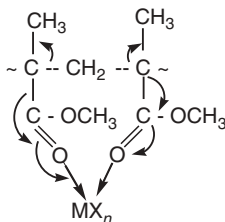
It should be noted that a homolytic radical break of a metal–macroligand bond has also been observed for MMC of poly- $\beta$ -ketoethers (scheme 3).<sup>24</sup>



**Scheme 3**

The resulting radicals have been shown to initiate graft polymerization of butadiene. Radicals photogenerated in the *macroligand*– $\text{MX}_n$  systems essentially accelerate the process. Decomposition usually occurs to form an intermediate complex, in which the metal plays an important role (i.e., a random break is realized through the  $\beta$ -position of a resulting polymer radical). For example, photolysis of isotactic poly(methylmethacrylic acid) (PMAAc) bound to  $\text{Cu}^{2+}$  in a complex proceeds much faster than that of the parent PMAAc. The chain scission rate constant increases with an increase in the value of  $\text{CuCl}_2$ :PMAAc ratio up to 0.04 and then remains unchanged.<sup>25</sup> At the latter ratio, chain scission is realized most likely at the sites of complex formation. The mechanism and kinetics of the free-radical decomposition of solid polymethylmethacrylate (PMMA) that is initiated by photoreduced  $\text{FeCl}_3$  complexes was studied in detail by Pokholok et al.<sup>26</sup> A more complicated process has been reported by Kanaev et al. for photolysis in composites based on PVA-I and metal halides.<sup>27</sup>

One cannot exclude decomposition as a thermally activated decay of interatomic bonds, which may occur as a result of a polymer chain scission affected by mechanical forces (i.e., stretching strain ( $\sigma$ )) like that described for PMMA by Zhurkov et al. (scheme 4).<sup>28</sup>



**Scheme 4**

This process results in a lower activation energy of the C–C bond cleavage down to  $E = E_0 - \gamma\sigma$ , where  $\gamma$  is a structural coefficient defining a strain distribution in bonds. An essential contribution can also be made by the changes in chain entropy as a result of breaking cyclic compound.

In addition to stretching strain, an important role is also played by the M–O bond energy and the conformation of a cyclic compound formed in the process. There are numerous examples of the combined effect of stretching strain and thermal motion that results in a lowering of the potential barrier for the C–C bond rupture. Moreover, it has been shown by Enikolopyan et al. that strained crown-ether macrocycles open and polymerize upon exocyclic coordination to  $\text{MX}_n$ .<sup>29</sup> In conclusion, one should consider macroligand decomposition while designing MMC and studying its composition, structure, and stability. Degradation is characteristic of all types polymers and occurs under appropriate kinetic conditions.

#### D. Changes in Origin of Functional Groups of Polymers in Their Reactions with $\text{MX}_n$

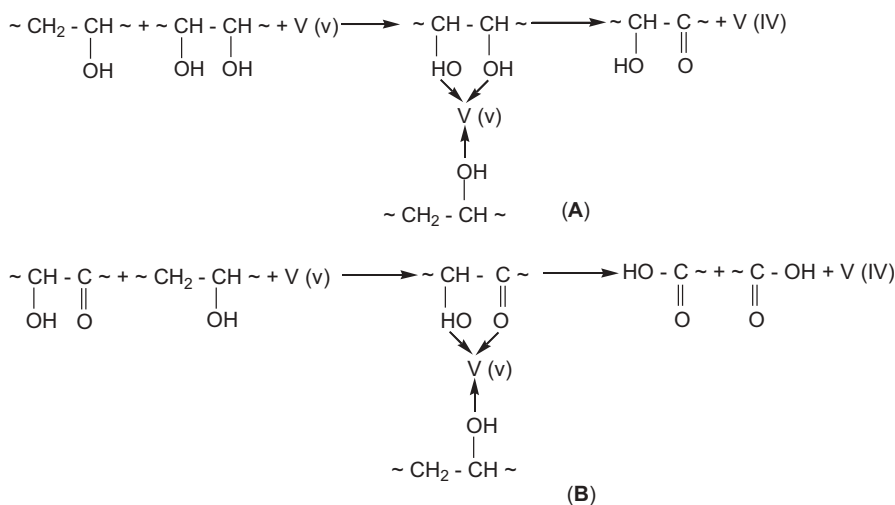
Local chemical bond stability in macrocomplexes can differ from bond stability in similar complexes with low molecular weight compounds. The difference may be attributed to rigid chain formation and is probably due to the changes in acid–basic,<sup>30</sup> donor–acceptor, and other properties of the functional groups that introduced into the macromolecule. For example, the lowering of the carbonyl vibrational stretching frequency ( $\Delta\nu_{\text{C=O}}$ ) may be interpreted in terms of the relative basicity of the carbonyl-containing ligand. For example,  $\Delta\nu_{\text{C=O}}$  in  $\text{TiCl}_4$  complexes with monomer and polymer ligands are quite different (e.g.,  $\delta\Delta\nu_{\text{C=O}} = 42 \text{ cm}^{-1}$ );  $\Delta\nu_{\text{C=O}}$  has the following order: monomer > saturated analog > oligomer > polymer. However, when analyzing the  $\Delta\nu_{\text{C=O}}$ -values that are observed on formation of a donor–acceptor bond in MMC,  $>\text{C=O} \rightarrow \text{M}$ , one should consider the differences in bond stability and the contributions to the vibrations made by structural changes in the chain. Therefore,  $\delta\Delta\nu_{\text{C=O}}$  in fact, manifests all the thermodynamic features of complex formation with macroligands (i.e., chain effects, neighboring group effects, and changes in chain conformation). For example, it is important that the rings in styrene copolymers with methylmethacrylate (MMA) are inert diluents of carbonyl groups. Thus the  $\Delta\nu_{\text{C=O}}$  is approximately the same for MMA as for the oligomer of MMA ( $132 \text{ cm}^{-1}$ ) vs. for statistical copolymers of MMA and styrene ( $125 \text{ cm}^{-1}$ ) (Table 3). An inverse effect of carbonyl groups frequency is observed if the MMA to styrene ratio decreases as in the MMA–styrene alternating copolymer ( $\delta\Delta\nu_{\text{C=O}} = 110 \text{ cm}^{-1}$ ;  $\delta\Delta\nu_{\text{C=O}} = 20 \text{ cm}^{-1}$ ). In general, the shorter the distance between functional groups of a copolymer chain, the stronger their reciprocal effect (i.e., neighboring group).

Consistent with the chain effect, which can be added to the neighboring group effect, the  $\Delta\nu_{\text{C=O}}$ -value is strongly affected by the molecular weight of a macroligand. For example, for  $\text{CoCl}_2$  complexes with poly(vinylpyrrolidone) with polymerization degrees of  $n = 100, 200, 360,$  and  $6300$  and  $\Delta\nu_{\text{C=O}}$  values of  $54, 49, 48,$  and  $43 \text{ cm}^{-1}$ , respectively, were found.<sup>31</sup>

**Table 3** The Comparison of Donor Properties of the Carbonyl Group of Macroligand and Its Low Molecular Weight

Ligand	$\Delta\nu_{C=O}$ , $\text{cm}^{-1}$	$\delta\Delta\nu_{C=O}$ , $\text{cm}^{-1}$
Methyl ether of isobutyric acid	115	25
Methylmethacrylate	132	42
Oligomer of methylmethacrylate ( $\bar{M}_n = 5000$ )	128	38
Statistical copolymer of styrene with methylmethacrylate (50:50 mol%)	125	35
Alternate copolymer of styrene with methylmethacrylate (50:50 mol%)	110	20
PMMA ( $\bar{M}_n = 1.1 \cdot 10^6$ )	90	0
PE-gr-PMMA	90	0

The nature of functional groups of a polymer changes as a result of protonation, ionization, quaternization, and alkylation. There are numerous examples of this effect; however, only a few will be described here. Particularly, PVA reaction with  $V^{5+}$  is accompanied by a partial conversion of hydroxyl to carboxyl groups (scheme 5).<sup>32</sup> In an acidic medium, complex **A** decomposes, 1,2-glycol units are oxidized, and  $V^{5+}$  reduces to  $V^{4+}$ . In addition, complex **B** is formed from  $V^{5+}$  and 1,2-ketol as a result of oxidation, which is accompanied by chain decomposition to reduce vanadium. The reaction is, to a certain extent, similar for  $Ce^{4+}$ .<sup>33</sup> Furthermore, free-radical steps are observed in these reactions. It should be noted that this occurs only for PVA, which forms with 1,2-glycol units as a result of abnormal head-to-head addition. This illustrates the importance of both functional and structural uniformity of macroligands.

**Scheme 5**

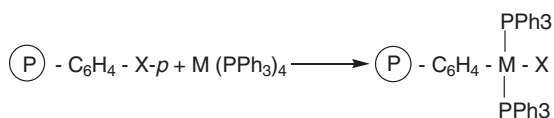
Chemical changes in the macroligand functional groups can involve transition metal ligands. For example, the reaction of polyacrylonitrile with  $\text{MoCl}_5$  is accompanied by partial conversion of the  $-\text{C}\equiv\text{N}$  groups to  $-\text{C}(\text{Cl})=\text{N}-$ .<sup>34</sup> Moreover, polymer ketones are formed in the case of the treatment of the chloromethylated copolymer of styrene and divinylbenzene with  $\text{Na}_2\text{Fe}(\text{CO})_4$ .<sup>35</sup> These types of conversions can be prevented by imposing strict requirements to the uniformity of polymer ligands and optimization of the conditions required for complex.

### III. TRANSFORMATION OF TRANSITION METAL COMPOUNDS IN REACTIONS WITH POLYMERS

The transformation of transition metal compounds in reactions with polymers is difficult to study. Only a few cases have been reported. The most noticeable changes that transition metal compounds can undergo have been reduced to the following: changes in metal valence state, nuclearity, and cooperativity if two or more metal complexes are involved in the reaction.

#### A. Oxidation–Reduction Conversion of Transition Metals

One of more often observed transformations is reduction or oxidation of transition metals. Metal oxidation on reaction with a polymer will be discussed first. One of the typical processes is oxidative addition of metal(0) to a macroligand. For example, *tetrakis*(triphenylphosphine)metal(0),  $\text{M}(\text{PPh}_3)_4$  ( $\text{M} = \text{Pt}, \text{Pd}, \text{Ni}$ ), is oxidized by halogenated polystyrene (PS) to a bivalent state as the functional groups on the polymer become metal ligands (scheme 6).<sup>1</sup>

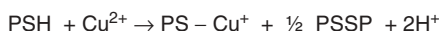


Scheme 6

Similar processes have been observed using metal(0) vapor deposition on polymers,<sup>36</sup> metal dissolution in the presence of polymers, mechanochemical syntheses involving macromolecular ligands, etc. However, transition metal reduction is most often observed in these processes. Hence compounds of  $\text{V}^{5+}$  and  $\text{V}^{4+}$  are reduced relatively easily, as it was shown with PVA as a model compound. A graft copolymer of cellulose is reduced in a similar manner.<sup>37</sup> The degree of reduction depends on the pH of reaction medium (maximum of 70% at pH 4.5–5.0), and if the resulting  $\text{V}^{4+}$  is fully bound to the polymer.

It is known that  $\text{Mo}^{5+}$  easily reduces to  $\text{Mo}^{4+}$ . Peptide complexes of  $\text{Mo}^{5+}$  and  $\text{Mo}^{6+}$ , which are formed as a result of  $\text{MoO}_2\text{Cl}_2$  or  $(\text{NH}_4)_2\text{MoOCl}_5$  reaction with

chloromethylated PS that contain peptide groups, undergo redox reactions,<sup>38</sup> Mo<sup>5+</sup> oxidizes to Mo<sup>6+</sup> according to a one-electron mechanism, and then Mo<sup>6+</sup> is reduced by PPh<sub>3</sub> to Mo<sup>4+</sup>. The latter can again be oxidized by nitrate ion to Mo<sup>6+</sup>. This cyclic mechanism of Mo reduction–oxidation in a polymer-bound complex is a model of a reductase or oxidase. It is important that isolated Mo<sup>5+</sup> complexes are formed. These complexes are long lived even in the presence of O<sub>2</sub> or H<sub>2</sub>O due to the hydrophobic properties of macroligands. Similar processes are also known for polymer (P) complexes of Cu<sup>2+</sup> in chelation of crosslinked poly[N-(acryloylamino)methyl]-mercaptoacetamide (scheme 7).<sup>39</sup>



**Scheme 7**

The Cu<sup>+</sup> complex again oxidizes to Cu<sup>2+</sup> in air. It is interesting that oxidation of Cu<sup>+</sup> bound to poly(1-vinylimidazole) is characterized by higher enthalpy and lower entropy compared to the low-molecular-weight imidazole complex.<sup>40</sup> These differences are attributed to the changes in polymer ligand conformation as a result of Cu<sup>+</sup> oxidation to Cu<sup>2+</sup> and is evidenced by viscosity measurements. It has been noted that copper ion doping in poly(thioether) stabilizes the oxidation state of Cu<sup>+</sup> and results in the formation of a Cu<sup>+</sup>–Cu<sup>2+</sup> system with a potential of 1 V in aqueous solution.<sup>41</sup>

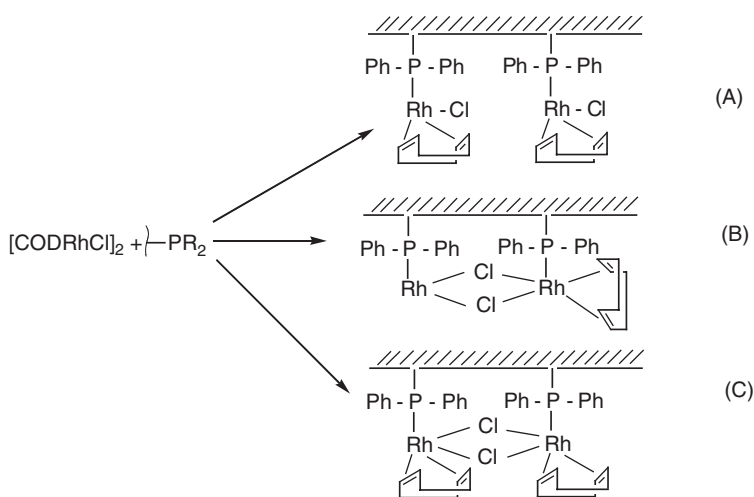
An abnormal behavior was observed for Cr<sup>2+</sup> macrocomplexes with polyether modified by amino groups<sup>42</sup>; Cr<sup>2+</sup> oxidizes to Cr<sup>3+</sup> on adding NaCl, and at ~–1.3 V the reverse reaction is observed. Such metal-containing polymers as woven fibers can serve as an electric muscle, electric resistance systems, etc. Fe<sup>3+</sup> → Fe<sup>2+</sup> reversible reduction in sandwich complexes of η<sup>5</sup>-pentamethylbenzylferrocene with PVC or chloromethylated PS was used to fabricate redox electrodes.<sup>18</sup>

Rh<sup>3+</sup> and Pd<sup>2+</sup> complexes are easily reduced on bonding to macroligands, especially in alcoholic solution, for a variety reasons. For example, if Pd<sup>2+</sup> cations are complexed to a Nylon-66 fiber, immobilization on the polymer powder is accompanied by partially formed Pd<sup>0</sup> even in the step that involves macrocomplex formation.<sup>43</sup> One of the causes is probably rapid oxidation of Pd<sup>0</sup> to Pd<sup>2+</sup> involving CuJ used as a stabilizer in polymer fiber fabrication. Thus redox processes in such systems can be either stimulated or inhibited using particularly a purposeful selection of reagents, solvents and reaction conditions.

## **B. Monomerization of Transition Metal Dimer Complexes in Reactions with Polymers**

It is known that many transition metal compounds are dimers (e.g., VCl<sub>4</sub>, TaCl<sub>5</sub>, MoCl<sub>5</sub> etc.), tetramers (e.g., Ti(OR)<sub>4</sub> etc.), and chlorine-bridged polymers (e.g., VCl<sub>3</sub>, TiCl<sub>3</sub>, and HfCl<sub>4</sub>). Their interaction with macroligands usually causes monomerization. The following factors should be considered in analyzing this phenomenon. The

mixing of different size particles (macroligands and dimer complexes) must be accompanied by monomerization of the associated particles near a polymer chain as a result of an increase in excess positive entropy of mixing with an increase in the difference in particle size. The degree of monomerization is defined as the increase or decrease in the complex formation constant. However, because of the propensity of chain molecules to associate, the proportion of associated complexes increases, particularly in concentrated solutions. The predominance of one of these causes results in either complete monomerization or the coexistence of both the monomer and dimer complexes. This phenomenon was observed by Brubbs et al. on reaction of *bis*(cyclooctadienylrhodium chloride) with phosphinated PS, which was crosslinked with a varying number of divinylbenzene molecules (scheme 8).<sup>44</sup>



Scheme 8

Different routes are defined by the reaction conditions, nature of the functional groups,  $\text{MX}_n$ , and the level of macroligand crosslinking. For example, at a low level of crosslinking (ca. 2% of divinylbenzene), the polymer is flexible enough and the dimer structures **B** and **C** form or remain unchanged on complex formation. Dimer complexes were nearly unobserved for a 20% of divinylbenzene crosslinked polymer, and coordinatively unsaturated structures (**A**) can possibly form as well.

The nature of the functional groups of the macroligands is also of great importance.<sup>1</sup> For instance, monomeric and polymeric amines dissociate the  $[\text{Rh}(\text{CO})_2\text{RS}]_2$  dimer complex in contrast to thiols that yield addition products. Similarly, the nature of the solvent affects chain flexibility and long-range action. For example, the  $\text{Co}^{2+}$  complex with a crosslinked PS polymer has a  $\text{Co:L}$  composition of 1:1 (L=monomer unit) in weakly swelling *n*-hexadecane, whereas a thermodynamically stable 1:2 complex forms in xylene.<sup>45</sup> This observation may be a result of the fact that a PS support is glassy at 70°C in *n*-hexadecane and gum-like in xylene.

Therefore, for highly flexible polymers, metal complex dimerization occurs either in a single chain (linear polymer) or in the chain site between the crosslinked knots. It was reported that a ratio of mononuclear and binuclear complexes of  $\text{Cu}^{2+}$  with polymeric acids depends on the degree of neutralization of the latter; low charge density provides binuclear complexes and monomer formation as the charge density increases.

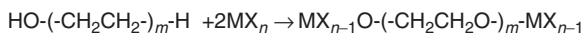
In general, many properties of MMC, including catalysis, depends on a type of complex that is formed (monomer or dimer). Unfortunately, contradictory data do not allow generalized conclusions.

### **C. Composite Inhomogeneity of Macromolecular Complexes**

Another important feature of complex formation with macroligands is the presence of different types decompositions that appear both within and between the polymer chains. As a result, several types of metal centers form simultaneously. Transformations between complexes sometimes do not occur and, therefore, result in the coexistence of fully coordinated macroligands or differently coordinated complexes in addition to the free macroligands, even at a low level of functional group conversion. Complex formation in solution proceeds rapidly and is accompanied by the loss of polymer ligand solubility that results in precipitation of different types of complexes, particularly at high values of  $\Theta$ . Both intramolecular and intermolecular complexes with a similar or different metal coordination number (CN) can form. Moreover, the number of defects in the coordination centers increases with rigidity of a molecular skeleton.

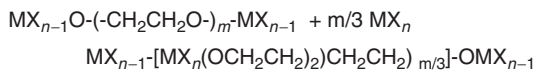
Linear polymers usually generate coordinately saturated complexes,<sup>1</sup> such as the complexes of  $[\text{MCl}_4 \cdot 2\text{D}]\text{D}$  and  $[\text{MCl}_4 \cdot 2\text{D}]\text{4D}$ , where D is a monomer unit. In this example, outer-sphere groups conform to a noncoordinated macrochain in PMMA or poly(vinylacetate) (PVA) and  $\text{MX}_n$  (e.g.,  $\text{TiCl}_4$ ,  $\text{VCl}_4$ ) system. Therefore, 33–66 mol% of ligand functional groups are involved in complex formation because of two possible reasons: (1) the neighboring group effect, which consists of changes in reactivity of functional groups that are adjacent to reacting groups and of a statistical distribution of the reacted and nonreacted units, and (2) the chain effect, in which a polymer chain becomes more rigid at a high degree of conversion. The decrease of unit lability complicates their favorable orientation with regard to coordinative metal ion. If the number of bonds between the metals and the chains is large, there is a greater entropy loss, which lowers the CN of metals. For example, the  $\text{CoCl}_2$  interaction with poly(propylene glycol) in methanol is accompanied by the decrease in the CN of  $\text{Co}^{2+}$  from 6 to 4. Moreover, the proportion of four-coordinated  $\text{Co}^{2+}$  increases with polymer concentration.<sup>46</sup> Similar effects were observed in the reaction of  $\text{Co}^{2+}$  with PEG, poly(ethyleneimine) (PEI), and other polymers. In all cases, a complex with higher CN forms when there is a loss of chain entropy due to chain folding. The entropy loss is compensated by a change in free energy due to additional coordination. The CN of metals is usually defined by the chain structure and less by the reaction conditions.

Because of high reaction rates, intermediate products have been isolated in only a few reactions. For example, in the reaction of *cis*-Ru(Dipy)<sub>2</sub>Cl<sub>2</sub> with a 4-ViPy copolymer with 4-methyl-4'-vinyl-2,2'-dipyridyl (unit ratio is 0.94 and 0.06), the 4-ViPy units react first and then Ru<sup>2+</sup> recoordinates to the dipyridyl rings of the polymer chain. The resulting ratio of the Ru<sup>2+</sup>-ViPy units and the Ru<sup>2+</sup>-dipyridyl rings is 0.01 and 0.025, respectively.<sup>47</sup> The situation is much more complicated for polydentate macroligands that make up functional groups of different origins. It is difficult to identify the step-by-step reaction products. One rare example is the interaction of low-molecular-weight ( $M_n = 300 - 20\,000$ ) PEG with MX<sub>n</sub> (e.g., TiCl<sub>4</sub>, VCl<sub>4</sub>).<sup>48</sup> At Q MX<sub>n</sub> to PEG molar ratio of 2, the formation of metal ethers due to terminal hydroxyl groups of oligomers is observed (scheme 9).



Scheme 9

If the MX<sub>n</sub> to PEG ratio is more than 2, there is coordination of each MX<sub>n</sub> molecule to the chain, making up three oxyethylene units: one noncoordinated and two coordinated ones (scheme 10).



Scheme 10

This is another example of structurally uniform macrocomplexes that require structural limitations on macroligand functional uniformity, which is not always achieved even for homopolymers.

There is still no resolution on the effect of macroligand stereochemistry on complex formation.<sup>1</sup> A particular case is the formation of a complex between P2ViPy and MCl<sub>2</sub> (M = Co, Ni, Cu, Zn). In that case, the order of reactivity is as follows: atactic > isotactic > crosslinked. However, the rate of complex formation for isotactic poly(acrylic acid) (PAAc) with Cu<sup>2+</sup> is 1.5 times greater than for the syndiotactic form, and the E<sub>a</sub> for these reactions is 6.0 and 7.0 kcal · mol<sup>-1</sup>, respectively.

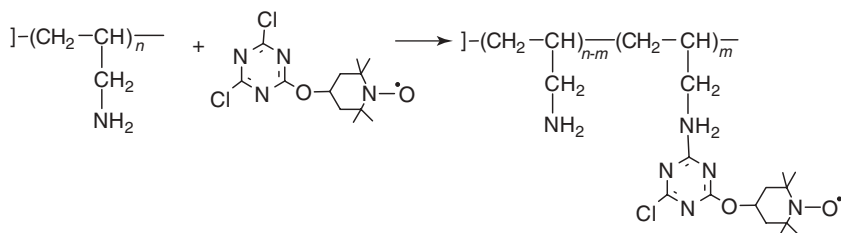
Thus only a fundamental analysis of the processes that occur in the macroligand-MX<sub>n</sub> systems will allow one to design macrocomplexes of desirable structure. Even then one cannot be sure that the MMC will be uniformly distributed throughout the polymer chain. In addition, the topochemistry of MMC should be considered—namely, specificity of the formation and distribution of mononuclear, binuclear, and polynuclear metal complexes in macroligands.

#### IV. PROBLEM OF TOPOCHEMISTRY OF MACROMOLECULAR COMPLEXES

The main usage of macromolecular metal complexes is catalysis.<sup>49</sup> Some important characteristics of immobilized catalysts are functional group distribution, their accessibility, and the uniformity of their bonding properties. These characteristics and their response to reaction conditions reflect the latent properties of immobilized catalysts and have been given the term *topochemistry of macromolecular metal complexes*.

##### A. Topochemistry of Polymer Macroligand Functional Layers

In the 1980s we reported on new types of macroligands. These macroligands are polyethylene (PE), polypropylene (PP), copolymer of ethylene with propylene (CPP), PS, and others. These materials provide a reaction center at or below the surface of an ordinarily inert polymer. Furthermore, the surfaces of the polymeric macroligands may be functionalized by gas-phase grafted polymerization with the corresponding monomers (allylic alcohol, allylamine and diallylamine, acrylic acid, 4-vinylpyridine etc.).<sup>50</sup> For example, in the case of PE, the products are denoted as PE-grafted-poly-diallylamine (PE-gr-PAIAm), PE-grafted-poly(4-vinylpyridine) (PE-gr-P4Vpy), and (PE-gr-PAC). The degree of grafting ranged from 1 to 10 wt%, and the thickness of grafted layer was 10–30 nm. To determine the accessibility of the functional groups for the reaction with transition metal compounds ( $MX_n$ ) and to study the topochemistry of metal complexes formed, the method of spin labels was used, which earlier was in wide use in the analysis of various biological,<sup>51</sup> polymeric,<sup>52</sup> and other materials.<sup>53</sup> Spin-labeling of macroligands in the case of PE-gr-PAIAm by using stable 2,2,6,6-tetramethyl-4-(2'-oxy-4',6'-dichlorotriaxine)piperidine-1-oxyl nitroxyl radicals ( $R^{\cdot}$ ) can be represented by scheme 11.<sup>54</sup> A calibration curve for the parameter  $\Delta - \bar{r}$ , where  $\Delta = d_1/d - (d_1/d)_0$  and  $d_1/d$  is the ratio of total intensities of end and middle components of the EPR spectra (for our systems,  $d_1/d = 1.76 - 0.036 A_{||}$ ) was used to determine the effective distances ( $\bar{r}$ ) between iminoxyl radicals on the polymers.

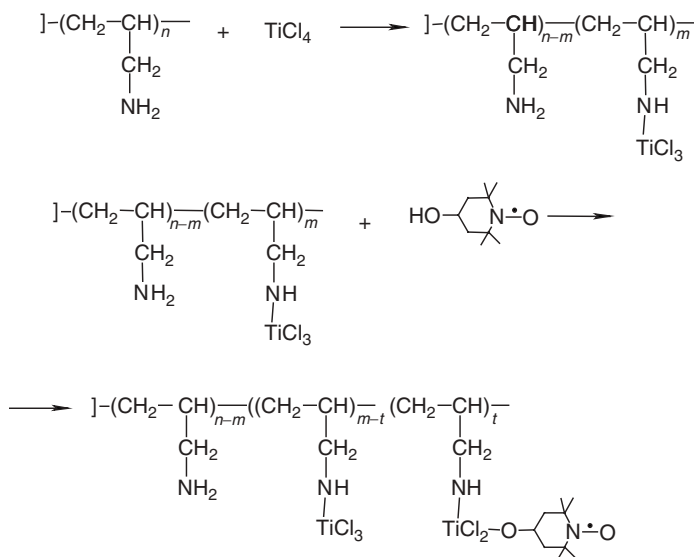


Scheme 11

It turned out that  $\bar{r} = 25\text{--}35 \text{ \AA}$  for the PE-gr-PAIAm-R' system at various concentrations of the fixed radical. When the concentration of the fixed R' is 10 times greater,  $\bar{r}$  decreases to  $10 \text{ \AA}$ . Taking into account the real surface of macroligands, this effect is possible only if there is a chromatographing of R' into a deep layer of the functional cover. In other words, the grafted layer is loose and all the polymer's functional groups are practically accessible for the interaction. The process of spin labeling proceeds in a layer-by-layer manner, and the number of layers is about 10.

## B. Topochemistry of Diamagnetic Complexes That Are Fixed to the Polymers

The same approach can be used for spin-labeling diamagnetic metal complexes bounded to the polymer. This is illustrated by the interaction of  $\text{TiCl}_4$  with PE-gr-PaAlAm (scheme 12).<sup>54</sup>



Scheme 12

A minor proportion of the immobilized metal complex is involved in cluster-like aggregations that effectively bond stable nitroxyl radicals by coordination of the  $-\text{N}-\text{O}^{\bullet}$  fragments. The effective distances between the radicals are less than  $10\text{--}12 \text{ \AA}$  in such aggregations. The proportion of the bonded metal complexes involved in these aggregations is considerably greater for titanium-containing polymers. The remaining proportion is uniformly distributed along the grafted functional layer as isolated complexes that covalently bond to the R' radical. It was shown that metallation of the functional covering makes the polymer more accessible for spin labeling.

Furthermore, metallation of the functional covering has a considerable effect on the dynamic behaviour of the polymer matrix.

### C. Topochemistry of Polymer-Bonded Paramagnetic Complexes

Polymer-bonded paramagnetic complexes provide the most information about topochemistry.  $\text{Cu}^{2+}$ ,  $\text{V}^{4+}$ ,  $\text{Mn}^{2+}$ , and other ions are used most as paramagnetic centers. Magnetochemistry and ESR spectroscopy are the main methods used to study these systems. Thus the temperature dependence of the magnetic susceptibility ( $\chi^{-1}$ ) of the  $\text{Cu}^{2+}$  complexes that are fixed to PE-gr-PAA<sup>55</sup> shows that, in all cases, there a break in the curve of  $\chi_{\text{M}}^{-1} = f(T)$  occurs (Fig. 5).

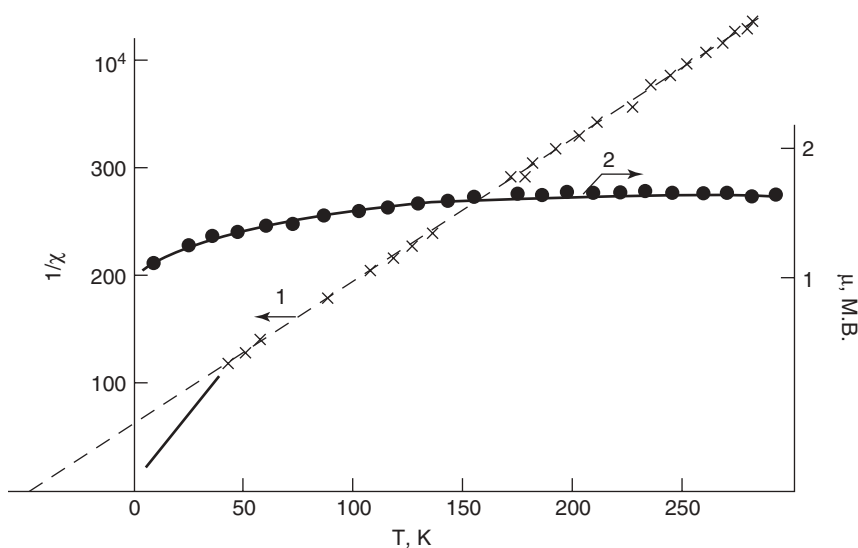


**Figure 5** Temperature dependence for (1)  $\chi^{-1}$  and (2)  $\mu_{\text{ef}}$  for PE-gr-PAA-Cu(II) (0.4 mmole/g).

The Weiss constant ( $\theta$ ) is equal to 50K. This can be explained by the presence of two types of bond complexes for  $\text{Cu}^{2+}$ : isolated complexes (that obeys the Curie law), and complexes that aggregate into clusters with an antiferromagnetic exchange. This may be expressed as follows:

$$\chi_{\text{exp}} = \chi_{\text{isol}} + \chi_{\text{exch}}$$

The copper content in theses complexes is estimated by the equation

$$\bar{C}_{\text{total}} = \bar{C}_{\text{isol}} + \bar{C}_{\text{bond}}$$

**Table 4** Distribution of Isolated Ions and Dipole-Bound aggregations in the PE-gr-PAA-Cu(II) System

Total Cu Content, %	Content, %		Cu Density in Clusters $\times 10^{20}$ , $\text{cm}^{-3}$	Total Cu Content, %	Content, %		Cu Density in Clusters $\times 10^{20}$ , $\text{cm}^{-3}$
	Isolated Ions	Clusters			Isolated Ions	Clusters	
0.2	100	0	—	1.51	1	99	19.4
0.29	100	0	—	2.48	2.5	97.5	31.4
0.55	16	84	6.0	3.18	2.0	98	40.6
0.94	4	96	11.7	18.4 <sup>a</sup>	0	100	17.2
1.37	2	98	17.4				

<sup>a</sup>For the Cu(II) complex with the polyacrylic acid homopolymer.

The experimental data show that at a concentration  $C_{\text{total}} = 0.1$  mmole/g, more than half of the copper ions is localized in cluster aggregations (Table 4). More detailed information can be obtained from the ESR spectra. As  $\bar{C}_{\text{total}}$  increases, the shape of the ESR spectrum is changed (Fig. 6); a wide asymmetrical singlet appears and grows.

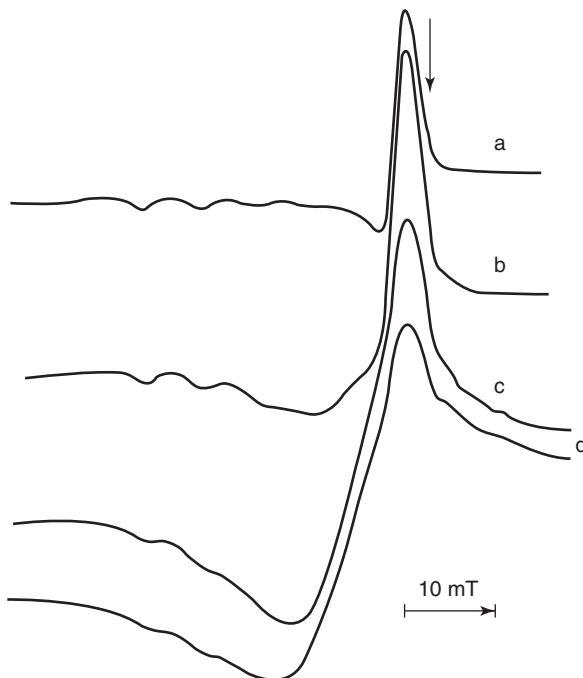


**Figure 6** Change in the form of the ESR spectrum (77 K) of Cu(II) complexes on PE-gr-PAA with increasing mean cupric ion concentration (in mmole/g), *a*, 0.03; *b*, 0.08; *c*, 0.15; *d*, 0.23. The arrow represents  $g = 2.0036$ .

The width of the signal monotonically increases. The average value of the  $g$ -factors ( $\bar{g} = 2.16 \pm 0.02$ ) agrees with the  $\bar{g}$ -factors of isolated complexes of Cu(II), and the peak width ( $\Delta H$ ) corresponds to the total length of the spectrum. These facts suggest that the close proximity of the of copper centers are responsible for both types of the spectra. By increasing  $\bar{C}_{\text{total}}$ , the width of the singlet signal increases and confirms the existence and growth of dipole–dipole interactions between copper ions. Applying Equation 1, the experimentally observed dependence of  $\bar{C}$  on  $\Delta H$  is approximately linear with a slope of  $(9.7 \div 2.3) \cdot 10^{-20} \text{ Gs cm}^3$ .<sup>56</sup>

$$\Delta H = \Delta H_0 + A \bar{C} \quad (1)$$

In addition, the contribution of copper in dipole–dipole bond aggregations as it affects  $\bar{C}_{\text{total}}$  may be estimated from the ESR data. It was shown that at a concentration exceeding 0.15 mmole/g, almost all the copper was bound as aggregates, in which the local concentration was  $(6.0 \pm 40.6) \times 10^{20} \text{ per cm}^3$ .<sup>55</sup>

Thus one can imagine the following distribution of copper in the grafted layer: (1) isolated complexes with an effective distance  $\bar{r}_{\text{isol}} \geq 15 \text{ \AA}$  (Fig. 7, type I), (2) part of the copper is in cluster-like aggregations with  $r_{\text{aggr}} \leq 7 \text{ \AA}$ , in which the complexes

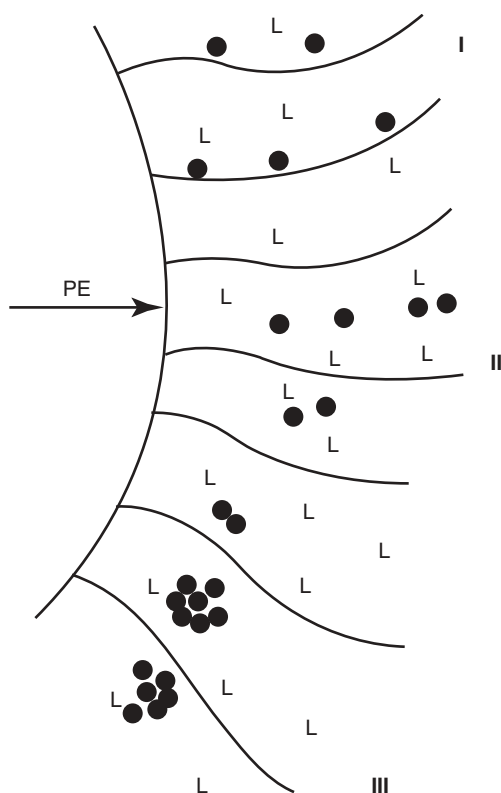


**Figure 7** The principal scheme of distribution of the metal ions in grafted layer of the polymer.

are not bound chemically (Fig. 7, type II), and (3) a considerable proportion of the copper is bound into clusters with strong exchange, (Fig. 7, type III), which is caused by chemical bonds of the complexes between each other. Most likely this topographic pattern has the same general character as any of the macroligands and any of the metal complexes. For example, this has been confirmed for V(IV) complexes bound to PE-gr-P4ViPy as a donor–acceptor bond.<sup>57</sup> In this case, a well-resolved, eight-component, broad signal with the same  $g$ -factors appears and increases with increasing  $VCl_4$  content (Fig. 8). The same type of spectrum is observed for complexes that exhibit broadening by dipole–dipole interactions. Furthermore, the width of the hyperfine lines remains constant with an increase in the  $VCl_4$  content—that is, the spectra are anisotropic. The distribution of V(4+) is characterized by following data after taking into account the thickness of the grafted layer (grafted with 5 wt% of 4-ViPy) at the lowest concentration of  $VCl_4$  ( $0.15 \times 10^{-4}$  mol/g); for bonded complexes of V(4+),  $\bar{C}_{isol} \leq \delta H/A_{min} \approx 2 \cdot 10^{-4}$  g-atom  $cm^{-3}$ ;  $r_{isol} \geq 22$  Å; and  $r_{clust} \geq 6.8 \div 9$  Å. At the distance of 7–9 Å, the energy of dipole–dipole interaction is much less than  $kT$ . Thus one can assume that dipole–dipole interactions do not occur; however, a spatial organization of metal ions is important and is preferred for the formation of cluster aggregations.

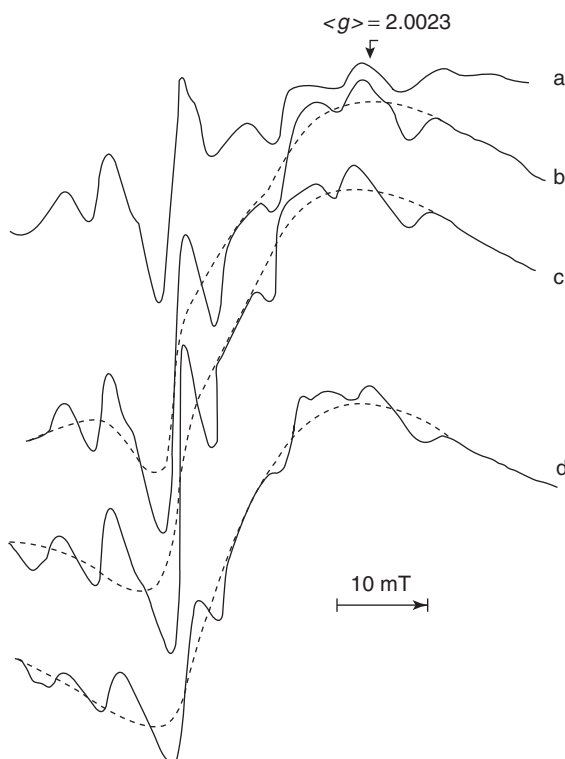


**Figure 8** ESR spectra of V(IV) fixed into PE-gr-P4VP (5 wt%). The content of  $V(IV) \cdot 10^4$  (g-atom/g): a, 0.15; b, 0.20; c, 0.85; d, 1.76.

It is likely that cluster aggregations arise around metal ions that bond two polymer chains. This effect can enhance the probability of additional bonding to other nearby metals. Clearly, further studies in this area are necessary to understand the main causes of these effects.

#### **D. The Main Data on MMC Topochemistry**

The distribution of polymer-bound metal ions is not homogeneous. Even at the low concentrations of bound complexes, the formation of three types of complexes is observed.

1. Isolated complexes, in which  $\bar{r} \geq 15 \text{ \AA}$ .
2. Aggregations of the cluster type, in which complexes of unbound paramagnetic metals occur between each other, in which  $\bar{r} \leq 7 \text{ \AA}$ .
3. Clusters in which there is a strong exchange interaction (i.e., exchange-bound clusters that are caused by chemical bonds as polynuclear complexes).

It is likely that the size of macromolecule segments that contain the bound complexes is large enough and their slow motions are unable to average the local environment of complexes. Moreover, complexes **I**, **II**, and **III** (Fig. 7) are dynamic; in principle, their realitive quantities can be altered, depending on both the concentration of metal complexes and the conditions (temperature, solvent, degree polymers swelling, etc.) under which bonding to the polymers occurs. The topochemistry pattern can be considerably altered when a reduction (e.g.,  $\text{Ti}(4+) \rightarrow \text{Ti}(3+)$ ,  $\text{V}(4+) \rightarrow \text{V}(3+)$ , etc.) or an oxidation of metal ions proceeds in the course of their bonding to the functional groups of the polymer. Introducing other metals into the system causes variations in the distribution of metal complexes. Thus the ESR spectrum of  $\text{Cu}(\text{II})$  remains unchanged even if  $\text{Pd}(\text{II})$  is introduced into a  $\text{PE-gr-PAA-Cu}^{2+}$  system in which vacant functional groups are still present even though  $\text{Pd}(\text{II})$  is reduced to  $\text{Pd}_0$ .<sup>58</sup>

The peculiarity of macrocomplexes topochemistry influences their catalytic properties. As a rule, the extremal dependence of the specific catalytic activity on the surface density of bond metal complexes in all catalytic processes (for example, polymerization, hydrogenation, and oxidation) is observed. However, their kinetic behavior correlates with neither  $\bar{C}_{\text{isol}}$  nor  $\bar{C}_{\text{clust}}$  of the complexes. This area too deserves further investigation.<sup>59-61</sup>

#### **V. PROBLEMS OF UNIT VARIABILITY IN METAL-CONTAINING POLYMERS OBTAINED BY COPOLYMERIZATION OF METAL-CONTAINING MONOMERS**

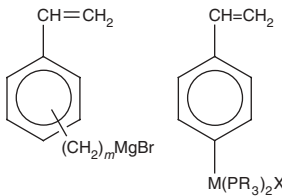
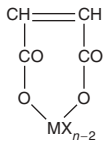
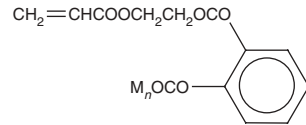
The concept of unit variability is used for all types of high-molecular-weight compounds.<sup>62</sup> It allows a deeper insight into the relationship between the structure

and properties of polymers. As applied to metal-containing polymers, the concept can be further developed and substantially enriched because the composition and structure of metal-containing groups can vary over wide limits. Metal-containing polymers can be produced by all the known methods that are used to synthesize high-molecular-weight compounds—namely, most often radical polymerization<sup>63,64</sup> or less often polycondensation of the corresponding monomers.<sup>65</sup> Polymerization and copolymerization of MCMs are of interest for the preparation of structurally homogeneous products with specified properties.<sup>66</sup> The main problem in this route is the synthesis of the corresponding monomers. Depending on the nature of the linkage between the metal of valency  $n$  and the ligands containing a multiple bond, MCMs can be classified into several types, which are presented in Table 5.<sup>67,68</sup>

In the general case, MCMs are metal complexes with specific ligands whose most important property is the ability to polymerize.<sup>69</sup> In these monomers, metals do not act as chain-forming centers (i.e., they are not included in the backbone), but serve as peculiar pendant groups. The reactivities of MCMs differ markedly; some polymerize even during their synthesis, whereas others are unable to polymerize or polymerize only with difficulty even under fairly drastic conditions (high temperature, pressure, and concentration of an initiator or catalyst). The limitations imposed on the polymerization of most known MCMs are associated with their solubility, possible dissociation and change in their composition in solution.

When analyzing polymerization of MCMs, it is reasonable to assume that the composition of the polymer formed corresponds to that of the initial monomer. In reality, this is not always true. In the formation of these polymers, some units appear

**Table 5** MCM Classification

$\sigma$ -MCM	Ionic type MCM
$(\text{CH}_2=\text{CH})_m\text{MCl}_{n-m}$ (M = Ti, Cr, Sn)	
 <p style="text-align: center;">R = Et, Bu; M = Pt, Pd</p>	$\text{M}(\text{OOC}(\text{R})=\text{CH}_2)_n$ (R = H, Me; M = Ti, V, Zr, Sn, Co, Ni, Fe, Cr, Mn, etc.)
	$(\text{C}_5\text{H}_5)_2\text{M}(\text{OOC}(\text{R})=\text{CH}_2)_2$ (R = H, Me; M = Ti, V, Zr)
$\text{Et}_3\text{Sn}-\text{CH}=\text{CH}-\text{C}\equiv\text{CR}$ ; $\text{RC}\equiv\text{C}-\text{M}(\text{PBu}_3)_2-\text{C}\equiv\text{CR}$ (R = Ph, $-\text{C}\equiv\text{CR}$ , M = Pt, Pd, Ni)	 <p style="text-align: center;">M = Co, Ni, Fe, Mn, Cu</p>
$\text{M}(\text{OR})_{n-m}(\text{OR}')_m$ (R = Me, Et, Pr <sup>i</sup> , Bu; R' is alkenyl; R'' = H, Me; M = Ti, V, Zr, Sn, Co, Ni, Fe, Cr, Mn)	 <p style="text-align: center;">M = Zn, Mg, Fe, Cu</p>

**Table 5** (Continued)

$\sigma$ -MCM		Ionic type MCM	
$\pi$ - MCM		Cluster type MCM	
$R = H, Me; M = Fe, Os, Ru$		$R_6(CO)_{15}(4-VinPy)$	$R_6(CO)_{14}(4-VinPy)_2$
<b>Donor - acceptor (nv) type MCM</b>		<b>Chelate type MCM</b>	
$MX_n(CH_2=CH)_m$ 	$MX_n(CH_2=CH)_m$ 		
$M = Pt, Pd, Rh, Co, Ni$		$M = Ti, Co, Ru, Os, Zn, Cu, Ni$	$M = Eu, Cu, Ni, NO, Co, Mn, Fe$
$MX_n(CH_2=C(R))_m$ 	$MX_n(CH_2=C(R))_m$ 		
$MX_n(CH_2=C(R))_m$ 			
$R = H, Me; M = Ti, V, Co, Ni, Cu, Zn, Sn, Mn, Fe, Cr, Y, Ba$			

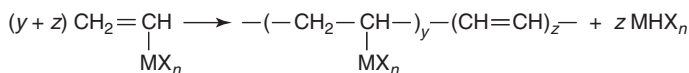
with a structure and geometry different from those of the main unit. As a consequence, the chemical and structural homogeneity of the macromolecular chain is disturbed (defective); thus real molecules cannot actually be represented as sequences of identical repeating units because diverse anomalous types of addition (i.e., unit variability, should also be taken into account). These problems are fairly important for the elucidation of the relationship between the composition, structure, and properties of the products formed upon MCM copolymerization. They often determine or restrict the particular applications of these polymers.

Metal-containing polymers can contain two types of abnormal units. For example, there are those that are characteristic of traditionally high-molecular-weight compounds, which cause violation of stereoregularity, residual multiple bonds, crosslinking and cyclization during polymerization and those that are specific. The latter includes partial elimination of metal-containing groups and the disturbance of the electronic structure of the units (e.g., changes in the valence state and nuclearity of the metal ion, the ligand environment, the shape of metal complex polyhedron particularly for polyvalent transition metals, the distribution of metal-containing groups along the polymer chain, and extra coordination during the formation of metal-containing polymers). In some cases, these factors are fundamentally important.

Since no systematic classification of the types of unit variability in the materials in question can be found in the literature, we shall analyze the general state of the problem and emphasize those aspects that present not only theoretical but also practical interest.

### A. Unit Variability Due to Elimination of a Metal-Containing Group During Polymerization

The unit variability caused by elimination by a metal-containing group during polymerization is one of the most important types of structural defects in metallopolymeric chains. Attempts to polymerize many MCMs have failed due to the elimination of a metal hydride and the formation of polymers devoid of the metal (scheme 13).<sup>70</sup> As a rule, introduction of a vinyl group into the ligand environment of a metal complex decreases its reactivity, apparently due to conjugation with the metal d-electrons. In the case of MCMs with other types of polymerizable groups (styryl, allyl, methacrylate, etc.), the probability of these processes occurring is low.



Scheme 13

Chemical transformations of MCMs in aqueous and polar solvents are accompanied by ionization and dissociation. This also can result in the formation of products devoid of the metal. The degree of dissociation depends both on the nature of solvent and the temperature (Fig. 9). This is especially so in the case of transition metal carboxylates, which are strong electrolytes in water. In aqueous or water-organic media at pH > 7, salts of unsaturated carboxylic acids are almost completely dissociated (the molar electrical conductivity at infinite dilution,  $\lambda_0$ , is 146–154 cm Ohm<sup>-1</sup> mol<sup>-1</sup>); hence instead of MCMs, other species such as acrylate and methacrylate ions (specially, metal acrylates and methacrylates) act as monomers.<sup>71</sup> Similarly, in the acrylonitrile-sodium prop-2-enesulfonate system, which undergoes copolymerization in DMSO–H<sub>2</sub>O mixtures at various pH values (at 45°C with AIBN as the initiator), the relative reactivities of the comonomers change in different media due to the increase in the solvation capacity of water. Actually, copolymerization in these systems involves three types of monomers: CH<sub>2</sub>=CH–CH<sub>2</sub>SO<sub>3</sub>…Na

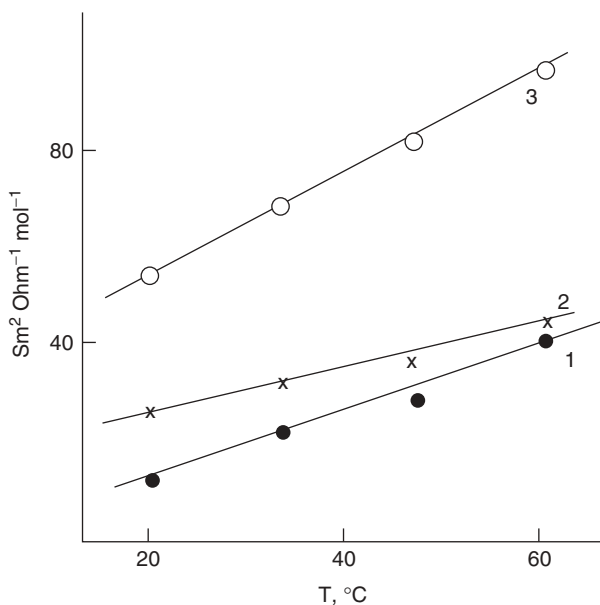


**Figure 9** The influence of temperature on the electroconductivity of nickel acrylate in (1) DMF, (2) ethanol, and (3) in water. The concentration =  $6.7 \cdot 10^{-5} \text{ mol L}^{-1}$ .

(in DMSO),  $\text{CH}_2=\text{CH}-\text{CH}_2\text{SO}_3^-$  (in aqueous DMSO), and  $\text{CH}_2=\text{CHCH}_2\text{SO}_3\text{H}$  (in DMSO at pH = 1.5).

Aqueous solutions of  $\text{Cu}^{2+}$ ,  $\text{Co}^{2+}$  and  $\text{Ni}^{2+}$  acrylates are medium-strength electrolytes; a plot of the molar electrical conductivity vs. concentration is described satisfactorily by the Kohlrausch equation.<sup>72</sup> For 0.05 M aqueous solutions of calcium acrylate (Acr) and methacrylate<sup>73</sup> at 25°C, the specific electrical conductivities,  $K$ , are  $5.16 \times 10^{-5}$  and  $2.787 \times 10^{-5} \text{ Ohm}^{-1} \text{ mol}^{-1}$ , and the degrees of dissociation,  $\alpha$ , are 0.46 and 0.2, respectively. The degrees of dissociation of Zn, Pb, and Ba acrylates ( $\text{M}(\text{Acr})_2$ ) in methanol are sufficient for the  $\text{M}(\text{Acr})^+$  cations that are formed to react with radical initiators (e.g., alkylcobalt chelates with tridentate Schiff bases) to give alkyl free radicals, which induce<sup>74</sup> radical polymerization of MCM even at low temperatures (5–10°C). For other types of MCM (*mv*-,  $\pi$ -types, see above), metal elimination processes are less typical; and in some cases (i.e., chelate type), these processes do not occur at all.

Thermal polymerization of MCM\* is also often accompanied by the elimination of metal-containing groups. Thus, in the case of copper acrylate,<sup>75</sup> the relatively weak Cu–O bond cleaves to give the  $\text{CH}_2=\text{CH}-\text{COO}'$  radical, whose interaction

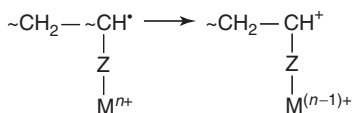
\*Thermal polymerization of MCMs (with transition metal acrylates as examples) is of interest in at least two aspects.<sup>75</sup> First, the structure of these salts contains many dislocations, that facilitate solid-state polymerization. Second, thermal decomposition and polymerization transformations are the stages for a potential method of the synthesis of polymer-immobilized, highly dispersed nanosize metal particles.

with the matrix can serve as a channel leading to the formation of units containing no metal. At 190–240°C, thermal decomposition is accompanied by polymerization in the solid phase. The polymers can incorporate metal-containing fragments formed on elimination of either CO<sub>2</sub> or Cu(COO)<sub>2</sub> group, depending on the temperature of the solid-phase recombination-polymerization process.<sup>76</sup>

It is significant that dissolution of the metal polymers that are obtained can also be accompanied by dissociation, particularly in polar solvents. Thus, in aqueous solutions at pH ≥ 7, alkaline and alkaline earth metal polyacrylates dissociate almost entirely, although dissociation can be suppressed by adding nonpolymerizable salt such as 0.15 M KCl. This is often accompanied by decomposition of the polymer to give products with lower molecular weight that contain no metal.

## B. Unit Variability Due to Different Valence States of the Transition Metal Ions

Different valence states are also a fairly widespread type of unit variability. By analogy with macromolecular complexes (Section II), it may be expected that homopolymerization and copolymerization of metal-containing monomers would prevent or retard redox processes involving participation of metal ions. Experimental data confirm the fact that a polymeric matrix stabilizes complexes of metals in low oxidation states (e.g., Pd<sup>+</sup>).<sup>77</sup> Moreover, the stability of the Cu<sup>+</sup> state during polymerization (including thermal polymerization) of copper acrylate controls the use of this method for the preparation of coordination compounds of Cu<sup>+</sup>.<sup>78</sup> The polymeric framework plays a stabilizing role, whereas the metal ions that are localized on the surface layer are oxidized<sup>79</sup> to Cu<sup>2+</sup>. However, polymerization of monomers that contain metal ions in high oxidation states is often accompanied by their reduction: V<sup>5+</sup> → V<sup>4+</sup> → V<sup>3+</sup>, Fe<sup>3+</sup> → Fe<sup>2+</sup>, and Mo<sup>5+</sup> → Mo<sup>4+</sup> (scheme 14). For example, polymerization of Cu<sup>2+</sup> and Fe<sup>3+</sup> acrylates may be accompanied by intramolecular chain termination.<sup>80</sup> This may be attributed to the relatively low standard reduction potentials of these metal ions ( $E_0(\text{Cu}^{2+} \rightarrow \text{Cu}^+) = 0.15$ ,  $E_0(\text{Fe}^{3+} \rightarrow \text{Fe}^{2+}) = 0.77$  V).



Scheme 14

In systems of this type, electron transfer occurs via a complex route and is accompanied by reduction of M<sup>n+</sup> to M<sup>(n-1)+</sup>. Monomolecular chain termination resulting in reduction has also been observed during graft postpolymerization of acrylate and acrylamide copper complexes<sup>81,82</sup> to λ-irradiated polyethylene (PE).\*

\*However, no reduction of Cu<sup>2+</sup> to Cu<sup>+</sup> was observed<sup>83</sup> during γ-initiated (beam-induced) copolymerization of copper bis-2-acetoacetoxyethyl methacrylate with various comonomers.

It is assumed that the set of eigen states of a dimeric copper dimethacrylate structural fragment allow delocalization of the excited  $\pi$ -electron of the C=C bond to the  $\text{COO}^-$  group during the initiation of graft post-polymerization.<sup>79</sup> This is accompanied by the reduction of copper and partial dissociation of the monomer (scheme 15).



**Scheme 15**

An estimate of the proportions of different valence forms of copper in copper polyacrylates shows that the  $\text{Cu}^{2+}$  content does not exceed 60%, and  $\text{Cu}^0$  is absent.<sup>84</sup> Most probably, autocatalytic  $\text{Cu}^{2+} \rightarrow \text{Cu}^+$  reduction occurs. The role of the ligand and their subsequent transformations during the reduction reaction are not entirely clear, although some of the possible routes will be analyzed below. It stands to reason that the geometry of complexes also changes on reduction of metal ions. For example, square-planar  $\text{Cu}^{2+}$  complexes add an additional ligand and are converted into square-pyramidal complexes, whereas  $\text{Cu}^+$  complexes are normally tetrahedral.

It has been suggested that the chemical reaction that accompanies electron transfer in the electrochemical polymerization of copper methacryloylacetate,  $\text{Cu}(\text{MAA})_2$ , involves replacement of the anionic  $\text{MAA}^-$  ligand by solvent molecules ( $\text{CH}_3\text{CN}$ ) and affords the neutral complex,  $(\text{MMA})^-\text{Cu}^+(\text{CH}_3\text{CN})_2$ , which is oxidized at  $E = -0.22 \text{ V}$ .<sup>85</sup>

Reduction processes also occur quite often in the synthesis of the corresponding monomers. This should be taken into account if the aim is to prepare a structurally homogeneous product. Thus in the aqueous  $\text{Fe}(\text{OH})_3$ -maleic acid system a mixture of  $\text{Fe}^{3+}$  maleinate and  $\text{Fe}^{2+}$  hydrogen maleinate is formed instead of the expected  $\text{Fe}^{3+}$  maleinate. According to the Mössbauer spectroscopy, the ratio of the  $\text{Fe}^{3+}$  to  $\text{Fe}^{2+}$  products is 9:1.<sup>86</sup> Dissolution of finely dispersed metallic Fe powder in an aqueous solution of maleic acid under inert atmosphere gave only  $\text{Fe}^{2+}$  hydrogen maleinate. It should be noted that special methods for the synthesis of monomers containing transition metal ions in low oxidation states ( $\text{Fe}^{2+}$ ,  $\text{Cu}^+$ ,  $\text{Cr}^{2+}$ ,  $\text{V}^{3+}$ , etc.) have been developed in our laboratories.<sup>78</sup>

The tendency of vanadium in high oxidation states to undergo reduction is well known and is due to the metal's low redox potential. Apparently, this process is accelerated in the presence of radical species ( $\text{I}^\cdot$ ); therefore, initiation of polymerization with elimination of alkoxy radicals occurs in parallel with the reduction of vanadium in mixed orthovanadates (scheme 16).<sup>87</sup>



**Scheme 16**

Elimination of a polymerizable fragment and its incorporation in the polymeric chain (viz., in situ copolymerization with the monomer and ligand)<sup>87</sup> can also lead to unit variability. In addition, radical fragments can initiate polymerization, recombine, and abstract a hydrogen atom from coordinated ligand.

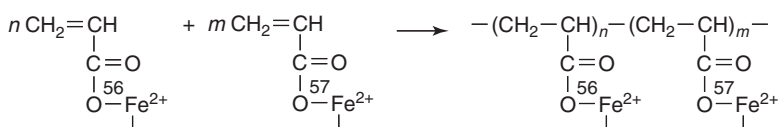
ESR studies of the transformation products of mixed ligand orthovanadates that contain a polymerizable group has shown that diamagnetic  $V^{5+}$  is partially reduced to paramagnetic  $V^{4+}$  during polymerization.<sup>88</sup> Although it is difficult to strictly characterize these processes, rough estimates of the  $V^{4+}$  content in the resulting homopolymers give a value of  $\sim 1$  mol% of the total vanadium. In copolymers with styrene, the value is much higher and reaches 14–16 mol%. In copolymers with acrylonitrile the value is even higher; 35–44 mol%. ESR and polarographic studies<sup>89</sup> of the thermolysis products of model  $Ti^{4+}$  complexes in the presence of a radical polymerization initiator (AIBN) show that  $Ti^{4+}$  is reduced to  $Ti^{3+}$  ( $\sim 5\%$ ). The reasons for this are, as yet, obscure.

Oxidation of a metal during polymerization is relatively rare. A typical example is vinylferrocene.<sup>63</sup> The ferrocenium cation, which is generated on the transfer of an electron from the Fe atom to the terminal radical, rearranges to give a high-spin  $Fe^{3+} 3d^5$  complex. This process is facilitated by the ferrocene conjugation. Evidently, the polymerization features of this MCM is unique, since effects of this type have not been observed for other  $\pi$ -type MCMs. At the same time, polymerization of praseodymium(III) maleinate induced by  $H_2O_2$  deserves attention. The reaction is accompanied by partial oxidation of  $Pr^{3+} \rightarrow Pr^{4+}$ ; and, a complex of the resulting ion catalyzes polymerisation.<sup>90</sup> An oxidative method has also been used in the synthesis of triphenylantimony and triphenylbismuth diacrylates.<sup>91</sup> In the presence of *t*-butyl peroxide or hydrogen peroxide and acrylic acid,  $Ph_3M$  is oxidized to  $M^{5+}$ .

In summary, knowing the character of redox processes in systems with metal-containing monomers enables polymerization. At a minimum, one can predict these processes and take them into account.

### C. Unit Variability Due to the Presence of Stable Metal Isotopes

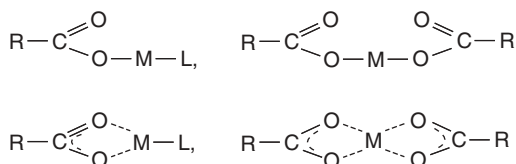
Unit variability as a result of stable metal isotopes is fairly well known for traditional polymers. It is associated and caused by stable isotopes of the polymer-forming elements ( $^{13}C$ ,  $^2H$ ,  $^{18}O$ ,  $^{15}N$  etc.). In some cases, certain metals isotopes are enriched during MCM synthesis. For example, enrichment in  $^{57}Fe$  is used for  $\gamma$ -resonance studies of the polymerization products of  $Fe^{2+}$  acrylates (scheme 17).<sup>87</sup> In other cases, stable isotopes of tin and vanadium, were used.



Scheme 17

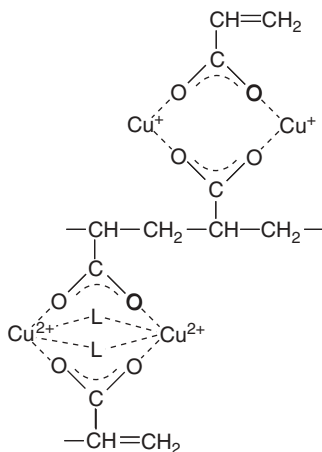
### D. Anomalies in Metallopolymeric Chains Caused by the Diversity of Chemical Binding of a Metal to Polymerizable Ligands

Unit variability as a result of the diversity of chemical binding of a metal to polymerizable ligands can be demonstrated most clearly by considering metal salts of unsaturated carboxylic acids. The polydentate properties of the carboxylate group,  $\text{RCOO}^-$ , are well known.<sup>92</sup> Monodentate and bidentate types of metal binding are typical (scheme 18). Nevertheless, carboxylates can also act as tridentate or tetradentate ligands in reactions with  $\text{M}^{2+}$ , even when multiple bonds do not participate in complexation.



Scheme 18

The metal–ligand bonds in metal acrylates were found to be mostly ionic with a degree of covalence of 0.13–0.16.<sup>93</sup> It is interesting that, going from acrylates to their saturated analogs, acetates, the metal–ligand bonds become longer and less covalent. During the syntheses of metal acrylates and methacrylates, for example, the  $\text{Cu}^{2+}$  salts, molecules of the initial acid, and solvating solvents (alcohols, acetone, DMF etc.) may also be included in the complex (e.g.,  $\text{Cu}_2(\text{CH}_2\text{CHCOO})_4 \cdot 2\text{CH}_2\text{CHCOOH}$  or  $\text{Cu}_2(\text{CH}_2\text{C}(\text{Me})\text{COO})_4 \cdot 3\text{CH}_2\text{C}(\text{Me})\text{COOH}$ ). When these components are removed, the MCMs are converted into chain-coordination polymers  $[\text{Cu}_2(\text{CH}_2\text{C}(\text{Me})\text{COO})_4]_n$  consisting of dimeric repeating units, some of which can contain these ligands (scheme 19).



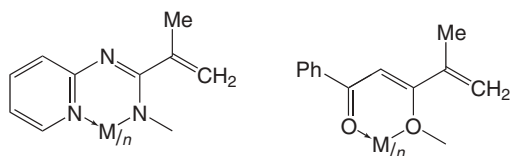
Scheme 19

The situation becomes even more complicated in the case of unsaturated dicarboxylic acids, which are tetradentate ligands that are capable of forming both neutral (e.g., cobalt maleinate  $\text{CoC}_4\text{H}_2\text{O} \cdot n\text{H}_2\text{O}$ ), and acidic (e.g., cobalt fumarate,  $\text{Co}(\text{OCOCH}=\text{CHCOOH})_2$ ) salts. Acidic salts are normally monomeric, while neutral salts are normally chain or three-dimensional (3D) coordination polymers in which the multiple bond does not participate in coordination.<sup>94</sup> The IR spectra of these materials suggest that the bridging structure of the carboxylate groups is retained on polymerization at least, on polymerization of copper diacrylate.<sup>84</sup> For example, the  $\nu_{\text{as}}(\text{COO}^-)$  and  $\nu_{\text{s}}(\text{COO}^-)$  absorption bands, which appear at 1575 and 1440  $\text{cm}^{-1}$  in the initial complex, are shifted to 1550 and 1410  $\text{cm}^{-1}$  in the spectrum of the polymerization product, while the difference in their frequencies—( $\nu_{\text{as}}(\text{COO}^-) - \nu_{\text{s}}(\text{COO}^-) \approx 130 \text{ cm}^{-1}$ ), which is typical of bridging  $\text{COO}^-$  groups—remains virtually unchanged.

In polymers (particularly in network polymers based on metal diacrylates),<sup>79</sup> the geometry of the bridging groups is distorted due to the presence of internal strain. Polymerization of the polynuclear  $\text{Cr}_3\text{O}$  monomer is accompanied most likely by the formation of monodentate carboxylate groups upon destruction of the bridging bonds.<sup>95</sup> The IR frequencies correspond to bridging and nonbridging bidentate carboxylate groups do not tend to merge.<sup>96</sup>

In the case of thermal polymerization, the number of modes of metal binding to carboxylate groups usually increases sharply, because of recombination polymerization processes. Both the monomer itself ( $\text{Cu}^{2+}$  diacrylate)<sup>76</sup> and the transient polymer can undergo thermolysis. At higher temperatures, the role of the latter route increases—that is, terminal metal carboxylate groups are much more susceptible to decarboxylation than the internal groups.

The situation is more complex in those cases in which the polymerizing ligand contains several metal binding sites. Thus, in metal chelates based on *N*-(2-pyridyl)-methacrylamide, the metal is coordinated to oxygen of the carbonyl group and nitrogen of the heterocycle (scheme 20).<sup>97</sup>



Scheme 20

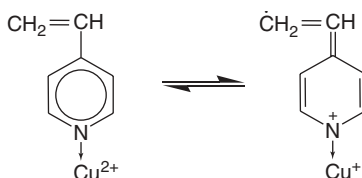
It follows from analysis of the Rack parameter and the degree of covalence (0.375) that the bond in these complexes is largely covalent, suggesting a substantial shielding of the d-shell from the nucleus and a decreasing effective positive charge on the metal. This is also true for metal chelates based on methacryloylacetophenone.<sup>98</sup> The electronic spectra of macrochelates such as transition metal polymethacryloylacetates, attests to some decrease in the orbital contribution to the metal–ligand bond in the polymer relative to that in the monomer.<sup>99</sup>

The potential unit variability of this type can also be manifested in metal–poly(acrylamide) complexes. Since it is impossible to obtain a single crystal of this polymer, the polymer structure is roughly modeled by the monomer structure. Acrylamide (AAM) can form complexes through both the oxygen and the nitrogen atoms. The complex  $\text{Co}(\text{NO}_3)_2 \cdot 4\text{AAM} \cdot 2\text{H}_2\text{O}$  was studied by x-ray diffraction analysis, which showed that the octahedral complex cations,  $[\text{Co}(\text{AAM})_4(\text{H}_2\text{O})_2]^{2+}$ , and the  $\text{NO}_3^-$  anions are joined by a 3D system of hydrogen bonds.<sup>100</sup> The octahedral environment of  $\text{Co}^{2+}$  is formed by the oxygen atoms of four AAM and two water molecules. Thus, in these MCMs, AAM is coordinated through the O atoms of the amide groups. The scatter of the Co–O distances from 2.065 to 2.114 Å reflects nonequivalence of the ligands. It is important, at least for subsequent polymerization transformations, that cations containing longer double bonds be arranged in a chain along a particular axis. Evidently, the double bonds are most reactive under the appropriate conditions. This assumption is also confirmed by thermally initiated frontal polymerization of acrylamide complexes of transition metals.<sup>101,102</sup> The cobalt environment apparently consists of only O atoms, because Co complexes that contain nitrogen atoms in the inner coordination sphere are typically tetrahedral ( $T_d$ ). The  $T_d$  symmetry is readily identified by the electronic absorption spectra, which is specific for octahedral chromophores. The d–d transitions observed in cobalt acrylate have low intensity.<sup>103</sup> This indicates an octahedral structure if allowance is made for the selection rules. Naturally, complexes with other metals and polymers based on them can have a different structure.

A frequently encountered type of structural anomaly in polymers, which may be predetermined at the stage of their synthesis, is artificial unit variability (i.e., different arrangements of the multiple bonds in the ligand molecules).<sup>63</sup> This type of unit variability is observed, for example, in vinyl-substituted heterocycles, such as isomeric vinylpyridines (ViPy), vinylimidazoles, and vinyltetrazoles. Since the degree of activation of an exocyclic C=C bond depends on its position in the ring, the rate of polymerization of zinc complexes of vinylpyridines decreases in the series 4-ViPy > 2-ViPy > 2-methyl-5-ViPy. This reflects the overall influence of many factors, including the steric accessibility of the double bond. Moreover, the results can be different even for similar ligands. For example,  $\text{M}(4\text{-ViPy})_4\text{X}_2$  and  $\text{M}(2\text{-ViPy})_4\text{X}_2$  complexes ( $\text{M}=\text{Co}^{2+}$ ,  $\text{Ni}^{2+}$ ,  $\text{X}=\text{Cl}^-$ ) are octahedral, whereas  $\text{Co}(4\text{-ViPy})_2\text{Cl}_2$  and  $\text{Co}(2\text{-ViPy})_2\text{Cl}_2$  exist either in the blue tetrahedral ( $\alpha$ ) form or in the pink octahedral ( $\beta$ ) form.\* These forms differ in the distance between the C=C bonds, which is 4.47 Å in the  $\alpha$ -form and 3.65 Å in the  $\beta$ -form. This difference has a substantial effect on the ability of these MCMs to polymerize; only crystals of the tetrahedral  $\alpha$ - $\text{Co}(4\text{-ViPy})_2\text{Cl}_2$  undergo thermal polymerization on heating in air or under nitrogen at 103–130°C, whereas the highly dense octahedral modification does not polymerize in the solid phase regardless of initiation. Nevertheless, polymers based on  $\text{Co}(2\text{-ViPy})_2\text{Cl}_2$  were obtained, but they were block copolymers formed by complexes with a smaller metal coordination number. In addition, they released ligands—that is, the

\*Note that the magnetic moments of octahedral and tetrahedral  $\text{Ni}^{2+}$  and  $\text{Co}^{2+}$  are significantly different: the  $\mu_{\text{eff}}$  values, equal to 3.15 and 4.52  $\mu_{\text{B}}$ , respectively, point to the high-spin state of these ions in the octahedral ligand fields.

unit variability was caused by ligand elimination in situ. Another example of this type is the polymerization of ViPy in methanol–pyridine media initiated by the complex  $(4\text{-ViPy})_2\text{Cu}(\text{OCOCH}_3)_2$ . Initiation was effected by the transfer of an electron from the monomer to the copper ion in the complex (scheme 21).



Scheme 21

The principal difference between this mechanism and the repeatedly mentioned redox process with participation of  $\text{Cu}^{2+}$  is that the electron transfer involves a  $\pi$ -electron of the double bond rather than the free radical electron. This accounts for the opening of the double bond as an extreme case of activation. Reactivation of the initiator is attained by oxidation of  $\text{Cu}^+$  to  $\text{Cu}^{2+}$  in air, because the end units contain  $\text{Cu}^+$ , which is also a source of unit variability.

As noted above, the coordination number of the metal can change during polymerization of MCM due to abstraction of some of the ligands. This can result not only in mixed-unit chains but also in a changed rate of polymerization. This process is difficult to follow; however, some examples have been documented in the literature.<sup>104,105</sup> Thus the rate of homopolymerization of vinylimidazole (VIA) complexes depends on the coordination number of the metal, which is determined by the number of attached VIA molecules (i.e.,  $\text{Mn}(\text{VIA})_4\text{Cl}_2 > \text{Mn}(\text{VIA})_2\text{Cl}_2 > \text{VIA}$ ).

### E. Unit Variability Due to Qualitatively and Quantitatively Different Ligand Environments of the Metal

Unit variability due to different ligand environments about the metal is a relatively widely distributed type of anomaly. For example, it was found by IR and  $^1\text{H-NMR}$  spectroscopy<sup>106</sup> that the equilibrium shown in scheme 22 occurs in a  $\text{Ti}(\text{OBu})_4$ -unsaturated alcohol system. In that scheme  $\text{R}'\text{OH}$  is the monomethacrylate of ethylene glycol (2-hydroxyethyl methacrylate, MEG), furfuryl alcohol, propargyl alcohol, and 2-methylhex-5-en-3-yn-2-ol ( $\text{CH}_2=\text{CHC}\equiv\text{CC}(\text{Me})_2\text{OH}$ ). The  $\text{Ti-O-Bu}$  bond in  $\text{Ti}^{4+}$  alkoxides is rather labile, which is confirmed by fast radical exchange as measured on the NMR time scale.



Scheme 22

Polymerization of some MCMs of this type can be accompanied by the formation of mixed-unit chains as a result of disproportionation during the process. This is particularly typical for vanadium-containing monomers. Thus all three isopropoxy

radicals in isopropyl orthovanadate ( $\text{VO}(\text{OPr}^i)_3$ ) can be substituted successively during the reaction with MEG to give polymerizable the vanadium-containing monomers,  $\text{VO}(\text{OPr}^i)_{3-n}(\text{OR}')_n$ .<sup>88</sup> On the one hand, the potential of these reactions imposes rigid restrictions on the stoichiometry of the initial compounds during their synthesis and on the conditions of the synthesis. On the other hand, when conducting polymerization of these monomers, unit variability in the polymer chains that is caused by different ligand environments of the metal should be taken into account. Some unsaturated alcohols (e.g.,  $\text{CH}_2=\text{CHC}\equiv\text{CC}(\text{Me})_2\text{OH}$ ) form vanadium-containing monomers that are susceptible to disproportionation (scheme 23).

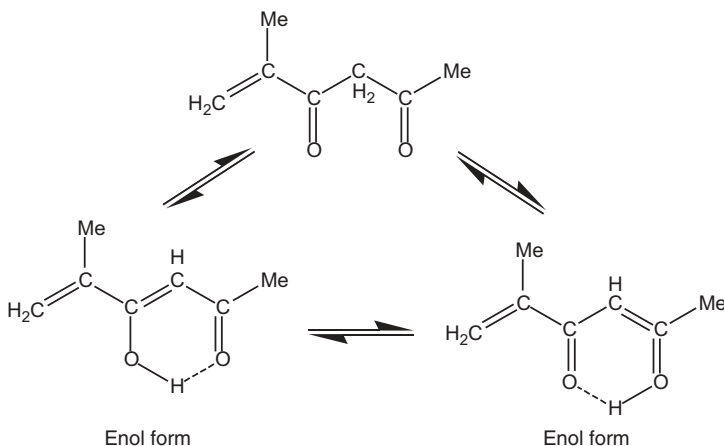


Scheme 23

Therefore, monomers of this type and their corresponding, polymers, with the exception of a few specific alcohols, are mixtures of related vanadium-containing complexes. Of the monomers of this class, compounds with identical ligands such as  $\text{VO}(\text{OR}^i)_3$  are the most stable since there appears to be no possibility for disproportionation.

Mention should be made of the type of unit variability caused by the fact that many MCMs (particularly organometallic species) are susceptible to hydrolysis in the presence of even traces of  $\text{H}_2\text{O}$ . Moreover, they may also react with traces of  $\text{O}_2$ . In other cases, the resulting compounds are able to polymerize, which violates the structural homogeneity in the polymers. For example, hydrolysis of acetone solutions of copper(II) acrylate<sup>107</sup> and methacrylate<sup>108</sup> has been reported.

Even more complicated processes occur in the case of ligands that isomerize during the formation and polymerization of MCMs. For example, methacryloylacetone (5-methylhex-5-ene-2,4-dione), which is the initial monomer for the synthesis of dicarbonyl type chelates, is susceptible to keto-enol tautomerism (scheme 24).<sup>109</sup>



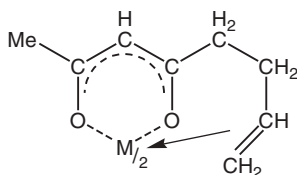
Scheme 24

The reaction of this ligand with, for example, copper ions, involves the enol form of methacryloylacetone (i.e., the ligand acts as an OH acid), whose fraction according to pH-titration data is quite large (~30% w/w). The formation of MCM by these ligands with doubly charged metal ions occurs in two steps and can generally be represented as in scheme 25.



Scheme 25

It is obvious that polymerization transformations of tautomers or monomers containing different numbers of ligands would result in the corresponding unit variability. The constants for successive addition ( $k_1$ ,  $k_2$ ) were used to calculate the stability constants and to optimize the synthesis of metal methacryloylacetones.<sup>109,110</sup> The greatest mole fraction of  $ML^{+}$  is observed at a pH of 5.4–5.8, and the formation of the neutral chelate  $ML_2$  is completed at a pH of 8. It is of interest that polymers prepared by the electrochemical method contain a higher fraction of keto-form units than those synthesized by conventional radical polymerization.<sup>85</sup> When the vinylic group of a ligand also participates in complexation, the number of possible types of anomalous units markedly increases. Thus, for oct-7-ene-2,4-dione, the possibility of tridentate coordination due to additional binding of the double bond has been shown (scheme 26).<sup>111</sup>



Scheme 26

The tridentate ligand occupies three adjacent vertices of the coordination polyhedron, and the stability of complexes differ markedly from that of bidentate coordination. As a rule,  $\pi$ -coordination inhibits, and often totally prevents, polymerization processes, although numerous  $\pi$ -complexes between comonomers were found to exist during copolymerization.<sup>112</sup>

Polymerization of MCMs can be accompanied by interaction of the monomer with an initiator (catalyst), which also results in the generation of anomalous units in the chains. These types of reactions have scarcely been studied. It is known, however, that alkoxy derivatives of many metals efficiently react with peroxide initiators.<sup>2</sup> Thus benzoyl peroxide (BP) readily reacts with alkyl titanates to give titanium acylates  $(BuO)_3Ti-O-Ti(OBu)_2OCOPh \cdot PhCOOBu$  and with allyltrimethyltin to give allyl benzoate and trimethyltin benzoate in quantitative yield. Therefore, BP

cannot induce polymerization of MCM of the  $(\text{BuO})_3\text{TiOCOC}(\text{Me})=\text{CH}_2$  type. However, the substrate does polymerize with AIBN; and at  $80^\circ\text{C}$ , the degree of conversion can reach 60% in 20–30 min. In general, other transformations of the ligand can also occur during polymerization. The most important of these is the oxidation of an acrylamide ligand, which is observed as exothermic effects observed during differential thermal analysis of an MCM that is based on metal nitrates.<sup>113</sup> The oxidation reaction is most likely initiated by the decomposition of the nitrate groups of the complexes. This effect is also typical for polymers.

## F. Extra-Coordination as a Spatial and Electronic Anomaly of the Polyhedron

The relatively low stability of some MCMs and polymers based on MCMs may be attributed to coordination unsaturation of the central metal, which facilitates a series of side processes. The coordination number of a metal can be increased complex formation;<sup>114</sup> for example, the structure of  $\text{Ni}^{2+}$ ,  $\text{Co}^{2+}$  and  $\text{Cr}^{3+}$  acrylates can be expanded to an octahedral geometry. Specifically introduced compounds like solvent molecules, (most often water) can act as the additional ligands. After polymerization, not all the addends chemically bonded to the metal are removed from the product. Thus they serve as a source of anomalous units in the polymers. Since the structure of coordination units in the metal-containing polymer is difficult to study due to a multiplicity of oxidation states, this type of unit variability is more convenient to examine in metal-containing monomers.

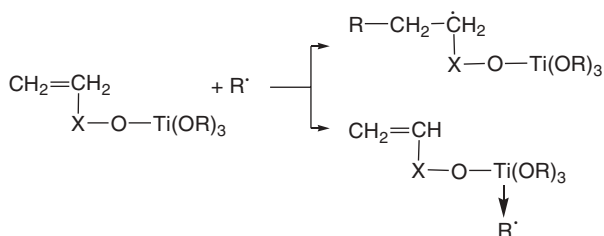
Many metal acrylates often contain water of crystallization.<sup>93</sup> The  $\text{M}\dots\text{OH}_2$  coordination bonds are generally the least stable; therefore, dehydration is usually the first step of thermal polymerization.<sup>115</sup> Chelates of the metals and *N*-(2-pyridyl)methacrylamide also tend to coordinate additional  $\text{H}_2\text{O}$  molecules to the axial positions to give octahedral structures.<sup>97</sup> Acrylamide complexes of metal nitrates (e.g.,  $\text{Mn}^{2+}$ ,  $\text{Co}^{2+}$ ,  $\text{Ni}^{2+}$  and  $\text{Zn}^{2+}$ ) contain water of crystallization.<sup>100</sup> All of these metals are high-spin octahedra. In the case of chelate compounds of Ni, Co, and Mn methacryloylacetates ( $\beta$ -diketonate type), additional axial coordination of  $\text{H}_2\text{O}$  molecules has been observed.<sup>116</sup> Thus the coordination unit is expanded to an octahedron. Unlike acetylacetates, which lose the water of crystallization in the  $70\text{--}100^\circ\text{C}$  range, methacryloylacetates are dehydrated at higher temperatures ( $110\text{--}160^\circ\text{C}$ );<sup>117</sup> however, this is accompanied by thermal polymerization of the corresponding MCMs. At even higher temperatures, partial decomposition and loss of the ligand molecules occur. The intermediate compound, which was considered above, retains the chelate structure. In metal-containing methacryloylacetates polymers, the  $\text{M}\text{--}\text{O}$  bond in the chelate unit is apparently weakened, resulting in a lower temperature for the onset of decomposition. As a rule, on going from a monomer to a polymer, the structure of the closest environment of the metal changes; for example,  $\text{Fe}^{3+}$  has a near-cubic local symmetry about the  $\text{Fe}\text{--}\text{O}$  bonds, which changes to a more asymmetric structure.<sup>118,119</sup> At the same time, the rate of spin-lattice relaxation of  $\text{Fe}^{3+}$  ions decreases.

It is significant that the use of an additional ligand can also influence the rate of polymerization of the MCM formed. For example, for postpolymerization of allyl alcohol into  $\gamma$ -irradiated PE, it was found<sup>120</sup> that, in the case of  $\text{CoCl}_2 \cdot 6\text{H}_2\text{O}$ , the rate of grafting is much lower than that in the presence of anhydrous  $\text{CoCl}_2$ . A study of the properties of the product formed by the spontaneous polymerization of concentrated aqueous solutions of acrylamide- $\text{Cr}(\text{NO}_3)_2 \cdot 9\text{H}_2\text{O}$  (at  $\sim 20^\circ\text{C}$ ) showed the formation of glassy polymers containing water.<sup>120</sup> The water of crystallization that evolved during polymerization either bonds to the polymer or forms microinclusions associated with the electrolyte solution within the bulk polymer. Perhaps this is one of the rare cases where the distribution of water in the polymer is exactly defined.

Of other solvents, alcohols such as ethanol are used most often for polymerization. Since the structure of nonsolvated  $\text{Cu}^{2+}$  acrylate is unknown, it may be expected that upon desolvation of its complex with ethanol, some of the bidentate carboxyl groups become tridentate (see above). Thus they can act simultaneously as a ligand and a solvation agent, which is absent. The increase in the dentate number of the  $\beta$ -diketonate groups leads<sup>75</sup> to a distortion of the oxygen environment about Cu; in particular, the Cu-O distances and, hence, the C-O bond lengths.

It should be noted that the spatial and electronic structure of MCMs can change on going from the solid state to solution. In the case of liquid-phase polymerization, the structural change is fixed in the polymer. Diverse dissociation processes that accompany dissolution can result in anomalous units in the chains of the polymers obtained by solution polymerization. Thus the cobalt chloride complex with AAm changes spatial structure in solution from a tetragonally distorted octahedron to a tetrahedron.<sup>121</sup> However, the coordination units of the  $\beta$ -diketonates were found to remain invariable on going from the crystalline state to chloroform solutions.<sup>116</sup> Similarly, complexes of nitrogen-containing vinyl heterocycles remain structurally invariable in the crystalline state and in methanolic and DMF solutions.<sup>122</sup> On the other hand, complexes of cobalt and nickel chlorides with these same ligands,  $\text{ML}_2\text{Cl}_2$ , are polymeric structures in which the metal ion lies in the plane of the chloride bridges and the ligands occupy the axial positions. When these MCMs are dissolved in methanol, the chloride bridges are cleaved and the arising coordination site vacancies are occupied by methanol molecules, which is a stronger high field ligand. DMF also disrupts the chloride chains and occupies some of the coordination sites that have been liberated (i.e., both six- and four-coordinate complexes are formed). Elucidation of the structural organization of metal-polymer complexes and identification of various types of polyhedra that result in unit variability in metal-containing polymer are puzzles that still need to be solved.

Additional coordination can also involve other components of the polymerizable system and can exert a substantial influence on the polymerization kinetics and the structures of the products formed. In particular, the formation of MCM complexes<sup>89</sup> with an initiator can both accelerate (generate the initiating species) and retard its decomposition and leads to a set of products that can be incorporated in the polymer as terminal groups. Thus the unusual kinetics (the order of the reaction with respect to the monomer is  $\sim 0.5$ ) of radical polymerization of  $\text{Ti}^{4+}$ -containing monomers are due to the occurrence of parallel reactions (scheme 27).<sup>123</sup>



Scheme 27

The  $\text{Ti}^{4+}$ -coordinated radicals thus formed can participate both mainly in chain termination and in chain growth. The metal ion acts as a sort of radical trap. The radical that is formed becomes passivated with respect to the initiation of new chains. These complexes can be relatively stable.\* As the first approximation, the situation is modeled by stable radicals (e.g., iminoxyl radicals). In fact, the initiating radical species in the reaction with the monomers of  $\eta^4$ -(hexatrienyl)tricarbonyliron<sup>125</sup> is accompanied by the formation of stable radicals, which are inefficient for chain initiation (scheme 28).



Scheme 28

Copolymerization of MCMs is even more complicated due to diverse complexation reactions between the monomers that participate in copolymerization. This accounts for both the unusual pattern of the monomer mixture composition–copolymer composition diagrams and the abnormal distribution of metal-containing sites along the chain. For example, in the  $\text{V}^{5+}$ -containing monomer–styrene system, the coordination interactions of the weak Lewis acid, MCMs with the electron donor, styrene yield mostly alternating copolymers.<sup>87</sup> The tendency for unit alternation in the product points to a complex radical mechanism of copolymerization.<sup>112</sup> In the ESR spectra of styrene copolymers with copper complexes of vinylporphyrins (see above), two types of signals for  $\text{Cu}^{2+}$  were detected,<sup>126</sup> and one of these signals apparently corresponds to an extracoordinated  $\text{Cu}^{2+}$  complex.

## G. Exchange Interactions between Metal Ions Incorporated in the Chain

Many properties of metal-containing polymers depend appreciably on the localized nature of the metal ions. This brings up the problem of describing the various

\*It is assumed<sup>124</sup> that the single-electron  $\text{Ti}^{\text{IV}} \rightarrow \text{R}'$  bond in the complex radical can prove to be fairly strong; its energy is estimated to be half that of the  $\sigma$ -Ti-C two-electron bond.



interchain interactions can appear. They are manifested as intense antiferromagnetic exchanges that are caused by conformational changes in the macrochains.<sup>130</sup> The structure of complexes, which are combined in clusters with antiferromagnetic interactions, is formed during the polymerization. It has been suggested<sup>131</sup> that the  $\text{Fe}^{3+}$  and  $\text{Zn}^{2+}$  ions in copolymers, which contain zinc and iron methacrylates in addition to unsubstituted methacrylic acid, undergo long-range interactions that are transferred along the polymer chain. This was explained by the relatively large inductive polarizability of the functional groups attached to  $\text{Fe}^{3+}$ . Formally, the presence of alternating and nonalternating units also results in metalopolymer unit variability, however, its influence on the properties of these polymers is currently difficult to elucidate.

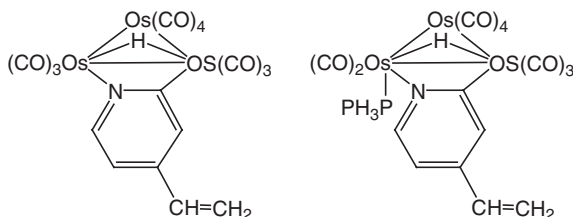
### H. Change in the Nuclearity of Metal Sites as a Type of Unit Variability

During MCM polymerization transformations in the solid phase or in solution, the nuclearity of the metal complexes can either increase or decrease. Under certain conditions, polynuclear, cluster, or even nanosize metal particles can be formed.<sup>132–134</sup> As mentioned above,<sup>93</sup> the binuclear structure of  $\text{Cu}^{2+}$  acrylate can be destroyed or retained during polymerization.

Monomers of the general formula  $[\text{M}_3\text{O}(\text{OCOCH}=\text{CH}_2)_6]\text{OH} \cdot 3\text{H}_2\text{O}$  ( $\text{M} = \text{Fe}^{3+}, \text{Cr}^{3+}$ ) are built as trinuclear clusters in which the metal atoms form a regular triangle with oxygen atom in the center, while the carboxy groups form bridges between the metal atoms.<sup>96</sup> It is not completely clear whether the  $\text{M}_3\text{O}$  clusters retain their individuality during polymerization when the spatial network of the polymer is formed. They can also decompose with the elimination of  $\text{H}_2\text{O}$  and  $\text{CH}_2=\text{CHCOO}$  groups. It is not certain in which particular step either occurs. However, it is known that after polymerization the structure of the local environment around the  $\text{M}^{3+}$  ion can both remain unchanged ( $\text{M} = \text{Cr}^{3+}$ ) and change substantially ( $\text{M} = \text{Fe}^{3+}$ ).<sup>110</sup> Moreover, the partial loss of the water of crystallization in the monomer decreases the coordination number of the iron ions—that is, the symmetry of their local environment decreases. This does not imply destruction of the cluster structure during polymerization, although the mass spectroscopy data lead to the conclusion that dissociation of the  $\text{M}-\text{O}$  bonds is energetically nonequivalent.<sup>95,96,118</sup> Thus polymers based on these monomers can contain several types of anomalous units: those caused by the change in nuclearity of the metal complex or its ligand environment and those due to the formation of branched polymers with retention of the  $\text{M}_3\text{O}$  framework during polymerization.

Similar structures can also be found in acrylates and methacrylates of other transition metals in high oxidation states and their polymers, such as zirconium methacrylate  $\text{Zr}_4[\text{OCOC}(\text{Me})=\text{CH}_2]_{10}\text{O}_2\text{X}_2 \cdot n\text{H}_2\text{O}$  ( $\text{X} = \text{HO}^-, \text{CH}_2=\text{C}(\text{Me})\text{COO}^-; n = 2, 4$ ).<sup>135,136</sup> Moreover, even acrylates of some transition metals in low oxidation states (e.g.,  $\text{V}^{3+}$ )<sup>78</sup> are formulated in the same way ( $\text{V}_3\text{O}$ ). This is also true for unsaturated dicarboxylic acids and their polymers.<sup>86,94</sup> Naturally, it becomes immeasurably more difficult to determine the detailed structure of these metalopolymers and

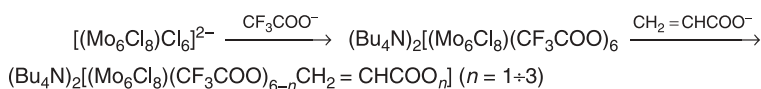
to take account of all the types of mixed units in them. The problem is somewhat simpler in the case of cluster-containing monomers that are obtained on interaction of ligands with individual clusters, which are capable of polymerization transformations. For example, the reaction of the carbonyl cluster  $\text{Rh}_6(\text{CO})_{16}$ -4-ViPy system in the presence of trimethylamine *N*-oxide under mild conditions affords the monosubstituted derivative  $\text{Rh}_6(\text{CO})_{15}$ (4-ViPy) as a major product and disubstituted compound,  $\text{Rh}_6(\text{CO})_{14}$ (4-ViPy)<sub>2</sub>, in a relatively low yield.<sup>137</sup> These two species can be isolated in a pure state by chromatography. The vinyl group in these MCMs lies in the plane of the pyridine fragment and does not interact with the rhodium cluster. In the case of  $\text{Rh}_4(\text{CO})_{12}$  and 4-ViPy, nonselective polysubstitution of the CO groups occurs and results in a number of products in relatively low yields. Thus the problem involved in the synthesis and subsequent polymerization of MCMs of this type is to introduce selectively specific ligands with retention of the noncoordinated double bond. Since the IR spectra in the region of vibrations of the cluster carbonyl groups provide a great deal of information, these spectra are used for elucidation of the nuclearity of metal-containing sites in polymers. Yet another specific feature—namely, the formation of a cluster with the orthometallated 4-ViPy ligand—was noted in a study of the triosmium carbonyl cluster.<sup>138,139</sup> In this case, the replacement of a CO group by  $\text{PPh}_3$  made it possible to prepare the phosphine derivative of the MCMs (scheme 30).



Scheme 30

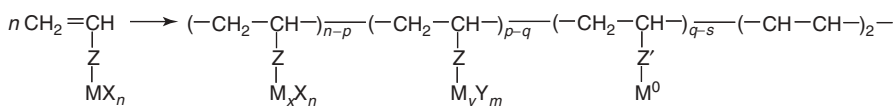
Heating  $(\mu\text{-H})\text{Os}_3(\mu\text{-OH})(\text{CO})_{10}$  with excess acrylic acid in benzene gives a new cluster complex with bridging bidentate coordination of the acid to two osmium atoms.<sup>138</sup> This complex is capable of polymerizing. Since the  $\text{Os}_3$  cage is highly stable during polymerization transformations, only anomalous units, which are caused by different ligand environments, can be detected in the products. The same is true for the product of the reaction of  $\text{Os}_3(\text{CO})_{12}$  with allylamine, which exists as two isomers of the complex  $(\mu\text{-H})\text{Os}_3(\mu\text{-O}=\text{CNHCH}_2\text{CH}=\text{CH}_2)(\text{CO})_{10}$  due to the hindered rotation around the C-N bond.<sup>138,140</sup> However, most often these reactions are accompanied by coordination of the double bond (e.g., as in tricobaltalkylidene complexes,  $\text{Co}_3(\mu_3\text{-CR})(\text{CO})_{9-x}(\text{PPh}_2\text{CH}=\text{CH}_2)_x$ , where  $x = 1, 2, 3$  are examples).<sup>141</sup> A similar product,  $\text{Rh}_6(\text{CO})_{14}(\mu\eta^2\text{-PPh}_2\text{CH}_2\text{CH}=\text{CH}_2)$ , was isolated on reaction of  $\text{Rh}_6(\text{CO})_{16}$  with allyldiphenylphosphine. In this case,  $\pi$ -coordination of the unsaturated ligand with the cluster core is also observed.<sup>142,143</sup>

Although homopolymerization of cluster-containing monomers occurs with difficulty (as a rule, low-molecular-weight oligomers are formed), their copolymerization with vinylic monomers occurs in high yields. Physicochemical studies show that Os<sub>3</sub>- and Ru<sub>3</sub>-containing monomers do not undergo substantial transformations that could complicate copolymerization with styrene or acrylonitrile and do not react with AIBN. However, when a cluster-containing monomer adds to a growing polymer chain with its structure remaining almost unchanged, chain growth is restricted.<sup>144</sup> Nevertheless, broadening of some bands in the IR spectra of copolymers (particularly, in the case of Rh<sub>6</sub>, can be interpreted as to the presence of anomalous units in the chain, which are formed on decarbonylation of some of the units and increase or decrease the nuclearity. The same phenomena were observed in the polymerization of molybdenum-containing cluster monomers such as depicted in scheme 31).<sup>145</sup> Detailed analysis of these types of processes and identification of the role of the cluster polymers in catalysis requires further research.



Scheme 31

Thus unit variability in metallopolymers can be represented in a simplified form by scheme 32, which takes into account the change in the metal valence state, ligand environment, nuclearity and the elimination of a metal-containing group.



*x* and *y* are the valences of the metal, *Y* and *Z'* are the products of transformation of *X* and *Z*.

Scheme 32

## I. Stereoregularity of Metallopolymeric Chains

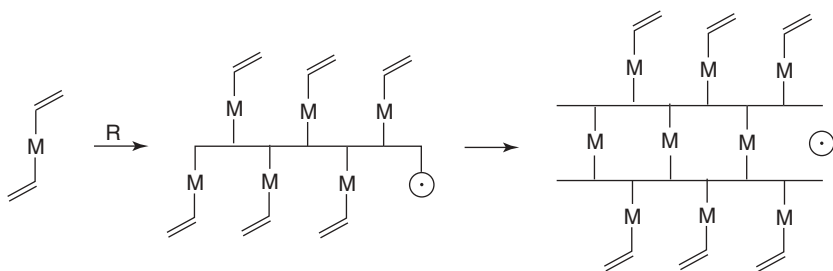
Unit variability as a result of the stereoregularity along the metallopolymeric chain, unlike those considered above, is frequently encountered in traditional polymers. Although the difference between the activation energies of iso- and syndio-addition during radical polymerization is small ( $<1 \text{ kcal mol}^{-1}$ ), in the case of MCM there exists prerequisites for the formation of stereoregular polymers. The prerequisites

are based, first of all, on the assumption that quadrupoles or ion pairs can affect the direction from which the monomer approaches the active center and the mechanism for opening the monomer's double bond (e.g., the orientation effect of the cation's coordination bond, and the electrostatic interaction between the ionized growing radical and the polar metal-containing group in MCMs). Thus, due to the presence of an ionized group in transition metal acrylates, the growing center changes its stereochemistry in each chain-lengthening event to that of the opposite stereochemistry. This should result in alternating configurations of the MCM units in the chain (i.e., in the formation of a syndiotactic polymer). Moreover, even small (to 2 mol%) amounts of transition metal acrylates added to the MMA–MAAc system during copolymerization not only influences the relative reactivity constants of the comonomers but also changes the microtacticity of the copolymers.<sup>146</sup>

It is of interest that the stereoregularity of metal-containing polymers changes markedly as a function of the MCM composition.<sup>2</sup> Thus polymerization of  $\text{Zn}(\text{MMA})_2\text{Cl}_2$  gives a polymer with a higher degree of syndiotacticity (60%) than polymerization of  $\text{Zn}(\text{MMA})\text{Cl}_2$  (48%), whereas in the case of  $\text{Sn}(\text{MMA})\text{Cl}_4$  and  $\text{Sn}(\text{MMA})_2\text{Cl}_4$ , the opposite relationship is observed (77% and 63%, respectively).

As for conventional monomers, a decrease in the polymerization temperature increases the content of the structurally ordered fraction in metal polyacrylates.<sup>74</sup> For a  $\text{Co}^{2+}$  salt, the syndiotactic fraction was 60% (i.e., polymerization of acrylic acid under the same conditions gives only 25–30%).<sup>147</sup> At low-temperatures (5–10°C) the radical polymerization of barium diacrylate gave 74% of the syndiotactic form and 80% for zinc diacrylate.<sup>74</sup>

The process of polymerization of bifunctional monomers (e.g., diacrylates) can be divided into two steps (scheme 33). The first step yields a linear comb-shaped polymer with a degree of stereoregularity that depends on the nature of the metal ion. The second step results in a spatial network polymer. In this step, chain growth involves predominantly the  $\text{C}=\text{C}$  sidechains of the macroradicals. Chain growth occurs under conditions of severe steric hindrance and with an increasing level of internal (shrinkage) stresses and results in the formation of an atactic structure.



Scheme 33

**Table 6** Degree of Stereoregularity of PAA Isolated from Different Metal Polyacrylates

<i>Original Polymer</i>	Yield of Fraction (%)	
	Soluble in Dioxane (atactic)	Soluble in Aqueous Dioxane (syndiotactic)
Zn polyacrylate <sup>a</sup>	20	80
Zn polyacrylate <sup>b</sup>	58	42
Polyacrylate acid <sup>b</sup>	59	41
Ba polyacrylate <sup>b</sup>	26	74

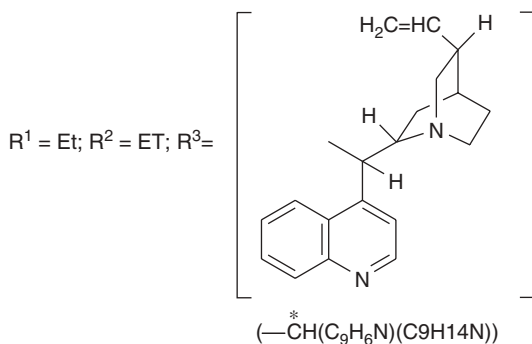
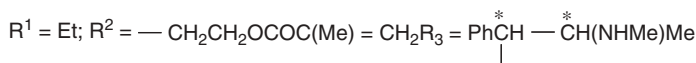
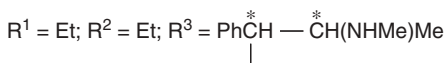
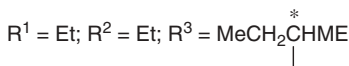
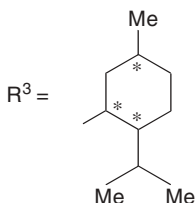
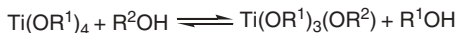
<sup>a</sup>Polymerization at 9°C.<sup>b</sup>Polymerization at 70°C.

Until recently not much attention has been paid to stereoregulated unit variability in the “daughter” chains, which are formed during matrix polymerization of MCMs. This is due to the parent polymeric chain (the matrix) bringing about structural and chemical control of the growth of the daughter chains formed from the MCM molecules adsorbed on the matrix. The orientation and nonvalence interactions in the MCMs adsorbed by the matrix units cause stereoregulation in the daughter chain growth events. The mechanism of the structural matrix effect was recently studied in relation to the polymerization of sodium acrylate<sup>148</sup> and sodium methacrylate<sup>149</sup> on poly(allylamine hydrochloride). The ideal route of matrix polymerization follows the “zipper” mechanism—that is, each growing chain propagates along a single matrix chain. This is the case at low degrees of conversion but deviations resulting in a peculiar unit variability appears during more extensive polymerization. The growing radical, which reaches the end of the matrix chain, can capture a monomer from the bulk or react with a monomer adsorbed on another chain. As a consequence, a network structure is formed. Moreover, a decrease in temperature is expected to increase the percentage of the structurally ordered fraction in the macromolecules (Table 6).

## J. Unit Variability Due to Chirality in Pendant Groups

Unit variability that results from pendant group optical chirality has scarcely been studied, although the presence of these units in metal polymer chains is important in, for example, asymmetric catalysis.<sup>150</sup> The first study along these lines was the synthesis of an optically active metal-containing monomer, a palladium complex with R- and S-1-(4-vinylphenyl)ethylamine,  $\text{PdCl}_2(\text{CH}_2=\text{CHC}_6\text{H}_4\text{CH}(\text{NH}_2)\text{CH}_3)_2$ .<sup>77</sup> Copolymers of these MCMs with styrene and divinylbenzene were chiral catalysts for the reduction of acetamidocinnamic acid azlactone and the products of its solvolysis. At least one more variant of this type of unit variability exists, which is caused by different ligand environments of the metal. This variant can be attained by introducing,

for example, an alcoholic group, which contain an asymmetric carbon atom within the ligand environment of the MCM (scheme 34).<sup>151,152</sup>



**Scheme 34**

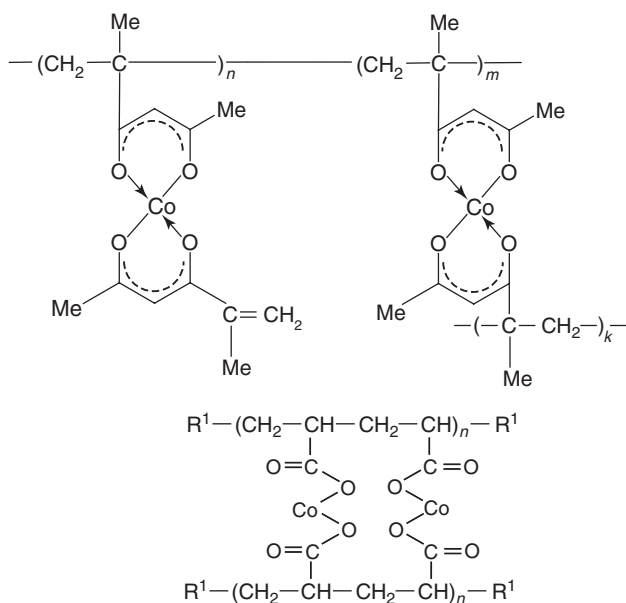
In this case, the difficulties associated with the transesterification of alkoxy derivatives of  $\text{Ti}^{4+}$  or  $\text{V}^{5+}$ , even in binary systems, have already been noted. In ternary systems, these difficulties grow immeasurably; however, in some cases, individual compounds still can be synthesized and characterized, such as the mixed

compounds in which  $R' = -CH_2CH_2OOC(CH_3)=CH_2$  and  $R^* =$  I-menthol residue. The product from this reaction is optically active, despite the fact that homopolymerization and copolymerization of these MCMs are accompanied by racemization.

## K. Unsaturation and Structurization of Metallopolymers

Unsaturation and structurization of metallopolymers can occur for different reasons: incomplete involvement of the multiple bonds in polymerization, specific features of chain restriction, and chain transfer reactions.

Metal-containing copolymers of Co or Ni acrylates, which contain up to 20 mol% of acrylate units, with styrene are readily soluble in DMF methanol, indicating that the process involves mostly one of the double bonds (scheme 35).<sup>129</sup> The same can be true for their graft polymerization.<sup>81</sup> During polymerization of transition metal methacryloylacetates, the structure of the coordination units does not change; however, the double bonds that do not participate in the polymerization can form either crosslinked structures or remain free.<sup>99</sup>



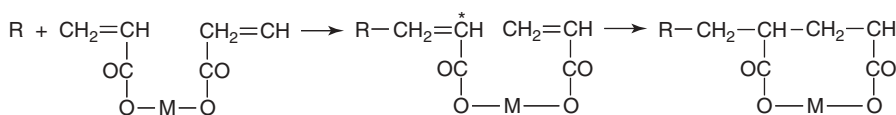
**Scheme 35**

Similarly, the polymer formed upon thermal polymerization of  $Co^{2+}$  acrylate can be both linear and crosslinked, depending on the temperature.<sup>76</sup> The fraction of unreacted double bonds in copolymers of transition metal diacrylates with traditional vinylic monomers increases in the order  $Zn^{2+}$  (4–35%) <  $Co^{2+}$  (14–39%) <  $Ni^{2+}$  (22–49%), which correlates with the ability of these acrylates to undergo homopolymerization (note: in the hypothetical case where only one acrylate group

reacts, the degree of unsaturation is 50%). Copolymerization of  $\text{Co}^{3+}$  complexes in which Schiff's bases with vinylic groups act as the ligands involves either one or two groups of the three groups coordinated to  $\text{Co}^{3+}$ , whereas in the  $\text{Cu}^{2+}$  chelate both vinylic groups participate in polymerization.

### L. Cyclization During Polymerization

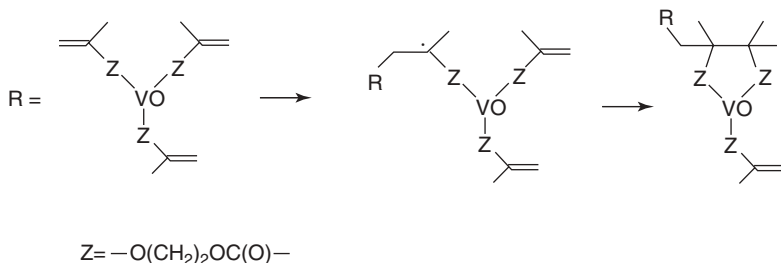
As a rule, MCMs based on polyvalent metals are bifunctional or trifunctional monomers with nonconjugated double bonds. The mechanism of formation of cyclic units is close to that of the polymerization of nonconjugated diene monomers (e.g., 1,5- or 1,6-dienes) and acrylic or methacrylic anhydride. The cyclization is based on the alternation of intermolecular and intramolecular chain growth events (scheme 36).



Scheme 36

The important role of metal ions is to ensure the orientation of polymerizing units and the close arrangement of their double bonds. The possibility of these processes is indicated by the known facts of higher efficiency of cycloaddition compared to an ordinary addition (i.e., the radical formed upon cleavage of one of the double bonds normally reacts with the second double bond in the same monomer). It is significant that cycloaddition is realized even in those cases in which the activities of the double bonds in the monomer are markedly different, for example, in the cyclopolymerization of allyl methacrylate.

It has been shown by a number of methods (e.g., measurement of the polymer solubility, comparison of the degree of polymerization with the number of double bonds in the polymer) that radical polymerization of the trisubstituted vanadium-containing monomer,  $\text{VO}(\text{O}(\text{CH}_2)_2\text{OC}(\text{O})\text{C}(\text{CH}_3)=\text{CH}_2)_3$ , follows the cyclopolymerization mechanism (scheme 37).<sup>87</sup>



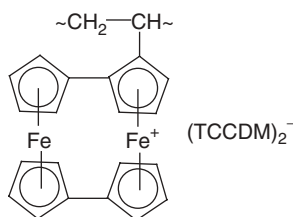
Scheme 37

These processes also occur in systems that undergo copolymerization, particularly if one of the monomers chemically changes during the reaction (e.g., copolymerization of sodium styrenesulfonate with sodium chloroacrylate, which is accompanied by a partial dehalogenation of the monomer and involves intramolecular cyclization leading to the appearance of lactone units in the copolymer).

## VI. SOME PRACTICAL APPLICATIONS OF UNIT VARIABILITY OF METAL-CONTAINING POLYMERS

The data presented here indicate that various types of unit variability in metallopolymeric chains can arise during polymerization of MCMs. Some of these metal-containing polymers serve as specific levers for controlling the composition and properties of the metallopolymer formed, whereas others are only hypothetical. The main point is the necessity of choosing conditions under which the metal-containing group is introduced into a polymer. It should be emphasized that polymerization of MCMs, which contain different metal isotopes, has already found practical applications; in particular, these materials have been used to separate effectively the isotopes of  $^{235}\text{U}$  and  $^{238}\text{U}$  based on the different rates of polymerization of their acrylates,  $\text{UO}_2(\text{OCOCH}=\text{CH}_2)_2$ , in magnetic fields.<sup>153</sup>

Polymers whose monomeric units contain metal ions in different oxidation states are of interest for a number of reasons. Thus homopolymerization of 3-vinyl-*bis*-fulvalenediiron is an efficient way to produce conductive polymers.<sup>154</sup> This process is accompanied by the oxidation of  $\text{Fe}^{2+}$  to  $\text{Fe}^{3+}$ , with the simultaneous formation of a charge transfer complex with the oxidant, tetracyanoquinodimethane (TCCDM) (scheme 38).



Scheme 38

The formally mixedvalence ( $\text{Fe}^{2+}$ ,  $\text{Fe}^{3+}$ ) polymeric complex thus obtained is a delocalized system with a single type of iron ions and possesses one of the highest electrical conductivities of those observed for organic polymers,  $(6-10) \times 10^{-3} \text{ Ohm}^{-1} \text{ cm}^{-1}$ . The unit variability caused by different spatial and electronic structures of metal-containing groups in polymers can also significantly influence their properties. For example, copolymers of  $\text{Cr}^{3+}$  alkyl vinyl sulfoxide complexes

with MMA exhibit thermochromism;<sup>155</sup> their color changes from emerald green (20–30°C) to violet (40°C). Evidently, on changing the temperature, the configuration of the complex changes due to the behavior of the polymeric matrix in which the complex is fixed. As the temperature decreases, the matrix becomes more rigid and distorts the configuration of the polymeric complex. At higher temperatures, the influence of the matrix is weaker, and the complex returns to its initial shape. Since the reactions of polymers are not quantitative, many intermediate states of the metal-containing polymeric complexes coexist.

It should be noted extra-coordination processes are also important in controlling the properties of metallopolymers. Thus mechanical parameters and performance of many metal-containing polymers are determined by the ability of the metals to form ionic or coordination crosslinks (i.e., additional interchain interaction), and to exhibit cohesion and adhesion properties. Formally, unit variability in these cases is determined by the presence of metals in the chain with different coordination numbers. The incorporation of cluster-containing  $Os_3$ -monomers into a polystyrene or poly(acrylonitrile) chain results in a mutual thermal stabilization of both the polymers and the clusters incorporated into the chains.<sup>156</sup> These effects are observed only in cases where the cluster monomers are chemically bound to the polymeric chain. The influence of the chain may be manifested as the transfer of energy from the rotation-vibration degrees of freedom of the cluster to the translational degrees of freedom of the polymer chain segments at elevated temperatures.

We have analyzed above the unit variability caused by the unsaturated character of metallopolymers and by their crosslinking. Many properties of metallopolymers are enhanced on the formation of crosslinked structures. For example, additional thermal polymerization with participation of the residual double bonds is aimed at producing crosslinked polymers with high strength, plasticity, and softening temperatures. Unsaturation in metallopolymers can also influence their color. In fact, the reaction mixture consisting of MMA, MAA, and  $Co^{2+}$  methacrylate changes color from pink to green when the number of  $C=C$  bonds decreases by 15%.<sup>146</sup> In addition, transition metal acrylates can participate in crosslinking of polymeric chains and result in unit variability that occurs during the photochemical crosslinking of gelatin.<sup>103</sup> Thus, on exposure to monochromatic radiation from a helium-neon laser, the amino and hydroxy groups of gelatin (e.g., hydroxyproline and lysine or arginine residues) react with the activated double bonds. The high photosensitivity of copper acrylate-based layers is due to the fact that the position of the absorption maximum corresponds closely to the laser radiation wavelength (633 nm) and these layers absorb light efficiently. Chain crosslinking can also occur by other mechanisms—for example, by coordination interactions of the metal ions of MCMs with functional groups of polymers.

Thus the analysis of unit variability in metallopolymer chains presented here may give the impression that polymerization of MCM is accompanied by many of side processes. As noted in the introduction to this chapter, it might appear problematic that the unique character of the polymerization products from these monomers is due to the structural iniformity of the macro complexes. Actually this is not so.

Many of the side reactions that were considered can be prevented, and some other reactions can be substantially suppressed. Numerous approaches exist for this

purpose: (1) the low-temperature convenient polymerization, including that which is initiated by radiation, and (2) the radiation-induced polymerization that can be carried out in all phase states of the monomer over a broad temperature range, including a postradiation variant. Attention was focused in this review and elsewhere on the nontraditional methods of MCM polymerization initiation (low-temperature, frontal, spontaneous, etc.). In each case, the researcher may choose the optimum variant. If the unit variability cannot be ruled out, it can be taken into account qualitative and/or quantitatively.

Depending on the fraction of anomalous units, metal-containing polymers can be divided into several types. According to the IUPAC nomenclature,<sup>157</sup> when the content of these units is low, the polymers can be classified as regular macromolecules, which consist mostly of identical repeating units linked to one another in the same way. When the content of unit variability is relatively large, they are called irregular macromolecules.

Many problems need to be solved before we can understand the reasons and the mechanism for the formation of anomalous units from MCMs and copolymers of MCMs, to elucidate their roles, and to use this phenomenon for practical purposes in modifying polymer properties during polymerization. At present, little is known about the relative reactivity constants of MCMs, except, perhaps, for organotin and ferrocene monomers. It was found that for the monomers  $\text{CH}_2=\text{CHX}$ , the parameter  $e$  (which is a measure of the polarity of the substituent  $X$  in the Alfrey Price  $Q$ - $e$  scheme) is correlated with the Hammett constant ( $\sigma_x$ ).<sup>158</sup> The  $e$  values of vinylic monomers range from  $-1$  to  $+1.5$ , while those for MCMs are normally large negative values; they vary from  $-1.96$  to  $-2.65$  for metal acrylates. This means that the metal-containing group is an electron-donating substituent (similar to  $p$ - $\text{NMe}_2$  or  $p$ - $\text{OMe}$  in the aromatic ring), with the electron density is markedly shifted toward the  $\text{C}=\text{C}$  bond.

Copolymerization of different MCMs is less studied. Thermal transformations and solid-state copolymerization (e.g., with co-precipitated  $\text{Fe}^{3+}$  and  $\text{Co}^{2+}$  acrylates) lead to the conclusion that the Fe- and Co-containing fragments influence each other during these processes.<sup>159</sup> This is manifested as initiation of polymerization routes that result from partial thermal decomposition of the Fe-containing monomer. It is also manifested as a decrease in the thermal stability of the Co-containing fragments in the resulting polymer.

The situation is far more complicated when copolymerization involves three or more monomers and when the production of uniform materials with a strictly defined ratio of the components is required in a multicomponent system. Examples of thermal polymerization are the styrene-acrylonitrile-zinc acrylate,<sup>160</sup> chromium acrylate or copper acrylate<sup>161</sup> systems.

A rare case is copolymerization of several different MCMs. The resulting polymers can contain mixed units of various types. This is particularly true for the development of high-temperature superconducting (HTSC) ceramics that are based on synthesized prepolymers. One of the methods that is used is the copolymerization of MCM acrylates (and perhaps maleinates)<sup>162</sup> or acrylamide complexes of  $\text{Y}^{3+}$ ,  $\text{Ba}^{2+}$ , or  $\text{Cu}^{2+}$  and the synthesis of superconducting bismuth cuprates (e.g.,  $\text{Bi}_2\text{Sr}_2\text{Ca}_{n-1} \cdot \text{Cu}_n\text{O}_{2n+4-\delta}$  where  $n=1-3$ ) by copolymerization of the corresponding metal-containing monomers. Thermolysis of these polymeric precursors affords a finely

dispersed mixture of metal oxides (e.g.,  $Y^{3+}:Ba^{2+}:Cu^{2+}=1:2:3$  (mol) ceramics). Thermolysis enables a relatively easy production<sup>163</sup> of single-phase high-temperature superconducting ceramics with a superconduction transition point of 110 K (Fig. 10). When there are variations in the alternation of the corresponding units in these thermocopolymers, as occurs when they contain long blocks of units incorporating the same metal, it becomes difficult to prepare a single-phase material. It is noteworthy that the products of solid-state polymerization of lithium acrylate, methacrylate, crotonate, fumarate, maleinate, and sorbate possess high-temperature (250°C) ionic conductivity ( $10^{-4}$ – $10^{-7}$  Ohm  $cm^{-1}$ , activation energy  $\sim 2$  eV).<sup>128,164</sup>

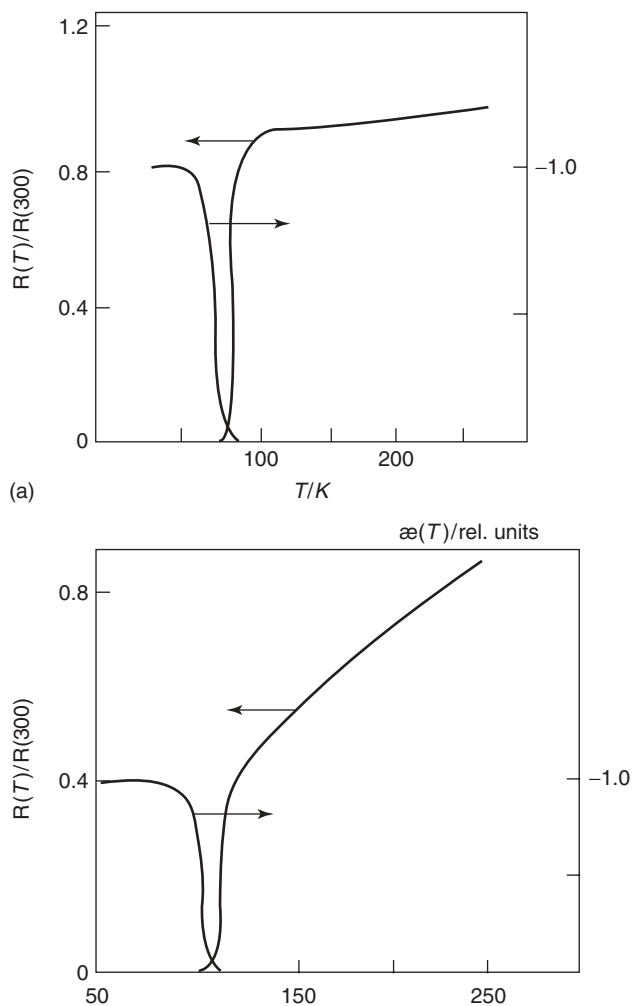


**Figure 10** Temperature dependences of the resistivity and the magnetic susceptibility of HTSC ceramics prepared from (a) the copolymer of  $Y^{III}$ ,  $Ba^{II}$ , and  $Cu^{II}$  acrylates and (b) the product of spontaneous polymerization of AAM complexes of  $Bi^{III}$ ,  $Ca^{II}$ ,  $Sr^{II}$ ,  $Pb^{II}$ , and  $Cu^{II}$  nitrates.

**Table 7** Activation Parameters for Hydrogenation of Acrylic Acid and Cobalt Acrylate

Substrate	$E$ , kJ/mole	$\Delta H^\ddagger$ , kJ/mole	$\Delta S^\ddagger$
$\text{CH}_2=\text{CHCOOH}$	14.2	18.1	-7.5
$\text{Co}(\text{OOCCH}=\text{CH}_2)_2$	33.3	32.2	-7.4

Development of a theoretical basis for the influence of coordination bonds that are formed by transition metals with functional groups of a monomer or with a polymer radical would ensure the possibility of efficiently regulating the stereochemistry of radical polymerization. Since the corresponding database is absent, we did not focus in this review on the manifestation of different types of unit variability in one metal-containing polymer (e.g., that caused by the different valence states of the transition metal ions in some units and the diversity of their chemical binding in other units) or on their multiple character of copolymers.

Finally, it should be noted that MCMs are metal complexes with specific ligands, and polymerization is only one of their functions. Generally, these compounds can participate in all the reactions typical of compounds with double bonds. Thus it was found under model conditions that, on hydrogenation, metal acrylates are converted into the corresponding propionates.<sup>165</sup> It should be mentioned that the effective energy of activation and enthalpy of the reaction is higher than that of acrylic acid (Table 7).

However, it is unclear whether the double bonds are hydrogenated simultaneously or involved in the catalytic process successively. This also refers to the residual double bonds in mixed-unit metallopolymers. Metallopolymers with this type of unit variability can also undergo other analogous polymer transformations (i.e., reactions that do not affect the backbone) such as alkyl hydroperoxide-induced epoxidation, carbonylation, hydrosilylation, and hydroformylation. Realization of these reactions could yield valuable products. However, solutions to these problems will require additional research.

## VII. ACKNOWLEDGMENTS

This work was financially supported by the Russian Foundation for Basic Research (Projects No. 04-03-32634 and 04-03-97233).

## VIII. REFERENCES

1. A. D. Pomogailo, *Polymer-Immobilized Metal Complexes Catalysts*, Nauka, Moscow, 1988 (and the references cited there).

2. N. A. Plate, A. D. Litmanovich, O. V. Noah, *Macromolecular Reactions*, Wiley, Chichester, UK, 1995.
3. I. E. Uflyand, E. F. Vainshtein, A. D. Pomogailo, *Russ. J. Gen. Chem. Polym. Sci. (Engl. Trans.)*, **61**, 1790 (1991).
4. E. F. Vainstein, G. E. Zaikov, in *Polymer Yearbook*, vol. 10, R. A. Pethric, ed., Harwood Academic, London, 1993.
5. E. Tsuchida, *Macromolecular Complexes. Dynamic Interactions and Electronic Processes*, VCH, New York, 1991.
6. H. Todokoro, Y. Chatani, T. T. Yoshihara, *Macromol. Chem.*, **73**, 109 (1964).
7. R. Iwamoto, Y. Saito, H. Ishikawa, H. Iadokoro, *J. Polym. Sci. A-2*, **6**, 1509 (1968).
8. J. M. Parker, P. V. Wright, C. C. Lee, *Polymer*, **22**, 1305 (1981).
9. N. Higuchi, T. Hiraoki, K. Nikichi, *Polym. J.*, **11**, 139 (1979).
10. R. Barbucci, P. Ferruti, *Polymer*, **20**, 1061 (1979).
11. H. Niside, E. Tsuchida, *Makromol. Chem.*, **177**, 2295 (1976).
12. S. Skaria, C. R. Rajan, S. Ponrathnam, *Polymer*, **38**, 1699 (1997).
13. Z. M. Michalska, K. Strzelec, *React. Funkt. Polym.*, **44**, 189 (2000).
14. M. G. Kolomeer, H. G. Taganov, Z. Z. Biglov, *Thermodynamics Org. Compounds*, **N7**, 58 (1978).
15. A. Warshawsky, R. Kalir, *J. Appl. Polym. Sci.*, **24**, 1125 (1979).
16. A. D. Pomogailo, I. E. Ufland, E. F. Vainshtein, *Russ. Chem. Rev.*, **64**, 857 (1995).
17. S. Yano, H. Yamashita, M. Matsushita, *Colloid Polym. Sci.*, **259**, 514 (1981).
18. E. Roman, G. Valenzuela, L. Gargallo, D. Radic, *J. Polym. Sci. Polym. Chem. Ed.*, **21**, 2057 (1983).
19. A. A. Popov, E. F. Vainstein, S. G. Entelis, *J. Macromol. Sci. A*, **11**, 859 (1977).
20. A. I. Kuzaev, A. D. Pomogailo, U. A. Mambetov, *Polym. Sci. (Engl. Trans.)*, **A**, **23**, 213 (1981).
21. A. D. Pomogailo, A. I. Kuzaev, F. S. Dyachkovskii, N. S. Enikolopyan, *Dokl. Chem. (Engl. Trans.)*, **256**, 132 (1981).
22. G. R. Joppien, *Angew. Macromol. Chem.*, **70**, 189, 199 (1978).
23. E. Roman, G. Valenzuela, L. Gargallo, *Am. Chem. Soc. Polym. Prepr.*, **23**, 81 (1982).
24. S. L. Davydova, N. A. Plate, *Coord. Chem. Rev.*, **16**, 195 (1975).
25. H. H. Jellinek, S. N. Lipovac, *J. Polym. Sci., C, Pt. 2*, 621 (1969).
26. T. V. Pokholok, G. V. Pariysky, N. I. Zaitzeva, D. Y. Toptygin, *Eur. Polym. J.*, **20**, 609 (1984).
27. B. V. Kanaev, I. V. Sokolov, A. P. Fedorova, *Russ. J. Phys. Chem. (Engl. Trans.)*, **58**, 1147 (1984).
28. S. N. Zhurkov, V. A. Zakrevskii, V. E. Korsunov, V. E. Korsunov, V. S. Kuksenko, *Phys. Solids*, **7**, 2004 (1971).
29. N. S. Enikolopyan, A. M. Bochkin, A. D. Pomogailo, *Dokl. Chem. (Engl. Trans.)*, **265**, 95 (1982).
30. A. S. Polinskii, V. S. Pshezhetskii, V. A. Kabanov, *Polym. Sci. (Engl. Trans.)*, **27**, 2295 (1985).
31. H. G. Biederman, W. Z. Graft, *Z. Naturforsch.*, **29b**, 65 (1974).
32. Y. Ikada, Y. Nishizaki, Y. Uyama, *J. Polym. Sci. Polym. Chem. Ed.*, **14**, 2251 (1976).
33. Y. Ikada, Y. Nishizaki, Y. Iwata, H. Sakurada, *J. Polym. Sci. Polym. Lett. Ed.*, **15**, 451 (1977).
34. S. B. Echmaev, I. N. Ivleva, A. V. Raevskii, A. D. Pomogailo, *Kinet. Catal.*, **24**, 1428 (1983).
35. C. Ungurenasu, C. Cotzur, *Polym. Bull.*, **6**, 299 (1982).
36. G. A. Ozin, C. E. Francis, *J. Mol. Struct.*, **59**, 55 (1980); *J. Mol. Struct.*, **59**, 55 (1980).
37. L. V. Miroshnik, A. M. Dubyna, V. N. Tolmachev, *Russ. J. Coord. Chem. (Engl. Trans.)*, **6**, 870 (1980).
38. J. Topich, *J. Inorg. Chim. Acta*, **46**, L97 (1980).

39. A. Deratani, B. Sebille, H. Hommel, A. P. Legrand, *React. Polym.*, **1**, 263 (1983).
40. M. Sato, K. Kondo, K. Takemoto, *J. Polym. Sci. Polym. Chem. Ed.*, **17**, 2729 (1979).
41. D. B. Rorabacher, in *Proceedings of the 179th American Chemical Societies National Meetings*, American Chemical Society, Washington, D.C., 1980.
42. S.C.H. Windler, *Nachr. Chem. Technol. Lab.*, **32**, 392 (1984).
43. R. P. McDonald, J. M. Winterbottom, *Rev. Port. Guim.*, **19**, 269 (1977).
44. R. H. Grubbs, C. Gibbons, L. C. Kroll, *J. Am. Chem. Soc.*, **95**, 2373 (1973).
45. S. L. Regen, D. P. Lee, *Macromolecules*, **10**, 1418 (1977).
46. Z. N. Medved', N. N. Zhegalova, *Polym. Sci. (Engl. Trans.)*, **B20**, 524 (1978).
47. X.-H. Hou, M. Kaneko, A. Yamada, *Kobunshi Ronbunshu*, **41**, 311 (1984).
48. A. D. Pomogailo, D. V. Sokol'skii, U. A. Mambetov, *Russ. J. Gen. Chem. (Engl. Trans.)*, **48**, 2101 (1978).
49. A. D. Pomogailo, *Catalysis by Polymer-Immobilized Metal Complexes*, Gordon & Breach, Amsterdam, 1998.
50. D. A. Kritskaya, A. D. Pomogailo, A. N. Ponomarev, F. S. D'yachkovskii, *J. Appl. Polym. Sci.*, **25**, 349 (1980); *J. Polym. Sci., Polym. Symp.*, **68**, 13 (1980).
51. G. I. Likhtenstein, *Method of Spin Labels in Molecular Biology*, Nauka, Moscow, 1974.
52. A. M. Vasserman, A. L. Kovarskii, *Spin Labels and Probes in Physicochemistry of Polymers*, Nauka, Moscow, 1986.
53. S. S. Eaton and G. R. Eaton, *Coord. Chem. Rev.*, **26**, 207 (1978).
54. N. M. Bravaya, A. D. Pomogailo, *J. Inorg. Organomet. Polym.*, **10**, 1 (2000).
55. A. T. Nikitaev, A. D. Pomogailo, N. D. Golubeva, I. N. Ivleva, *Kinet. Catal.*, **27**, 709 (1986).
56. O. Ya. Grinberg, A. T. Nikitaev, K. I. Zamaraev, Ya. S. Lebedev, *Russ. J. Strukt. Khim.*, **10**, 230 (1969).
57. A. D. Pomogailo, A. T. Nikitaev, F. S. D'yachkovskii, *Kinet. Catal.*, **25**, 166 (1984).
58. A. D. Pomogailo, N. D. Golubeva, *J. Inorg. Organomet. Polym.*, **11**, 67, (2001).
59. A. D. Pomogailo, paper presented at the *IUPAC 8th International Symposium on Macromolecule-Metal Complexes*, Waseda University, Tokyo, 1999.
60. A. D. Pomogailo, in *Proceedings of the International Symposium on Macromolecule Metal Complexes (MMC-9)*, Polytechnic University Brooklyn, (New York, 2001).
61. A. D. Pomogailo, *Macromol. Symp.*, **186**, 15 (2002).
62. V. V. Korshak, *Unit Variability in Polymers*, Nauka, Moscow, 1977.
63. A. D. Pomogailo, V. S. Savost'yanov, *Metal Containing Monomers and Polymers Based on Them*, Khimiya, Moscow, 1988.
64. V. V. Korshak, ed., *Advances in the Synthesis of Organoelement Polymers*, Nauka, Moscow, 1988.
65. G. I. Dzhardimalieva, A. D. Pomogailo, in *Metal-Containing Polymeric Materials*, C. U. Pittman Jr., C. E. Carraher, Jr., M. Zeldin, J. E. Sheats, B. M. Culbertson, eds., Plenum Press, New York, 1996.
66. A. D. Pomogailo, V. S. Savost'yanov, *Synthesis and Polymerization of Metal-Containing Monomers*, CRC Press, Boca Raton, FL, 1994.
67. A. D. Pomogailo, V. S. Savost'yanov, *Russ. Chem. Rev. (Engl. Trans.)*, **52**, 973 (1983).
68. A. D. Pomogailo, V. S. Savost'yanov, *J. Macromol. Sci., Rev.*, **25**, 375 (1985).
69. A. D. Pomogailo, in *Polymeric Materials Encyclopedia*, J. C. Salamone, ed., CRC Press, Boca Raton, FL, 1996.
70. C. U. Pittman Jr., in *Organometallic Reactions*, E. I. Becker and M. Tsutsui, eds., Marcel Decker, New York, 1977.
71. V. A. Kabanov, D. A. Topchiev, *Polymerization of Ionizing Monomers*, Nauka, Moscow, 1975.

72. B. S. Selenova, G. I. Dzhardimalieva, E. B. Baishiganov, O. N. Efimov, A. D. Pomogailo, *Bull. Acad. Sci. AN SSR Div. Chem. Sci. (Engl. Trans.)*, **38**, 927 (1989).
73. U. Kh. Agaev, G. Z. Ponomareva, F. M. Alieva, A. T. Alyev, R. Z. Gasanova, E. S. Abdullaeva, *Russ. Polym. Sci. B (Engl. Trans.)*, **38**, 1769 (1996).
74. B. S. Selenova, G. I. Dzhardimalieva, M. V. Tsikalova, S. V. Kurmaz, V. P. Roshchupkin, I. Ya. Levitin, A. D. Pomogailo, M. E. Vol'pin, *Russ. Chem. Bull. (Engl. Trans.)*, **42**, 455 (1993).
75. A. S. Rozenberg, G. I. Dzhardimalieva, A. D. Pomogailo, *Dokl. Phys. Chem. (Engl. Trans.)*, **356**, 294 (1997).
76. E. I. Aleksandrova, G. I. Dzhardimalieva, A. S. Rozenberg, A. D. Pomogailo, *Russ. Chem. Bull. (Engl. Trans.)*, **42**, 264 (1993).
77. L. B. Krentsel', A. D. Litmanovich, N. A. Plate, E. I. Karpeiskaya, L. F. Godunova, E. I. Klabunovskii, *Polym. Sci. A (Engl. Trans.)*, **34**, 10 (1992).
78. G. I. Dzhardimalieva, I. N. Ivleva, E. N. Frolov, A. D. Pomogailo, *Russ. Chem. Bull. (Engl. Trans.)*, **47**, 1113 (1998).
79. P. A. Vasil'ev, A. L. Ivanov, A. N. Glebov, *Russ. J. Coord. Chem.*, **23**, 132 (1997).
80. G. I. Dzhardimalieva, A. D. Pomogailo, S. P. Davtyan, V. I. Ponomarev, *Bull. Acad. Sci. USSR, Div. Chem. Sci. (Engl. Trans.)*, **37**, 1352 (1988).
81. V. S. Savost'yanov, A. D. Pomogailo, D. A. Kritskaya, A. N. Ponomarev, *Bull. Acad. Sci. USSR, Div. Chem. Sci. (Engl. Trans.)*, **35**, 36, 325 (1986).
82. V. S. Savost'yanov, V. N. Vasilets, O. V. Ermakov, E. A. Sokolov, A. D. Pomogailo, D. A. Kritskaya, A. N. Ponomarev, *Bull. Russ. Acad. Sci. Div. Chem. Sci. (Engl. Trans.)*, **41**, 1615 (1992).
83. M. Bertolin, M. Zecca, G. Favero, G. Palma, S. Lora, D. Ajo, B. Corain, *J. Appl. Polym. Sci.*, **65**, 2201 (1997).
84. Yu. M. Shul'ga, O. S. Roshchupkina, G. I. Dzhardimalieva, A. D. Pomogailo, *Russ. Chem. Bull. (Engl. Trans.)*, **42**, 1498 (1993).
85. A. B. Gavrilov, T. I. Movchan, A. D. Pomogailo, *Russ. Chem. Bull. (Engl. Trans.)*, **43**, 232 (1994).
86. N. P. Porollo, Z. G. Aliev, G. I. Dzhardimalieva, I. N. Ivleva, I. E. Uflyand, A. D. Pomogailo, N. S. Ovanesyan, *Russ. Chem. Bull. (Engl. Trans.)*, **46**, 362 (1997).
87. A. D. Pomogailo, N. D. Golubeva, *Russ. Chem. Bull. (Engl. Trans.)*, **43**, 2020 (1994).
88. A. D. Pomogailo, N. D. Golubeva, A. N. Kitaigorodskii, *Bull. Acad. Sci. USSR Div. Chem. Sci. (Engl. Trans.)*, **40**, 418 (1991).
89. N. M. Bravaya, A. D. Pomogailo, *Bull. Puss. Acad. Sci. Div. Chem. Sci. (Engl. Trans.)*, **41**, 1351 (1992).
90. N. A. Orlin, K. I. Petrov, *J. Appl. Spectr. USSR (Engl. Trans.)*, **24**, 171 (1976).
91. A. V. Gushchin, V. A. Dodonov, paper presented at the *International Conference on Fundamental Problems of Polymer Science*, Moscow, 1997.
92. M. A. Porai-Koshits, *Kristalloghimiya, Crystal Chemistry: Advances in Science and Engineering* VINITI, Acad. Sci. USSR, Moscow, 1981.
93. G. I. Dzhardimalieva, A. D. Pomogailo, V. I. Ponomarev, L. O. Atovmyan, Yu. M. Shul'ga, A. G. Starikov, *Bull. Acad. Sci. USSR Div. Chem. Sci. (Engl. Trans.)*, **37**, 1346 (1988).
94. N. P. Porollo, G. I. Dzhardimalieva, I. E. Uflyand, A. D. Pomogailo, *Mendeleev Chem. J. (Engl. Trans.)*, **40**, 190 (1996).
95. Yu. M. Shul'ga, I. V. Chernushevich, G. I. Dzhardimalieva, O. S. Roshchupkina, A. F. Dodonov, A. D. Pomogailo, *Russ. Chem. Bull. (Engl. Trans.)*, **43**, 983 (1994).
96. Yu. M. Shul'ga, O. S. Roshchupkina, G. I. Dzhardimalieva, I. V. Chernushevich, A. F. Dodonov, Yu. V. Baldokhin, P. Ya. Kolotyarkin, A. S. Rozenberg, A. D. Pomogailo, *Russ. Chem. Bull. (Engl. Trans.)*, **42**, 1661 (1993).
97. I. E. Uflyand, I. A. Il'chenko, A. G. Starikov, V. N. Sheinker, A. D. Pomogailo, *Bull. Acad. Sci. USSR Div. Chem. Sci. (Engl. Trans.)*, **38**, 2271 (1989).

98. I. E. Uflyand, I. A. Il'chenko, A. G. Starikov, V. N. Sheinker, A. D. Pomogailo, *Bull. Acad. Sci. USSR Div. Chem. Sci. (Engl. Trans.)*, **39**, 388 (1990).
99. T. I. Movchan, I. S. Voloshanovskii, A. D. Pomogailo, *Russ. Chem. Bull. (Engl. Trans.)*, **42**, 1972 (1993).
100. V. S. Savost'yanov, V. I. Ponomarev, A. D. Pomogailo, B. S. Selenova, I. N. Ivleva, A. G. Starikov, L. O. Atovmyan, *Bull. Acad. Sci. USSR Div. Chem. Sci. (Engl. Trans.)*, **39**, 674 (1990).
101. V. S. Savost'yanov, A. D. Pomogailo, B. S. Selenova, D. A. Kritskaya, A. N. Ponomarev, *Bull. Acad. Sci. USSR Div. Chem. Sci. (Engl. Trans.)*, **39**, 680 (1990).
102. V. S. Savost'yanov, D. A. Kritskaya, A. N. Ponomarev, A. D. Pomogailo, *J. Polym. Sci. Part A Polymer Chem.* **32**, 1201 (1994).
103. A. V. Botsman, L. N. Fedorova, A. I. Vasil'chenko, G. I. Dzhardimalieva, A. D. Pomogailo, *Bull. Russ. Acad. Sci., Div. Chem. Sci. (Engl. Trans.)*, **41**, 454 (1992).
104. E. N. Danilovtseva, A. I. Skushnikova, V. V. Annenkov, E. S. Domnina, *Russ. Polym. Sci. (Engl. Trans.)*, **39**, 146 (1997).
105. L. I. Skushnikova, E. S. Domnina, G. G. Skvortsova, *Russ. Polym. Sci. B (Engl. Trans.)*, **24**, 11 (1982).
106. G. I. Dzhardimalieva, A. D. Pomogailo, A. N. Shupik, *Bull. Acad. Sci. USSR Div. Chem. Sci. (Engl. Trans.)*, **34**, 411 (1985).
107. P. A. Vasil'ev, *Russ. J. Inorg. Chem.*, **39**, 1688 (1994).
108. P. A. Vasil'ev, A. L. Ivanov, O. N. Rubacheva, A. N. Glebov, *Russ. J. Inorg. Chem. (Engl. Trans.)*, **41**, 1748 (1996).
109. T. I. Movchan, I. I. Zheltvai, I. S. Voloshanovskii, A. D. Pomogailo, *Bull. Russ. Acad. Sci. Div. Chem. Sci. (Engl. Trans.)*, **41**, 1609 (1992).
110. I. I. Zheltvai, T. I. Movchan, I. S. Voloshanovskii, A. D. Pomogailo, *Russ. Chem. Bull. (Engl. Trans.)*, **42**, 1016 (1993).
111. I. I. Zheltvai, I. S. Voloshanovskii, T. D. Butova, A. D. Pomogailo, *Russ. Chem. Bull. (Engl. Trans.)*, **44**, 2299 (1995).
112. V. A. Kabanov, V. P. Zubov, Yu. D. Semchikov, *Complex Radical Polymerization*, Khimiya, Moscow, 1987.
113. V. S. Savost'yanov, G. P. Belov, D. A. Kritskaya, A. D. Pomogailo, A. N. Ponomarev, *Bull. Acad. Sci. USSR Div. Chem. Sci. (Engl. Trans.)*, **39**, 905 (1990).
114. I. E. Uflyand, I. V. Kokareva, A. G. Starikov, V. N. Sheinker, A. D. Pomogailo, *Bull. Acad. Sci. USSR Div. Chem. Sci. (Engl. Trans.)*, **38**, 2265 (1989).
115. A. S. Rozenberg, E. I. Aleksandrova, G. I. Dzhardimalieva, A. N. Titkov, A. D. Pomogailo, *Russ. Chem. Bull. (Engl. Trans.)*, **42**, 1666 (1993).
116. T. I. Movchan, A. G. Starikov, I. N. Ivleva, I. S. Voloshanovskii, A. D. Pomogailo, *Bull. Russ. Acad. Sci. Div. Chem. Sci. (Engl. Trans.)*, **41**, 545 (1992).
117. T. I. Movchan, T. I. Solov'eva, I. N. Ivleva, L. A. Petrova, I. S. Voloshanovskii, G. P. Belov, A. D. Pomogailo, *Russ. Chem. Bull. (Engl. Trans.)*, **43**, 35 (1994).
118. A. T. Shuvaev, A. S. Rozenberg, G. I. Dzhardimalieva, N. P. Ivleva, V. G. Vlasenko, T. I. Nedoseikina, T. A. Lyubeznova, I. E. Uflyand, A. D. Pomogailo, *Russ. Chem. Bull. (Engl. Trans.)*, **47**, 1460 (1998).
119. A. D. Pomogailo, V. G. Vlasenko, A. T. Shuvaev, A. S. Rozenberg, G. I. Dzhardimalieva, *Colloid J. (Engl. Trans.)*, **64**, 472 (2002).
120. V. S. Savost'yanov, A. D. Pomogailo, D. A. Kritskaya, A. N. Ponomarev, *Bull. Acad. Sci. USSR Div. Chem. Sci. (Engl. Trans.)*, **35**, 33 (1986).
121. I. E. Uflyand, A. G. Starikov, V. S. Savost'yanov, A. D. Pomogailo, *Bull. Acad. Sci. USSR Div. Chem. Sci. (Engl. Trans.)*, **39**, 1185 (1990).
122. A. G. Starikov, G. I. Dzhardimalieva, I. E. Uflyand, T. K. Goncharov, A. D. Pomogailo, *Russ. Chem. Bull. (Engl. Trans.)*, **42**, 66 (1993).

123. G. I. Dzhardimalieva, A. O. Tonoyan, A. D. Pomogailo, S. P. Davtyan, *Bull. Acad. Sci. USSR Div. Chem. Sci. (Engl. Trans.)*, **36**, 1612 (1987).
124. P. E. Matkovskii, N. S. Enikolopov, *Hypothesis of Coordination-Radical Mechanism of Polymerization of Olefins on Organometallic Complex Catalysts*, Inst. Chem. Phys., Acad. Sci. USSR, Chernogolovka, 1983.
125. C. U. Pittman, Jr., O. E. Ayers, S. P. McManus, *J. Macromol. Sci.-Chem.*, **7**, 1563 (1973).
126. A. D. Pomogailo, N. M. Bravaya, V. F. Razumov, I. S. Voloshanovskii, N. A. Kitsenko, V. V. Berezovskii, A. I. Kuznev, A. G. Ivanchenko, *Russ. Chem. Bull., (Engl. Trans.)*, **45**, 2773 (1996).
127. V. F. Razumov, A. G. Ivanchenko, A. D. Pomogailo, I. S. Voloshanovskii, A. I. Kuzaev, *Polym. Sci., Ser. A (Engl. Trans.)*, **39**, 1451 (1997).
128. S. M. Schitter, H. P. Beck, *Chem. Ber.*, **129**, 1561 (1996).
129. G. I. Dzhardimalieva, A. Pomogailo, *Bull. Acad. Sci. USSR Div. Chem. Sci. (Engl. Trans.)*, **40**, 297 (1991).
130. G. I. Dzhardimalieva, V. A. Zhorin, I. N. Ivleva, A. D. Pomogailo, N. S. Enikolopyan, *Dokl. Chem. (Engl. Trans.)*, **287**, 654 (1986).
131. K. C. Tripathi, P. R. Sarma, H. M. Gupta, *J. Polymer Sci. Polym. Lett. Ed.*, **16**, 750 (1978).
132. A. D. Pomogailo, *Russ. Chem. Rev. (Engl. Trans.)*, **66**, 750 (1997).
133. A. S. Rozenberg, A. V. Raevskii, E. I. Aleksandrova, O. I. Kolesova, G. I. Dzhardimalieva, A. D. Pomogailo, *Russ. Chem. Bull., Intern. Ed.*, **50**, 901 (2001).
134. A. D. Pomogailo, A. S. Rozenberg, G. I. Dzhardimalieva, M. Leonovicz, *Adv. Mater. Sci.*, **1**, 19 (2001).
135. Ger. Pat. No. 3137840 (1981).
136. U. Schubert, *Chem. Mater.* **13**, 3487 (2001).
137. S. P. Tunik, S. I. Pomogailo, G. I. Dzhardimalieva, A. D. Pomogailo, I. I. Chuev, S. M. Aldoshin, A. B. Nikol'skii, *Russ. Chem. Bull. (Engl. Trans.)*, **42**, 937 (1993).
138. V. A. Maksakov, V. P. Kirin, S. N. Konchenko, N. M. Bravayn, A. D. Pomogailo, A. V. Virovets, N. I. Podberezskaya, I. G. Barakovskaya, S. V. Tkachev, *Russ. Chem. Bull. (Engl. Trans.)*, **42**, 1236 (1993).
139. V. A. Ershova, A. V. Golovin, L. A. Sheludyakova, P. P. Semyannikov, S. I. Pomogailo, A. D. Pomogailo, *Russ. Chem. Bull. (Engl. Trans.)*, **49**, 1455 (2000).
140. V. A. Maksakov, V. A. Ershova, V. P. Kirin, A. V. Golovin, *J. Organomet. Chem.*, **532**, 11 (1997).
141. G. A. Acum, M. J. Mays, P. R. Raithby, G. A. Solan, *J. Organomet. Chem.*, **508**, 137 (1996).
142. A. D. Pomogailo, G. I. Dzhardimalieva, S. I. Pomogailo, N. D. Golubeva, O. A. Adamenko, *Organometallic Chemistry on the Eve of the 21st Century (Workshop-INEOS'98)* Moscow, Russia, 1998.
143. S. I. Pomogailo, G. I. Dzhardimalieva, V. A. Ershova, S. M. Adoshin, A. D. Pomogailo, *Macromol. Symp.*, **186**, 155 (2002).
144. N. Bravaya, A. D. Pomogailo, V. A. Maksakov, V. P. Kirin, V. P. Grachev, A. I. Kuzaev, *Russ. Chem. Bull. (Engl. Trans.)*, **44**, 1062 (1995).
145. O. A. Adamenko, G. V. Lukova, N. D. Golubeva, V. A. Smirnov, V. A. Boiko, A. D. Pomogailo, I. E. Uflyand, *Dokl. Phys. Chem. (Engl. Trans.)*, **381**, 360 (2001).
146. E. A. Gonyukh, V. N. Serova, L. Kh. Khazryatova, E. N. Kuznetsov, in *Chemistry and Technology of Organoelement Compounds*, Kazan Chemical Technology Institute, 1984.
147. M. R. Muidinov, G. I. Dzhardimalieva, B. S. Selenova, A. D. Pomogailo, I. M. Barkalov, *Bull. Acad. Sci. USSR Div. Chem. Sci. (Engl. Trans.)*, **37**, 2258 (1988).
148. P. Cerrari, G. D. Guerra, S. Maltini, M. Tricoli, P. Giusti, L. Petarca, G. Polacco, *Macromol. Rapid Commun.*, **15**, 983 (1994).
149. G. Polacco, M. G. Cascone, L. Petarca, G. Maltini, C. Cristallini, N. Barbani, L. Lazzeri, *Polym. Intern.*, **41**, 443 (1996).

150. A. D. Pomogailo, *Catalysis by Polymer-Immobilized Metalcomplexes*, Gordon & Breach, London, 1998.
151. G. I. Dzhardimalieva, N. D. Golubeva, A. D. Pomogailo, paper presented at the, *Polymer and Organic Chemistry, 7th International Conference on Polymer Supported Reactions in Organic Chemistry*, Wroclaw, Poland, 1996.
152. E. I. Klabunovskii, E. I. Karpeiskaya, G. I. Dzhardimalieva, N. D. Golubeva, A. D. Pomogailo. *Russ. Chem. Bull.*, **48**, 1717 (1999).
153. D. A. Bennett, Br. Pat. 2.201.828; *Chem. Abstr*, 1989, **111**, 30095 n.
154. C. Pittman Jr. B. Sutnarayanan, *J. Am. Chem. Sec.*, **96**, 7916 (1974).
155. V. A. Nikonov, G. V. Leplyanin, Yu. I. Murinov, A. R. Derzhinskii, *Bull. Acad. Sci. USSR Div. Chem. Sci. (Engl. Trans.)*, **33**, 2427 (1984).
156. N. M. Bravaya, A. D. Pomogailo, V. A. Maksakov, V. P. Kirin, G. P. Belov, T. I. Solov'eva, *Russ. Chem. Bull. (Engl. Trans.)*, **43**, 381 (1994).
157. A. D. Jenkins, P. Kratochvil, R.F.T. Stepo, U. W. Suter, *Pure, Appl. Chem.*, **68**, 2287 (1996).
158. J. Furukawa, T. Tsuruta, *J. Polym. Sci.*, **36**, 275 (1959).
159. A. S. Rozenberg, E. I. Aleksandrova, G. I. Dzhardimalieva, N. V. Kir'yakov, P. E. Chizhov, V. I. Petinov, A. D. Pomogailo, *Russ. Chem. Bull. (Engl. Trans.)*, **44**, 858 (1995).
160. B. P. Agrawal, A. K. Srivastava, *Polym. Eng. Sci.*, **34**, 528 (1994).
161. P. Shukla, A. K. Srivastava, *Polymer*, **35**, 4665 (1996); *Polym. Int.*, **41**, 407 (1996).
162. A. S. Rozenberg, E. I. Aleksandrova, G. I. Dzhardimalieva, N. P. Ivleva, I. E. Uflyand, A. D. Pomogailo, *Russ. Chem. Bull. (Engl. Trans.)*, **47**, 259 (1998).
163. A. D. Pomogailo, V. S. Savost'yanov, G. I. Dzhardimalieva, A. V. Dubovitskii, A. N. Ponomarev, *Russ. Chem. Bull. (Engl. Trans.)*, **44**, 1056 (1995).
164. H. P. Beck, P. Trubenbach, *Chem. Ber.*, **125**, 331, 613 (1992); **126**, 339 (1993).
165. M. V. Klyuev, L. V. Tereshko, G. I. Dzhardimalieva, A. D. Pomogailo, *Bull. Acad. Sci. USSR Div. Chem. Sci. (Engl. Trans.)*, **35**, 2318 (1986).

---

# Index

---

- Absorbed light intensity, polymer photodegradation, 103–104
- Acetylene derivatives, titanacycle-containing polymer synthesis and reactions, 73–74
- Alkyl system, metal-carbon  $\sigma$ -bonds, 37–38
- Alkyne bridges, metallocene polycondensation, 13–15
- Alkyne metathesis polymerization, substituted metallocenes, 11–12
- Alkynes, transition metal polyynes, 34–36
- Alumina catalysts, zirconocene and hafnocene, 116–119
- Aluminum-ether catalyst (TIBA), zirconocene and hafnocene, 118–119
- Amidoxines, zirconocene and hafnocene catalysts, condensation reactions, 128–136
- Anomalous unit formation, metallopolymer unit variability and, 200–201
- Ansa bridged systems, zirconocene and hafnocene catalysts, 117–119
- Aqueous mediums:  
metal polymers, metal monomer copolymerization, unit variability, 176–177  
zirconocene and hafnocene catalysts, condensation reactions, 122–136
- Arene-transition metal polymers:  
chemical properties, 6–7  
nucleophilic aromatic substitution, chloroarene complexes, 23–26  
olefin-containing polymerization, 21–22  
organometallic moieties coordination, 29–30  
polycondensation, 27–28  
ring-opening metathesis polymerization, substituted norbornenes, 22–23  
supramolecular assembly, 30–31
- Artificial unit variability, chemical binding diversity, metal-polymer ligands, metallopolymeric chain anomalies, 182–183
- Aryl systems, metal-carbon  $\sigma$ -bonds, 37–38
- Atomic force microscopy (AFM), polyferrocenylsilane resists:  
electron-beam lithography, 53  
reactive ion etching, 53–54
- Auto-oxidation mechanism, photodegradation, metal-metal polymer bonds, 79–80
- Azobisisobutyronitrile (AIBN) catalyst:  
metal-metal bonded systems, 39–41  
olefin-containing arene polymerization, 22  
olefin-functionalized metallocene polymerization, 9–11
- Backbone structures:  
metallocene polycondensation, 13–15  
metal-metal bonds, photodegradation mechanisms:  
auto-oxidation, 79–80  
cage effects, 95–98  
difunctional dimer synthesis, 86–88  
Fries photochemical rearrangement, 82–83  
hydroperoxide species, 80–82  
intentional design, 83–85  
polymer characterization, 90–91  
polymer synthesis, 88–90  
polyvinyl chlorides, 82  
solid state photochemistry, 94  
solution-based photochemistry, 91–94  
synthesis and characterization, 85–86
- Bifunctional hydroxyl monomers, carbonyl complexes, 32–34

- Bis-(cyclopentadienyl) complexes:  
alkyne metathesis substituted metallocene polymerization, 11–12  
basic principles, 7–8  
cyclopentadienyl rings, metal coordination to, 18–19  
metallocene polycondensation, 13–15  
olefin-functionalized metallocene polymerization, 8–11  
preformed polymer metallocenes, 20–21  
ring-opening polymerization, 15–18
- Bond photolysis, photodegradation, tensile stress effects, 98
- Boron bridge, ring-opening polymerization, 17–18
- Cage effects, photochemical degradation, 95–98
- Carbon-carbon bonds, macromolecular macroligand transformation, decomposition, 159
- Carbon disulfide, mainchain organometallic polymers, reactive metallacycles, cobaltacyclopentadiene-containing polymers, 65–66
- Carbon-halogen bonds, photochemical reactions, 93–94
- Carbon monoxide bonds:  
olefin-containing arene polymerization, 22  
photodegradable polymer design, 84–85  
solid state photochemical reactions, 94  
solution-based photochemical reactions, 91–94
- Carbonyl complexes:  
backbone photodegradation, metal-metal polymer bonds, 81–82  
photodegradable polymer design, 83–85  
polyferrocenylsilanes, ultraviolet photoresists, 55–56  
transition-metal polymers, 32–34
- Carbonyl vibrational stretching frequency, macromolecular macroligand transformation, functional polymer groups, origin changes, 159–161
- Cationic initiators, ring-opening polymerization, 17–18
- Chain effect, macromolecular macroligand transformation, composite inhomogeneity, 164–166
- Chain structure:  
anomalies:  
chemical binding diversity, metal-polymer ligands, 180–183  
transition metal ions, exchange interactions, 188–190  
length, photochemical degradation, cage recombination efficiency, 97–98  
rigidity, macromolecular macroligand transformation, polymer chain conformation, 155
- Chirality, transition metal pendant groups, unit variability and, 194–196
- Chloroarene complexes, nucleophilic aromatic substitution polymerization, 23–26
- Chromium complexes, oxidation-reduction conversion, 162
- Chromium tricarbonyl ( $\text{Cr}(\text{CO})_3$ ):  
arene polycondensation, 27–28  
supramolecular assembly, 30–31
- Chromophores, photodegradable polymer design, 83–85  
concentration effects, 106
- Cobaltacyclopentadiene-containing polymers, mainchain organometallic polymers, reactive metallacycles, 61–69  
isocyanate conversion, 66–69  
yellow polymers, 63–66
- Cobalt complexes:  
metal-metal bonded systems, 40–41  
polyferrocenylsilane resists:  
electron-beam lithography, 52–53  
reactive ion etching, 53–54  
ultraviolet photoresists, 55–56  
polyferrocenylsilanes, lithographic applications, 51–52
- Cobalticium complexes:  
metallocene polycondensation, 15  
zirconocene and hafnocene catalysts, condensation reactions, 126–136
- Composite inhomogeneity, macromolecular complexes, 164–166
- Condensation reactions, zirconocene and hafnocene:  
Lewis acid-base reactions, 121–136  
natural products, 137–139
- Conductive polymers, unit variability and development of, 198–199
- Conjugated polymers:  
arene polycondensation, 27–28  
cyclopentadienyl ring coordination, 19  
organometallic-arene coordination, 29–30  
zirconocene and hafnocene catalysts, 140
- Cooperative effects, polymer chain conformation, macromolecular macroligand transformation, 152
- Coordination compounds:  
bis-(cyclopentadienyl) complexes, cyclopentadienyl ring coordination, 18–19  
metallopolymer unit variability and, 202  
organometallic compounds *vs.*, 2–3
- Coordination number, macromolecular macroligand transformation, composite inhomogeneity, 164–166
- Copolymers:  
carbonyl complexes, 32–34

- ethylene with propylene, macroligand topochemistry, 166–167
- metallopolymer unit variability and, 200–201
- olefin-functionalized metallocene polymerization, 8–11
- synthesis reactions, 89–90
- zirconocene and hafnocene catalysts, 118–119
- Copper complexes:
- exchange interactions, chain anomalies, 189–190
  - oxidation-reduction conversion, 162
  - paramagnetic polymer-bound complexes, topochemistry, 168–172
  - unit variability, valence states, 177–179
- Corrosion-protective coatings, zirconocene and hafnocene catalysts, 142
- Covalent properties, chemical binding diversity, metal-polymer ligands, metallopolymeric chain anomalies, 180–183
- Crosslinking mechanisms:
- macromolecular macroligand transformation, polymer chain conformation, 153–154
  - metallopolymer unit variability and, 199
  - photodegradation and, 105
  - transition metal dimer complexes, 163–164
  - zirconocene and hafnocene catalysts, 119–121
    - condensation reactions, 122–136
    - polymer formation, 137–139
- Cyanide complexes, zirconocene and hafnocene catalysts, 142
- Cyclization reactions, metal polymerization unit variability, 197–198
- Cyclobutadienes:
- mainchain organometallic polymers, reactive metallacycles, cobaltacyclopentadiene-containing polymers, 61–66
  - metal-coordinated structures, 31–32
- Cyclodiborazane groups, transition metal polyynes, 35–36
- Cyclopentadienyl (Cp) derivatives:
- arene polycondensation, 28
  - bis-(cyclopentadienyl) complexes, 7–8
  - chloroarene complexes, nucleophilic aromatic substitution polymerization, 24–26
  - difunctional dimers, 86–88
  - ion fragmentation patterns, 134–136
  - metal-coordinated cyclobutadienes, 31–32
  - reactive metallacycles, in mainchain, cobaltacyclopentadiene-containing polymers, 61–63
    - isocyanate conversion, 66–69
    - yellow polymers, 63–66
  - ring structures, metal coordination, 18–19
  - transition metal chemistry, 4–5
  - zirconocene and hafnocenes, 112–113
  - condensation reactions, monomeric Lewis bases, 121–136
  - silica and alumina catalysts, 116–119
- Decomposition, macromolecular macroligand transformation, 155–159
- composite inhomogeneity, 164–166
- Decreased radical recombination efficiency (DRRE)
- hypothesis, photodegradation, tensile stress effects, 100
  - quantum yields, 101–102
- Degree of conversion, polymer chain conformation, macromolecular macroligand transformation, 150–152
- Dehydroxylated silica (DA), zirconocene and hafnocene catalysts, 118–119
- Depth profiling, polymer photodegradation, oxygen diffusion, 105–106
- Dextran modification, zirconocene and hafnocene catalysts:
- condensation reactions, 125
  - natural product reactions, 137–139
- Diamagnetic complexes, topochemistry, polymer fixation, 167–168
- Diamine synthesis, difunctional dimers, 87–88
- Dicarboxylic acids:
- chemical binding diversity, metal-polymer ligands, metallopolymeric chain anomalies, 181–183
  - metallocene catalysts, condensation reactions, 125–136
- Dichlorides, condensation reactions:
- metallocene catalysts, 122–136
  - natural products, 137–139
- Diels-Alder reaction, zirconocene and hafnocene structures, crosslinked polystyrene, 120–121
- Diene-arylene polymers, zirconocene and hafnocene catalysts, 141–142
- Diene-containing polymers:
- difunctional dimers, 86–88
  - titanacycle-containing polymer synthesis and reactions, 69–74
- Differential scanning calorimetry, chloroarene complexes, nucleophilic aromatic substitution polymerization, 25–26
- Difunctional dimers:
- prepolymer synthesis, 90
  - solution-based photochemical reactions, 91–94
  - synthesis, 86–88
- Dihexylfulvalene dianion, cyclopentadienyl ring coordination, 18–19
- Dimer complex monomerization, macromolecular transition metal complexes, 162–164

- Diethyl phthalate (DOP), photodegradation, tensile stress effects, quantum yields, polymer **3**, 102
- Diols, zirconocene and hafnocene catalysts, condensation reactions, 123
- Dipole-bound aggregation, paramagnetic polymer-bound complexes, topochemistry, 169–172
- Dissociation, metal polymers, metal monomer copolymerization, unit variability, 175–177
- Diyne monomers:  
mainchain polymer reactions, 74–75  
titanacycle-containing polymer synthesis and reactions, 70–74
- Double bond complexes, metallopolymer unit variability and, 202
- Drug-containing polymers, zirconocene and hafnocene catalysts, condensation reactions, 132–136
- Ecolyte polymers, carbonyl compounds, 83–85
- Ecosystem restoration, zirconocene and hafnocene catalysts, condensation reactions, 130–136
- Electron-beam lithography (EBL), polyferrocenylsilanes and, 50  
resists, 52–53
- Electron energy-loss spectroscopic (EELS), polyferrocenylsilane resists, reactive ion etching, 54
- Electron spectroscopic imaging (ESI), polyferrocenylsilanes, lithographic applications, 51–52
- Electron spin resonance (ESR):  
paramagnetic polymer-bound complexes, topochemistry, 168–172  
unit variability, valence states, 179
- $\beta$ -Elimination:  
metal-aryl/metal-alkyl systems, metal-carbon  $\sigma$ -bonds, 37–38  
zirconocenes and hafnocenes, 114–115
- Elimination reactions, unit variability, metal polymers, metal monomer copolymerization, 175–177
- Exchange interactions, transition metal ions, chain incorporation, 188–190
- Extra-coordination anomalies:  
metallopolymer unit variability and, 199  
unit variability in transition metals, 186–188
- Face-to-face polymetalloenes, cyclopentadienyl ring coordination, 19
- Ferrocenedicarboxylic acid (FDCA), zirconocene and hafnocene catalysts, condensation reactions, 126–136
- Ferrocenes:  
bis-(cyclopentadienyl) complexes, 7–8  
cyclopentadienyl ring coordination, 18–19  
metallocene polycondensation, 13–15  
ring-opening polymerization, 16–18
- metal-metal bond-containing polymers, 85–86
- olefin-functionalized metallocene polymerization, 8–11
- polyferrocenylsilanes, lithographic applications, 50–52
- preformed polymer introduction, 20–21
- zirconocene and hafnocene catalysts, condensation reactions, 126–136
- Free energy, macromolecular macroligand transformation, decomposition, 156–159
- Fries rearrangement, backbone photodegradation, metal-metal polymer bonds, 82–83
- Functional polymer groups:  
macromolecular macroligand transformation, changes in origin, 159–161  
transition metal dimer complexes, 163–164
- Gel-penetrating chromatography (GPC), macromolecular macroligand transformation, decomposition, 155–159
- Gibberellic acid, zirconocene and hafnocene catalysts, condensation reactions, 130–136
- Glass transition temperatures, chloroarene complexes, nucleophilic aromatic substitution polymerization, 25–26
- Gold acetylide polymers, transition metal polyynes, 36
- Grignard reagent, metal-aryl/metal-alkyl systems, metal-carbon  $\sigma$ -bonds, 37–38
- Hafnocene reactions:  
acetylene polymers, transition metal polyynes, 36  
catalysts, 113–116  
inorganic supported catalysts, 116–119  
existing polymers, 137–142  
inorganic supports, 119–121  
macromolecules, 112–113  
monomeric Lewis bases, condensation reactions, 121–136
- Hard-soft acid-base (HSAB) theory, zirconocene and hafnocene catalysts, condensation reactions, 124–136
- Heck reaction, mainchain organometallic polymers, reactive metallacycles, cobaltacyclopentadiene-containing polymers, 64–66
- Helical structures, polymer chain conformation, macromolecular macroligand transformation, 150–152
- Hematoporphine derivatives, zirconocene and hafnocene catalysts, condensation reactions, 130–136

- Heteroatom monomers, zirconocenes and hafnocenes, 115
- Hexamethylene diisocyanate (HMDI), metal-metal bond-containing polymers, 86
- High molecular weight polymers:  
macromolecular complexes, 149  
ring-opening polymerization, 16–18
- High-resolution electron impact mass spectrometry (HREI-MS), zirconocene and hafnocene catalysts, condensation reactions, 133–136
- High-temperature superconducting (HTSC) ceramics, metallopolymer unit variability and, 200–202
- Homolysis, photodegradation, tensile stress effects, 98–99
- Hydrocarbon macromolecule, zirconocene and hafnocene catalysts, 140
- Hydrolysis susceptibility, unit variability, ligand environment, 184–186
- Hydroperoxide reactions, backbone photodegradation, metal-metal polymer bonds, 80–82
- Hydroquinone, zirconocene and hafnocene catalysts, condensation reactions, 124
- Hydroxyketone functional group, zirconocene and hafnocene catalysts, 141–142
- In-cage trapping hypothesis, photochemical degradation, cage recombination efficiency, 96–98
- Initiator reactions, unit variability in transition metals, 185–186
- Inorganic catalysts, zirconocene and hafnocene, 116–119
- Interfacial systems, zirconocene and hafnocene catalysts, condensation reactions, 122–136
- Intermolecular complexes, polymer chain conformation, macromolecular macroligand transformation, 151–152  
structuring process, 152–154
- Intramolecular complexes, polymer chain conformation, macromolecular macroligand transformation, 151–152
- Ion fragmentation:  
condensation reactions, 133–136  
paramagnetic polymer-bound complexes, topochemistry, 169–172
- Ionization, metal polymers, metal monomer copolymerization, unit variability, 175–177
- Iron polymers:  
arene polycondensation, 28  
chloroarene complexes, nucleophilic aromatic substitution polymerization, 26  
exchange interactions, chain anomalies, 189–190  
metal-metal bonded systems, 39–41  
olefin-functionalized metallocene polymerization, 9–11
- Isomerization reactions, unit variability, ligand environment, 184–186
- Isotopic abundance, zirconocene and hafnocene catalysts, condensation reactions, 133–136
- Ketones, zirconocene and hafnocene catalysts, condensation reactions, 128–136
- Kinetic analysis:  
polymer photodegradation, oxygen diffusion, 105–106  
zirconocene and hafnocene catalysts, condensation reactions, 126–136
- Kinetin polymers, zirconocene and hafnocene catalysts, condensation reactions, 131–136
- Lability properties, polymer chain conformation, macromolecular macroligand transformation, 150–152
- Lewis acid-base reactions, zirconocene and hafnocene, 112–113  
condensation reactions, 121–136  
inorganic catalysts, 116–119
- Ligand environments, transition metal macromolecules, unit variability and, 183–186
- Linear products, zirconocene and hafnocene reactions, 137–139
- Linkage analysis, zirconocene and hafnocene catalysts, condensation reactions, 133–136
- Liquid-crystalline polymers:  
metallocene introduction, preformed polymer, 20–21  
metallocene polycondensation, 14–15  
olefin-functionalized metallocene polymerization, 11
- “Living” polymerization, alkyne metathesis polymerization, substituted metallocenes, 12
- Low critical solution temperatures (LCSTs), olefin-functionalized metallocene polymerization, 11
- Low-molecular-weight polymers:  
macromolecular complexes, 149  
metallocene polycondensation, 15
- Macrocycles, macromolecular complex polymerization, 149
- Macroligands, macromolecular complexes:  
composite inhomogeneity, 164–166  
functional layer topochemistry, 166–167  
structural principles, 148–149  
transition metal binding and transformation of, 150–161  
chain conformation, changes in, 150–152

- decomposition, 155–159
  - functional group origins, 159–161
  - structuring process, 152–155
- Macromolecular metal complexes (MMC):
- basic principles, 148–149
  - macroligand transformation, transition metal binding, 150–161
  - chain conformation, changes in, 150–152
  - decomposition, 155–159
  - functional group origins, 159–161
  - structuring process, 152–155
- topochemistry, 166–172
- diamagnetic complexes, polymer fixation, 167–168
  - paramagnetic polymer-bonded complexes, 168–172
  - polymer macroligand functional layers, 166–167
  - structural data, 172
- transition metal transformation, polymer reactions, 161–165
- composite inhomogeneity, 164–165
  - dimer complex monomerization, 162–164
  - oxidation-reduction conversion, 161–162
- unit variability:
- applications, 198–202
  - monomer copolymerization, 172–198
    - cyclization during polymerization, 197–198
    - extra-coordination, spatial/electronic polyhedron anomalies, 186–188
    - metal group elimination during polymerization, 175–177
    - metal ion chain exchange interactions, 188–190
    - metallopolymeric chain anomalies, 180–183
    - metallopolymeric chain stereoregularity, 192–194
    - metallopolymer unsaturation and structuring, 196–197
    - metal site nuclearity, 190–193
    - pendant group chirality, 194–196
    - qualitative/quantitative metal ligand environments, 183–186
    - stable metal isotopes, 179
    - valence states, transition metal ions, 177–179
- Magnetic force microscopy (MFM), polyferrocenylsilane resists, electron-beam lithography, 53
- Mainchain organometallic polymers, reactive metallacycles:
- cobaltacyclopentadiene-containing polymers, 61–63
    - isocyanate conversion, 66–69
    - yellow polymers, 63–66
  - diyne monomers, 74–75
  - titanacycle-containing polymers, 69–74
- Manganese compounds, paramagnetic polymer-bound complexes, topochemistry, 168–172
- Mass spectrometry, zirconocene and hafnocene catalysts, condensation reactions, 133–136
- Matrix-assisted laser desorption ionization (MALDI) spectrometry, zirconocene and hafnocene catalysts, condensation reactions, 133–136
- Metal-carbon  $\sigma$ -bonds:
- metal-aryl/metal-alkyl systems, 37–38
  - transition metal polyynes, 34–36
- Metal-containing monomers (MCM), macromolecular complexes, structural principles, 149
- Metal-coordinated cyclobutadienes, basic properties, 31–32
- Metallacycles, mainchain organometallic polymers:
- cobaltacyclopentadiene-containing polymers, 61–63
    - isocyanate conversion, 66–69
    - yellow polymers, 63–66
  - diyne monomers, 74–75
  - titanacycle-containing polymers, 69–74
- Metallocenes:
- bis-(cyclopentadienyl) complexes, 7–8
  - alkyne metathesis polymerization, substituted metallocenes, 11–12
  - olefin-functionalized metallocene polymerization, 8–11
  - polycondensation, 13–15
  - preformed polymers, 20–21
  - ring-opening polymerization, 15–18
  - transition metal macromolecules and, 6–7
- Metallopolymeric chain anomalies:
- chemical binding diversity, metal-polymer ligands, 180–183
  - stereoregularity, 192–194
- Metal-metal bonded systems:
- difunctional dimers, 86–88
  - polymer synthesis, 88–90
  - transition-metal polymers, 38–41
- Metal-metal polymers, photodegradation mechanisms, backbone structure:
- auto-oxidation, 79–80
  - cage effects, 95–98
  - difunctional dimer synthesis, 86–88
  - Fries photochemical rearrangement, 82–83
  - hydroperoxide species, 80–82
  - intentional design, 83–85
  - polymer characterization, 90–91
  - polymer synthesis, 88–90
  - polyvinyl chlorides, 82
  - solid state photochemistry, 94

- solution-based photochemistry, 91–94  
synthesis and characterization, 85–86
- Metal-oxygen bonds, macromolecular macroligand transformation, decomposition, 159
- Metal site nuclearity, unit variability and, 190–192
- Methylalumoxane (MAO) reaction, zirconocenes and hafnocenes, 114–115  
silica and alumina catalysts, 116–119
- Microcontact printing, polyferrocenylsilanes and, 50
- Mixed-unit chain formation, transition metal macromolecules, unit variability and, 183–186
- Molecular weight averaging:  
macromolecular macroligand transformation:  
decomposition, 155–159  
functional polymer groups, origin changes, 159–161  
polymer chain conformation, 154  
metallocene catalysts, condensation reactions, 125–136
- Molybdenum compounds:  
metal-metal bonded systems, 39–41  
metal-metal polymers, 92–94  
organometallic-arene coordination, 29–30  
oxidation-reduction conversion, 161–162  
photochemical degradation, cage recombination efficiency, 96–98
- Monomeric structures:  
carbonyl complexes, 32–34  
diynes:  
mainchain polymer reactions, 74–75  
titanacycle-containing polymers, 70–74  
transition metal dimer complexes, 162–164  
unit variability in transition metals, ligand environment, 185–186  
zirconocene and hafnocene, condensation reactions, 121–136
- Nanocomposites:  
olefin-containing arene polymerization, 22  
polyferrocenylsilane resists, reactive ion etching, 54–55
- Nanotransfer printing, polyferrocenylsilanes and, 50
- Natural products, zirconocene and hafnocene catalysts, condensation reaction, 137–139
- Neighboring group effect, macromolecular macroligand transformation, composite inhomogeneity, 164–166
- Nickel compounds, mainchain organometallic polymers, reactive metallacycles, cobaltacyclopentadiene-containing polymers, 63–66
- Nitriles, mainchain organometallic polymers, reactive metallacycles, cobaltacyclopentadiene-containing polymers, 67–68
- Nitroxyl radicals, diamagnetic polymer fixation, topochemistry, 167–168
- Nonlinear optical (NLO) properties:  
metallocene polycondensation, 14–15  
olefin-functionalized metallocene polymerization, 9–11
- Norbornene complexes, ring-opening metathesis polymerization, 22–23
- Norfloxacin, zirconocene and hafnocene catalysts, condensation reactions, 133–136
- Norrish pathways, photodegradable polymer design, 83–85
- Noyes's prediction, photochemical degradation, cage recombination efficiency, 95–98
- Nuclearity of metal sites, transition metal unit variability and, 190–192
- Nucleophilic aromatic substitution polymerization, chloroarene complexes, 23–26
- Olefin-containing arenes, polymerization, 21–22
- Olefin-functionalized metallocene polymerization, bis-(cyclopentadienyl) complexes, 8–11
- Oligomer structures, metal-metal bonded systems, 38–41
- Organometallic compounds:  
arene polymer coordination, 29–30  
bis-(cyclopentadienyl) complexes, 7–21  
ring-opening polymerization, 15–18  
chloroarene complexes, nucleophilic aromatic substitution polymerization, 25–26  
defined, 2  
historical background, 5–7  
olefin-containing arene polymerization, 21–22
- Osmium complexes, unit variability, metal site nuclearity and, 191–192
- Oxidation-reduction:  
transition metal conversion, macromolecular complexes, 161–162  
unit variability, valence states, transition metal ions, 179
- Oxygen diffusion, polymer photodegradation and, 105–106
- Palladium catalyst:  
arene polycondensation, 28  
oxidation-reduction conversion, 162
- Paramagnetic polymer-bound complexes, topochemistry, 168–172
- PDA (partially dehydroxylated silica), zirconocene and hafnocene catalysts, 118–119
- Pendant group chirality, unit variability and, 194–196
- Pendant phenyl ring structure, backbone photodegradation, metal-metal polymer bonds, 83  
pH levels, zirconocene and hafnocene catalysts, condensation reactions, 123–124
- Phosphine complexes, arene polycondensation, 28

- Photochemical reactions:  
  cage effects, 95–98  
  solid state, 94  
  solution reactivity, 91–94
- Photodegradation:  
  absorbed light intensity, 103–104  
  chromophore concentration, 106  
  metal-metal polymer backbone mechanisms:  
    auto-oxidation, 79–80  
    cage effects, 95–98  
    difunctional dimer synthesis, 86–88  
    Fries photochemical rearrangement, 82–83  
    hydroperoxide species, 80–82  
    intentional design, 83–85  
    polymer characterization, 90–91  
    polymer synthesis, 88–90  
    polyvinyl chlorides, 82  
    solid state photochemistry, 94  
    solution-based photochemistry, 91–94  
    synthesis and characterization, 85–86  
  oxygen diffusion, 105–106  
  polymer morphology, 104–105  
  tensile stress effects, 98–102  
    Plotnikov hypothesis, 99  
    quantum yields, 101–102  
    radical reactions, 100  
    radical recombination efficiency hypothesis, 100  
    theoretical principles, 98  
    Zhurkov equation, 100–101
- Photon reagents, polymer photodegradation, absorbed light intensity, 103–104
- Photo-oxidative mechanism, photodegradation, metal-metal polymer bonds, 79–80
- $\pi$ -orbital complexed polymers:  
  carbonyl complexes, 33–34  
  olefin-containing arene polymerization, 21–22  
  titanacycle-containing polymer synthesis and reactions, 72–74  
  transition metal polyynes, 34–36
- Plant growth, zirconocene and hafnocene catalysts, condensation reactions, 131–136
- Plasma-induced crystallization, polyferrocenylsilane resists, reactive ion etching, 54–55
- Platinum bonds, metal-metal bonded systems, 38–41
- Plotnikov hypothesis, photodegradation, tensile stress effects, 99
- Polyacrylamide, zirconocene and hafnocene catalysts, natural product reactions, 138–139
- Poly(acrylic acid), zirconocene and hafnocene catalysts, natural product reactions, 139
- Polyamides, arene polycondensation, 27–28
- Polyarylenediynes, zirconocene and hafnocene catalysts, 140–141
- Polyarylenes, mainchain organometallic polymers, reactive metallacycles, cobaltcyclopentadiene-containing polymers, 63–66
- Polyaspartamides, preformed polymer introduction, 20–21
- Polycondensation:  
  arene complexes, 27–28  
  metallocenes, 13–15
- Polydimethylsiloxane systems, zirconocene derivatives, 119–121
- Polyene complexes, backbone photodegradation, metal-metal polymer bonds, 2
- Polyesters, condensation reactions, 124
- Polyethers, condensation reactions, 122–123
- Polyethylene, macroligand topochemistry, 166–167
- Polyferrocenylsilanes, lithographic applications:  
  basic principles, 50–52  
  electron beam lithography resists, 52–53  
  reactive ion etch resists, 53–55  
  ultraviolet photoresists, 55–56
- Polyhedral structures, extra-coordination anomalies, 186–188
- Polymer **3**, photodegradation, tensile stress effects, quantum yields, 101–102
- Polymer chain conformation, macromolecular complexes, macroligand transformation, 150–152
- Polymer morphology, photodegradation and, 104–105
- Poly(methylsiloxanes), metallocene introduction, preformed polymer, 20–21
- Poly(*n*-hexylphenylene) (PHP), organometallic-arene coordination, 29–30
- Polynorbornenes, ring-opening polymerization, 1–18
- Polyoxide polymers, zirconocene and hafnocene catalysts, condensation reactions, 140
- Polyoximes, zirconocene and hafnocene catalysts, condensation reactions, 128–136
- Polyparaphenylene (PPP), arene coordination, 29–30
- Polyphosphazenes, organometallic-arene coordination, 30
- Poly(*p*-phenylene), titanacycle-containing polymer synthesis and reactions, 72–74
- Poly(*p*-phenylene terephthalamide) (PPTA), arene polycondensation, 27–28
- Polypropylene (PP):  
  macroligand topochemistry, 166–167  
  zirconocene and hafnocene catalysts, 117–119  
  styrene-divinylbenzene copolymers, 119–121
- Polysilanes, zirconocene and hafnocene structures, 120–121
- Polysiloxanes, metal-metal bonded systems, 39–41

- Polystyrene:  
  macroligand topochemistry, 166–167  
  organometallic-arene coordination, 29–30  
  zirconocene and hafnocene structures, 119–121
- Polythioethers, zirconocene and hafnocene catalysts, condensation reactions, 127–136
- Polyurethane, synthesis reactions, 88–90
- Poly(vinyl alcohol), zirconocene and hafnocene catalysts, natural product reactions, 138–139
- Polyynes, transition metal-carbon  $\sigma$ -bonds, 34–36
- Pore accessibility, macromolecular macroligand transformation, polymer chain conformation, 153–154
- Powder X-ray diffraction (PXRD), polyferrocenylsilanes, lithographic applications, 51–52
- Preformed polymers:  
  metallocene introduction, 20–21  
  synthesis, 90
- Pyridone moieties, mainchain organometallic polymers, reactive metallacycles, cobaltacyclopentadiene-containing polymers, 66–69
- Qualitative/quantitative ligand environments, transition metal macromolecules, unit variability and, 183–186
- Quantum yields:  
  photodegradation, tensile stress effects, 101–102  
  polymer photodegradation, absorbed light intensity, 103–104
- Rack parameters, chemical binding diversity, metal-polymer ligands, metallopolymeric chain anomalies, 181–183
- Radical reaction rates:  
  macromolecular macroligand transformation, decomposition, 157–159  
  photodegradation, tensile stress effects, 100
- Reaction intermediates, macromolecular macroligand transformation, composite inhomogeneity, 165–166
- Reactive ion etching (RIE), polyferrocenylsilanes:  
  lithographic applications, 50–52  
  resists, 53–55
- Reduction processes, metal polymers, metal monomer copolymerization, unit variability, 178–179
- $\alpha$ -Relaxation, macromolecular macroligand transformation, polymer chain conformation, 155
- Rhodium complexes:  
  arene polycondensation, 28  
  oxidation-reduction conversion, 162  
  unit variability, metal site nuclearity and, 191–192
- Ricinoleic acid, zirconocene and hafnocene catalysts, condensation reactions, 129–136
- Rigid-chain polymer interactions, macromolecular macroligand transformation, 155
- Ring-opening metathesis polymerization (ROMP):  
  metallocene complexes, 16–18  
  substituted norbornenes, 22–23
- Ring-opening polymerization (ROP):  
  bis-(cyclopentadienyl) complexes, 15–18  
  polyferrocenylsilanes, lithographic applications, 50–52
- Ruthenocene complexes, ring-opening polymerization, 15–18
- Scanning electron microscopy (SEM), polyferrocenylsilane resists, electron-beam lithography, 52–53
- Schrock molybdenum catalyst, alkyne metathesis polymerization, substituted metallocenes, 12
- Selenium compounds, mainchain organometallic polymers, reactive metallacycles, cobaltacyclopentadiene-containing polymers, 68–69
- Side reactions, metallopolymer unit variability and, 199–200
- Silica catalysts, zirconocene and hafnocene, 116–119
- Silole units, carbonyl complexes, 32–34
- Silver compounds, zirconocene and hafnocene catalysts, condensation reactions, 125–136
- Sodium hydroxide, zirconocene and hafnocene catalysts, condensation reactions, 124
- Solid state photochemistry, metal-metal polymers, 94
- Solution-based photochemical reactions, metal-metal polymers, 91–94
- Solvatochromism, mainchain organometallic polymers, reactive metallacycles, cobaltacyclopentadiene-containing polymers, 65–66
- Solvent properties, zirconocene and hafnocene catalysts, condensation reactions, 132–136
- Spatial/electronic structure, macromolecular complexes, extra-coordination anomalies, 186–188
- Spectroscopic characterization:  
  metal-metal polymers, 90–91  
  zirconocene and hafnocene catalysts, condensation reactions, 133–136
- Stable metal isotopes, unit variability, transition metal ions, 179
- Step polymerization, metal-metal bond-containing polymers, 85–86
- Stepwise constants, polymer chain conformation, macromolecular macroligand transformation, 152

- Stereoregularity mechanisms, metallocopolymeric chains, 192–194
- Stirring rate, zirconocene and hafnocene catalysts, condensation reactions, 123
- Structurization, metallocopolymer unit variability and, 196–197
- Styrene-divinylbenzene copolymers, zirconocene and hafnocene catalysts, 119–121
- Superconducting quantum interference device (SQUID) magnetometry, polyferrocenylsilanes, lithographic applications, 52
- Supramolecular assembly:  
  arene polymers, 30–31  
  macromolecular macroligand transformation, polymer chain conformation, 154–155
- Tautomeric forms:  
  polymer chain conformation, macromolecular macroligand transformation, 150–152  
  unit variability in transition metals, ligand environment, 185–186
- Tensile stress effects, photodegradation, 98–102
- Plotnikov hypothesis, 99
- quantum yields, 101–102
- radical reactions, 100
- radical recombination efficiency hypothesis, 100
- theoretical principles, 98
- Zhurkov equation, 100–101
- Tetrahedral structures, zirconocene and hafnocenes, 112–113
- Thermal polymerization:  
  chemical binding diversity, metal-polymer ligands, metallocopolymeric chain anomalies, 181–183  
  extra-coordination anomalies, polyhedral structures, 186–188  
  metal polymers, metal monomer copolymerization, unit variability, 176–177
- Thermogravimetric analyses (TGAs), mainchain organometallic polymers, reactive metallacycles, cobaltacyclopentadiene-containing polymers, 62
- Thiophene polymers, mainchain organometallic polymers, reactive metallacycles:  
  cobaltacyclopentadiene-containing polymers, 68–69  
  titanacycle-containing polymer synthesis and reactions, 72–74
- Time-of-flight secondary ion mass spectrometry (TOF SIMS), polyferrocenylsilane resists, electron-beam lithography, 52–53
- Titanacycle-containing polymers, mainchain reactive metallacycles, 69–74
- Titanacyclobutene, titanacycle-containing polymer synthesis and reactions, 73–74
- Titanium:  
  basic chemistry, 3–5  
  diamagnetic polymer fixation, topochemistry, 167–168
- Titanocene compounds:  
  condensation reactions, 122, 125–136  
  isotopic abundance, 134–136  
  Natta-Ziegler mechanisms, 113–114  
  structure and properties, 112–113
- Top-down approach, olefin-containing arene polymerization, 22
- Topochemistry, macromolecular metal complexes, 166–172  
  diamagnetic complexes, polymer fixation, 167–168  
  paramagnetic polymer-bonded complexes, 168–172  
  polymer macroligand functional layers, 166–167  
  structural data, 172
- Toxicity properties, metallocene introduction, preformed polymer, 20–21
- Transition metal macromolecules:  
  basic chemistry, 3–5  
  compositional and structural irregularities, 148–202  
  historical background, 5–7  
  polymer reaction and transformation of, 161–165  
  composite inhomogeneity, 164–165  
  dimer complex monomerization, 162–164  
  oxidation-reduction conversion, 161–162  
  structure and properties, 2–3
- Transmission electron microscopy (TEM), polyferrocenylsilanes:  
  lithographic applications, 51–52  
  reactive ion etch resists, 53–54
- Tridentate ligands, unit variability in transition metals, 185–186
- Trimethylaluminum (TMA), zirconocenes and hafnocenes, 117–119
- Triphenylphosphine, mainchain organometallic polymers, reactive metallacycles, cobaltacyclopentadiene-containing polymers, 64–66
- Tungsten complexes, metal-metal polymers, 92–94
- Ultraviolet photoresists, polyferrocenylsilanes, 55–56
- Ultraviolet-visible spectroscopy:  
  mainchain organometallic polymers, reactive metallacycles, cobaltacyclopentadiene-containing polymers, 62

- titanacycle-containing polymer synthesis and reactions, 71–74
- Unit variability, metal polymers, metal monomer copolymerization, 172–198
- cyclization during polymerization, 197–198
  - extra-coordination, spatial/electronic polyhedron anomalies, 186–188
  - metal group elimination during polymerization, 175–177
  - metal ion chain exchange interactions, 188–190
  - metallopolymeric chain anomalies, 180–183
  - metallopolymeric chain stereoregularity, 192–194
  - metallopolymer unsaturation and structuration, 196–197
  - metal site nuclearity, 190–193
  - pendant group chirality, 194–196
  - qualitative/quantitative metal ligand environments, 183–186
  - stable metal isotopes, 179
  - valence states, transition metal ions, 177–179
- Unsaturation, metallopolymer unit variability and, 196–197
- “Vacant” orbitals, zirconocene and hafnocenes, 112–113
- Valence states, transition metal ions, metal polymers, metal monomer copolymerization, unit variability, 177–179
- Vanadium compounds:
- exchange interactions, chain anomalies, 189–190
  - oxidation-reduction conversion, 161–162
  - paramagnetic polymer-bound complexes, topochemistry, 168–172
- unit variability:
- ligand environment, 183–186
  - metal site nuclearity and, 190–192
  - valence states, 178–179
- Weiss constant, paramagnetic polymer-bound complexes, topochemistry, 168–172
- X-ray photoelectron spectroscopy (XPS), polyferrocenylsilane resists, electron-beam lithography, 52–53
- Yellow-colored polymers, mainchain organometallic polymers, reactive metallacycles, cobaltacyclopentadiene-containing polymers, 63–66
- Zeolites, zirconocene and hafnocene structures, 119–121
- Zhurkov equation, photodegradation, tensile stress effects, 100–101
- Ziegler-Natta catalysts, zirconocenes and hafnocenes, 113–115
- Zirconium complexes, unit variability, metal site nuclearity and, 190–192
- Zirconocene complexes:
- acetylene polymers, transition metal polyynes, 36 catalysts, 113–116
    - inorganic supported catalysts, 116–119
  - existing polymers, 137–142
  - inorganic supports, 119–121
  - macromolecules, 112–113
  - monomeric Lewis bases, condensation reactions, 121–136